

Chapter 1

The climate of the Eastern Mediterranean and Greece: past, present and future*

1.1 Introduction

During the four and a half billion years of our planet's history, the parameters that determine the Earth's climate have varied considerably. When the composition of our planet's atmosphere started to come close to its present-day characteristics, some three billion years ago, alternating warm and cold glacial and interglacial periods began to take place. The most recent geological period, the Holocene began 11,500 years ago, i.e. after the last ice age (18,000 years ago) and continues to this day. During the current interglacial period, the air temperature began to rise and almost reached present temperature levels in the 11th century A.D. (Luterbacher et al., 2011). This period was also marked by the so-called 'Little Ice Age' from the 15th to the 19th century, during which substantially lower temperatures prevailed both at middle latitudes and in Greece, with estimates showing that temperatures were 1.5°C lower than today (Repapis et al., 1989; Zerefos et al., 2010; Zerefos, 2007; Zerefos, 2009; Luterbacher et al., 2006; 2010; 2011).

Since the end of the 19th century, a warming of the atmosphere, with some variations, has been ongoing. The average rate of warming of the Earth's atmosphere during the 20th century was 0.7°C per 100 years (IPCC, 2007). The international scientific consensus is that a significant part of this warming is attributable to a change in the atmosphere's composition caused by human (anthropogenic) activity. This is commonly referred to as the 'anthropogenic component of climate change' or simply 'anthropogenic global warming'. In fact, this period is often described, quite accurately, as the 'anthropocene' a term originally coined by Eugene F. Stoermer and later popularised by Prof. Paul Crutzen. As estimated by Jones and Moberg (2003), the increase in air temperature averages in the Earth's land areas in the course of the 20th century was 0.78°C per 100 years. It should be noted that the increase was not constant throughout the 20th century: a warming was recorded in 1920-1945 and from 1975 onwards, while many studies have tried to explain the cooling observed between 1945 and 1975, which, it was concluded,

* Chapter 1 was co-authored by Ch. Zerefos, Ch. Repapis, Ch. Giannakopoulos, J. Kapsomenakis, D. Papanikolaou, M. Papanikolaou, S. Poulos, M. Vrekoussis, C. Philandras, G. Tselioudis, E. Gerasopoulos, C. Douvis, M. Diakakis, P. Nastos, P. Hadjinicolaou, E. Xoplaki, Juerg Luterbacher, P. Zanis, Ch. Tzedakis, D. Founda, K. Eleftheratos and K. Repapis.

could be attributed to the sun's light being blocked by anthropogenic atmospheric aerosols and volcanic dust (global dimming). In any case, the recent upward trend in temperature is statistically significant at a confidence level of 95% in almost all inhabited areas of the planet and, according to the World Meteorological Organisation, the 1995-2005 period was the warmest decade on record in the last 500 years (WMO, 2006).

According to the Intergovernmental Panel on Climate Change (IPCC, 2007) the atmospheric temperature is projected to continue to rise throughout the 21st century in most areas of the planet. In particular, on the basis of average results over a number of climate model simulations, the average atmospheric temperature is expected to increase by 1.8-4°C by 2100, depending on developments in the concentration of greenhouse gas emissions. The increase in temperature is expected to be greater at higher latitudes and in continental regions as opposed to the oceans (IPCC, 2007). Global warming is expected to cause a decline in sea and land ice cover, and an increase in the mean sea level. In fact, in many regions the observed and expected increase in atmospheric temperature is also accompanied by an increasing frequency of extreme weather events, as mentioned in the Special Report on extreme weather events of the Intergovernmental Panel on Climate Change (IPCC, 2012). Future precipitation is more difficult to estimate because local factors including terrain affect the amount of rainfall. In the 20th century, the amount and the distribution of rainfall in continental areas tended on average to increase in a large part of middle and high latitudes, whilst, by contrast, tending to decrease in tropical regions. Similar patterns are expected in the amount of rainfall in the 21st century, according to results of climate model simulations. Precipitation is generally expected to increase at mid and high latitudes and also in the Intertropical Convergence Zone, and to decrease at tropical latitudes (IPCC, 2007).

Southern Europe and the wider Mediterranean region have been identified as vulnerable to the impact of anthropogenic climate change (Hulme et al., 1999; Giorgi, 2006; IPCC, 2007), because these regions are situated at the edge of semi-arid zones; as a result, a northward shift of baroclinic instability due to climate change could bring about drastic changes, particularly in the balance of precipitation in the Mediterranean. In particular, as shown by the results of a series of climate model simulations under various emission scenarios for the Mediterranean region, temperatures are projected to rise significantly by the end of the 21st century, while precipitation is projected to decrease (Gibelin and Déqué, 2003; Pal et al., 2004; Giorgi and Bi, 2005; Giorgi and Lionello, 2008; Zanis et al. 2009; Kapsomenakis, 2009; Douvis, 2009). Recent studies by Gao et al. (2006), Hertig and Jacobeit (2007), Zerefos et al. (2010), using statistical downscaling methods, concluded that precipitation is projected to decline substantially in SE Mediterranean regions, mostly from October to May. Other studies focusing on changes in temperature and rainfall extremes project that heat stress (Diffenbough et al., 2007; Kuglitsch et al., 2010) and the duration of drought periods (Goubanova and Li, 2007) will drastically increase in the Mediterranean region in the future, leading, inter alia, to a significant rise in for-

est fire risk (Giannakopoulos, 2009a). These changes are expected to have a significant impact on the region's ecosystems, as well as on a number of sectors and implications of human activity (health, agriculture, tourism, energy demand, natural disasters, loss of biodiversity, etc.). The following sections present a more detailed analysis of climate change in the Eastern Mediterranean and in various regions of Greece, at different time scales in the past, present and future.

1.2 Paleoclimatic changes

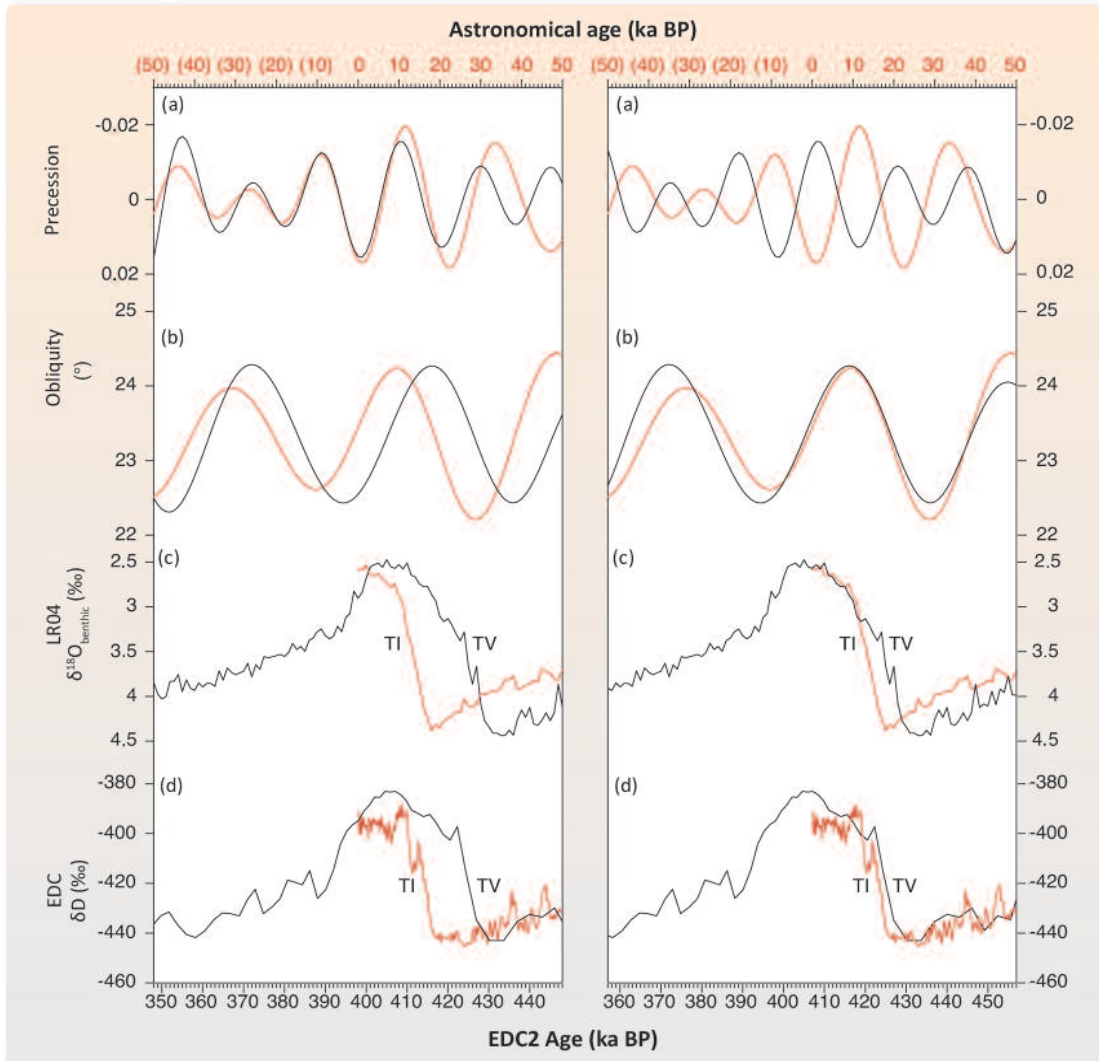
At the beginning of the Eocene, fifty-five million years ago, the Earth's climate was warmer than it is today (The Geological Society, 2010), with deep-sea paleotemperature estimates derived from the analysis of benthic foraminifera oxygen isotopes (Zachos et al., 2001; Miller et al., 2005) suggesting that temperatures were about 6°C higher. Evidence also points to a subsequent long-term downward trend in temperature over the last 50 million years (Zachos et al., 2001). Antarctic ice sheets formed 34 million years ago (Barrett, 1996), while Northern Hemisphere glaciation started 2.6 million years ago (Maslin et al., 1998). This marked the beginning of the Quaternary, i.e. the most recent geological period, characterised by alternations between relatively short interglacial periods (lasting 10-30 thousand years), and prolonged glacial ones. The sequence of alternating glacial/interglacial periods became distinctly more intense, but also less frequent during the last one million years (Middle and Late Pleistocene).

In brief, climate is determined by both external and internal factors (Bradley, 1999; Alverson et al., 2003). External factors include Earth-Sun orbital parameters, i.e. eccentricity, obliquity and precession, as well as solar activity. Internal factors include volcanic activity, feedback processes between the hydrosphere – atmosphere – lithosphere – biosphere – cryosphere (e.g. albedo, cloud cover, etc.), variations in ice-sheet volume, changes in speed and circulation of ocean currents, changes in atmospheric greenhouse gases (e.g. CO₂, CH₄) and their impact on incoming and outgoing thermal radiation, and anthropogenic forcing.

The impact of variations in the Earth's orbital parameters on long-term climate change was first described by Adhemar (1842), Croll (1875) and Milankovitch (1941); since then, numerous studies have documented the effect of the three orbital parameters, occurring at periodicities of 400 and 100, 41 and 19-21 thousand years (ka), on various paleoclimatic indices. Astronomical solutions and calculations of the Earth's orbital parameters in the past (Berger and Loutre, 1991) and the future (Berger et al., 1998) are important tools in a range of paleoclimatic studies. For instance, they allow for comparisons between the current interglacial period – which started 11.5 thousand years before present (ka BP) – and past ones marked by similar orbital parameters and, then, for an estimate of the current phase of the climate cycle, as well as of its future development. According to estimates from the 4th IPCC assessment report (2007), at least 30 thousand

Figure 1.1

Alignment of past isotopic records, based on precession and obliquity parameters, with those of the present and the future. Comparison of the two alignment schemes

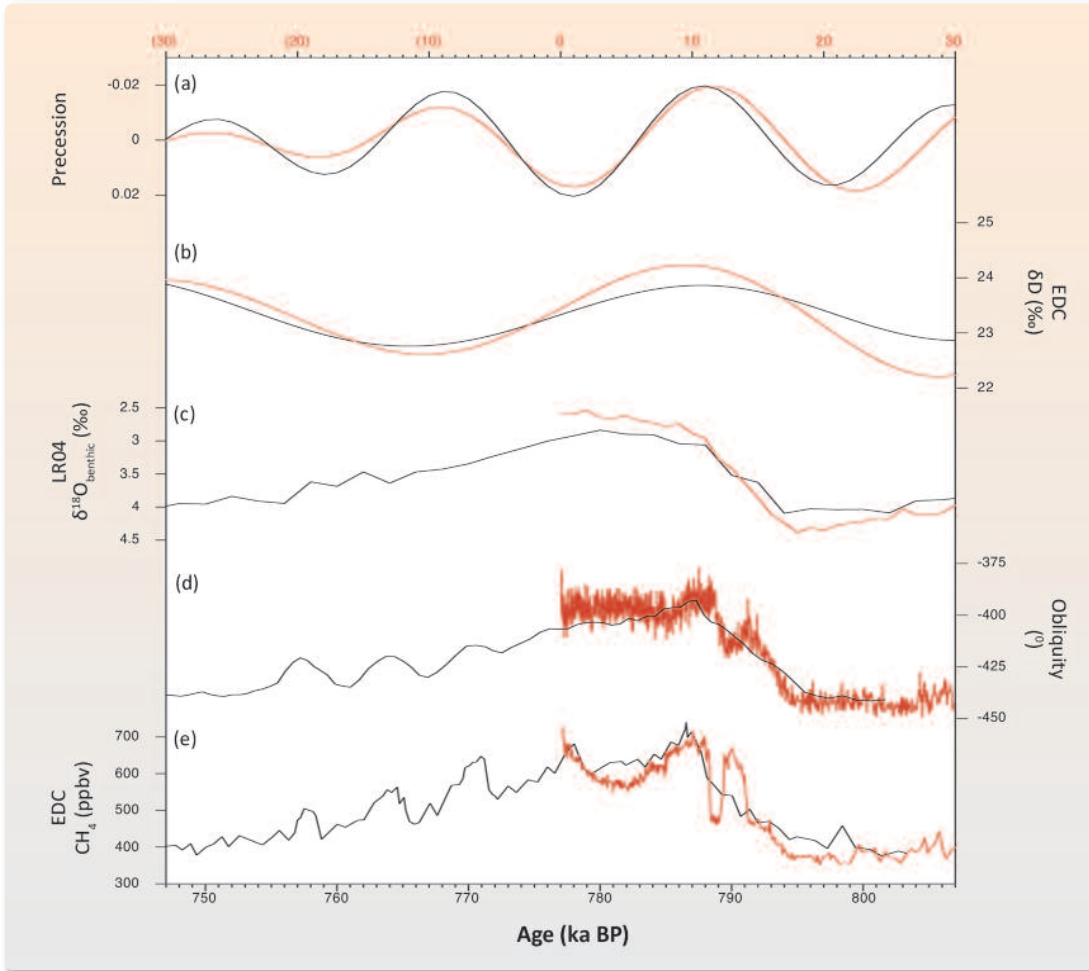


The bottom horizontal axis (in black) refers to a 100-ky interval in the past, namely 350-450 ka (MIS 11) (according to Masson-Delmotte et al., 2006). The upper horizontal axis (in red) refers to the past 50 ka, but also extends 50 ka into the future (ages in parentheses denote thousand years after present, ka AP). Left panel shows synchronization of the precession signal between MIS 1 and 11 and right panel synchronization of the obliquity signal. (a) precession index (Berger and Loutre, 1991); (b) obliquity (Berger and Loutre, 1991); (c) $\delta^{18}\text{O}_{\text{benthic}}$ record from the LR04 stack (Lisiecki and Raymo, 2005); (d) Deuterium (δD) composition of ice in EDC ice core (EPICA Community Members, 2004). The EPICA data in this figure are plotted on the EDC2 timescale used in the EPICA Community Members (2004) paper. Chart from Tzedakis (2010).

years would have to pass before the Earth's orbital configuration would favour the occurrence of very cold summers in the Northern Hemisphere, similar to the ones that occurred 116 ka BP at the beginning of the last glacial period). However, the scientific community remains sceptical today both about which specific past interglacial period to choose for comparison with the current warm period, and about which analogue to use for such a comparison. For instance, if we were to compare the current interglacial period (isotopic stage 1, or MIS 1) with MIS 11 (~ 400

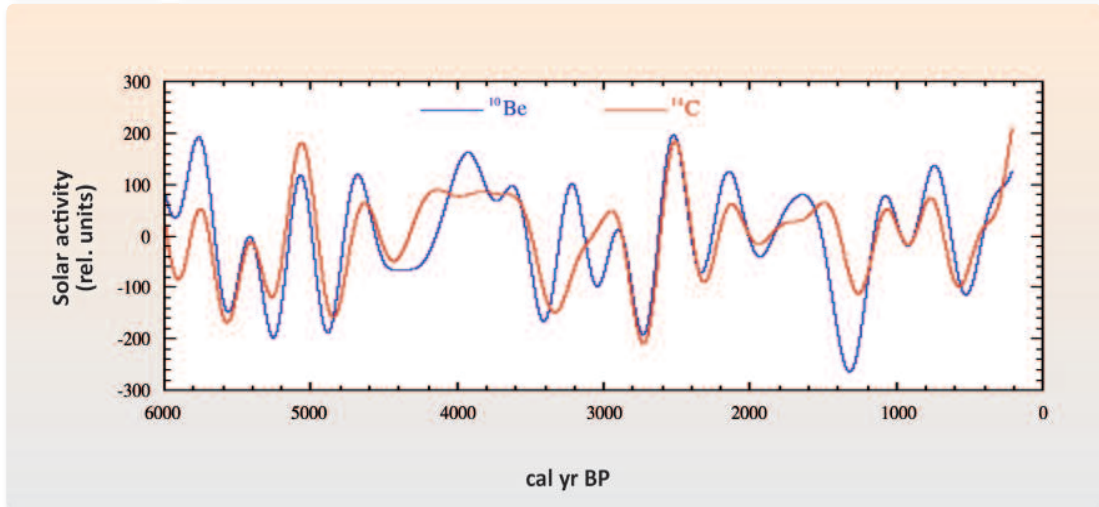
Figure 1.2

Alignment of past isotropic records, based on precession and obliquity parameters, with those of the present and future. Comparison of the two alignment schemes



The bottom horizontal axis (in black) refers to a 60-ky interval in the past, around 800 to 750 ka BP (MIS 19). The upper horizontal axis (in red) refers to the past 30 ka, but also extends 30 ka into the future (ages in parentheses denote thousand years after present, ka AP). (a) Precession index (Berger and Loutre, 1991); (b) obliquity (Berger and Loutre, 1991); (c) $\delta^{18}\text{O}_{\text{benthic}}(\text{‰})$ record from the LR04 stack (Lisiecki and Raymo, 2005); (d) δD composition of ice in the EDC ice core, Antarctica (Jouzel et al., 2007), plotted on the EDC3 timescale; (e) atmospheric CH_4 concentration from the EDC ice core (Loulergue et al., 2008), plotted on the EDC3 timescale.

ka BP) – which had a long duration (28 ka) and similar insolation and CO_2 values – and if we aligned the precession curves of the two interglacial periods, we would probably deduce that the current interglacial period must be nearing its end (Figure 1.1) (Loutre and Berger, 2000; 2003; Ruddiman, 2007; Tzedakis, 2010). However, the alignment of the obliquity curves of the two warm periods (Masson-Delmotte et al., 2006; Broecker and Stocker, 2006) indicates that the current warm period should continue another 12 ka, before conditions could favour the onset of the next glacial period (Figure 1.2). On the other hand, if we compare the current MIS 1 period with MIS 19 (~770 ka BP), which also has similar orbital parameters, then we would deduce that the current warm period could last another 9 ka (see Loutre and Berger, 2000; and Figure 1.2).

Figure 1.3**Reconstruction of solar activity based on ^{10}Be and ^{14}C** 

The ^{10}Be production rate was derived from ^{10}Be concentrations measured in the GRIP ice core, Greenland (Vonmoos et al., 2006). The ^{14}C production rate was calculated with the Bern3D dynamic ocean carbon cycle model (Müller et al., 2006) by prescribing the tree-ring records of both hemispheres (Reimer et al., 2004; McCormack et al., 2004). Chart from Wanner et al. (2008).

Climate variability can, depending on the observed frequencies of variability, be broken down into (a) periodicities of 400 to ~20 thousand years, closely associated with astronomical forcing, (b) periodicities of 1,500 years and its multiples (i.e. 3,000 years, etc.), related to rapid global cooling events, known as ‘Dansgaard-Oeschger events’ and non-periodical ‘Heinrich events’ and, lastly, (c) shorter decadal or even annual periodicities, attributable to interactions between the atmosphere – biosphere – cryosphere – hydrosphere, such as ‘El Niño’, the North Atlantic Oscillation, the Arctic Oscillation, the Quasi-Biennial Oscillation, etc.

Measurements of solar activity based on sunspot number observations date back to the 17th century and show periodic variations at cycles of 11, 22 and 75 years. Solar activity in the historical and geological past can be reconstructed using such proxies as changes in cosmogenic isotope concentrations (^{10}Be in polar ice cores and ^{14}C in tree rings, where strong production rates of isotopes are associated with lower solar irradiation). Reconstructions of this sort were made by Wanner et al. (2008) for the past 6,000 years and by Vonmoos et al. (2006) for the past 10,000 years. The discrepancies between ^{10}Be and ^{14}C records over the last 6,000 years are visible in Figure 1.3

The scale of solar activity impacts on climate variability is also suggested by the correlation of changes in cosmogenic isotopes with changes in various climate proxies, such as oxygen isotopes (Karlén and Kuylenstierna, 1996; Bond et al., 2001; Fleitmann et al., 2003; Wang et al., 2005). Scafetta and West (2006) calculated that 75% of the global warming during the period 1900-1980 came from solar contribution, a proportion that falls to 30% for the following two decades (1980-2000). Others, like Wanner et al. (2008), are more sceptical both about how to

physically interpret the climatic impact of solar activity and about how marked the effect of solar activity variations may have been on Quaternary climatic change (glacier advances and retreats) and on current global warming (Bard and Frank, 2006), claiming that the effect of solar activity is probably only secondary. It is, in other words, possible that solar activity may contribute to small climatic variations on a timescale of a few centuries (Steinhilber et al., 2009), like the climatic variations that took place over the last millennium, e.g. the medieval climate anomaly (a relatively warm period between 900 and 1400 A.D.) and, the ‘Little Ice Age’ (1500-1800 A.D.). Given the considerable uncertainty within the scientific community as to the impact of solar activity at small timescales, solar activity will not be discussed further in the present study (IPCC, 2007).

1.3 Climate change in the Holocene

The high-resolution study of the climatic evolution over the last 11.5 thousand years (Holocene) is important for estimating the trends, patterns, ranges and rates of change in various climate proxies. The climate regime of the elapsed part of the Holocene is comparable to today’s and provides high-resolution sediment records containing potentially valuable biological and paleoclimatic indicators. The dating of these records can, depending on the case, be achieved quite accurately, using either absolute dating (e.g. radioactive isotopes ^{14}C , ^{210}Pb) or relative dating methods (e.g. tephrostratigraphic markers, sapropel stratigraphy, etc.). The availability of high-resolution records of climate parameters (e.g. temperature, salinity, precipitation) either from instrumental measurements (for the last two centuries) or from sediment records (on a millennial or centennial timescale) point to a strong variability on a decadal and centennial timescale. Meanwhile, adequate instrumental climate measurements are available only for the past 150 years, while the combination of various parameter datasets from tree rings, ice cores, speleothems, historical records, etc. barely covers the last two millennia in the Mediterranean (e.g. Luterbacher et al., 2011).

The present and following two sub-chapters aim to compare the duration, range and rate of past climate change with present-day data, focusing primarily on the Eastern Mediterranean and Greece.

The Holocene, the most recent warm interglacial period, is currently in its final stages. However, a significant number of studies point to substantial climatic variability, in the form of abrupt global cooling events. It is absolutely essential to determine the characteristics (duration, intensity, and rate) of these events, as well as the driving forces behind them, and to compare the findings with respective data for the last millennial-to-centennial timescale. Mayewski et al. (2004) in their extensive review of global Holocene proxy records identify six major periods of rapid climate change, i.e. cooling events within a generally warm period.

The first severe climatic disruption of the Holocene occurred 9-8 thousand years ago. Also called the '8.2 ka event' (Alley et al., 1997), this cooling event coincided with:

- at least one large pulse of glacier meltwater into the North Atlantic (Barber et al., 1999), probably enhancing the production of sea ice, providing a positive feedback on climate cooling;
- a decline in summer insolation;
- no clear evidence of variations in solar activity (^{10}Be remains unchanged in ice cores, while the pronounced depressions in $\Delta^{14}\text{C}$ probably reflect a change in thermohaline circulation because of increased meltwater production) and high rates of SO_4 , suggesting a possible contribution of volcanic eruptions to both cooling in the Northern Hemisphere and aridity in low latitudes (as a result of weakened Afro-Asian monsoons circulation).

The 9-8 ka event was followed by other abrupt climate events that occurred during the time periods 6-5 ka BP, 4.2-3.8 ka BP, 3.5-2.5 ka BP, 1.2-1 ka BP and 600-150 a BP (Mayewski et al., 2004). The climate regime and the driving forces associated with these cooling events are different from the ones of the earlier 9-8 ka BP event, in the sense that these later (post 9-8 ka BP) cooling events provide no evidence of massive freshwater releases or significant ice growth in the Northern Hemisphere. Also, there are no systematic changes in the concentrations of volcanic aerosols and atmospheric CO_2 . Although during 9-8 ka BP event, Northern Hemisphere glaciers still played a significant role in climate change, some of the more recent events seem to be largely determined by solar variability. Cooling at high latitudes in the Northern Hemisphere generally coincides with aridity at low latitudes (Mayewski et al., 2004; Staubwasser and Weiss, 2006), including the Mediterranean. More specifically, the 6-5 ka BP and the 3.5-2.5 ka BP intervals are associated with:

- a decline in solar output, as suggested by the maxima in the ^{10}Be and $\Delta^{14}\text{C}$ records; and
- a steady rise in atmospheric methane concentrations after ~5 ka BP.

The subsequent abrupt climate events of 4.2-3.5 ka BP and 1.2-1 ka BP are more difficult to attribute to specific forcing mechanisms: the 4.2-3.5 ka BP interval, for instance, coincides with a maximum in ^{10}Be , but only little change in $\Delta^{14}\text{C}$ to suggest a solar association. On the other hand, the aridity at low latitudes may be attributable to the southward displacement of the Intertropical Convergence Zone (ITCZ, Hodell et al., 2001), which would be consistent with the strengthening of the westerlies over the North Atlantic. The drought of the 4.2-3.5 ka BP period seems to have been a factor in the collapse of the Akkadian civilisation (deMenocal et al., 2000a). The 1.2-1 ka BP event coincides with a slight increase in atmospheric CO_2 and the drought-related collapse of Maya civilisation (Hodell et al., 2001). Under cooler conditions, tropical aridity may result from a variety of factors, including the weakening of the monsoonal system, reduced evaporation from cooler oceans, and weakened thermal convection over tropical landmasses (Mayewski et al., 2004).

The most recent cooling interval (<600 years BP) is characterised by low temperatures at high latitudes together with increased moisture at low latitudes. It has seen a drop in CO₂ and a rise in CH₄, suggestive of wet conditions. High levels of volcanic aerosols at early stages of this event may have contributed to its onset. Moreover, a distinct peak in ¹⁰Be and Δ¹⁴C (Beer, 2000; Stuiver and Braziunas, 1989; 1993) suggests that solar variability had a major influence on climate during this interval (Bond et al., 2001; Denton and Karlén, 1973; Mayewski et al., 1997; O’ Brien et al., 1995) and may be associated with the solar activity minimum (Spörer Minimum) of the 15th century A.D. A sequence of sunspot minima, such as the Wolf Minimum (1280-1350 A.D.), the Spörer Minimum (1460-1550 A.D.), the Maunder Minimum (1645-1715 A.D.) and the Dalton Minimum (1790-1820 A.D.), can be regarded as representing the cold interval known as the ‘Little Ice Age’, during which volcanic activity is estimated to have contributed to a further drop in temperature (Gao et al., 2008). Between the Oort minimum (1040-1080 A.D.) and the Wolf Minimum (1280-1350 A.D.), there was an interval of nearly 200 years marked by higher solar activity, which coincides with the Medieval Climate Anomaly.

The most important conclusions to be drawn from this brief presentation are that the abrupt climate change events of the Holocene (more frequent from the Middle Holocene onward) were the result of a combination of climate forcing mechanisms and therefore did not take place at the same time or with the same intensity across the globe. Each cooling event is the outcome of a distinct and unique combination of climate forcing mechanisms (Mayewski et al., 2004).

1.4 Past rates of increase in atmospheric temperature and the role of carbon dioxide

Current climate change has been estimated to account for a temperature increase of about 1°C (ground surface temperature) in the last 500 years (Pollack and Smerdon, 2004; Huang et al., 2000) and of 0.76°C in the last 100 years (IPCC, 2007). Temperatures in the second half of the 20th century were, as estimated, very likely to have been higher than during any other 50-year period in the last 500 years, and likely the highest in the past 1,300 years (IPCC, 2007). However, uncertainty remains considerable as to whether the last 100 years have had a higher incidence of climate extremes than the last 400 years, due to the accuracy margin of paleoclimate data derived from paleoclimatic proxy indicators and historical records for the last 400 to 500 years BP, and to the fact that these data are not sufficiently calibrated and bridged with the instrumental records available for the last 150 years (Xoplaki et al., 2005).

Although it is difficult to assign specific numbers to the change and rate of change in global temperatures, given the considerable differences between regions, a number of temperature esti-

Table 1.1**Global temperature change and rate during sub-periods of the present interglacial, along with the respective data sources**

Time period	ΔT ($^{\circ}\text{C}$)	ΔT rate ($^{\circ}\text{C}/\text{years}$)	Source
100 a BP	+ 0.7		IPCC (2007)
500 a BP	+1		Pollack and Smerdon (2004)
18 ka-11 ka BP*		+ 1/100	North Atlantic foraminifera
18 ka-11 ka BP		+ 0.6–0.8/100	Pollen from France
18 ka-11 ka BP		+ 1.7–2/100	Coleoptera from Britain
6 ka BP		+ 0.4/100	
900-1350 A.D. (Middle Ages)	+1		Greenland ice
Cold periods in the 19th century	- 0.6-0.7		Dahl-Jensen et al. (1998)
Cold periods in the 17th century (Little Ice Age)	- 0.5		Dahl-Jensen et al. (1998)
1980-1999 – 2090-2099	+ 1.8-4.0		IPCC (2007) (Meehl and Stocker, 2007) climate projections

* ka: thousand years, BP: before present.

mates have been advanced by the scientific community for different periods of the geological past, quoted below in chronological order and also summarised in Table 1.1.

The global mean surface temperature during the last interglaciation (125-120 thousand years ago, or ka BP), is estimated to have been higher (by 0°C to 4°C , and by 2°C to 3°C for northern Europe) than today (Otto-Bliesner et al., 2006). Temperature variability from the end of the last glaciation (21-18 thousand years ago) to the beginning of the current warm period (11-10 thousand years ago) is estimated to have been in the order of 4°C to 7°C (Jansen et al., 2007). In the course of the current warm period (i.e. the last 11,500 years), estimates show that the mid-Holocene (between 9 and 4 thousand years ago) experienced a warm peak, with temperatures $1\text{-}3^{\circ}\text{C}$ higher than present levels (based on surface and ice-core data, Dahl-Jensen et al., 1998; Masson-Delmotte et al., 2005). As shown by Greenland ice-core data, temperatures during the Medieval Warm Period (900-1350 A.D.) were 1°C higher than in the hundred-year period from 1880 to 1980 (Vinther et al., 2010). All reconstructions indicate that the Middle Ages were warmer and the Renaissance and Enlightenment periods were colder, and that the 20th century presents particularly high rates of temperature increase. It should, at any rate, be noted that the maximum temperatures in the Middle Ages, for instance in Greenland, were close to 1950 A.D. temperature levels (Kobashi et al., 2010).

The rates of temperature increase during the transition from the last glaciation (21-18 thousand years ago) to the beginning of the Holocene warm period (11,500 years ago) have been estimated at around $1^{\circ}\text{C}/100$ years based on data from deep-sea foraminifera in the North

Atlantic (Austin and Kroon, 1996), 0.6-0.8°C/100 years based on the analysis of pollen time series from France (Guiot, 1987) and 1.7-2°C/100 years based on the analysis of coleoptera remains from Britain and France (Atkinson et al., 1987; Ponel and Coope, 1990). Even higher rates of temperature increase have been advanced on the basis of the Greenland ice sheet, with the temperature estimated to have increased by 5-10°C in less than 1,500 years (Severinghaus et al., 1998) and in some extreme estimates even by as much as 5-10°C/100 years (Alley, 2000).

The rate of temperature increase in the Mid-Holocene (6 thousand years ago) is estimated to have reached no more than 0.4°C/100 years at mid-latitudes.

At this stage, it should be noted that, as estimated by the Intergovernmental Panel on Climate Change, the anthropogenic component in the temperature increase over the next 80 years is projected to be between 1.8°C and 4.0°C (IPCC, 2007).

The high temperatures, the glacier retreat and the rise in sea level to higher-than-current levels during the Early- to Mid-Holocene are consistent with higher insolation, which peaked at the beginning of the Holocene (~11 ka BP) and then began to trend downward. Given that current insolation levels are low, one would expect temperatures to be lower and glacier volume to be greater than the observed values. Furthermore, the rates of temperature increase of 0.6-0.8°C and 1°C/100 years mentioned above concern the transition from a glacial to an interglacial period, during which higher rates of increase can be expected, whereas the current rate of increase of 0.76°C/100 years likely corresponds to the final stages of the current interglacial period.

The global warming of the last 150 years has been largely attributed to the increase in anthropogenic greenhouse gas emissions (Hegerl et al., 2011). As for the changes of the last few decades, human forcing, e.g. air pollution, but also natural variability and processes in the atmosphere-hydrosphere system have played their part (IPCC, 2007). As noted by The Geological Society of London in a recent report (November 2010), evidence from the geological record is consistent with the physics that shows that adding large amounts of CO₂ to the atmosphere causes the temperature to rise ('greenhouse effect'), which in turn leads to higher sea levels, changed patterns of rainfall (Alverson et al., 2003), increased acidity of the oceans (Barker and Elderfield, 2002; Caldeira and Wickett, 2003) and decreased oxygen levels in seawater (Keeling et al., 2010).

As shown by the analysis of air bubbles trapped in the Antarctic ice sheet, atmospheric CO₂ concentrations have fluctuated over the last 800 thousand years. Temperature and CO₂ concentration time-series evolved in parallel during earlier glacial-interglacial cycles of the Quaternary, with CO₂ concentrations ranging from 180 to 280 ppm, respectively. However, since the end of the previous glacial period, the increase in CO₂ has been lagging behind the rise in temperature by a few centuries, more likely suggesting that CO₂ is not the only culprit in climate change during this interval. Scientists believe that the continued global cooling from the end of

the Eocene (34 million years ago) to the Holocene is probably associated with a decline in CO₂ values from ~1000 ppm to 180-280 ppm during the Quaternary. CO₂ is currently at 390 ppm, having increased by almost 35% in the last 200 years, with half of this increase having occurred in the last 30 years. As mentioned in the aforementioned report of The Geological Society of London (2010), similar rates of increase in CO₂ have been found for 183 million years ago (Lower Jurassic) and for 55 million years ago (Paleocene-Eocene), although the calculations of the rate of CO₂ increase are fraught with considerable uncertainty (sediment dating, rate of sedimentation, estimates of total CO₂). Similarly high CO₂ levels are estimated to have existed during the Pliocene (at times between 5.2-2.6 million years ago), with CO₂ concentrations in the atmosphere reaching 330-400 ppm. During those times, global temperatures were 2-3°C higher than now (Seki et al., 2010), and the mean sea level was higher than today by 10-25 m.

Evidence preserved in a wide range of geological settings (e.g. ice sheets, marine and lake sediments, speleothems, etc.) has helped to establish that the Earth has undergone a number of warming periods in the past. Each warming event/episode can be explained by, or related to, geological events, such as orbital forcing, the breakdown of methane hydrates beneath the seabed, changes in ocean circulation, variations in volcanic activity, continental displacement and changes in the energy received from the sun. The concern about current global warming (since 1970) stems from the fact that it cannot be related to anything recognisable as having a geological cause, like the events mentioned above. For one, a rise in temperature as a result of internal climate variability (e.g. El Niño) should cause regional rather than global warming (Hegerl et al., 2007). The recent increase in temperature coincides with a sharp increase in anthropogenic CO₂ emissions which, based on geological analogues and physical theory, is likely to raise global temperatures (Solomon et al., 2007). It has been estimated that a doubling of CO₂ concentrations in the atmosphere translates into a temperature increase in the order of 2°C to 4.5°C, with a best estimate of about 3°C (climate sensitivity).

1.5 Paleoclimatic changes in the Eastern Mediterranean during the Holocene

The Mediterranean climate is influenced by the subtropical high pressure system over the arid zones of North Africa's deserts, the westerlies from central and northern Europe, the African and Asian monsoons (Lionello and Galati, 2008), the Siberian High Pressure System, the North Atlantic Oscillation (NAO) and the Southern Oscillation (SO) (Lionello et al. 2006; Xoplaki, 2002). Apart from atmospheric circulation in the Mediterranean, the NAO can also have an impact on river runoff and thermohaline circulation in the region (e.g. Tsimplis et al., 2006). Specifically, according to the patterns of at least the last 500 years (Luterbacher et al., 2006), a negative NAO index is associated with wet (low-pressure anomalies) and usually

cooler conditions in the Mediterranean, whereas a positive NAO index is linked with strong westerlies at high- and mid-latitudes and dry (anticyclonic), warm conditions in the Mediterranean. Heavy rainfall from the African and Asian monsoons contributes to the inflow of freshwater, mostly into the Eastern Mediterranean, from the Nile and other river systems, while precipitation variability is also affected by the El Niño Southern Oscillation (ENSO); Alpert et al. (2006); Brönnimann et al. (2007); Karabörk and Kahya (2009). Thus, the reconstruction of the Mediterranean paleoclimate and interpretation of climatic changes, whether gradual or abrupt, often involve correlating with variations in monsoon intensity, periodicity of the Earth's orbital parameters, solar activity, as well as the North Atlantic Oscillation (NAO).

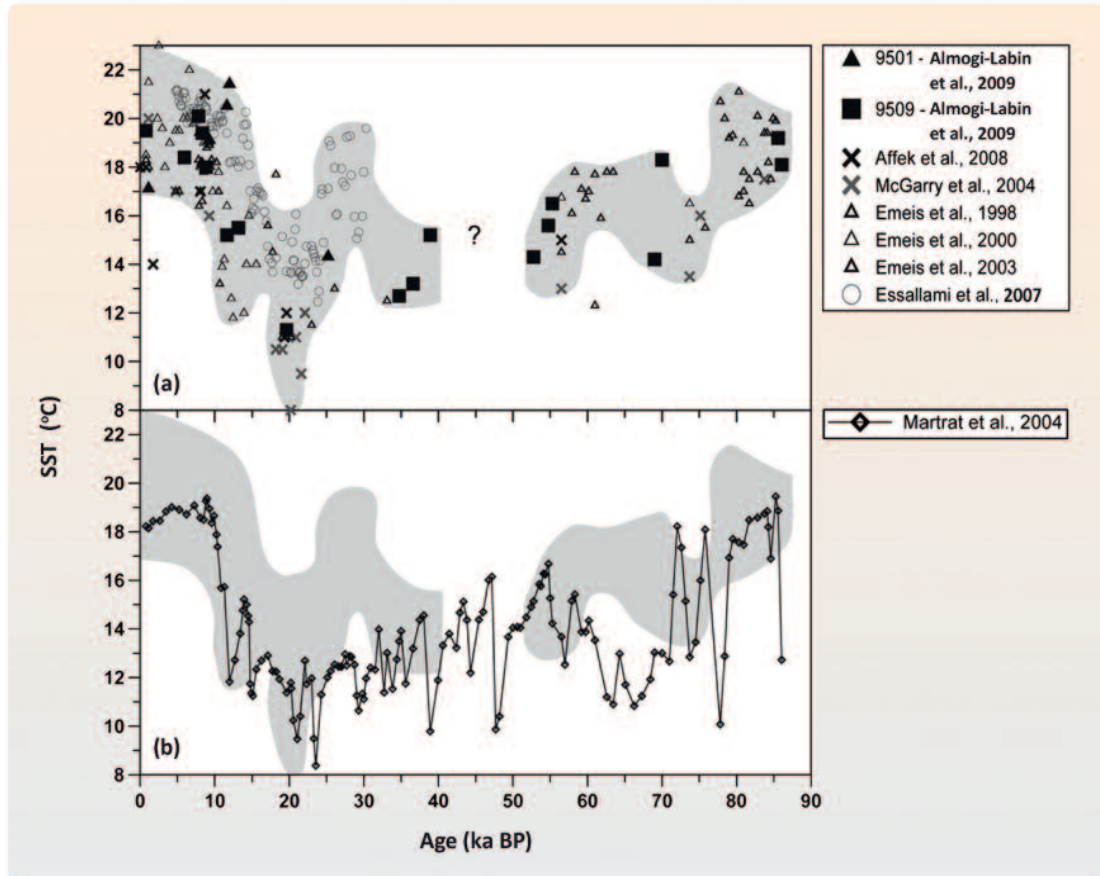
The main physico-geographical factors that determine climatic conditions in the Mediterranean region are atmospheric circulation, latitude, altitude/orography, Atlantic and Mediterranean sea surface temperatures, land-sea interaction (distance from the sea), as well as smaller-scale processes. Oceans have a direct influence on the atmosphere, through the continuous exchange of heat and moisture, and through the significant role they play in the atmosphere's chemical balance. Sea Surface Temperature (SST) is an important geophysical parameter, capable – via the air-sea interaction mechanism – of shaping local weather conditions, but also of affecting the long-term climate (IPCC, 2007).

Both the marine geological record (paleotemperature reconstruction using e.g. foraminifera, coccolithophores, alkenones) on a multi-millennial to centennial timescale and the proxy-based reconstruction of temperature, precipitation and atmospheric pressure for the past 500 years point to the existence of different climatic sub-regions in the Mediterranean, the clearest demarcation being between the Eastern Mediterranean, on one hand, and the Western and Central Mediterranean (Luterbacher and Xoplaki, 2003). Thus, winter air temperature in the Eastern Mediterranean appears to be negatively correlated with the NAO index, in contrast with the Western and Central Mediterranean where there seems to be a small positive correlation. Evidence of these regional differences is also found in the geological record in the paleotemperatures of marine surface waters estimated from long-chain alkenones (i.e. the Uk'37 index) in the coccolithophorid *Emiliana huxleyi* that blooms in spring. According to Emeis et al. (2003), sea surface temperatures over the last 300 ka are estimated to have ranged between 9°C and 21°C in the Western Mediterranean and between 17°C and 25°C in the Eastern Mediterranean. Comparable sea surface temperature data for the past 90 thousand years are graphically represented in Figure 1.4 (Almogi-Labin et al., 2009).

A combined analysis of the fossil coral record from the northernmost Red Sea and of simulations using the coupled atmosphere-ocean climate model ECHO-G reveals an impact of the NAO on both seasonal variability and on inter-annual long-term mean values during the Late Holocene (2.9 ka BP) and the previous interglacial (122 ka BP) in the Eastern Mediterranean and the Middle East (Felis et al., 2004).

Figure 1.4

Sea surface temperatures (SST) derived from alkenones



(a) From the Eastern Mediterranean, (b) from the Western Mediterranean. Figure taken from Almogi-Labin et al. (2009).

Present-day winter conditions in the Aegean are influenced by dry polar/continental northerlies that are orographically channelled through the Axios, Strymon and Evros river valleys, lowering the SSTs to 12-14°C in the Northern Aegean and to 16°C in the Southern Aegean (Theocharis and Georgopoulos, 1993; Poulos et al., 1997). The SST range in the Mediterranean is 3.6°C in spring (from 16.6°C to 20.2°C) and 3.4°C in winter (from 13.9°C to 17.3°C) (Brasseur et al., 1996). The temperature difference between the Western and the Eastern Mediterranean is in the order of 2-3°C (Emeis et al., 2000).

Paleoceanographic data from the Aegean suggests that short cooling events during the Holocene are associated with intense northerly winds superimposed on the tropical/sub-tropical influence on the regional hydrography and ecosystems (Rohling et al., 2002b; Casford et al., 2003; Gogou et al., 2007; Marino, 2008). These findings suggest that the NE Mediterranean climate was more variable during the last climate cycle than generally believed.

After the last glacial maximum (LGM, 21 ka BP) and until 13 ka BP, Mediterranean SSTs averaged 11-15°C based on the alkenone Uk'37 index (Emeis et al., 2000), while the total tem-

perature change during the transition to the ‘warm’ Holocene (11.5 ka BP) is estimated at about 10°C (Emeis et al., 2003). Significant during this period was the brief episode with relatively high SSTs (e.g. 22.9°C in the Northern Aegean; Gogou et al., 2007), between 15 and 13 ka BP and corresponding to the Bølling-Allerød event (Bar-Matthews et al., 1997; Geraga et al., 2000; Sbaffi et al., 2001). Distinct and abrupt cold events, known as the Older and Younger Dryas, then followed between 14.7 and 11.7 ka BP, with SSTs as low as 13-14°C at ca 14 ka BP in the Ionian Basin (Emeis et al., 2000) and 14.5°C in the Northern Aegean (Gogou et al., 2007) and throughout the Mediterranean (Vergnaud-Grazzini et al., 1986; Rossignol-Strick, 1995; Geraga et al., 2000; Sbaffi et al., 2001; Asioli et al., 2001; Aksu et al., 1995; Bar-Matthews et al., 1997; Zachariasse et al., 1997; De Rijk et al., 1999).

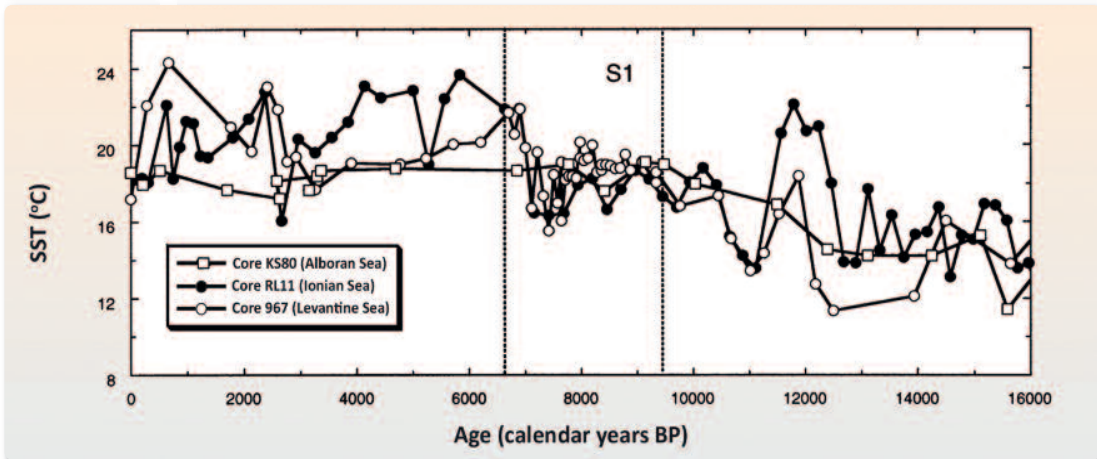
During the early to mid-Holocene, the enhancement of Northern Hemisphere monsoons, resulting from orbitally induced changes in the latitudinal and seasonal distribution of insolation created substantially wetter conditions over much of NE Africa (Jolly et al., 1998). This resulted in a periodic intensification of the African summer monsoon, with increased precipitation along the northern African and the Sahel and possibly an increased discharge of freshwater from the Nile (Rossignol-Strick, 1985; Rohling et al., 2002). At the same time, the northern fringe of the Mediterranean may also have experienced increased precipitation in autumn/winter (Tzedakis, 2007) due to significant regional atmospheric pressure variations (Duplessy et al., 2005). The greater discharge of freshwater into the Eastern Mediterranean affected thermohaline circulation and inhibited deep water formation processes. This resulted in bottom water oxygen depletion and stagnation, which, combined with increased organic material productivity and deposition on the sea floor, led to the formation and preservation of the most recent sapropel,¹ S1 (Rohling and Hilgen, 1991; Rohling, 1994). In the Aegean, sapropel formation began at ca 10-9.6 ka BP (Perissoratis and Piper, 1992; Aksu et al., 1995; Zachariasse et al., 1997; De Rijk et al., 1999; De Lange et al., 2008) and continued until ca 6.5 ka BP, with an interruption between 7.9 and 7.3 ka BP (see e.g. Figure 1.7).

The period preceding sapropel S1 formation, i.e. before 9 ka BP, was characterised by low SSTs. More specifically, the SST has been estimated at 13-14°C in the Ionian Basin at ca 11 ka BP (Emeis et al., 2000), 17°C in the SE Aegean between 10.8 and 9.7 ka BP (Triantaphyllou et al., 2009a, b) and ~16°C in the Northern Aegean at 10.5 ka BP (Gogou et al., 2007) (Figure 1.7). During sapropel S1 formation (9.5-6.6 ka BP), the SST reached 16-19°C in the Eastern, Central and Western Mediterranean (Emeis et al., 2000, Figures 1.5 and 1.6) and 17.5-22.9°C in the Northern Aegean (Gogou et al., 2007, Figure 1.7). A characteristic interruption in sapropel S1 formation is signalled by the global cold event of 8.2 ka BP, with markedly lower SSTs (Ger-

¹ Sapropel is a dark-coloured sediment, rich in organic material and thought to develop during episodes of reduced oxygen availability.

Figure 1.5

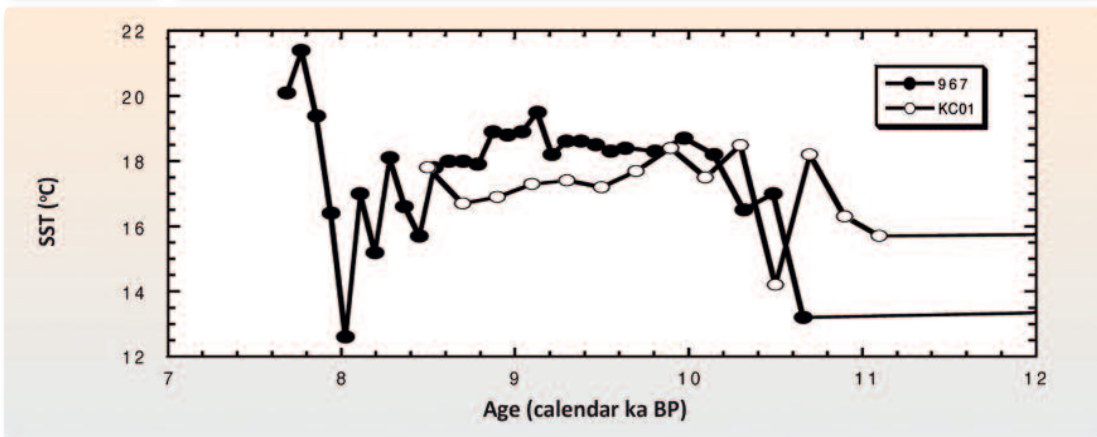
Sea surface temperature (SST) estimates derived from alkenones



Emeis et al. (2000).

Figure 1.6

Sea surface temperatures (SST) derived from alkenones in cores ODP 967 in the Levantine Basin and KC01 in the Ionian Sea



Emeis et al. (1998).

aga et al., 2008) in the Eastern Mediterranean (de Rijk et al., 1999; Geraga et al., 2000; 2005) and arid conditions, as suggested by the sedimentary record of the Aegean sea (e.g. Rohling et al., 2002; Triantaphyllou et al., 2009a, b). This cold dry event has also left archaeological imprints, for instance in Knossos (Crete), where a Neolithic age settlement between ca 9.8-8 ka BP, as confirmed by pottery finds, seems to have been partly abandoned between 9 and 7.5 ka BP (Efstratiou et al., 2004). The absence of material remains from human activity during this period has also been noted in a number of other locations, such as the Cyclops' Cave in the Northern Sporades, the Theopetra Cave (Thessaly), Sidari (Corfu, Berger and Guilaine, 2009) and elsewhere in the Mediterranean.

Table 1.2

Sea surface temperature (SST)* and its rate of change during various time intervals (ka BP) in Greece**

Time period	SST rate of change (°C/yr)	SST (°C)	Region
13 ka	+ 8/1000	from 14 to 22	Ionian Sea (Emeis et al., 2000)
9.8 ka	- 1.6/91		SE Aegean (Triantaphyllou et al., 2009)
9.7 ka	- 2-3/70		SE Aegean (Triantaphyllou et al., 2009)
9.7 ka	+ 3/92		SE Aegean (Triantaphyllou et al., 2009)
8.2 ka	- 2/50		Southern Aegean (Rohling et al., 2007)
2.8 ka	+ 6/~250	from 16 to 22	Ionian Sea (Emeis et al., 2000)
2.9 ka	- 4/~250	from 20 to 16	Ionian Sea (Emeis et al., 2000)
1500-1850 A.D.	- 2		Sicily (Silenzi et al., 2004)
1860-2000, with 1961-1990 as reference period	0.9/90		IPCC (2001)

* Based on alkenones (except for Silenzi et al., 2004, which is based on Vermetidae shells).

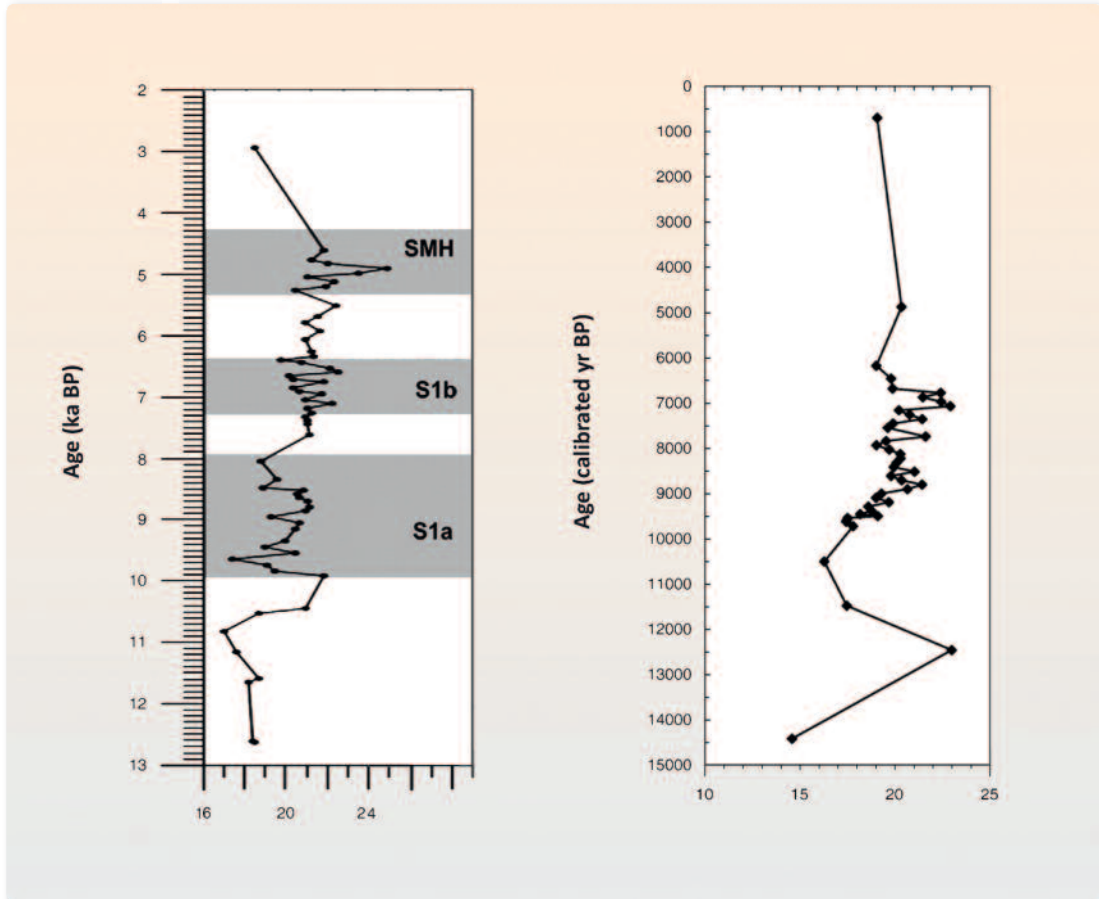
** ka BP: thousand years before present.

Following the S1 sapropel deposition (less than 6.6 ka BP), SSTs ranged around 20°C in the Ionian Sea and Levantine basin, reaching a maximum of 24°C (Emeis et al., 2000) at ca 6 ka BP and averages of 19°C in the Northern Aegean (Gogou et al., 2007), i.e. levels similar to the current annual SST (Worley et al., 2005) at the same location. The Mid-Holocene (4.9 ka BP) saw the highest SST recorded in the SE Aegean, i.e. 25°C (Triantaphyllou et al., 2009).

The abrupt changes in Holocene SSTs in the Eastern Mediterranean are summarised in Table 1.2. Specifically, during the Allerød period (ca 13 ka BP) core RL11 in the Ionian Basin (Emeis et al., 2000) saw a sharp increase in SST from 14 to 22°C in less than 1,000 years, followed during the Younger Dryas by a decrease in SST over the next 1,000 years (Figure 1.5). This variation may be associated with seawater density changes and a shift of intermediate and deep water formation to the Ionian Basin during the Younger Dryas. At 9.8 ka BP, core NS-14 in the SE Aegean (Figure 1.7) saw a decrease of 1.6°C in SST within 91 years, followed at 9.7 ka BP by a rise of 3°C within 92 years. The fact, however, that these high-amplitude and abrupt changes are not observed throughout the Aegean underscores the importance of local hydrologic and bathymetric conditions. Subsequently, during the cold and dry ‘8.2 ka event’ and based on paleotemperature proxies (e.g. oxygen isotopes and foraminifera concentrations), temperatures in the LC21 core in the Southern Aegean dropped by 2°C in roughly 50 years (Rohling et al., 2002a, b), likely associated with fierce NW polar winds prevailing in the area. According to the LC21 record, the decrease in temperature continued for about 150-250 years, while several centuries elapsed before temperatures resumed an upward trend. Rohling and Pälike (2005) note that the 8.2 ka BP cold event was part of a longer anomaly spanning 400-600 years (based for

Figure 1.7

Sea surface temperatures (SST), Uk/'37 Index



Derived from the alkenone Uk/'37 index, (a) in NS-14 core, south of Nissyros (Triantaphyllou et al., 2009), left panel, and (b) in MNB3 core in the Northern Aegean (Gogou et al., 2007), right panel.

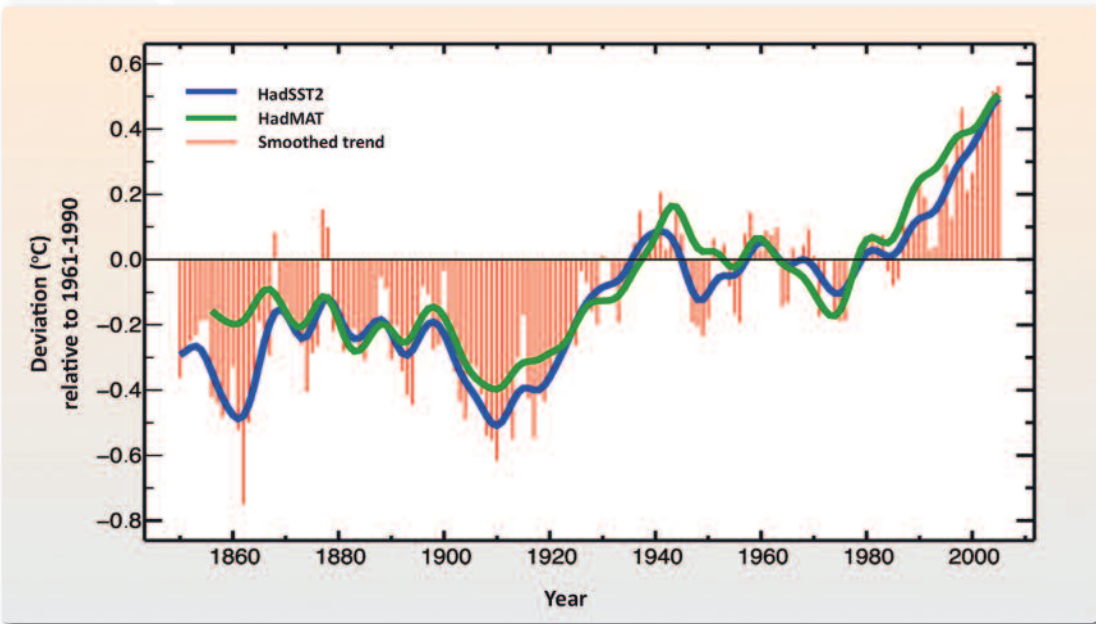
instance on records from Asia), but in Greenland lasted only 150 years (based on temperature records derived from ice cores).

At about 2.9-2.8 ka BP, records from the RL11 sediment core in the Ionian basin (Emeis et al., 2000) indicate that SSTs dropped sharply from 20°C to 16°C, and then rose from 16°C to 22°C in less than 500 years (see Figure 1.5). A decrease in SSTs (from 21-24°C to 18.5°C) is also recorded in the NS14 core in the Southern Aegean (Triantaphyllou et al., 2009a, b) during the same period.

As can be seen in Figure 1.8 representing the annual anomalies of Northern Hemisphere sea surface temperatures relative to the 1961 to 1990 mean, the decadal smoothed annual values indicate a total temperature deviation of about 1.0°C within 150 years. This rate of change does not seem to exceed estimated paleotemperature SST changes (e.g. a drop of 2-3°C in 70 years at 9.7 ka BP, or a rise from 21°C to 23.4°C in 72 years at 5 ka BP, Triantaphyllou et al., 2009a, b), derived from alkenone measurements for specific periods in the Aegean.

Figure 1.8

Annual sea surface temperature (SST) deviations relative to the 1961-1990 reference period in the Northern Hemisphere



Source: IPCC, 2007.

Table 1.3

Total range of change in sea surface temperature (SST) in the Mediterranean during the Holocene (11.5 ka BP until before the industrial revolution)

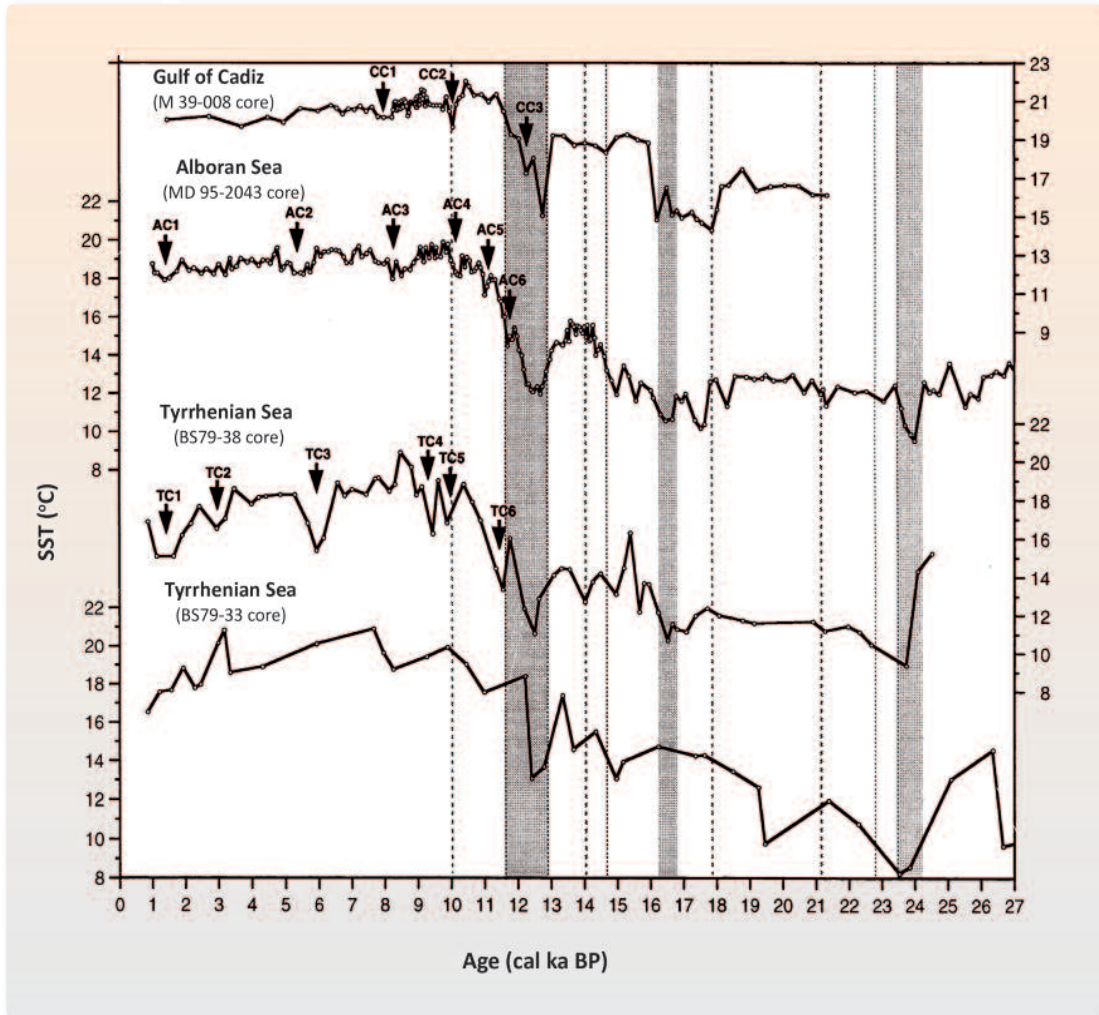
SST variation (°C)	Region	References
2-6	E Mediterranean	Emeis et al. (2000, 2003), Triantaphyllou et al. (2009)
8	N Aegean	Gogou et al. (2007)
4-12	SE Mediterranean, north of the Nile	Castañeda et al. (2010)
4	W Mediterranean	Cacho et al. (2001)
5	Tyrrhenian Sea	Sbaffi et al. (2001)

As shown by the recapitulation in Table 1.3, Holocene climate variations are reflected in SST variations of about 2-6°C in the Eastern Mediterranean (Emeis et al., 2000; 2003; Triantaphyllou et al., 2009a, b), up to 8°C in the Northern Aegean (Gogou et al., 2007), 4-12°C in the SE Mediterranean (north of the Nile; Castañeda et al., 2010), 4°C in the Western Mediterranean (Cacho et al., 2001; Figure 1.9) and about 5°C in the Tyrrhenian Sea (Sbaffi et al., 2001).

There are indications that the periodicity of these changes was 2,300 years for the Aegean Sea (Rohling et al., 2002a, b) and ca 730 years for the Western Mediterranean (Cacho et al., 2001).

Figure 1.9

Sea surface temperatures (SSTs) in the Western and Central Mediterranean



Source: Cacho et al., 2001.

Estimates about the variation in temperature and rainfall during the Holocene have been made possible by analysing the calcite formations (speleothems) of karstic caves in the Eastern Mediterranean for stable oxygen and carbon isotope ratios ($\delta^{18}\text{O}$ and $\delta^{13}\text{C}$). The Soreq Cave in central Israel, situated at an altitude of 400 m and 40-50 m below ground, has been the focus of many paleoclimate investigations, such as the ones by Bar-Matthews et al. (2003) and Bar-Matthews and Ayalon (2005). The analysis of these stable isotope data revealed a similarity in temperature variation between sea surface water (Emeis et al., 2000; McGarry et al., 2004) and atmospheric air, while a reconstruction of precipitation for the past 10 ka showed that there was 50% more rainfall at the beginning of the Holocene than today. The 8.2 ka BP cold event corresponds, at low latitudes, to an arid period within a humid period (i.e. the African humid period of 15-5 ka BP, deMenocal et al., 2000a, b). Maximum rainfall values prevailed until 7 ka BP,

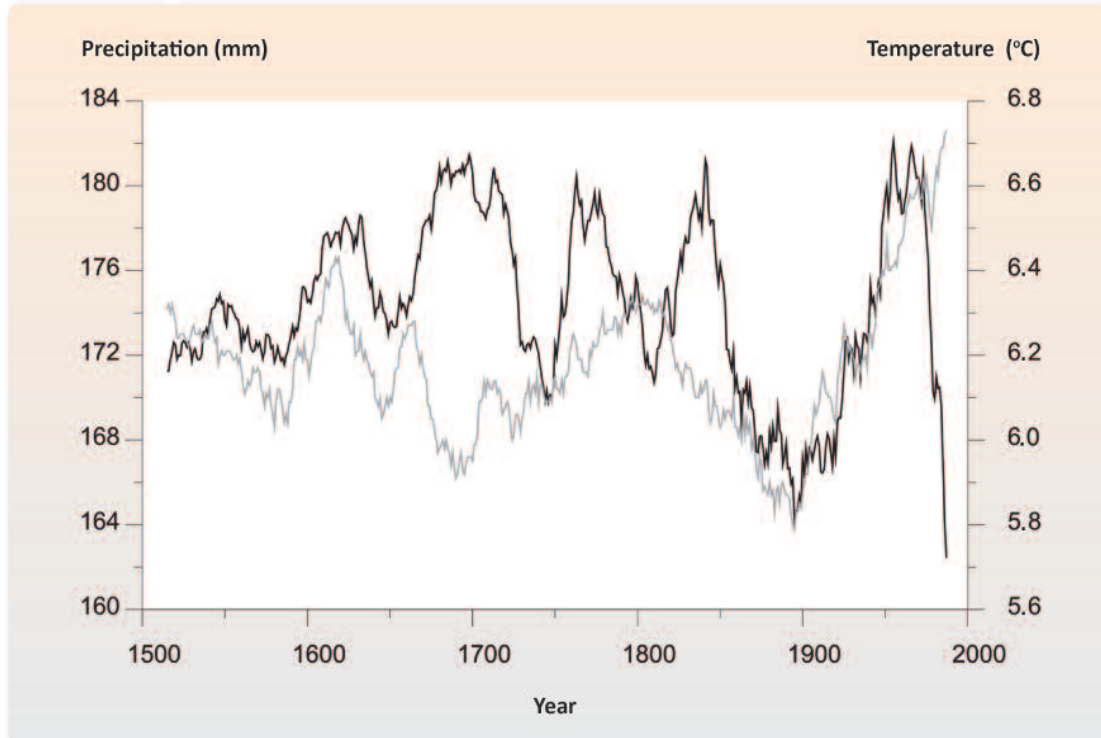
while 6-5 ka BP marks the end of the tropical African humid period (Gasse, 2000; 2001), with evidence of a gradual decrease in precipitation in the Eastern Mediterranean at ca 6.2 to 5.8 ka BP (Bar-Matthews et al., 1997; 2003; Frisia et al., 2006) and increased aridity in the Aegean (Rohling et al., 2002a, b). A period of increased precipitation followed between 5 and 4 ka BP, reflected in a sapropel-like layer, possibly younger than S1, called SMH (sapropel mid Holocene) and found in the Southern Aegean (Triantaphyllou et al., 2009a, b).

Subsequently, between 4.6 and 4.2 ka BP, precipitation levels in northern Italy (Drysdale et al., 2006), the Levant (Bar-Matthews et al., 1997; Enzel et al., 2003) and the northern Red Sea (Arz et al., 2006) decreased significantly from 600 to 400 mm and then remained below current levels for a long period of time. The late Holocene (from 4 ka BP to present) is characterised by a general cooling trend, coupled with progressive aridity (Cacho et al., 2001; Scaffi et al., 2001; Marchal et al., 2002; Rohling et al., 2002a, b). The arid period is in line with the general aridity trend, suggested by theory, for North Africa and the Middle East, more likely driven by earth orbital variations (e.g. precession), (deMenocal et al., 2000a).

1.6 The last millennium

A series of distinct climatic episodes have occurred during the last millennium in the Mediterranean, including the Medieval Warm Period (also known as the Medieval Climate Anomaly, 900-1350 A.D.), the cold Little Ice Age (1500-1850 A.D.) and other cold events of shorter duration. The latter, which comprise the Late Maunder Minimum (LMM, ca 1675-1715 A.D.) and the Spörer Minimum (SM, ca 1460-1550 A.D.), appear to be associated with solar activity minima, although there remains considerable scepticism among the scientific community about long-term solar irradiance changes (Jansen et al., 2007, etc.). Atmospheric circulation during the LMM, for instance, was also affected by volcanic activity, internal climate variability and changes in the North Atlantic Ocean circulation (Luterbacher et al., 2001; Luterbacher and Xoplaki, 2003).

Turning to Greece, documentary data (historical documents, manuscript monastic sources) provide evidence of severe winter extremes during the period 1200-1900 (Repapis et al., 1989). Repapis et al. conclude that the coldest periods occurred in the first half of the 15th century (concurring with the cold period reported by Mayewski et al., 2004), the second half of the 17th century and the mid-19th century. Indices of temperature, precipitation, drought and flooding for Greece and Cyprus during the period 1675-1830 have been reconstructed on a monthly discontinuous basis (Xoplaki et al., 2001). The wettest weather during the Little Ice Age was recorded during the periods 1650-1710 and 1750-1820 (Figure 1.10), while the SST, based on the $\delta^{18}\text{O}$ analysis of vermetid reefs (formed by thermophilic gastropods) in NW Sicily (Silenzi

Figure 1.10**Reconstruction of low-frequency temperature and precipitation variations in winter**

Mean values (for every 31 years) of winter temperatures (grey line) and precipitation (black line) in the Mediterranean during the 1500-2002 period (Luterbacher et al., 2006).

et al., 2004), is estimated to have been $1.99 \pm 0.37^\circ\text{C}$ lower during the Little Ice Age than today. As can be seen from Figure 1.11, the SST based on the reconstruction by Silenzi et al. (2004) was higher in the early 1500s A.D. than today, an observation also corroborated by the SST records from the Bermuda Rise in the Sargasso Sea (Keigwin, 1996).

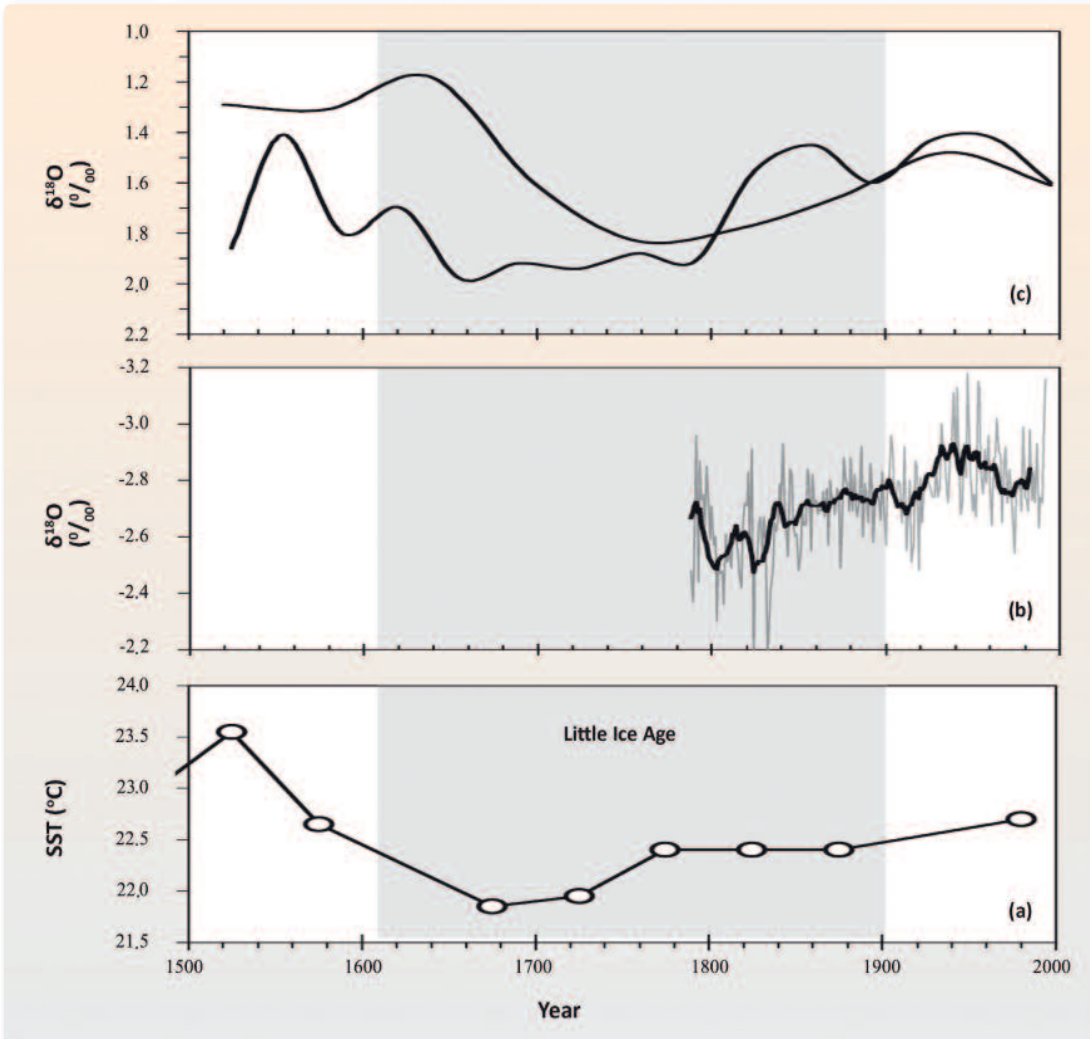
Evidence dating back to the Middle Ages and the beginning of the Little Ice Age in the Eastern Mediterranean has been collected by the University of Thessaloniki, the Patriarchal Institute for Patristic Studies and Utrecht University.

It should be noted that the period between 1500 and 1900 saw intense volcanic activity throughout the Mediterranean, but also across Europe.

Regarding the last few centuries, there is a considerable shortage of high-resolution (annual, seasonal) SST data for the Mediterranean, due to a lack of appropriate indices (such as the coral reef indices available for tropical-subtropical seas). One exception, though, is the annually-banded coral reefs of the Red Sea (Felis and Rambu, 2010). New paleoenvironmental indicators are being sought in vermetid reefs (for the last 500-600 years; 30-50 year resolution; Silenzi et al., 2004; Montagna et al., 2008; 2009; Sisma-Ventura et al., 2009), non-tropical corals (for the last 100-150 years; seasonal to weekly resolution; Montagna et al., 2009) and deep-water corals (similar to non-

Figure 1.11

Comparison of paleotemperature indices



(a) Vermetid $\delta^{18}\text{O}$ records from Sicily (Silenzi et al., 2004), (b) $\delta^{18}\text{O}$ records from the Red Sea, and (c) sea surface temperature (SST) in the Bermuda area, Sargasso Sea (Keigwin, 1996).

tropical corals; Montagna et al., 2006; McCulloch et al., 2010). These new records could complement the paleoclimatic database derived from such key climate indicators as foraminifera, alkenones, dinoflagellates, nannofossils, as well as serpulid overgrowth in submerged speleothems (Antonioli et al., 2001). The above-mentioned marine indicators provide low-resolution information (i.e. 100-200 years between samples), with the exception of areas with a high sediment accumulation rate (>80 cm/ka), such as the Southern Levantine basin, where the time resolution over the last millennium reaches 40-50 years between samples (Schilman et al., 2001). The stable isotope composition of foraminifera in this high-resolution sedimentary record clearly delimits the Medieval Warm Period from the Little Ice Age. Kuniholm and Striker (1987) conducted a large number of dendrochronological investigations, mostly in Greece and Turkey, in

Table 1.4

Published papers on the paleoreconstruction of sea surface temperatures (SST) (Based mostly on the alkenone Uk'/37 index and for the Eastern Mediterranean in particular during the Quaternary)

Core/location	Reference	Location	Paleotemperature index	Age range ka BP
NS-14	Triantaphyllou et al. (2009)	Nissyros (SE Aegean)	alkenones	(3) 4.5-12.7 ka
MNB-3	Gogou et al. (2007)	Skyros (N Aegean)	alkenones	(1.5) 6-10.5(14.5) ka
ODP967D ODP964 KC01/01B	Emeis et al. (1998)	Levantine, Ionian basins	alkenones	7.69 ka-3 ma
KS8230,967,RL11	Emeis et al. (2000)	Alboran, Ionian, Levantine basins	alkenones, planktonic oxygen isotopes	16 ka
M40/87, RL11, 964, M40/71, 969, M40/67, 967	Emeis et al. (2003)	Alboran, Ionian, S Aegean, Levantine basins	alkenones	340 ka
BS7933, BS7938, MD952043, M39008	Cacho et al. (2001)	Tyrrhenean, Alboran Sea, Gulf of Cadiz	alkenones	25 ka
9509, 9501	Almogi-Labin et al. (2009)	N and S Levantine Basins	alkenones	0.240-86 ka
	McGarry et al. (2004)	Peqiin cave, Israel	speleothemes	0-140 ka
GeoB 7702-3	Castaneda et al. (2010)	E Mediterranean, north of the Nile	alkenones and TEX86	27 ka
BS79 38/33/22, MD 95-2043, GISP2, GRIP	Sbaffi et al. (2001)	North of Sicily, Alboran Sea, Greenland	Forams, pteropods, d ¹⁸ O, alkenones	0-34 ka

order to date archaeological sites. The various investigations of tree-ring data from Turkey showed that drought periods typically lasted 1-2 years and rarely more than three. By combining the results of different studies, it appears that 1693, 1735, 1819, 1868, 1878, 1887 and 1893 were the driest years in the Eastern Mediterranean basin (Akkemik and Aras, 2005; Büntgen et al., 2008; 2010; Till and Guiot, 1990; Serre-Bachet et al., 1992; Glueck and Stockton, 2001; Esper et al., 2007; Touchan et al., 2008; 2010; Touchan et al., 2003; 2005; 2007).

The data and characteristics of leading published studies of paleo-sea surface temperature reconstruction in the (Eastern) Mediterranean over the past 340 thousand years, based mostly on the alkenone Uk'/37 index, are recapitulated in Table 1.4.

1.7 A comparison of current climate change to earlier changes in the Earth's history

Comparisons of the relative and absolute changes in SST in the Mediterranean over the last 21 thousand years with current temperature changes (assuming that the current mean SST of the

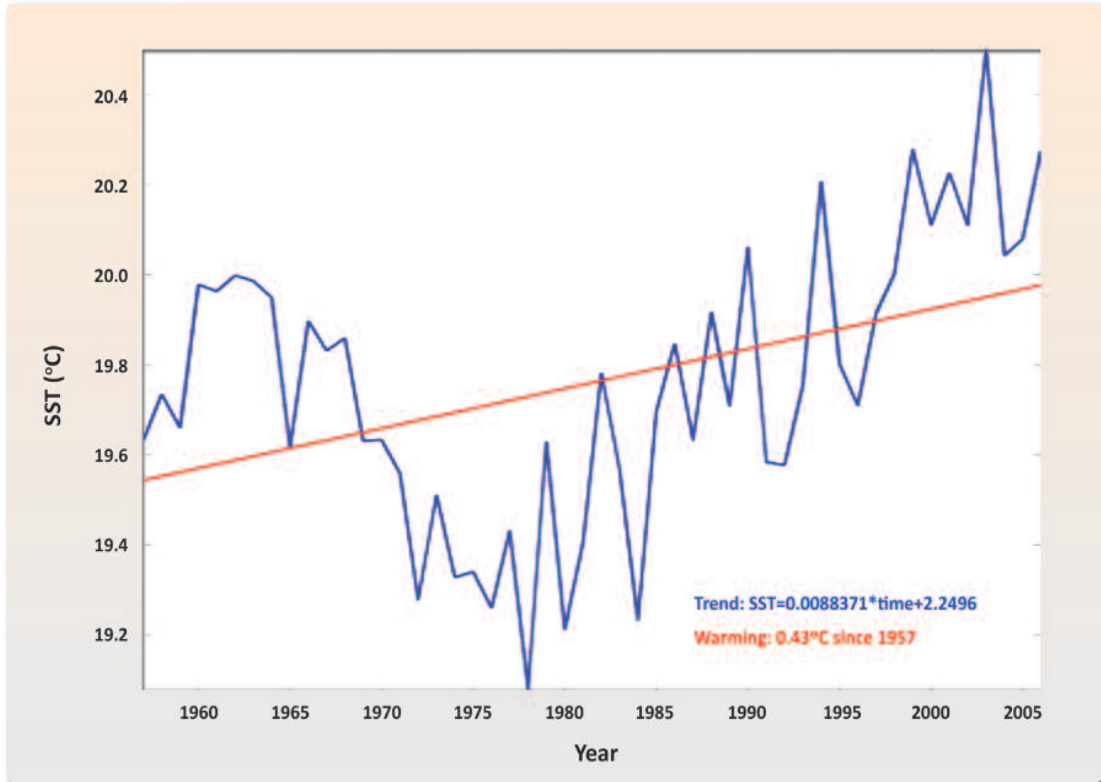
Mediterranean is 19.4°C, within a range of 18.4-20.5°C) reveal that, based on the alkenone Uk'37 index for paleotemperature estimation (considered to reflect spring SSTs), lower but also higher temperatures have been recorded in the recent geological past. More specifically, an SST of 25°C has been estimated for the SE Aegean at 4.9 ka BP (Triantaphyllou et al., 2009a, b), when comparable current spring values for the Southern Aegean are <9°C (Skloris et al., 2010). Similarly, an SST of 24°C has been estimated for the Ionian Basin at 6 ka BP (Emeis et al., 2000), when current mean SSTs for the Ionian Sea are <18°C (Malanotte-Rizzoli et al., 1997). The Northern Aegean is estimated to have had an SST of 22.9°C at 13 ka BP (Gogou et al., 2007), while current spring values are <8°C (Skloris et al., 2010), and the Ionian Basin is estimated to have had an SST of 22°C at ca 1000 A.D. (Emeis et al., 2000), while estimates based on oxygen isotope data from Vermetid reefs show that the SSTs in the Tyrrhenian Sea were higher in the early 1500s A.D. than today (Silenzi et al., 2004).

The mean rate of SST change in the Mediterranean from the early-19th century to 2008 was +0.04°C/decade, but much lower, in the order of +0.01°C/decade, in the Aegean (Axaopoulos and Sofianos, 2009). However, since the mid-1980s, the SST of the Aegean has shown a much stronger rate of increase, in the order of 0.024°C/decade (Axaopoulos and Sofianos, 2009). As discussed in Sub-chapter 1.5, the following rates of SST change (using alkenone-based reconstruction) have been estimated for the Mediterranean during the Holocene (11.5 ka BP): a decrease of 1.6°C in approximately 90 years (at 9.8 ka BP), followed by an increase of 3°C in 92 years (at 9.7 ka BP) (Triantaphyllou et al., 2009a, b) in the SE Aegean; a decrease of 2°C in 50 years in the Southern Aegean at 8.2 ka BP (Rohling et al., 2002a, b); an increase of 2.4°C (from 21°C to 23.4°C) in 72 years at 5 ka BP in the SE Aegean (Triantaphyllou et al., 2009); and an increase from 16°C to 22°C at 2.8 ka BP in the Ionian Sea (Emeis et al., 2000, see Figure 1.5).

As also noted in Sub-chapter 1.5, the annual deviations of mean SSTs in the Northern Hemisphere available for the period 1860-2000 relative to the reference period 1961-1990 (Figure 1.8) recorded a total change of an order of 0.9°C in the course of a 90 year-interval (namely 1910-2000 A.D.), which is less than other changes observed during the last 21 thousand years. However, a more recent record (1957-2006) of mean SSTs for the Mediterranean shows a stronger change in temperature, i.e. of 1.2°C in 28 years (Figure 1.12), which is consistent with the rate of increase of 0.067°C/year derived from satellite measurements for the period 1990-2006 (Del Rio Vera et al., 2006). Unfortunately, the inevitably low time resolution (over the last 21 ka) and poor spatial distribution of available paleoclimatic data do not allow for a more valid comparison of current and past SST variability in the Mediterranean. Based on high-resolution ocean circulation models, it is estimated that that SSTs could increase by 3°C by 2100 (Somot et al., 2006), i.e. at a rate not unheard of in the recent geological past, for instance at 9.7 ka BP in the SE Aegean.

Figure 1.12

Mean annual sea surface temperature (SST) in the Mediterranean during the 1957-2006 period (Based on Hadley climatology, Belkin, 2009)



A comparison of the global warming signal of 0.7°C over the past century (IPCC, 2007) with respective rates of warming during the last 21 thousand years indicates that similar or even greater changes occurred in the recent geological past. However, these earlier cases of warming coincided with glacial-interglacial transitions, during which higher rates of warming are to be expected. The rate of warming during the Mid-Holocene (6-4 ka BP) dropped to $0.4^{\circ}\text{C}/100$ years, i.e. a rate that reflects a period of more stable background climate state, as the climatic transition had essentially been completed. The current rate of warming ($0.7^{\circ}\text{C}/100$ years) therefore exceeds that of the Mid-Holocene, despite the fact that the estimated paleotemperatures are, in absolute terms, $1\text{-}3^{\circ}\text{C}$ higher than today's temperatures.

The difference between current climate change and earlier episodes of climate warming is that the rate of increase is now higher, when our position in the climate cycle is taken into account. It should be noted that the projections of a temperature increase of $1.8\text{-}4.0^{\circ}\text{C}$ over the next 80-90 years (Meehl and Stocker, 2007, IPCC), exceed the average warming rates recorded in paleoclimatic data. The highest estimated rate of warming during the initial stages of the current interglacial reached the extremes of $5\text{-}10^{\circ}\text{C}/100$ years; however, this estimate comes from

Arctic ice core measurements during the transition period from 18 ka BP to 11.5 ka BP, and therefore has limited spatial significance. The paleoclimatic record for the last 500 years in the Mediterranean consists of an instrumental record that goes back 150 years and compilations of proxy data for the period prior to 1860. The inconsistency and lack of homogeneity of this record does not allow safe conclusions, as to the change in frequency of extreme weather events during the past 100 years relative to the previous 400 years.

An overview of the paleoclimate of the last 21 ka in the Mediterranean shows that although all regions usually experienced a similar climate change trend (i.e. warming or cooling), they did not experience the same range or rate of temperature change (Tables 1.2 and 1.3). This is also evidenced by the modern instrumental SST record, which shows that during the recent warming period 1975-1990, the temperature increase was 0.8°C in the Western Mediterranean, 0.6°C in the Ionian Sea and almost nil in the Levantine Sea (Belkin, 2009). This suggests that the anticipated increase in SST based on the respective scenario will vary in intensity and duration across the different sub-basins of the Mediterranean, due to their distinct hydrological, climatic and oceanographic features. For instance, Eastern Mediterranean basin SSTs display stronger seasonal variability, most likely due to the deep water mass temperatures that are consistently lower than those of the other Mediterranean sub-basins (Berman et al., 2003). Moreover, the Eastern Mediterranean is strongly influenced by the Indian Monsoons, whereas the Western Mediterranean is more affected by the North Atlantic climatic variability.

In conclusion, today's rate of warming is indeed high, given the current climate background (phase of the climate cycle), but it remains within the range observed at other times during the past 21 thousand years. The contribution of CO₂ to current global warming seems to be significant, as this increased rate of warming cannot be explained or directly associated with specific geological events, such as changes in the Earth's orbital parameters, breakdown of methane hydrates, ocean circulation changes, volcanic activity, continental drift and changes in solar activity, each one of which has, in the geological past, been a cause of global warming and climate change.

1.8 Greece's present-day climate

1.8.1 Climate type and sub-types

The regions around the Mediterranean basin have a particular type of climate, known as 'Mediterranean', characterised for the most part by mild to cool wet winters and warm to hot dry summers.

Situated at the southern end of the Balkan Peninsula (Aemos Peninsula), Greece has a complex topography which, together with the prevailing weather systems, accounts for a strong spa-

tial variability of climate conditions. As a result, the climate can vary from Mediterranean to alpine within just a few dozen kilometres. Another predominant feature is Greece's extensive coastline, which along with the topography influences a number of local climate characteristics, sometimes causing significant differences from what is considered a typical Mediterranean climate. Three facts worth mentioning at this stage are the average altitude of the Greek mainland (close to 600 m), the gradient in elevation (typically between 100 m and 200 m per km), and – as mentioned – the impressively lengthy total coastline (16,300 km, i.e. more than a third of the Earth's equatorial circumference). Broadly speaking, Greece's climate can, according to Mariolopoulos (1938, 1982), be broken down into four main sub-types:

- i) a maritime Mediterranean climate, with pleasant temperate characteristics, encountered along Greece's western coast and on the Ionian Islands;
- ii) a lowland Mediterranean climate, found in SE Greece, part of Eastern-Central Greece, parts of the Eastern Peloponnese, the islands and coastal areas of the Central Aegean and Crete, with drier summers and colder winters than at respective latitudes around the Ionian Sea;
- iii) a continental Mediterranean climate, over the larger part of Thrace, Macedonia and Epirus and part of Thessaly, with some of the continental climate characteristics typical of Balkan regions further north; and
- iv) a highland Mediterranean climate, encountered in the mountain ranges running through Greece. These mountain ranges include woodlands with a forest climate, as well as small high-altitude areas with an alpine climate during winter.

The islands of the Northern Aegean have a transitional type of climate (continental-to-lowland), whereas the climate of the Dodecanese islands has temperate maritime characteristics.

1.8.2 Seasonal climate characteristics

The weather patterns over the Southern Balkans and the Eastern Mediterranean are affected by high pressure systems (anticyclones) and low pressure systems (depressions) that determine air mass movement. These centres of atmospheric activity, whether permanent or temporary/seasonal, are influenced by local factors and therefore take on characteristics specific to the region they move over and whose climate they in turn also affect.

The atmospheric circulation systems and centres of atmospheric activity that directly affect the winter weather patterns in the region are the Azores High, the Siberian High, and primary and secondary low pressure systems in the Mediterranean. The southward movement of the Azores High enables storm systems from the Atlantic to penetrate over the Mediterranean, while other low pressure systems also form over the Mediterranean as a result of the interaction between a low pressure trough in the upper atmosphere and the topography. The low pressure systems are mostly driven by the polar jet stream, in the upper troposphere, in trajectories

roughly corresponding to the polar front. As the polar front moves south-east in winter, the tracks of the low pressure systems also move south-east, causing the Eastern Mediterranean to become a centre of low pressure activity. This activity results in subtropical air masses moving over Greece and accounts for the mild temperatures and the seasonal rainfall.

The effects that these low pressure systems moving over Greece have on the weather and the climate depend on both the track of these systems and the topography. Because of the presence of mountain ranges in Western Greece, the low pressure systems coming in from the west produce large amounts of rainfall on the windward side of the ranges and lose strength by the time they reach the Aegean; there, they gather strength again and moisture as they rotate over the warm sea, causing new rainfall in Greece's eastern islands and on the Asia Minor coast. The impact of the Siberian High results in very low temperatures and severe winter cold, due to the advection of continental polar air masses into the region. The southward movement of the high pressure systems that form over the North Atlantic and northern Europe and the fact that they can remain stationary for extended periods of time cause very cold, albeit sometimes sunny days.

Spring in Greece is usually short, as winter generally lasts through March, with short frequent cold spells. The onset of summerlike weather is fairly rapid, rainfall declines as the atmospheric stability increases, especially toward end-March. From April onward, the average air temperature increases markedly throughout the country, paving the way to a generally warmer May, the prelude to summer.

Summer sets in during the month of June, with stable, fair and dry weather, abundant sunshine throughout the season and only brief rainy interludes in the form of thermal storms. Low pressure systems are, of course, not non-existent, but they are usually weak. More specifically, although the Balkan Peninsula and Anatolia are both regions where thermal low pressure systems form, the temperature of the sea at this time of the year is generally cooler than the surface temperature of the land it surrounds. As a result, the upward movement of the overheated air, which would normally be conducive to summer rainfall, is inhibited. The summer heat is rather intense throughout the country, with heat waves, known since ancient times, usually associated with atmospheric stability and calm.

In many areas of Greece, the heat, though severe, is tolerable due to the dryness of the air and the cooling effect of sea and land breezes. In Eastern Greece and in the Aegean in particular, the seasonal, but intermittent strong dry winds from the North (known formally as 'Etesians' and colloquially as 'meltemia') temper the heat considerably. In Western Greece, where the humidity is higher and the low-lying inland areas are too far for the sea breezes to cool and where the Etesians are rare, the heat can be unbearable. The temperature in Greece's mountainous areas, on the other hand, is quite tolerable. Summer nights are pleasant, especially in Eastern Greece, owing to the dryness of the atmosphere mentioned previously, the light land

breeze and the more subdued Etesians at night. Summer weather, with its high temperatures, often lasts through September, particularly in the southern regions and on the islands.

Autumn is one of the more pleasant seasons in Greece, especially in the southern regions and on the islands where it can last well into December. The mean temperature is higher in autumn than in spring. The first rains of autumn come around mid-September/early October, when the eastward expansion of the Azores High ceases rather abruptly, and the southward shift of the high pressure zone brings the first incursion of cold air masses. The high pressure systems that form in eastern Europe often around mid-autumn are responsible for the Indian summers with calm fair weather encountered in SE Europe, including Greece.²

1.9 Greece's climatic parameters

1.9.1 Solar radiation

The amount of solar radiation that reaches any given spot on the Earth's surface depends on such factors as location latitude, season, local climate and local topography.

In theory, the geographical distribution of insolation follows the annual cycle of solar declination.³ In the Northern Hemisphere, maximum incident solar radiation occurs at the time of the summer solstice (June 21st), and minimum incident solar radiation at the time of the winter solstice (December 21st).

However, atmospheric factors (such as absolute humidity, cloud cover, suspended particles) can account for considerable deviations from the theoretical values of incident solar radiation. In Athens, for instance, direct solar radiation, i.e. the solar radiation energy to reach the Earth's surface, measured on a surface perpendicular to the sun's beam, is stronger in spring than in summer. The reason for this is simple: despite the fact that the sun is at its maximum altitude in summer, the amounts of water vapour and (because of the etesian winds) dust in the atmosphere, i.e. two factors that absorb and scatter solar radiation, are greater in summer than in spring. The mean annual cycle of global solar radiation in a given region, i.e. the sum of the direct and diffuse radiation it receives, generally follows the annual variation in solar altitude, with maximum values in summer and minimum values in winter. Indicatively, the mean maximum values of global solar radiation for Athens are 200-250 W/m² in winter and 800-850 W/m² in summer, while diffuse radiation averages between 90-100 W/m² in winter and 190-200 W/m² in summer.

² The Indian summer phenomenon is sometimes still referred to in Greece as the 'little summer of St Demetrius' (e.g. Mariolopoulos, 1982; Kotini-Zambaka, 1983). Note: the feast of St Demetrius is celebrated in October.

³ Interestingly, the Greek word for climate ('κλίμα'), derived from the verb 'κλίνειν' (to slope, to incline), denotes the relationship between the angle of the sun's rays and air temperature.

1.9.2 Cloud cover and sunshine

Average annual cloud cover in Greece is greater in the inland regions, where the air masses are forced upward by the orography, causing water vapour convergence and condensation to take place. On average, maximum cloud cover (i.e. the fraction of the sky covered by clouds) is slightly above 50% inland and progressively declines the closer one moves to the coast, where maximum cloud cover falls below 40%. During the course of the year, cloud cover evolves roughly in parallel with rainfall, with maximum values in winter and minimum values in summer. In SE Greece, cloud cover is close to zero.

The number of mostly clear days (cloud cover under 20%) is rather high in all seasons, while the number of overcast days (cloud cover over 80%) is small.

The highest average annual sunshine durations in the country (around 3,000 hours) are recorded in the Southern Aegean, the southern coast of Crete and the Southern Dodecanese, while durations of over 2,800 hours are recorded in the Southern Ionian, the southern coast of the Peloponnese, the Argolis region (Eastern Peloponnese), the Saronic Gulf and the Central Aegean. The number of annual sunshine hours progressively decreases as the distance from the coast increases, with annual sunshine falling to its lowest levels (under 2,300 hours) in the country's north-western mountainous regions. As can be expected, during the course of the year, sunshine duration varies inversely with cloud cover, with maximum sunshine of about 300-400 hours/month recorded in July and minimum sunshine of about 90-100 hours/month in winter.

1.9.3 Air temperature

Air temperature in Greece varies not only with latitude, but also with the topography. Winters are milder in regions where the mountain configuration blocks the inflow of cold winds from the North, and much colder in areas where the geomorphology allows these cold air masses to penetrate. The tempering influence of the sea also accounts for the milder climate (milder winters and cooler summers) of the coastal regions and islands, compared with nearby regions situated inland. The annual isotherms (i.e. the contour lines that connect points of equal mean annual air temperature on a geographic map) run almost parallel to latitude, with the 19°C isotherm following the western coast of the Peloponnese, the 20°C isotherm the SE coast of Crete, and the 15°C isotherm the lowlands of Macedonia and Thrace. The mean annual temperature is about 10°C in the mountains of the Peloponnese and about 5°C in the mountains of Northern and Central Greece. The coastal areas of the Ionian and the islands of the Eastern Aegean enjoy a milder climate than regions in Eastern Greece at similar latitudes, with differences of about 0.5-1.0°C in mean annual temperature, while winters on the western coast are almost 3°C warmer. The winter isotherms again run almost parallel to latitude and temperature differences in various regions are more pronounced than in summer, when the air temperature is regulated by land-sea distribution.

In high summer, i.e. July and August, the daily maximum air temperature ranges between 32°C and 36°C, but can climb above 40°C, as daily absolute maximum temperatures of over 45°C have been recorded in certain areas of Central and Southern Greece. The climate of the Aegean is tempered by the etesian winds and summer sea breezes. In most parts of Greece, minimum air temperatures are recorded between end-January and February, indicating the prevalence of a continental climate and occurring earlier in the inland regions than on the coasts. Daily absolute minimum temperatures of -20°C are not unheard of in certain areas in Northern Macedonia and Northern Thrace, as well as at high altitudes in Central Greece. From March onwards, the air temperature gradually increases, peaking between end-July and August, later along the coast than inland. The temperature slowly begins to drop countrywide by end-September, earlier in the north than in the south.

The mean annual temperature range (the difference between the monthly mean temperature of July or August and the monthly mean temperature of January or February) is more than 20°C in Northern Greece, characteristic of a continental climate, but much smaller in the southern regions. In the southern islands, in fact, it is typically below 15°C. The diurnal air temperature variation in most parts of the country reaches a high in the afternoon, at around 2 pm (a little later in summer, at around 3 pm), and a low at around 7 am in winter (5 am in summer). The mean daily temperature range (the difference between the mean maximum and the mean minimum daily temperature) ranges from 8°C in summer to 4°C in winter.

Northern Greece sees days with total frost, i.e. days when the temperatures never climbs above 0°C, a phenomenon quite rare for Southern Greece, especially the coastal regions and Aegean islands. In fact, not a single day with total frost has ever been recorded in the low-lying areas of Crete since instrumental observations began. Days of partial frost, when the air temperature dips below 0°C at some point during the day, are common in winter and early spring. The air temperature drops by 0.6-0.8°C for every gain of 100 m in altitude. Ground surface temperature, like air temperature, varies on an annual and daily basis, but on a much larger scale, as the ground heats up more than the air in summer and also cools more in winter. Ground temperature variation evens out at greater depths, and at depths exceeding 1 m daily fluctuations are inexistent.

1.9.4 Air humidity

The annual course of absolute air humidity, i.e. the quotient of the mass of water vapour in a given volume of air, expressed by partial water vapour pressure, follows the annual temperature cycle, with maxima in summer and minima in winter. In maritime Mediterranean climates, the absolute humidity maxima and minima, just like the sea-surface temperature, lag slightly behind the corresponding air temperature maxima and minima. The mean annual absolute humidity shows maximum values of 11-12 mm Hg along the coast of Western Greece, and

decreases as one moves inland with minimum values of 8-9 mm Hg; the values then increase again towards the coast of Eastern Greece and on the Aegean islands, but remain lower than in Western Greece. The daily course of absolute air humidity presents a double fluctuation year-round, just as in the case of continental climates.

Relative humidity is expressed in percentage terms as a ratio of water vapour mass in the air to water vapour in the air at saturation (the maximum vapour mass that would be present in the air at a given temperature) or as a percentage ratio of partial water vapour pressure (absolute humidity) to maximum water vapour pressure (at saturation point). The concept of relative humidity is of particular bioclimatic interest, as low relative humidity makes summer heat waves and winter cold more tolerable. Mean annual relative humidity ranges around 60% in Attica-Boeotia and Argolis and around 75% along the coast of Western Greece and the islands. The climate is, generally speaking, more humid in Western Greece than in the SE regions. Relative humidity evolves conversely to air temperature on both an annual and a daily basis, as relative humidity is, by definition, inversely proportional to maximum water vapour pressure, which depends on air temperature. Mean relative humidity shows a simple annual variability pattern throughout Greece, with a maximum in December and a minimum in July-August. The annual range in atmospheric water vapour content is greater in continental Greece and Crete than that of temperate climates, approaching the typical range for continental climates; the annual range for Western Greece is somewhere between that of continental and marine climates, while the range for the coastal regions of the Peloponnese and Crete and the islands is close to that of maritime climates. Similarly, mean atmospheric relative humidity presents a simple daily variation, conversely to temperature variation, with a maximum near sunrise, between 4 am (in summer) and 7 am (in winter), and a minimum – almost always – at 2 pm.

1.9.5 Precipitation

Rainfall and air temperature are major determinants of regional climate. As already mentioned, the topography of Greece plays an important part in the shaping of its climate, especially with regard to the amount of rainfall. Greece's geographic position, the fact that the country is on most sides surrounded by sea, together with the presence of high mountains and mountain ranges spanning in different directions make for considerable regional differences in rainfall distribution and levels. The rainfall pattern typical of Mediterranean coastal areas is, of course, predominant, with dry spells in summer and a rainy season from mid-autumn to mid-spring. Rainfall distribution throughout the year tends to be more even in Northern Greece. Mean annual precipitation for Greece as a whole is roughly estimated at 800 mm, but the geographical distribution of the annual amount of precipitation and of the yearly rainy season generally follows Greece's geomorphology. As in the Iberian and the Italian peninsulas, annual precipitation in Greece generally declines from west to east and from north to south. The warm, moist,

rain-producing air masses of depressions moving in from the west, and the warm moist air masses coming in from the south butt up against almost perpendicular mountain ranges (the bulk of Greece's mountain ranges run north-south). These air masses, thus uplifted, subsequently cool and release most of their moisture on the windward side. Once over the mountain ridges, the air masses descend and heat by compression, producing some rainfall on the leeward side (rain shadow).

The mean annual precipitation received by Greece's mountain ranges is as follows: >2,200 mm in the Pindos range (continental Greece); 1,800 mm in Crete's White Mountains (Lefka Ori); and 1,600 mm in the mountains of the Peloponnese. The lowest amounts of annual precipitation, i.e. <400 mm, are recorded in the Saronic Gulf, Argolis (Eastern Peloponnese) and the islands of the Southern Aegean. Mean annual precipitation reaches 1,000-1,400 mm in the Ionian Islands, 1,000-1,200 mm on the western coast of Epirus, and increases progressively with the gain in altitude up to 2,000 m, but then decreases sharply on the leeward eastern slopes of the mountains and on the Greek peninsula's eastern side. Annual precipitation increases again somewhat, further east, in Euboia and the Northern Sporades Islands, and in the mountains of Macedonia and Thessaly, but once again decreases over the Aegean coast. Finally, annual precipitation increases over the islands and coast of Asia Minor. In Greece's NE regions, Eastern Macedonia and Thrace, annual precipitation increases as the distance from the coast increases, reaching its highest level in the region's northern mountains. Similarly, in Crete, annual precipitation declines from west to east, with levels of almost 800 mm recorded in the NW and of below 500 mm in the SE.

The temporal distribution of annual precipitation is fairly even in the cold months of the year, although precipitation levels increase from autumn to winter and decrease towards spring. In summer, the scarce rainfall events to interrupt the protracted dry spell are usually brief local thermal thunderstorms, which, without major differences between west and east, can produce substantial amounts of rain within just a few hours. In most parts of Greece, the summer drought begins in May, as the depressions over the Eastern Mediterranean become less frequent. The duration of the drought increases from north to south, from 2 months (July-August) in Northern Epirus, Macedonia and Thrace to as many as 4-5 months in the country's SE regions. The annual pattern of precipitation can present particularities in terms of maxima and minima depending on proximity to the sea, altitude, latitude, etc., without ever deviating too much from the typical characteristics of a Mediterranean climate, i.e. a cool wet winter and an arid summer. July and August are the driest months. The first autumn rains usually come in September, first at the higher altitudes, and later (October) in the lowland regions and the Aegean islands. The highest monthly rainfall is, on average, recorded in November and especially December. Annual precipitation levels can vary considerably from year to year, while consecutive years of dry or wet weather are also recorded. Annual precipitation in Athens has, for instance, ranged

from minimums of 115.7 mm (1898), 150.6 mm (1989), 199.3 mm (1990) and 206.2 mm (1891) to maximums of 987.3 mm (2002), 846.4 mm (1883), 713.0 mm (1885), 612.0 mm (1955) and 601.9 mm (1910). It should be noted that, based on the observations of the National Observatory of Athens, the mean annual precipitation of Athens during the period 1891-2010 was close to 400 mm.

The spatial distribution of the annual number of rainy days is similar to the spatial distribution of precipitation amounts. More specifically, the annual number of rainy days exceeds 110 days in the western coastal regions, increases farther inland, peaks in the central mountain ranges, and then decreases towards the Aegean coast, before increasing again in the coastal regions of Asia Minor. The smallest annual number of rainy days (below 80) is observed in the same region as the smallest amount of annual rainfall, i.e. in certain Cyclades islands and in the region of Argolis and the Saronic Gulf.

The amount of 24-hour precipitation and rainfall intensity, i.e. the amount of rain divided by its duration, are important data to be taken into consideration, especially at the designing and construction phases of public works. 24-hour precipitation levels in excess of 150 mm are not unheard of, even in regions with low annual precipitation: Athens has had 24-hour precipitation as high as 150.8 mm (16 November 1899) and 160 mm (2 November 1977), when the mean daily precipitation in November for Athens is 1.9 mm and total annual precipitation is roughly 400 mm. 24-hour precipitation and rainfall intensity have the same geographical and seasonal distribution as annual precipitation. Mean annual rainfall intensity declines from west to east and from north to south. Rainfall intensity in most parts of Greece is highest in October and November.

The meteorological conditions that favour thunderstorm development are similar to the ones that generate rainfall, except that there also has to be a high degree of atmospheric instability. Thunderstorms occurring in the Mediterranean are generally the result of an incursion of cold polar air masses (cold fronts), particularly in the autumn when the sea is relatively warm, and in areas where warm, moist, tropical air masses converge (warm fronts). The orography plays an important role, as the uplifted air masses subsequently cool and their water vapour content condenses. In Greece, autumn and winter storms are generally more common in the coastal regions, as the sea is warmer than the atmosphere. What are known as thermal thunderstorms take place in summer in the continental regions, as a result of the very high ground surface temperatures and the conditions that favour instability in the free atmosphere. Such instability is, on the contrary, negligible in the coastal regions, as the sea is cooler than the land.

1.9.6 Winds

As already mentioned, the Mediterranean winter is determined by high pressure systems over Eurasia and the North Atlantic. These systems steer respectively cold dry or warm moist

air masses towards the Mediterranean, thereby creating centres of cyclogenesis or rejuvenation of low-pressure systems. This explains why winter winds are so variable in direction and intensity. The same conditions roughly prevail in autumn and spring. The predominant wind from autumn to spring is a south-southwesterly wind, known today as *livas*.⁴ Caused by high pressure systems from the Atlantic and North Africa, this wind carries warm moist air masses and is associated with depressions in the Mediterranean. When forced by the topography over a mountain range, it becomes katabatic on the leeward side, warms up and moves further away from saturation, thus giving rise to warm dry winds with Foehn characteristics, particularly warm and dry in summer. The combination of a high pressure system over the Balkans and a low pressure system over the Aegean gives rise to the cold northerly wind, Vardar, in the Axios valley. As mentioned previously, winter is sometimes marked by an incursion of very cold air masses from the North.

Whereas the wind systems prevailing in winter are complex and variable, the winds prevailing in summer, known as “Etesians” (“meltemia”) , are predominantly northerly (north-westerly in the Ionian and Greece’s western coast, north-easterly in the Northern Aegean, becoming northerly in the Central and Southern Aegean). The intensity of the Etesians in the boundary layer of the atmosphere (from surface to 800-1,000 m) usually peaks at midday, when the mixing of upper and lower atmospheric layers reaches a maximum; these winds then subside, sometimes almost entirely, at night. Because of the lesser friction, the winds are generally stronger over sea expanses. Typically of moderate intensity (4-5B, 8-9 m/sec), the Etesians can easily gain strength over open seas (6-7B, 10-15 m/sec or more) and occasionally reach gale force (over 9B, >20 m/sec). The Etesians reach their highest intensity and frequency in July-August, particularly in certain channels of the Aegean, such as the one between the islands of Naxos and Paros (Repapis et al., 1977). On summer days without Etesians, the air in the inland areas is quite still, with light mountain and valley breezes, while the coastal areas and the islands enjoy sea breezes at daytime, alternating with land breezes at night. The velocity of sea breezes is of the order of 5-6 m/sec, while the velocity of land breezes is much lower.

1.9.7 Evaporation, dew, frost, fog, snow and hail

Evaporation, i.e. the amount of surface water that evaporates into the air, depends on a combination of factors: firstly, the water temperature, but also on air temperature and humidity, as well as the wind. Evaporation in Greece broadly follows the annual and daily air temperature range, with lower rates recorded in the west and north and higher rates in the south and east. Average annual evaporation amounts to roughly 1,650 mm in Athens and 1,350 mm in Thessaloniki.

⁴ Formerly the $\Lambda\iota\psi$ of the ancient Greeks.

Dew, i.e. the condensation of water vapour on exposed surfaces in the form of liquid droplets, is recorded almost year-round in most parts of Greece, with maximum occurrence in winter and minimum occurrence in summer.

Frost, i.e. the condensation of water vapour on exposed surfaces in the form of tiny ice crystals, is less frequent than dew and recorded only in the cold season, when ground surface temperature is below 0°C.

Fog, i.e. the low-lying cloud caused by the cooling and condensation of moisture contained in the adjacent to the ground surface air layer of a moist and warmer than the ground air mass. Fog forms as a result of the advection of warm, humid air masses over a cold ground surface or as a result of ground surface cooling – through radiation – during cold, fair nights. More days with fog are observed in Northern Greece than in the southern regions.

Snowfall increases from south to north, from coast to inland and from low-lying to high-lying regions. The occasional incursion in winter of north-easterly cold air masses associated with the Siberian High is another cause of snowfall, mainly in Eastern Greece. The snow season can last from end-September to end-May in the mountainous regions of Northern Greece, but is far shorter – starting later and ending earlier – in the southern regions and along the coast. Snow accounts for 0 to 20% of Greece's total annual precipitation.

Hail, i.e. the precipitation in the form of spherical or irregular pellets of ice that falls during thunderstorms, is an important climate phenomenon, because of the potentially substantial damage to agriculture. The annual number of days with hail decreases from west to east, but then increases again close to the Asia Minor coast. During the cold season, hail is more common on the coast than it is further inland, mainly due to frontal storms. Conversely, hail occurrence in the warm season increases inland on account of thermal thunderstorms.

1.10 The climatic characteristics of Greece's marine regions

The warm Asia Minor current that enters the Aegean Sea from the East, after flowing northward along the Eastern Mediterranean coast, and the colder current that enters the Northern Aegean from the Black Sea through the narrow strait of the Dardanelles and then flows southward along the western coast of the Aegean explain why the sea surface temperatures (SSTs) of the Aegean are slightly colder along the western coast than along the eastern coast (Metaxas, 1973). SSTs are generally highest in August and lowest in February and, as is well established, lag behind the air temperatures over land, due to the seas' high heat capacity, while the mean annual SST is higher than the mean annual marine air temperature (MAT). From September through March the mean monthly SST is higher than the mean monthly MAT (in the Northern and Central Aegean by as much as ~3°C in January-February), whereas from

April through August the mean monthly SST is lower than the mean monthly MAT (in the Central Aegean by $\sim 2^{\circ}\text{C}$ in July). In the Northern Aegean, the SST reaches a maximum of $\sim 24^{\circ}\text{C}$ in August and a minimum of 12.5°C in February, when the respective MAT values are 24.5°C and 9.5°C . In the Central Aegean, the maximum (minimum) SST is 25.0°C in August (14.5°C in February), when the corresponding maximum (minimum) MAT is 26.0°C in July (12.0°C in January). In the Southern Aegean, the maximum (minimum) mean monthly SST is 25.0°C in August (15.5°C in February), when the corresponding maximum (minimum) MAT is 26.0°C in August (14.0°C in February). In the Ionian Sea, the maximum (minimum) SST is 25.5°C (15.0°C), whereas the maximum (minimum) MAT is 26.0°C (13.5°C). In the cold season, the SST of the Southern Aegean is somewhat higher than that of the Ionian, while the opposite is the case in summer. During the months of July and August, the prevailing Etesian winds cause cooler water at greater depths to rise to the sea surface (upwelling) in the Eastern Aegean. The highest mean annual SST in Greece is recorded in the region of Rhodes ($\sim 20^{\circ}\text{C}$), while the lowest mean annual SST is recorded in the wider area of Alexandroupolis ($\sim 15.5^{\circ}\text{C}$). The lowest mean monthly SST in Greece is recorded in the NE Aegean, just outside the Dardanelles ($\sim 11^{\circ}\text{C}$ in February), while the highest mean monthly SST is recorded in the Southern Ionian ($\sim 26^{\circ}\text{C}$, in August).

Mean annual sea surface evaporation is estimated at $\sim 2,000$ mm on the eastern coast of the Aegean, at $\sim 1,800$ mm in the Southern Aegean, and at $\sim 1,600$ mm along the coasts of the Ionian and south of Crete. In both the Aegean and the Ionian seas, sea surface evaporation is generally more pronounced in the northern than in the southern parts, due to the prevalence of northern winds. All year round, the isoevaporation lines run almost parallel to the axis of the Aegean. The highest estimated daily values of ~ 7 mm/day are recorded on the eastern coast in January (where northern winds prevail and the sea-air temperature difference is greatest along the eastern coast of the Central Aegean), as well as in July-August, when strong Etesian winds prevail. The lowest estimated daily values of sea surface evaporation, under 3 mm/day, are recorded in May, due to the weak speed of winds (Metaxas and Repapis, 1977).

1.11 Urban climate and bioclimatic indexes

The settlement of human populations inevitably brings about changes to the environment. Human activity affects atmospheric conditions in three ways: i) by modifying land surface characteristics and land use (urbanisation, deforestation, draining e.g. of wetlands and swamps, etc.); ii) by releasing energy into the atmosphere (industries, heating, electric lighting, etc.); and iii) by loading the air with gaseous and particulate pollutants. Man's impact on the atmosphere is most evident in big cities, as *urbanisation* results in a significant alteration

of the urbanised environment's climate parameters. The quality of urban air, as opposed to that of rural air, is further degraded by the presence of various pollutants. Apart from the adverse effects that air pollutants and suspended particulates have on health, they also reduce visibility. This often results in the formation of a "microclimate", or "urban climate", the characteristics of which, especially as far as air quality is concerned, largely depend on the city's size, population, percentage of built-up areas and green spaces, building materials, paved surfaces, energy source use and industrial activity. The influence of all of these factors, conducive to what is known as "urbanisation-induced warming", is particularly evident in terms of the air temperature, as the energy emitted by urban human activity contributes to an increase in air temperature. The presence of buildings, pavements and roads also alters the radiation balance, as these elements absorb and re-emit heat differently than a rural environment would. The air is thus warmer on average in cities than in non-urbanised environments, with the size of the deviation basically increasing with urban population size. This phenomenon is known as the "urban heat island" effect.

Athens is a typical metropolitan area, with a high building density in the central districts and a lower building density in the suburbs (urban fringe). According to Eurostat data, the larger urban zone of Athens is among the eight most populated areas in the European Union, with a population of over 4,000,000 since 2004, i.e. nearly one third of the country's population (Note: the true figures for the population of Athens are in fact higher, given that illegal immigrants have not been taken into consideration). Despite decentralisation efforts made in the 1980s, most of the country's administrative, commercial, economic, social and cultural activities remain concentrated in Athens. Rapid population growth and the pursuit of a better quality of life have been the main drivers of urban sprawl, towards areas with more green space, associated with a higher quality of living index (Stathopoulou and Cartalis, 2006). During the period 1990-2000 alone, urbanised areas in Athens increased by 4.6% (Stathopoulou et al., 2009). This, of course, is not only a Greek phenomenon. According to a report by the European Environment Agency, during the ten year period 1990-2000 the growth of urban areas and associated infrastructure throughout Europe consumed more than 8,000 km², equivalent to complete coverage of the entire territory of Luxembourg or Crete. By 2020, approximately 80% of Europeans will be living in urban areas, while in some countries the proportion will be 90% or more. Greece's growth model has led to a distorted overcrowding of both people and activities in five major areas: the wider urban areas of Athens (with Piraeus), Thessaloniki, Patras and Herakleion and the zone between the two cities of Volos and Larissa. In the specific case of Athens, the transfer of the main airport to Spata (some 20 kms east of Athens) and the construction of high-speed motorways have in the past few years accelerated the relocation of Athenians to the city fringe, mostly to the north-east and south-east. As a result, former resort/secondary residence areas have evolved into primary residence areas and have undergone a considerable

growth in urban activity. Today, the predominant trend sees immigrants moving into the run-down neighbourhoods of central Athens and Piraeus, while veteran city dwellers move out, in pursuit of a better living environment in the burgeoning suburbs to the north and east. It should also be noted that this urban sprawl has been accompanied by considerable illegal construction activity, across all classes of society. With the continuous expansion of the urban fabric, motorways and paving, the urban environment encroaches ever increasingly upon the natural environment. This only exacerbates the urban heat island effect, as well as the changes to the climatic conditions in the area.

As mentioned earlier, the urban heat island effect is primarily due to the different thermal properties of commonly used urban building materials, as opposed to those of the natural environment (Park, 1986). Asphalt and cement, for instance, have different thermal and reflective properties than the natural environment. These materials alter the energy balance, as they absorb solar radiation, instead of reflecting it, thereby causing an increase in temperature. The lack of trees and natural vegetation in urban regions also affects the energy balance, as it inhibits evapotranspiration and the associated cooling effect provided. Moreover, air pollution, altered wind patterns (low winds), waste heat and the geometry of a city further intensify the urban heat island effect (Hassid et al., 2000; Santamouris et al., 2001; Livada et al., 2002; Mihalakakou et al., 2004). The urban heat island effect is seen during both the warm and the cold season (Santamouris et al., 2001), but is much higher in intensity (expressed as the difference in maximum air temperature between urban and rural areas) in the summer, when it approaches 10°C in the day and 5°C at night. The lack of urban green areas seems to be a key culprit in the development of the urban heat island effect in Athens, given that the phenomenon is considerably mitigated in areas of the city with tall, dense vegetation, such as the National Gardens at the heart of the city (Livada et al., 2002). The cooling effect of this public park vanishes within just a few metres, on the adjacent avenues with their dense traffic (Zoulia et al., 2008).

As a result of the urban layout, the traffic load, waste heat and the overall balance of each area, the temperature difference between the National Gardens and other parts of the city can range between 0°C and 13°C during the day (mean temperature difference between ~7 °C and 8°C). The smallest temperature difference is recorded with the central pedestrian zone on Ermou Street, as opposed to other parts of the city, such as Ippokratous Street. During the day the temperature is generally much higher in the city centre than in the suburbs (roughly 7-8°C higher). However, in areas with a high traffic load such as Ippokratous Street (where a monitoring station is located), the temperature difference can reach as much as 12-13°C. The increases in temperature in the Athens are not consistent throughout the different districts, but depend on the heat load.

Human health and well-being are directly dependent upon the weather and climate, in particular on such factors as air temperature and humidity, sunshine, wind and atmospheric pres-

sure. According to many climatologists, a comfortable climate (for humans) corresponds to a temperature range of 18-22°C, with a relative humidity of 30-60% and mild winds up to 2 m/sec. A number of bioclimatic indexes have been devised to quantify human discomfort due to various climate parameters, starting with Thom's very simple 'Discomfort Index', first proposed in 1959, that provides a combined index of the air temperature and relative humidity, to the far more elaborate 'Physiological Equivalent Temperature' (PET), an indicator of thermal comfort based on meteorological parameters, but also on the energy balance of the human body. An analysis of PET index values for Greece showed that winter afternoons in the low-lying regions and the islands were perceived as thermally neutral, i.e. comfortable (18-23°C), whereas in the highland regions the bioclimatic conditions were perceived as cold (4-8°C). In contrast, on July and August afternoons, the thermal environment was perceived as hot (35-41°C) in the low-lying regions, but as slightly warm (23-29°C) in the islands and highlands. According to climate model forecasts, bioclimatic conditions in Greece are expected to change substantially. Especially in the summer, the PET value for the period 2071-2100, compared with the reference period 1961-1990, is likely to move up three levels on the physiological stress scale in the southern regions and two levels in the northern regions. During the remainder of the year, the PET value is likely to move up one to two levels on the physiological stress scale (Matzarakis and Nastos, 2011). In addition, an analysis of the projected changes in the 'humidex' discomfort index showed a significant increase in the future in the number of days with index values of over 38°C (Sub-chapter 1.16, Figure 1.39).

1.12 Sources and emissions of air pollutants in Greece over the period 1990-2008

The deterioration in urban air quality as a result of human activity warrants particular interest. Air pollution can be defined as the perturbation of the atmosphere's natural chemical composition, due to increased concentrations of some of its components and/or to the introduction of additional substances, mainly of anthropogenic origin. Almost all megacities have some degree of air pollution, due to the activities of their populations (industry, traffic, energy and heat production, etc.; Gurjar et al., 2007), with pollutants classified as primary or secondary. Primary air pollutants are emitted directly into the atmosphere from the pollutant source and can include soot, sulphur dioxide, carbon monoxide, nitrogen oxides, hydrocarbons and other organic gases, lead oxides and various suspended particles of organic and inorganic compounds of anthropogenic or natural origin. Secondary air pollutants are not directly emitted as such, but form when primary pollutants react in the atmosphere (physico-chemical transformation), especially in areas and time periods with abundant sunshine. One such secondary pollutant is tro-

Table 1.5

Emissions of the most significant primary pollutants in Greece in kilotonnes (kt) and statistical data on the share (%) of Greece in total European emissions, as well as per capita emissions in kilograms per year in Greece

Pollutant	1990 emissions (kt)	2008 emissions (kt)	Percentage change	Ranking in EU-27 in 2008	Percentage share in total emissions in EU-27	Kg per inhabitant (2000-2008)	Source
NO _x	296.0	356.9	20.6	7	3.5	31.8	EEA
SO ₂	493.0	447.6	-9.2	7	7.6	39.9	EEA
NM ₁₀ VOC	255.0	218.0	-14.3	8	2.6	19.5	EEA
CO	1,281.3	685.0	-46.5	8	3.0	61.0	EMEP, EEA
NH ₃	79.0	63.1	-20.1	14	1.7	5.6	EEA
PM _{2.5}	49.3*	62.81	22.0	-	-	-	EMEP
PM ₁₀	26.1*	37.2	31.0	-	-	-	EMEP

EEA: European Environmental Agency, <http://www.eea.europa.eu/>

EMEP: European Monitoring and Evaluation Programme, <http://www.emep.int/>

* Emissions since 2000.

ospheric ozone. Immediately below is a brief outline of the prevalent primary air pollutants encountered in Greece (see also Table 1.5).

Nitrogen oxides – NO_x

Nitrogen oxides play an important role in atmospheric chemistry, particularly in the formation and destruction of tropospheric ozone. Two of the most prevalent oxides of nitrogen – nitrogen oxide, NO, and nitrogen dioxide, NO₂ – are essentially formed from the breakdown of nitrogen gas and its reaction with oxygen during combustion processes.

Certain nitrogen oxides, for instance NO₂, are particularly toxic. Short-term exposure to concentrations of less than 3 ppm can cause irritation to the respiratory tract, while concentrations of over 3 ppm may lead to pulmonary dysfunction. Prolonged exposure to low concentrations can affect lung tissue, causing emphysema. Certain groups, such as asthmatics and young children, are particularly vulnerable to the effects of nitrogen oxides. Nitrogen oxides also contribute to the formation of fine suspended particles and to ozone production, which costs billions of dollars on a global scale in terms of morbidity and mortality.

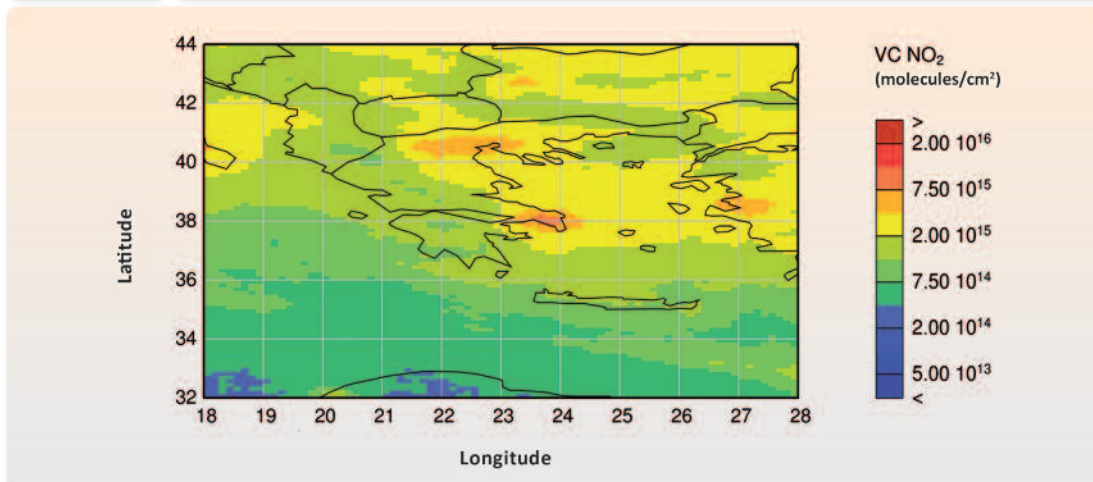
The main sources of NO_x emissions in Greece are energy production (fossil fuel combustion) which accounts for 59% of the total, road transport (29%) and other types of transportation (11%).⁵ As can be seen in Figure 1.13,⁶ the highest NO₂ emission levels are recorded in the

⁵ <http://www.eea.europa.eu/> (see file: greece-air-pollutant-emissions-country-factsheet.pdf, 2008)

⁶ <http://www.doas-bremen.de/>

Figure 1.13

Tropospheric column density of NO₂ over Greece in the 2003-2009 period, based on satellite observations from SCIAMACHY spectrometer



In the colour range, blue represents the lowest values of NO₂ and red the highest.

Attica Basin and in Central/Western Macedonia (Thessaloniki/Ptolemais), i.e. regions with intense anthropogenic activity.⁷

From 1990 to 2008, total NO_x emissions in Greece increased by 21%, putting Greece in the 7th position among the EU-27.⁸ It should be stressed that Greece is one of the few countries whose NO_x emissions increased, whereas emissions in the EU-27 as a whole decreased by 31%.⁹ For the period 2000-2008, NO_x emissions in Greece were estimated to have risen by 0.9 kg/capita to reach 31.8 kg/capita.

Sulphur dioxide – SO₂

Sulphur dioxide is released into the atmosphere mostly from anthropogenic activities, although one-fourth of total emissions come from natural sources, such as volcanic activity. The presence of SO₂ in the atmosphere is important to monitor because of the compound's high water solubility. When combining with water, sulphur dioxide forms sulphuric acid (H₂SO₄), a constituent of acid rain, the deposition of which has adverse effects on ecosystems. Sulphur dioxide is an oxidising agent that can cause pulmonary dysfunction, especially in asthmatics. It poses an even greater health risk when combined with increased concentrations of particulate matter and other gaseous pollutants.

⁷ <http://prtr.ec.europa.eu/>

⁸ The EU-27 consists of Austria, Belgium, Bulgaria, Cyprus, Czech Republic, Denmark, Estonia, Finland, France, Germany, Greece, Hungary, Ireland, Italy, Latvia, Lithuania, Luxemburg, Malta, Netherlands, Poland, Portugal, Romania, Slovakia, Slovenia, Spain, Sweden and United Kingdom.

⁹ <http://www.eea.europa.eu/> (file: greece-air-pollutant-emissions-country-factsheet.pdf, 2008)

Energy production, mainly from fossil fuel combustion, is the predominant source of SO₂ emissions in Greece (93%), with the rest coming from non-road transport and industrial processes.¹⁰ From 1990 to 2008, total SO₂ emissions in Greece declined by 9%, which, however, was far less than the average reduction (66%) achieved by the EU-27. With annual emissions of 448 kilotonnes in 2008, Greece ranked 7th among the EU-27.¹¹ Another fact worth noting is that Greece accounts for roughly 8% of total EU-27 SO₂ emissions. Lastly, in 2008 SO₂ emissions were estimated at 39.9 kg per capita.

Non-methane volatile organic compounds – NMVOC

Volatile organic compounds (VOCs), together with nitrogen oxides, are precursors of tropospheric ozone, high concentrations of which cause toxic photochemical smog with adverse effects on vegetation and human health (Williams, 2004). In addition, volatile hydrocarbons also have a significant effect on the oxidative capacity of the atmosphere (Vrekoussis et al., 2004; Monks, 2005), i.e. the atmosphere's ability to convert various gases and to cleanse itself of air pollutants. Lastly, VOCs are primary precursors for the formation of particulate matter in the atmosphere, as well as of cloud condensation nuclei (CCN) (Roberts et al., 2002).

VOCs are emitted into the atmosphere from anthropogenic and natural processes (Vrekoussis et al., 2009; 2010). The production of fossil fuels, the use of solvents and biomass burning are the main anthropogenic sources, while the main biologically generated source of VOC is isoprene, a compound released by plants. The sources of NMVOC in Greece can be divided into four categories: energy production and consumption (26%), road transport (23%), industrial processes (25%), while the remaining 25% comes from a number of other sources (farming, solvent use and waste management).¹²

Over the period 1990-2008, the EU-27 was able to reduce NMVOC emissions by a substantial 41%, while Greece, with a contribution of 2.6% to total EU-27 NMVOC emissions, reduced its emissions by 14%. The 218 kilotonnes of NMVOC emitted in Greece correspond to emissions of 19.5 kg per capita.¹³

Carbon monoxide – CO

Carbon monoxide, produced from the incomplete combustion of carbon-containing substances, is toxic to humans because it acts as an antagonist to haemoglobin, i.e. the protein in the bloodstream that transfers oxygen from the lungs to the rest of the body. It is present in the natural environment in very low concentrations of 100 ppbv (part per billion per volume). Emis-

¹⁰ [http://www.eea.europa.eu/ \(file: greece-air-pollutant-emissions-country-factsheet.pdf, 2008\)](http://www.eea.europa.eu/ (file: greece-air-pollutant-emissions-country-factsheet.pdf, 2008)

¹¹ [http://www.eea.europa.eu/ \(file: greece-air-pollutant-emissions-country-factsheet.pdf, 2008\)](http://www.eea.europa.eu/ (file: greece-air-pollutant-emissions-country-factsheet.pdf, 2008)

¹² [http://www.eea.europa.eu/ \(file: greece-air-pollutant-emissions-country-factsheet.pdf, 2008\)](http://www.eea.europa.eu/ (file: greece-air-pollutant-emissions-country-factsheet.pdf, 2008)

¹³ [http://www.eea.europa.eu/ \(file: greece-air-pollutant-emissions-country-factsheet.pdf, 2008\)](http://www.eea.europa.eu/ (file: greece-air-pollutant-emissions-country-factsheet.pdf, 2008)

sions from natural sources, such as volcanoes and wildfires, are relatively low compared with emission levels in urban centres. CO concentrations in urban areas, typically at 10 ppmv (parts per million per volume), are 100 times higher than in non-urban areas.

Most CO emissions in the EU-27 come from road transport, followed by household activities and industrial processes.¹⁴ Between the years 1990 and 2008, CO emissions in Greece were reduced by a substantial 47% (from 1,302 kilotonnes in 1990 to 685 kilotonnes in 2008), with per capita emissions (2000-2008) estimated at roughly 61 kg. Greece accounts for some 3% of total CO emissions in the EU-27.¹⁵

Ammonia – NH₃

Ammonia has recently become the focus of much debate because of the effects that the deposition of atmospheric nitrogen can have on ecosystems, thereby leading to eutrophication and increased acidity. Ammonia is also associated with the formation of secondary particulate matter with adverse effects on human health and the climate. Agriculture remains the major source of ammonia emissions in Greece (96%), with the remaining 4% associated with road transport. Between the years 1990 and 2008, ammonia emissions in Greece were reduced by 20%, with emissions in 2008 estimated at 5.6 kg per capita. Greece accounts for 1.7% of all NH₃ emissions in the EU-27.¹⁶

Particulate matter – PM

Particulate matter (PM) is a collective term used to describe solid or liquid particles suspended in the atmosphere, such as dust, pollen, soot, smoke, liquid droplets. Distinctions are made between coarse particulate matter (PM₁₀) which is less than 10 microns in diameter and fine particulate matter (PM_{2.5}) which is less than 2.5 microns in diameter, including ultrafine particulate matter (PM₁) which is less than 1 micron in diameter. Long-term exposure to high PM concentrations, especially fine particles, can cause severe respiratory and cardiovascular disorders.¹⁷

Primary particulate matter arises from both anthropogenic activity (agriculture, industry, fossil fuel combustion) and natural processes (windblown dust, wildfires and volcanoes). Secondary particulate matter comes from the oxidation of precursor gaseous compounds, such as nitrogen oxides, sulphur oxides, ammonia and VOCs. In the specific case of Greece, secondary particulate matter stemming mainly from NO_x and SO₂ account for the bulk of airborne particulate matter.¹⁸ Their main sources in 2007 were industrial processes, road transport and energy

¹⁴ [http://www.eea.europa.eu/ \(file: LRTAP1990-2008.pdf\)](http://www.eea.europa.eu/ (file: LRTAP1990-2008.pdf))

¹⁵ [http://www.eea.europa.eu/ \(file: LRTAP1990-2008.pdf\)](http://www.eea.europa.eu/ (file: LRTAP1990-2008.pdf))

¹⁶ [http://www.eea.europa.eu/ \(file: greece-air-pollutant-emissions-country-factsheet.pdf, 2008\)](http://www.eea.europa.eu/ (file: greece-air-pollutant-emissions-country-factsheet.pdf, 2008))

¹⁷ <http://www.who.int/en/>

¹⁸ <http://www.ekpaa.greekregistry.eu/>

production industries. Between the years 2000 and 2008, PM emissions in Greece increased both for fine particulate matter (PM_{2.5}) and coarse particulate matter (PM₁₀), by 22% and 31%, respectively.¹⁹ In contrast, EU-27 emissions decreased by ~10% in both PM categories over the same period.²⁰

1.13 Climate change trends in Greece

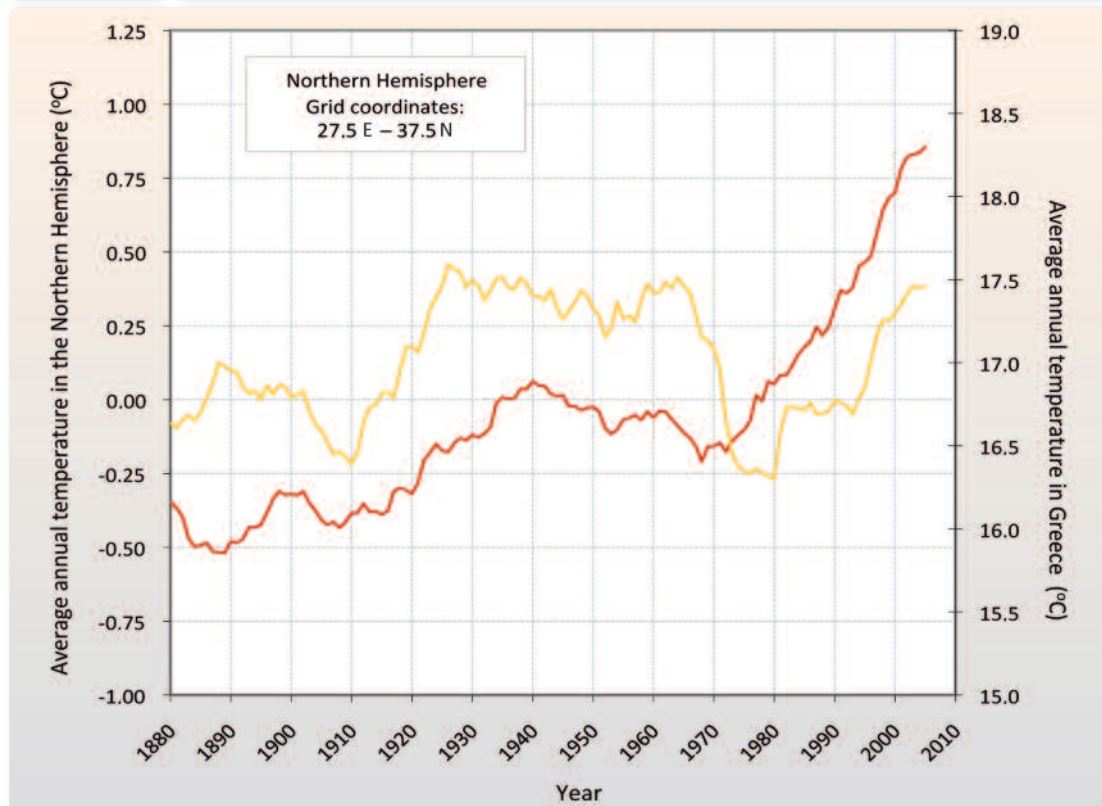
From the late 19th century to the 1970s, the mean air temperature time series for the Eastern Mediterranean and Greece has been consistent with the upward trend recorded for the Northern Hemisphere – NH (Repapis and Philandras, 1988; see also Figures 1.14 and 1.15). However, the cooling recorded in the NH in the period 1940-1970 was more pronounced in the

¹⁹ <http://www.emep.int/>

²⁰ <http://www.eea.europa.eu/> (file: LRTAP1990-2008.pdf)

Figure 1.14

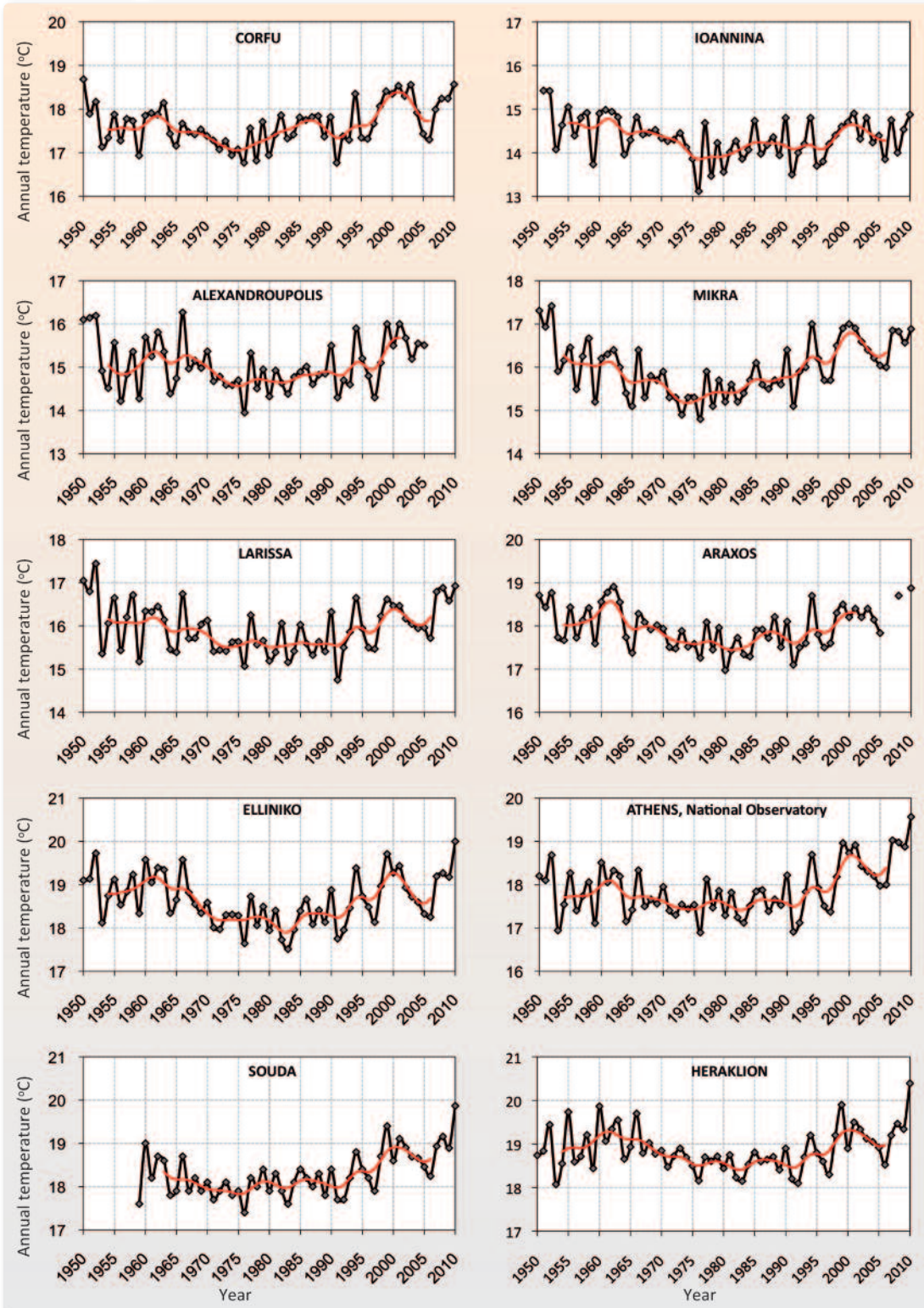
Mean annual temperature time series, 1880-2000
(Values smoothed with 10-year moving average)



(a) in the Northern Hemisphere (red line), and (b) in the grid box which includes Greece (yellow line).

Figure 1.15

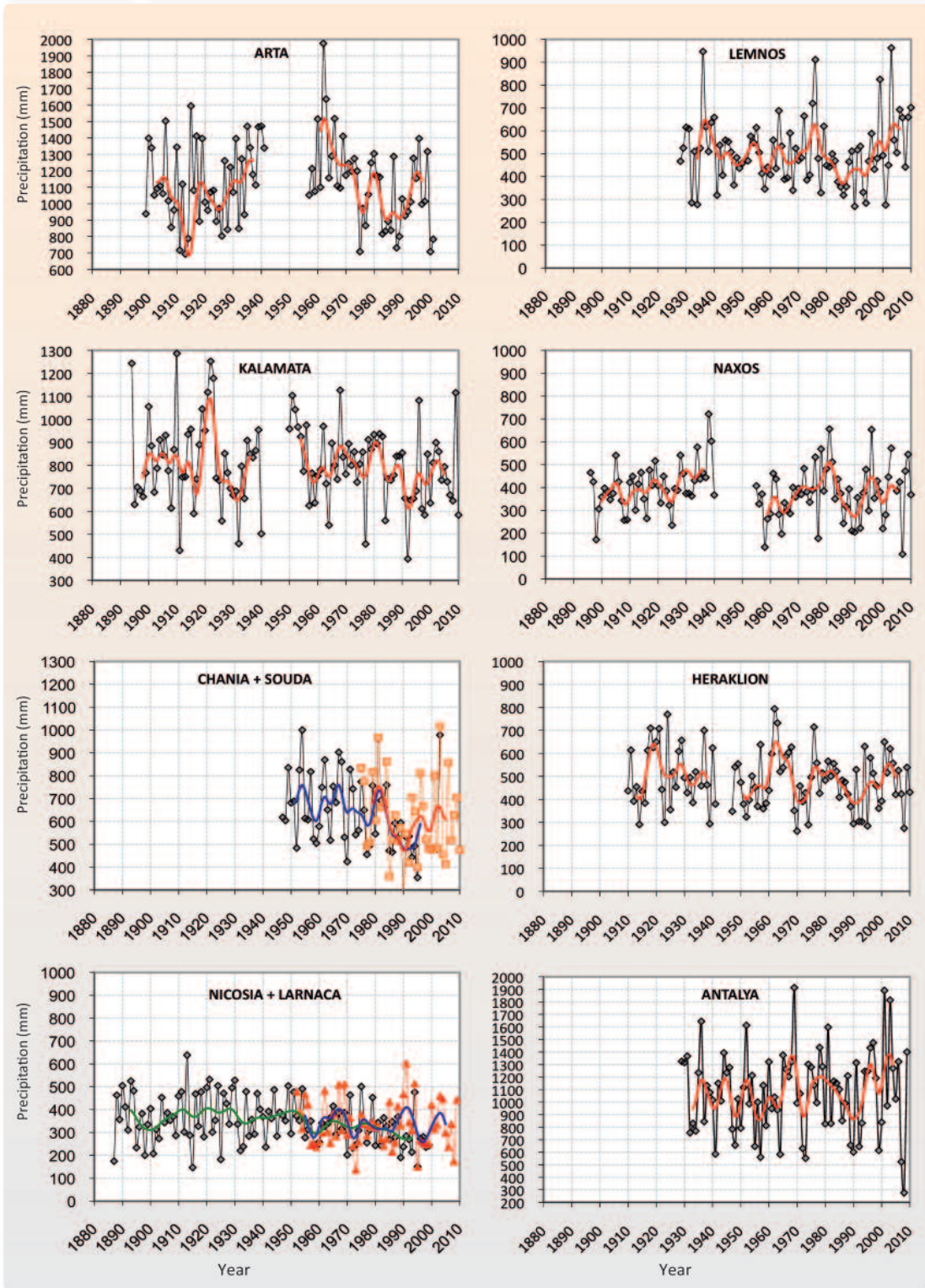
Mean annual air temperature time series observed at selected Greek stations (1950-2010)



The red line represents values smoothed with Gaussian 9.

Figure 1.16

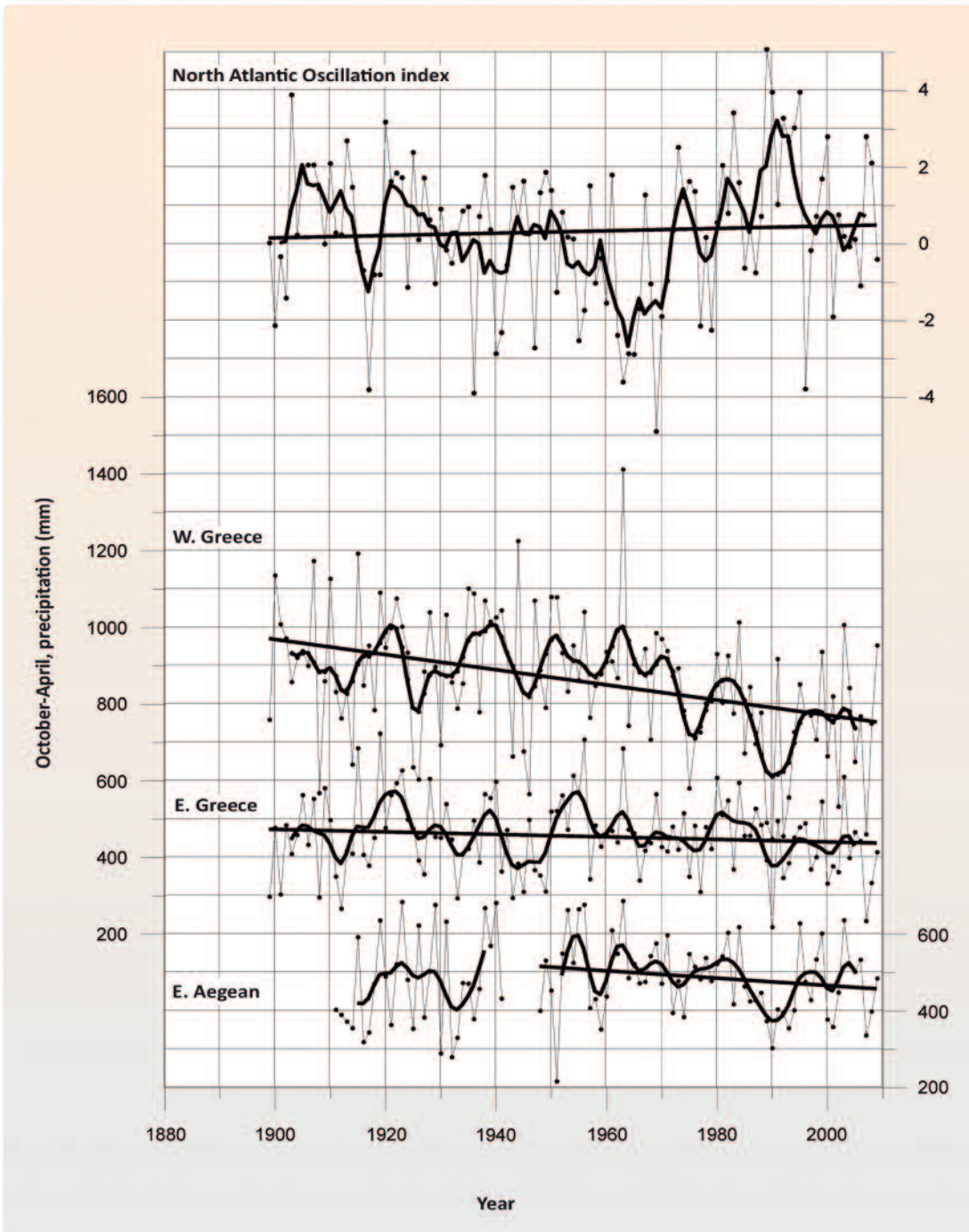
Time series of precipitation at selected stations in Greece, Cyprus (Nicosia) and Turkey (Antalya)



The orange time series for Chania and the red time series for Nicosia were completed with data from adjacent stations (Souda and Larnaca, respectively). Smooth lines were created using Gaussian filter with $\sigma=9$.

Figure 1.17

North Atlantic Oscillation (NAO) index time series and April-October precipitation (rainy season) time series in Western Greece, Eastern Greece and the Eastern Aegean Islands



The bold curves represent values smoothed with Gaussian 9. The straight lines show regressions.

Eastern Mediterranean: thus, whereas mean temperatures in the NH soon rebounded and from the early 1980s exceeded the values of the previous 100 years, in the Eastern Mediterranean

they only began to rise again in the 1980s and 1990s (Repapis et al, 2002; Saaroni et al., 2003; Feidas et al., 2004; Repapis et al., 2007).

In terms of precipitation levels, a clear positive trend in annual precipitation was recorded for northern Europe, with the exception of Finland, in contrast with a clear negative trend recorded for southern Europe and the Mediterranean (ECSN, 1995; IPCC, 1996; 2001). Rainfall in the Eastern Mediterranean decreased, with sizeable differences across regions and intense variability from year to year, depending on the topography and the tracks of passing low pressure systems. As far as Greece is concerned, most regions experienced a negative trend in rainfall in the second half of the 20th century, statistically significant in some regions (Kandyliis et al., 1989; Mantis et al., 1997; Hatzioannou et al., 1998; Paz et al., 1998; Maheras et al., 2004; Xoplaki et al., 2004; Feidas et al., 2007; Zanis et al., 2009).

In Greece, the negative trend in annual rainfall in the course of the 20th century ranges from 20% in Western Greece to 10% in Eastern Greece, and can be attributed partly to the trend observed in the North Atlantic Oscillation (see Figures 1.16 and 1.17; Zerefos et al., 2010).

1.14 Climatic trends in the Athens region

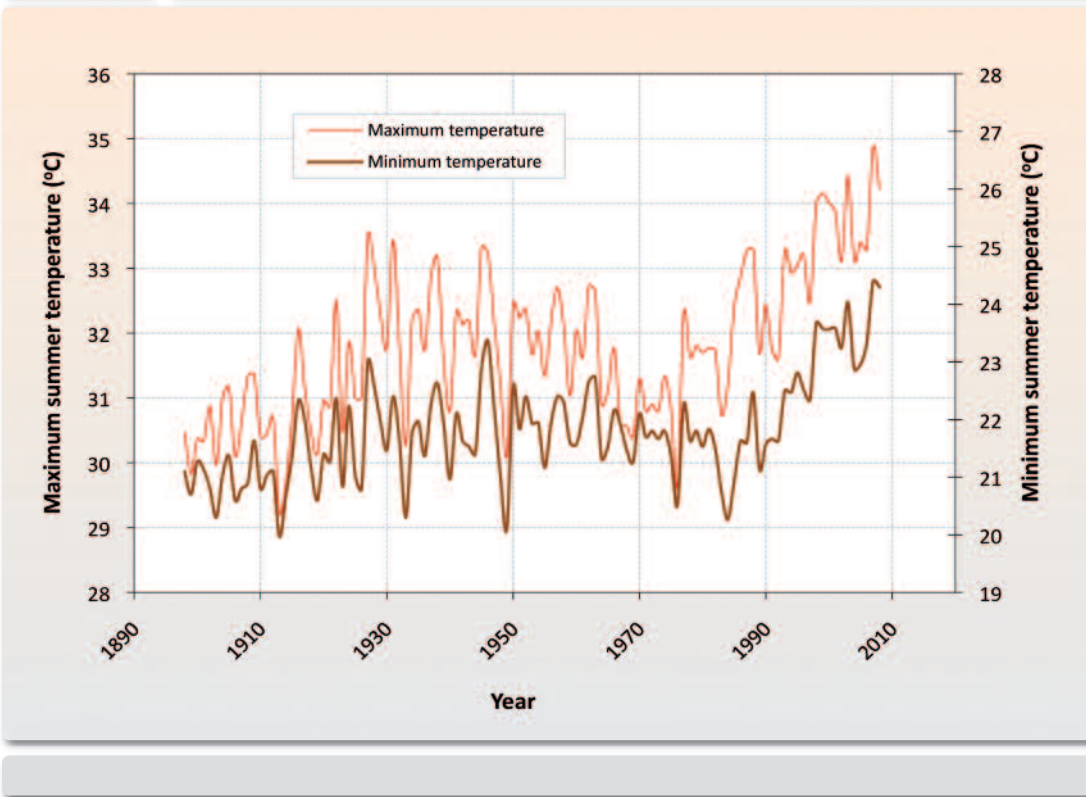
Athens has undergone particularly acute climatic changes over the past decades, due to the combined influence of various – mostly anthropogenic – factors, including:

- intensified urbanisation, leading to a greater ‘urban heat island’ effect;
- global climate change, due to the greenhouse effect;
- loss of peri-urban green areas to forest fires; and
- natural climate variability.

In order to determine the climatic influence of the above factors, it is necessary to have a continuous record of meteorological observations (time-series) that are long-term, reliable and homogeneous. The case of Athens can be considered ideal, as the meteorological observations (time-series) kept on record by the historic meteorological station of the National Observatory of Athens (NOA), in the city’s central district of Thisseion, go back more than a century and were all made at the exact same location, amid surroundings that have remained unchanged within a radius of several hundred meters (Founda et al., 2004). The area where the NOA station is located has no urban traffic, considerable green areas, and low-density low-height construction, i.e. features that are more typical of a suburban station (Livada et al., 2002). The temporal temperature variations, as recorded at the NOA station, seem to be predominantly attributable to the combined effects of global climate change (natural and anthropogenic) and intensified urbanisation in the wider area (Philandras et al., 1999; Founda et al., 2004).

Figure 1.18

Variation of the mean maximum and mean minimum summer temperatures in Athens (1900-2008/Thisseion Station, National Observatory of Athens)

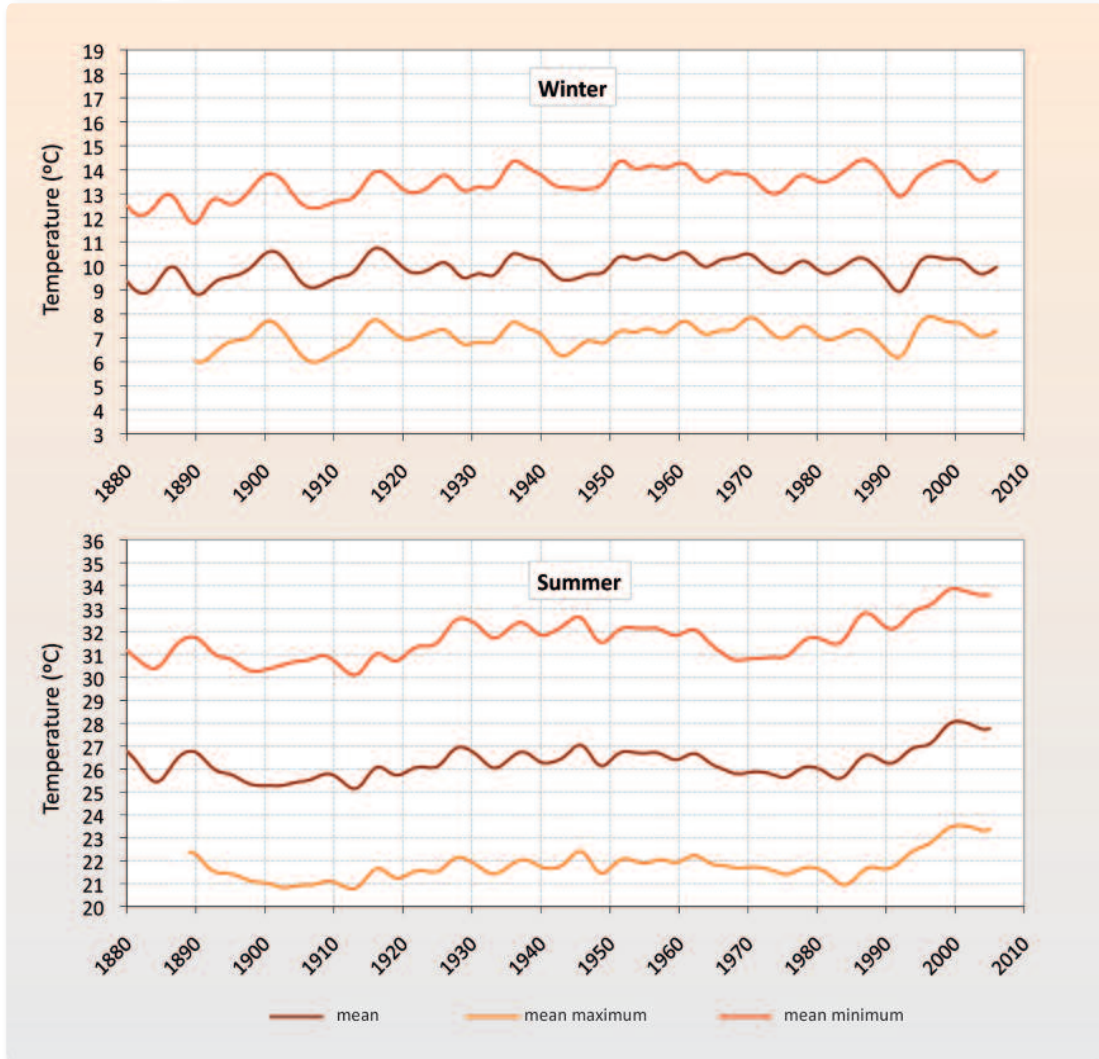


Based on NOA observations, the time-series of the annual mean air temperature for Athens has qualitatively followed the time-series for the Northern Hemisphere from the beginning of the previous century till today, with alternating warm and cooler periods, along a generally upward trend in the order of 0.5°C over the long term (1900-2008). Since the mid-1970s, however, the overall trend in annual mean temperature has, despite yearly variations, been clearly upward (+1.3°C from 1976 to 2008). Similar and concurrent has been the overall upward trend in annual mean maximum temperature (i.e. also starting in the mid-1970s), whereas the upward trend in annual mean minimum temperature (night temperature) began with a lag of several years, but has been faster paced (+1.8°C from 1984 to 2008; Founda, 2011).

Particularly striking is the difference in temperature variation trends between the warm and cold seasons of the year, with the marked upward trend in summer temperature largely accounting for the upward trend recorded on an annual basis (Founda et al., 2004; Founda, 2011). Specifically, the mean summer temperature (June to August) in Athens has been trending clearly upward since the mid-1970s, with an average increase of ~1°C per decade. Similar has been the overall trend in mean maximum temperature (+3.2°C/1976-2008), whereas the upward trend in mean minimum (night) temperature in summer once again began with a lag of several years,

Figure 1.19

Time series of the mean, mean maximum and mean minimum temperatures in Athens in winter and summer (1880-2008, Thisseion Station, National Observatory of Athens)



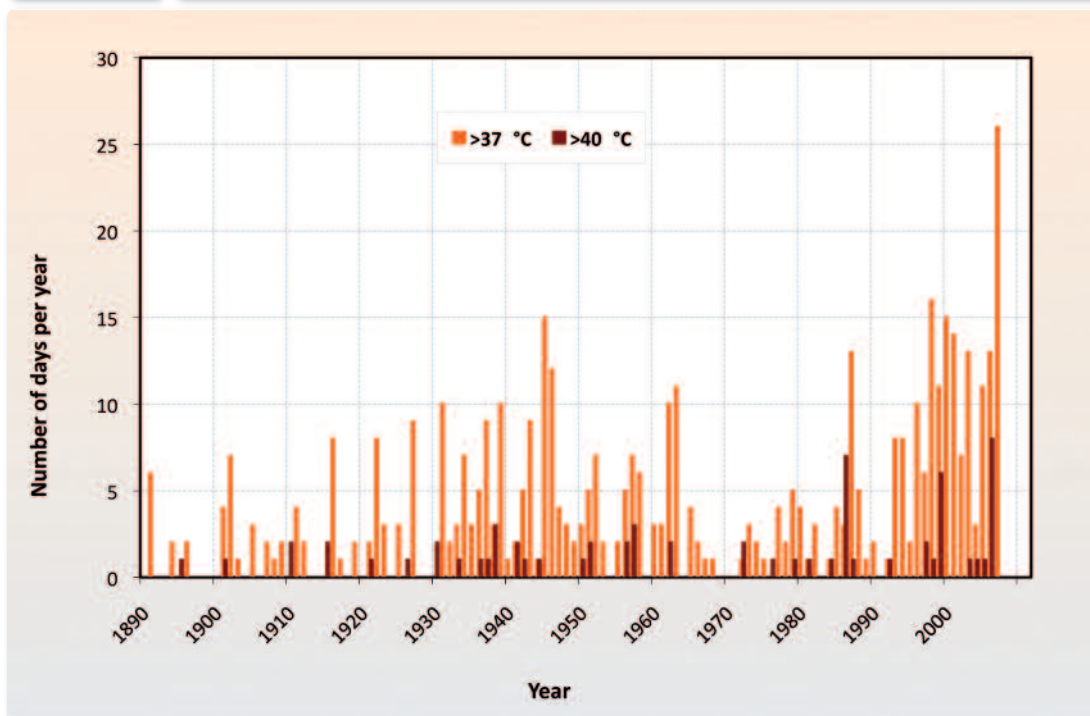
Values smoothed with Gaussian 9.

but has been faster paced ($+3.3^{\circ}\text{C}/1984\text{-}2008$), most probably on account of the urban heat island effect (Figures 1.18 and 1.19). Although many researchers associate the rise in summer temperatures in the centre of Athens with the weakening and warming of sea breezes as a result of higher building density (Metaxas et al., 1991; Philandras et al., 1999), interestingly similar rates of temperature increase in the summer months have also been recorded along the coast of Attica, for instance by the meteorological station of Ellinikon (Founda, 2011).

According to a recent study (Founda and Giannakopoulos, 2009), 1998-2007 was the warmest decade on record for Athens in terms of maximum summer temperatures (1937-1946 was the second warmest). On the contrary, no significant trend in temperature (either positive

Figure 1.20

Number of days per year with maximum temperature >37°C and >40°C (1890-2007/Thisseion Station, National Observatory of Athens)



In 2007, the number of days with maximum temperature >37°C exceeded 25.

or negative) has been observed during winter. According to recent records,²¹ 2001-2010 was the warmest decade on record for Athens in terms of annual temperature values (mean, maximum and minimum), once again on the basis of NOA observations. Six of the warmest years on record belong to this decade, with 2010 the warmest year ever with a mean temperature of 19.6°C and a departure from the climatic mean of almost 2°C. This is attributable for the most part to the months of August and November 2010, which were respectively 3.8°C and 3.5°C warmer than their climatic monthly mean.

Apart from the long-term trends in mean temperatures, another interesting change in the climate of Athens over the past few years concerns the incidence of extreme weather events (particularly high temperatures) in the summer months. This change in warm spells is characterised by:

- higher frequency (both in the number of separate days with extremely warm weather and in the number of warm spells (heat waves) lasting at least three consecutive days, Figures 1.20 and 1.21, Founda and Giannakopoulos, 2009);
- higher intensity (higher absolute maximum temperatures);

²¹ Climatological Bulletin, National Observatory of Athens.

Figure 1.21

Number of extreme hot spells (at least 3 consecutive days with temperatures >37°C) per year (1900-2007/Thisseion Station, National Observatory of Athens)

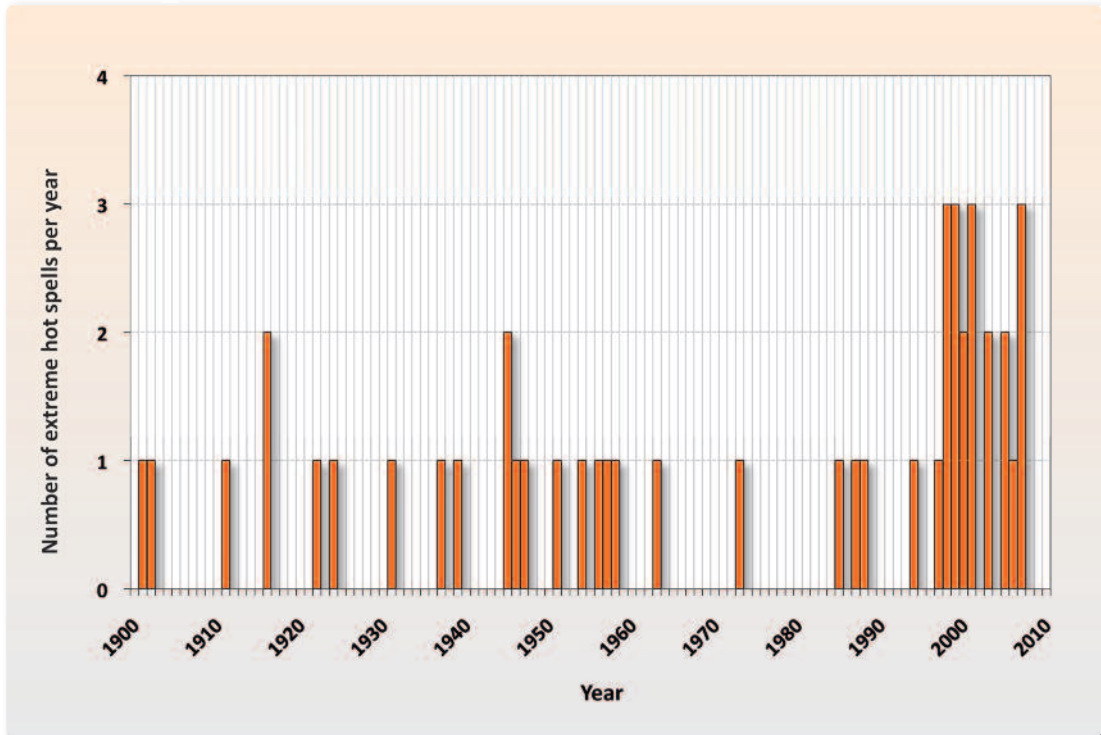
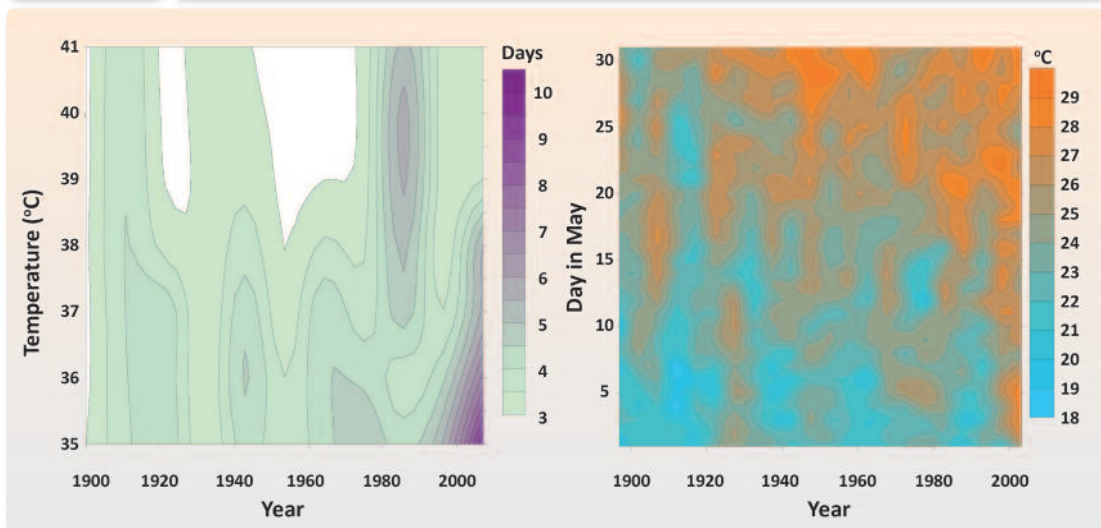


Figure 1.22

Average duration of extreme hot spells per year for various temperature thresholds (1900-2005/Thisseion Station, National Observatory of Athens, left panel) and maximum daily temperatures in May (1900-2005, National Observatory of Athens, right panel)



A shift towards earlier high temperature occurrences can be observed.

- longer duration (persistence) (Figure 1.22, left panel; Founda, 2009); and
- first occurrences earlier in the year (Figure 1.22, right panel, Founda, 2009).

As can be seen from Figure 1.20, the number of days with temperatures above 37°C/40°C has increased markedly since the mid-1990s, accounting for more than 35% of the entire time series. The increase in heat wave incidence (i.e. at least three consecutive days with temperatures above 37°C) has been of a similar order (Figure 1.21). According to Founda and Giannakopoulos (2009), the summer of 2007 was, in terms of air temperature, the most extreme on record in Athens. The temperature of 44.8°C recorded on 24 June 2007 at the NOA (>46°C at neighbouring stations) was an all-time high in the 150 years of NOA records, while the heat wave of June 2007 was the earliest on record (although an even earlier, but not as extreme, heat wave occurred in 2010). As almost half of the days had a maximum air temperature that exceeded the 90th percentile of temperature in the reference period (1961-1990), the summer of 2007 felt like a continuous heat wave. As shown by comparisons with climate simulation estimates made for the future (Founda and Giannakopoulos, 2009; and Tolika et al., 2009), the temperature conditions in the summer of 2007 were found to be similar to those projected to occur at increased frequency in the latter part of the 21st century. The heat wave index increased in general throughout the country over the period 1958-2000, whereas the frequency of cold nights both in summer and in winter declined (Kostopoulou and Jones, 2005).

Although the incidence of high temperature events in Greece is mostly associated with anticyclonic conditions and circulation anomalies in the upper atmosphere (Xoplaki et al., 2003), their effects are amplified in large urban centres by the urban heat island effect. Anticyclonic conditions have the general effect of exacerbating the urban heat island effect throughout the year, although less so in winter, due to cyclonic circulation and to the wind patterns that prevail during the cold season (Livada et al., 2002; Mihalakakou et al., 2002).

As for the future of Athens' climate over the next few decades, the outlook, based on projections, seems rather bleak. The region of the Eastern Mediterranean, to which Athens belongs, is considered one of the most vulnerable to the anthropogenic component of climate change (Giorgi and Lionello, 2008). It should be noted that, even though climate model projections developed by different research institutions often present considerable divergences, they are generally consistent with each other when it comes to the Mediterranean region, which significantly increases confidence in the specific projections. Researchers studying the effects of climate change on extreme weather events have concluded that the climate of the Mediterranean basin will become significantly warmer, with prolonged heat waves, less rainfall, but also more intense extreme rainfall events (Diffenbough et al., 2007; Goubanova and Li, 2007; Tolika et al., 2008).

After combining the results of three Regional Climate Models (RCMs) for the Athens area, the mean maximum summer temperature is projected to increase by 2°C in the period 2021-

2050 (with respect to 1961-1990) and by 4°C in the period 2071-2100 (Founda and Giannakopoulos, 2009). In parallel with the increase in mean temperature, the models also point to a rise in temperature variability around the mean value, resulting in a more frequent occurrence of extremely high temperatures. According to a recent study jointly conducted by WWF Hellas and NOA (WWF Hellas, 2009), Athens is projected to experience up to 15 more days a year with a maximum temperature >35°C (compared with the reference period 1961-1990) and up to 30 more 'tropical nights' with lowest night temperatures >20°C in the near future (2021-2050).

Projecting the extreme conditions of the summer 2007 into the future, it was estimated that the probability density function of the projected summer month maximum temperatures for the period 2070-2100 practically coincides with the respective one for the summer of 2007 in Athens, while similar results were obtained for minimum (night) temperatures (Founda and Giannakopoulos, 2009). In other words, the summer of 2007 was a 'foretaste' of the conditions that will prevail in the city in the future; and conditions considered today to be particularly extreme will, in the second half of this century, be typical of an Athens summer. The same approach, when applied to less urbanised areas around Athens, produced similar results with regard to maximum temperatures. However, the results in terms of minimum temperatures varied, signalling the cumulative impact of the urban heat island effect in the presence of extreme weather events, especially at night.

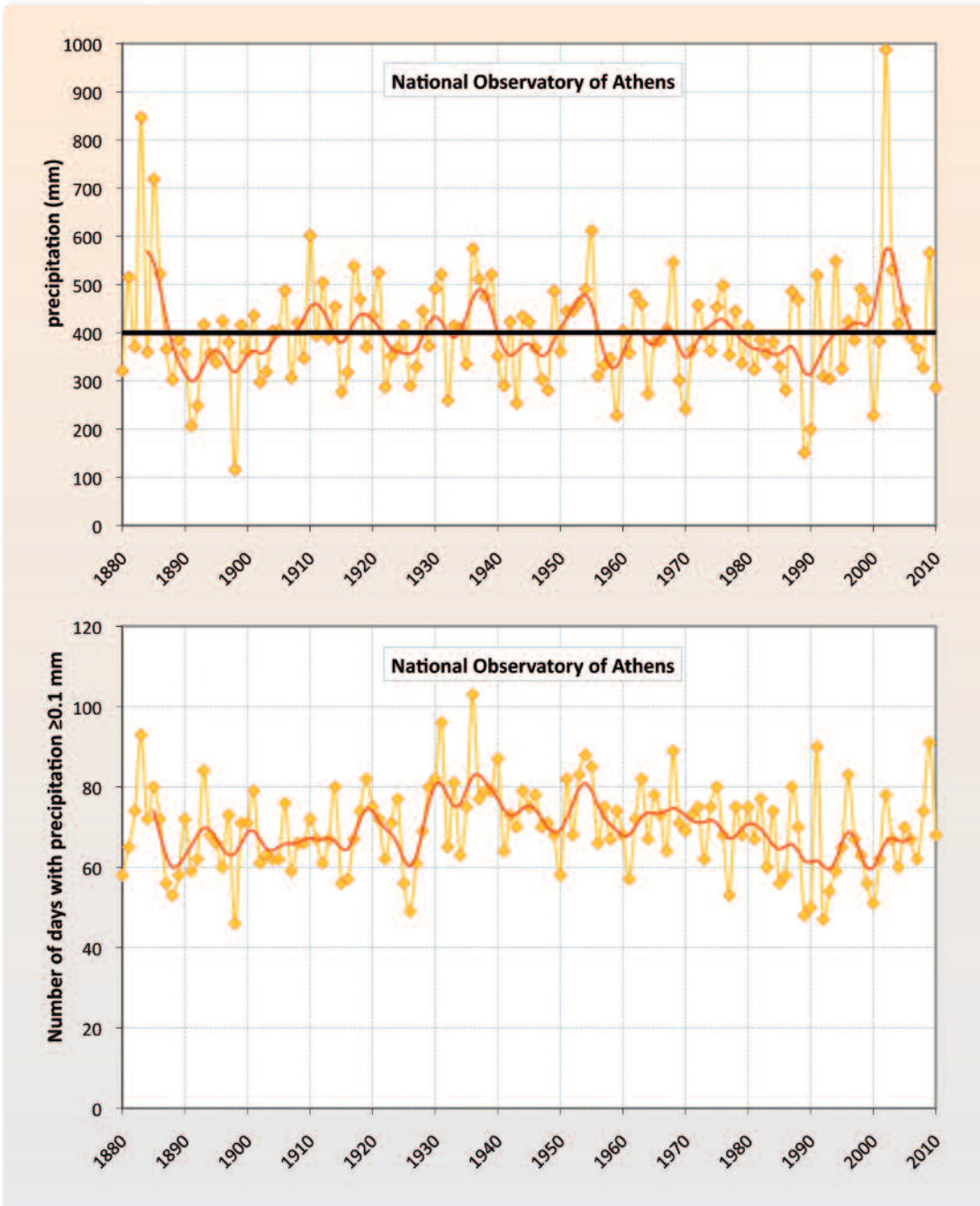
In addition to the above, note should also be taken of the projected expansion of the urban fabric in the next decades, and the respective expansion and exacerbation of the urban heat island effect.

As regards extreme precipitation events, Nastos and Zerefos (2007), after studying daily precipitation records from the National Observatory of Athens (NOA) covering the period 1891-2004, reported a clear overall increase in extreme precipitation events. Maheras et al. (2004) also provide evidence that extreme precipitation events are increasing, despite the decline in total precipitation (see also Figure 1.23).

Moreover, according to a recent study (Founda et al., 2009), a decrease in total precipitation is projected for Athens in the following decades, together with a higher occurrence of extreme precipitation events. Lower precipitation would obviously have an adverse effect on groundwater quality, and will become an additional factor in expected climatic changes (Fischer et al., 2007). Decision makers must be prepared to deal with such variability and the serious effects it is likely to have in our region, as shown by recent flooding and drought spells. Interestingly, the Ancient Greeks had plans for such contingencies, as evidenced by surviving texts, involving for instance the construction of ditches and dams in the surrounding mountains and of rainwater reservoirs in the cities (Aeginitis, 1908; 1926). Plato (in his *Laws*, Book 6, Sections 761b, c) says that rural patrols "shall dam the outflows of their flooded dales

Figure 1.23

Time series of annual precipitation (upper panel) and number of rainy days (with precipitation ≥ 0.1 mm, lower panel) (Thisseion Station, National Observatory of Athens)



Values smoothed with Gaussian 9 (red line). The straight line shows regressions.

by means of walls and channels, so that by storing up or absorbing the rains from heaven, and by forming pools or springs in all the low-lying fields and districts, they may cause even the driest spots to be abundantly supplied with good water. As to spring-waters, be they streams or

fountains, they shall beautify and embellish them by means of plantations and buildings, and by connecting the pools by hewn tunnels they shall make them all abundant, and by using water-pipes they shall beautify at all seasons of the year any sacred glebe or grove that may be close at hand, by directing the streams right into the temples of the gods”.²² Similarly, Aristotle (in his *Politics*, Section 1330) mentions that a city “must possess if possible a plentiful natural supply of pools and springs, but failing this, a mode has been invented of supplying water by means of constructing an abundance of large reservoirs for rain-water, so that a supply may never fail the citizens...”.²³

1.15 Estimating future climate variation for Greece's 13 climate zones until the end of the 21st century

1.15.1 Determining Greece's different climate zones

Our first task was to divide Greece into different climate zones on the basis of climatic and geographical criteria, the most significant of which are: (i) the mountain range running north to south through most of the country, dividing continental Greece into a western windward area and an eastern rain shadow area; (ii) the Eastern Aegean and the Dodecanese Islands, where precipitation levels resume an upward trend, after reaching their lowest values in the Cyclades; (iii) the north-to-south temperature gradient, as well as the temperature difference between island and continental regions; (iv) the topography and climatic homogeneity. These climatic and geographical considerations enabled us to identify the following 13 climate zones (see Figure 1.24): 1. Western Greece (WG); 2. Central and Eastern Greece (CEG); 3. Western and Central Macedonia (WCM); 4. Eastern Macedonia-Thrace (EMT); 5. the Western Peloponnese (WP); 6. the Eastern Peloponnese (EP); 7. Attica (AT); 8. Crete (C); 9. the Dodecanese islands (D); 10. the Cyclades islands (CY); 11. the Eastern Aegean (EA); 12. the Northern Aegean (NA); and 13. the Ionian (I).

1.15.2 Projecting climate variation for Greece's 13 climate zones, on the basis of four different greenhouse gas emissions scenarios

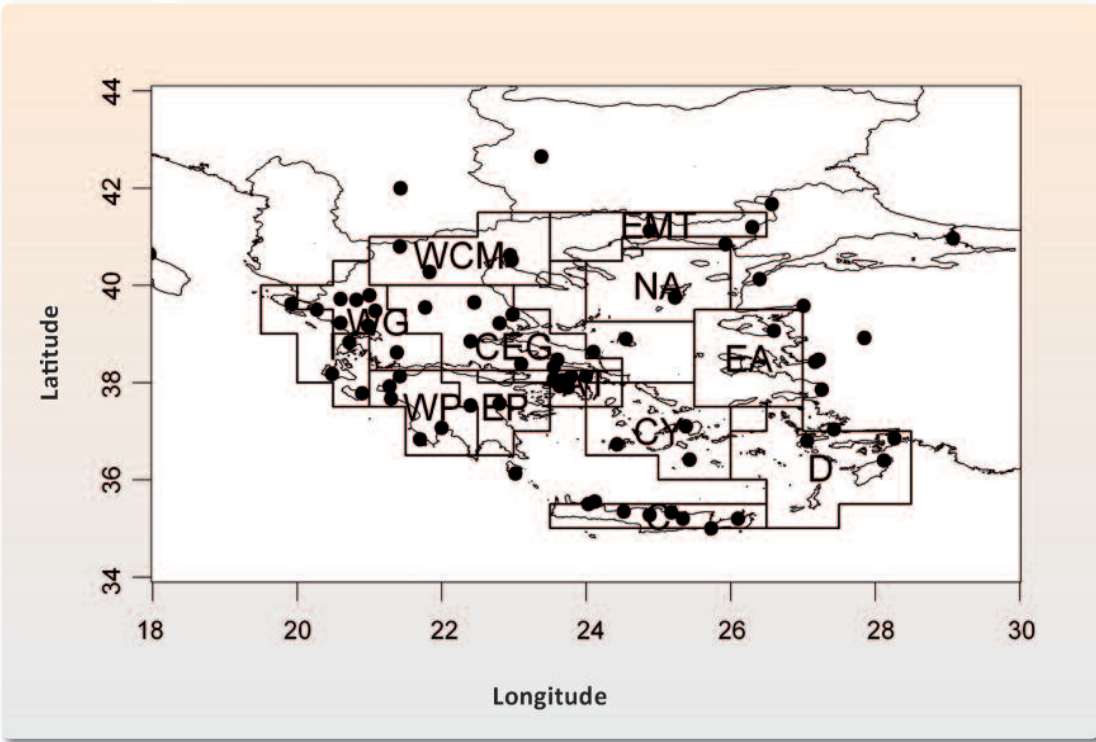
The Research Centre for Atmospheric Physics and Climatology of the Academy of Athens (RCAPC) has developed model simulation datasets for Greenhouse Gas Emission Scenarios A2, A1B, B2 and B1. Table 1.6 summarises the characteristics of each scenario, as developed

²² As translated by R.G. Bury (Plato in Twelve Volumes, Vols. 10 & 11, Cambridge, MA, Harvard University Press; London, William Heinemann Ltd. 1967 & 1968).

²³ As translated by H. Rackham (Aristotle in 23 Volumes, Vol. 21, Cambridge, MA, Harvard University Press; London, William Heinemann Ltd. 1944).

Figure 1.24

The division of Greece into 13 climate zones



For an explanation of the initials denoting each zone, see Section 1.15.1.

Table 1.6

Greenhouse gas emission scenarios used in the present study*

Scenario A2	Moderate increase in global average per capita income. Particularly strong energy consumption. Rapid rise in global population. Slow and fragmented technological change, and modest to major changes in land uses. Rapid rise in CO ₂ concentration in the atmosphere, to 850 ppm by 2100.
Scenario A1B	Rapid economic growth. Particularly strong consumption of energy, but also spread of new and efficient technologies. Use of both fossil fuels and alternative energy sources. Small changes in land uses. Rapid rise in global population by 2050 and gradual decline thereafter. Large increase in CO ₂ concentration in the atmosphere, to 720 ppm by 2100.
Scenario B2	Development of global economy at modest rates. Smaller technological change compared to Scenarios A1 and B1. Rapid rise in global population. Increase in CO ₂ concentration in the atmosphere at modest but steady rates , to 620 ppm by 2100.
Scenario B1	Large increase in global per capita income. Low energy consumption. Reduced use of conventional energy sources and shift towards renewable energy. Rapid rise in global population by 2050 and gradual decrease thereafter. Increase in CO ₂ concentration in the atmosphere at a relatively mild pace , particularly as of 2050, to 550 ppm by 2100.

* IPCC, 2007. More detailed information on the emission scenarios can also be found in the complete text on climate, in the relevant page of the Climate Change Impacts Study Committee (CCISC) on the Bank of Greece website (www.bankofgreece.gr).

in the context of the United Nations IPCC Third Assessment Report on Climate Change (Nakićenović et al., 2000).

For each of the respective 13 climate zones and for the country as a whole, we estimated the anticipated variation (based on the simulations) in the seasonal mean and the annual mean values of six climate parameters for two different periods 2021-2050 and 2071-2100, for comparison with the reference period 1961-1990. The six climate parameters are:

- mean air temperature (°C);
- precipitation (mm/year);
- relative humidity (%);
- cloud cover (%);
- total incident short-wave radiation (W/m²); and
- wind speed at 10 m above ground (m/sec).

It should be noted that we were able to estimate the variation in all six climate parameters only under three of the four scenarios (specifically under Scenarios A2, B2 and A1B). Under Scenario B1, it was only possible to estimate the variation in mean air temperature, due to the lack of available data from high spatial resolution simulations based on Regional Climate Model simulations (RCMs).

More specifically, the variation in the six climate parameters under Scenarios A2 and B2 was assessed by analysing the results of an array of simulations with the regional climate models (RCMs) developed under the EU-financed project, PRUDENCE.²⁴ A recent study (Zanis et al., 2009) presented the detailed results for Greece of nine RCMs from the PRUDENCE project, as well as the projections of these models for the period 2071-2100 using Scenario A2.

Datasets from 13 simulations were used for Scenario A2, and from 8 simulations for Scenario B2. In both cases, the estimates cover 30-year time-slices for the reference climate (1961-1990) and for a future period (2071-2100). The horizontal resolution of the RCMs used in the PRUDENCE project was 0.5°x0.5° (~50 km²). In the case of Scenario A1B: the assessment of climate variation was based on 12 simulations, conducted as part of the ENSEMBLES project.²⁵ The climate datasets cover 30-year time-slices for the reference climate (1961-1990) and for two future periods, 2021-2050 and 2071-2100. The horizontal resolution of the RCMs used in the ENSEMBLES project was 0.25°x0.25° (~25 km²). Lastly, in the case of Scenario B1, the variation in mean air temperature was estimated by statistically downscaling the mean values obtained with a set of 10 simulations with Atmosphere-Ocean General Circulation Models (AOGCMs) conducted for the United Nations IPCC Fourth Assessment Report on Climate Change (AR4). The variation of the climate parameters for Scenarios A2, A1B and B2 are based on the ‘ensemble mean’ of the 13, 12 and 8 simulations, respectively. Detailed information on the simulations used in the different scenarios and on the methodology used to estimate the vari-

²⁴ <http://prudence.dmi.dk/>

²⁵ <http://ensemblest3.dmi.dk/>

Table 1.7.1.a

Mean values of air temperature at 2 m above ground (T, °C), for time periods 1961-1990*, 2071-2080, 2081-2090 and 2091-2100, as well as absolute (Δ) and percentage (%) changes in these values between the periods 2071-2080, 2081-2090, 2091-2100 and the reference period 1961-1990

Climate zones	Periods	T (°C)		Δ T		(%)	
		A2	B2	A2	B2	A2	B2
Western and Central Macedonia	1961-1990	11.85±1.13	11.91±0.95				
	2071-2080	15.85±1.50	14.89±1.14	4.00±1.05	2.98±0.41	34.1±10.0	25.1±3.4
	2081-2090	16.40±1.54	15.11±1.23	4.56±1.07	3.20±0.51	38.8±10.3	26.9±4.0
	2091-2100	17.08±1.56	15.31±1.26	5.24±1.02	3.40±0.58	44.6±9.8	28.6±4.7
Eastern Macedonia and Thrace	1961-1990	12.24±1.39	12.36±1.06				
	2071-2080	16.29±1.74	15.42±1.15	4.05±1.06	3.05±0.41	33.5±9.8	24.8±4.0
	2081-2090	16.84±1.80	15.63±1.29	4.60±1.11	3.27±0.56	38.0±10.3	26.5±4.7
	2091-2100	17.52±1.81	15.79±1.26	5.28±1.08	3.42±0.62	43.6±10.1	27.8±5.6
Northern Aegean	1961-1990	16.37±0.65	16.19±0.66				
	2071-2080	19.63±0.76	18.82±0.73	3.26±0.19	2.63±0.11	19.9±1.0	16.3±0.7
	2081-2090	19.85±0.63	18.87±0.54	3.48±0.22	2.68±0.23	21.3±1.8	16.6±2.0
	2091-2100	20.56±0.69	19.23±0.65	4.19±0.25	3.04±0.31	25.6±1.9	18.8±2.2
Cyclades	1961-1990	17.98±0.35	17.94±0.36				
	2071-2080	20.97±0.44	20.43±0.41	3.00±0.18	2.49±0.13	16.7±1.0	13.9±0.7
	2081-2090	21.20±0.40	20.49±0.42	3.22±0.26	2.55±0.27	17.9±1.6	14.2±1.6
	2091-2100	21.91±0.45	20.86±0.36	3.93±0.33	2.92±0.34	21.9±2.0	16.3±2.1
Eastern Aegean	1961-1990	16.76±0.81	16.79±0.56				
	2071-2080	20.18±0.92	19.45±0.61	3.42±0.48	2.67±0.09	20.4±3.1	15.9±0.6
	2081-2090	20.46±0.92	19.54±0.59	3.70±0.55	2.75±0.29	22.1±3.6	16.4±1.9
	2091-2100	21.15±0.89	19.86±0.61	4.39±0.42	3.07±0.31	26.3±2.9	18.3±2.1
Dodecanese	1961-1990	18.62±0.41	18.57±0.38				
	2071-2080	21.75±0.52	21.13±0.46	3.12±0.20	2.56±0.17	16.8±1.0	13.8±0.9
	2081-2090	21.99±0.46	21.24±0.45	3.37±0.24	2.67±0.24	18.1±1.4	14.4±1.4
	2091-2100	22.65±0.57	21.57±0.57	4.03±0.34	3.00±0.40	21.6±1.8	16.2±2.2
Crete	1961-1990	17.50±0.62	17.53±0.54				
	2071-2080	20.81±0.96	20.03±0.65	3.31±0.92	2.50±0.18	19.0±5.7	14.3±0.8
	2081-2090	21.13±1.00	20.16±0.67	3.63±0.98	2.63±0.29	20.8±6.1	15.0±1.6
	2091-2100	21.86±0.86	20.51±0.70	4.36±0.82	2.98±0.32	25.0±5.2	17.0±1.8
Central and Eastern Greece	1961-1990	15.02±0.95	14.96±0.96				
	2071-2080	18.81±1.18	17.77±1.07	3.79±1.02	2.81±0.29	25.5±8.1	18.8±2.0
	2081-2090	19.26±1.25	17.97±1.21	4.24±1.09	3.01±0.45	28.5±8.6	20.1±2.8
	2091-2100	19.90±1.22	18.21±1.22	4.88±0.97	3.25±0.50	32.7±7.7	21.8±3.2
Attica	1961-1990	15.94±0.98	15.94±0.95				
	2071-2080	19.83±1.49	18.78±1.00	3.89±1.35	2.84±0.27	24.6±9.5	17.9±2.0
	2081-2090	20.29±1.55	19.02±1.15	4.35±1.42	3.08±0.46	27.5±10.0	19.3±2.9
	2091-2100	20.94±1.47	19.25±1.13	5.00±1.28	3.31±0.50	31.6±9.1	20.8±3.4
Eastern Peloponnese	1961-1990	15.41±0.85	15.36±0.75				
	2071-2080	19.17±1.26	18.11±0.94	3.76±1.14	2.75±0.29	24.6±8.4	17.9±1.6
	2081-2090	19.64±1.28	18.33±1.04	4.23±1.15	2.97±0.45	27.6±8.5	19.3±2.6
	2091-2100	20.31±1.24	18.59±1.04	4.91±1.05	3.22±0.45	32.0±7.7	21.0±2.6
Western Greece	1961-1990	12.94±1.52	13.10±1.16				
	2071-2080	16.92±1.76	16.06±1.39	3.98±1.07	2.96±0.45	31.3±10.2	22.7±3.3
	2081-2090	17.52±1.82	16.30±1.48	4.58±1.06	3.21±0.56	35.9±10.1	24.5±3.9
	2091-2100	18.24±1.87	16.54±1.53	5.30±1.01	3.45±0.65	41.4±9.6	26.4±4.7
Ionian	1961-1990	17.11±0.73	17.10±0.58				
	2071-2080	20.24±0.81	19.61±0.71	3.13±0.35	2.50±0.38	18.3±2.2	14.7±2.3
	2081-2090	20.51±0.80	19.72±0.66	3.40±0.41	2.62±0.50	19.9±2.6	15.3±3.1
	2091-2100	21.29±0.83	20.13±0.64	4.18±0.41	3.03±0.47	24.5±2.6	17.7±2.9
Western Peloponnese	1961-1990	15.69±1.14	15.81±0.77				
	2071-2080	19.26±1.40	18.53±0.96	3.57±0.60	2.72±0.34	22.8±3.8	17.2±1.9
	2081-2090	19.72±1.42	18.74±0.99	4.03±0.61	2.93±0.45	25.8±3.8	18.5±2.7
	2091-2100	20.44±1.42	19.03±0.99	4.75±0.55	3.22±0.51	30.4±3.4	20.4±3.2
Greece	1961-1990	16.17±0.68	16.14±0.56				
	2071-2080	19.58±0.80	18.81±0.67	3.41±0.42	2.66±0.19	21.1±2.8	16.5±1.0
	2081-2090	19.93±0.82	18.94±0.71	3.76±0.49	2.80±0.34	23.3±3.2	17.3±2.1
	2091-2100	20.64±0.80	19.25±0.72	4.46±0.38	3.11±0.39	27.6±2.6	19.3±2.5

Results are given as the mean value and standard deviation of 13 simulations for Scenario A2 and of 8 simulations for Scenario B2, respectively, and are based on the PRUDENCE project.

* The small differences in estimates of climate parameters in the reference period 1961-1990 for the different emission scenarios are due to the fact that climate parameters are estimated on the basis of different sets of climate simulations for the different scenarios.

Table 1.7.1.b

Mean values of rainfall (R, mm/year), for time periods 1961-1990*, 2071-2080, 2081-2090 and 2091-2100, as well as changes in these values between the periods 2071-2080, 2081-2090, 2091-2100 and the reference period 1961-1990

Climate zones	Periods	R (mm/year)		ΔR		(%)	
		A2	B2	A2	B2	A2	B2
Western and Central Macedonia	1961-1990	532.6±108.7	561.3±101.3				
	2071-2080	475.3±130.8	530.6±124.5	-57.3±51.2	-30.7±67.8	-11.4±10.2	-5.4±12.4
	2081-2090	422.9±103.0	521.4±110.3	-109.6±39.7	-39.9±50.7	-20.9±7.2	-7.1±9.8
	2091-2100	444.0±116.5	555.8±144.8	-88.5±53.5	-5.5±72.6	-17.1±10.1	-1.5±13.0
Eastern Macedonia and Thrace	1961-1990	608.3±132.4	663.6±115.4				
	2071-2080	526.8±131.1	625.6±137.2	-81.5±56.6	-38.0±92.3	-13.4±8.6	-5.3±14.4
	2081-2090	465.1±102.8	599.9±116.7	-143.2±64.0	-63.7±64.7	-23.3±8.5	-9.3±9.9
	2091-2100	487.6±126.1	652.1±159.1	-120.7±57.5	-11.5±93.8	-20.1±8.6	-1.8±14.6
Northern Aegean	1961-1990	481.8±104.4	500.7±118.7				
	2071-2080	445.5±124.8	496.1±135.5	-36.3±60.7	-4.6±84.2	-8.3±13.4	-0.4±17.1
	2081-2090	397.4±105.3	470.7±117.8	-84.4±56.8	-30.0±50.5	-17.8±10.9	-5.7±11.4
	2091-2100	451.3±134.9	532.2±151.6	-30.6±87.3	31.5±80.2	-6.9±18.1	6.2±16.3
Cyclades	1961-1990	400.6±106.0	411.7±125.2				
	2071-2080	334.3±89.6	400.6±110.1	-66.3±32.3	-11.1±27.6	-16.4±5.5	-1.7±6.1
	2081-2090	313.4±95.8	379.4±122.2	-87.3±27.0	-32.3±36.5	-22.4±6.3	-8.0±12.1
	2091-2100	361.9±106.7	436.8±138.1	-38.7±36.9	25.1±36.9	-10.3±10.1	5.6±11.1
Eastern Aegean	1961-1990	544.1±127.2	546.9±133.6				
	2071-2080	479.2±133.6	526.0±129.3	-65.0±43.4	-20.9±60.3	-12.4±8.0	-3.4±11.1
	2081-2090	431.6±125.5	500.5±127.6	-112.5±38.6	-46.4±33.7	-21.4±7.2	-8.5±6.8
	2091-2100	485.1±149.5	582.6±160.7	-59.0±63.9	35.7±65.3	-11.5±11.1	6.3±12.7
Dodecanese	1961-1990	433.2±160.8	428.4±188.0				
	2071-2080	369.7±130.7	416.8±183.1	-63.5±40.5	-11.6±37.2	-13.6±6.0	-2.7±7.8
	2081-2090	340.3±133.1	401.2±174.9	-92.9±40.8	-27.2±22.2	-22.0±5.5	-6.4±4.8
	2091-2100	376.7±152.9	450.0±207.3	-56.5±49.5	21.6±65.6	-14.8±12.3	3.8±15.3
Crete	1961-1990	351.6±187.2	315.5±144.4				
	2071-2080	280.3±151.4	287.5±127.9	-71.3±47.0	-28.1±29.8	-18.9±7.6	-7.4±9.1
	2081-2090	264.9±151.4	268.1±115.2	-86.6±47.5	-47.5±36.3	-24.7±8.1	-14.1±7.2
	2091-2100	300.2±179.6	297.9±130.9	-51.4±50.6	-17.6±34.1	-15.6±12.2	-5.1±10.1
Central and Eastern Greece	1961-1990	473.5±102.5	490.6±100.1				
	2071-2080	408.2±125.4	461.3±110.0	-65.2±43.3	-29.4±39.1	-14.8±9.3	-6.1±8.3
	2081-2090	378.3±103.6	449.3±114.3	-95.2±40.3	-41.3±45.8	-20.6±8.3	-8.8±10.7
	2091-2100	420.8±133.5	483.6±132.2	-52.6±72.6	-7.0±51.6	-11.9±15.4	-2.2±10.2
Attica	1961-1990	375.1±108.6	388.2±84.2				
	2071-2080	311.6±121.9	363.6±97.3	-63.5±36.7	-24.5±27.8	-18.1±9.1	-6.8±7.2
	2081-2090	293.9±107.7	342.8±100.0	-81.2±39.8	-45.3±41.3	-22.6±11.0	-12.3±11.9
	2091-2100	333.7±139.0	381.1±108.8	-41.4±60.2	-7.1±37.6	-12.7±15.8	-2.6±8.9
Eastern Peloponnese	1961-1990	479.9±166.6	517.4±171.5				
	2071-2080	395.4±164.1	469.4±176.7	-84.5±41.4	-48±33.9	-18.7±8.1	-9.8±7.2
	2081-2090	352.2±134.5	440.4±149.2	-127.8±53.6	-77±49.8	-27.2±7.6	-14.8±8.9
	2091-2100	392.0±166.7	483.4±177.0	-87.9±70.1	-34±32.2	-19.1±13.7	-7.1±7.4
Western Greece	1961-1990	861.1±174.2	912.4±102.0				
	2071-2080	744.0±187.8	842.2±148.0	-117.1±86.3	-70.2±126.1	-13.8±8.9	-7.5±13.8
	2081-2090	641.0±139.1	804.8±97.0	-220.1±85.0	-107.6±92.2	-25.3±8.1	-11.4±9.7
	2091-2100	654.0±164.6	842.5±165.8	-207.1±94.4	-69.9±116.8	-23.8±10.0	-7.8±12.5
Ionian	1961-1990	789.6±225.4	775.7±242.9				
	2071-2080	725.6±241.4	740.8±242.7	-64.0±83.1	-35.0±97.3	-9.2±11.5	-4.2±11.7
	2081-2090	598.6±195.9	711.3±233.0	-191±75.7	-64.5±69.7	-25.0±7.7	-8.4±9.0
	2091-2100	652.4±225.2	767.1±287.0	-137.3±89.9	-8.6±67.7	-18.6±11.9	-2.9±10.3
Western Peloponnese	1961-1990	613.5±159.6	629.4±120.8				
	2071-2080	510.2±164.9	568.6±112.4	-103.2±49.2	-60.8±66.0	-17.6±8.3	-9.4±9.9
	2081-2090	442±131.6	540.0±114.7	-171.4±52.6	-89.4±47.4	-28.4±6.4	-14.4±8.1
	2091-2100	475.6±175.7	584.5±146.0	-137.9±73.9	-44.9±46.9	-23.5±11.9	-7.9±9.0
Greece	1961-1990	510.1±108.0	524.1±113.8				
	2071-2080	442.7±112.9	497.4±108.6	-67.4±34.6	-26.7±50.2	-13.8±7.6	-4.6±9.8
	2081-2090	397.1±99.6	475.7±109.0	-113.0±29.5	-48.4±36.4	-22.6±5.5	-9.2±8.2
	2091-2100	437.7±126.6	525.2±138.0	-72.4±51.1	1.1±54.5	-15.2±10.9	-0.4±11.2

Results are given as the mean value and standard deviation of 13 simulations for Scenario A2 and of 8 simulations for Scenario B2, respectively, and are based on the PRUDENCE project.

* The small differences in estimates of climate parameters in the reference period 1961-1990 for the different emission scenarios are due to the fact that climate parameters are estimated on the basis of different sets of climate simulations for the different scenarios.

Table 1.7.1.c

Mean values of relative humidity (H, %) at 2 m above ground for time periods 1961-1990*, 2071-2080, 2081-2090 and 2091-2100, as well as changes in these values between the periods 2071-2080, 2081-2090, 2091-2100 and the reference period 1961-1990

Climate zones	Periods	H		ΔH		(%)	
		A2	B2	A2	B2	A2	B2
Western and Central Macedonia	1961-1990	61.58±9.41	61.82±11.51				
	2071-2080	57.27±7.22	59.83±12.43	-4.31±5.12	-1.99±2.85	-6.5±6.2	-3.4±4.2
	2081-2090	55.11±6.83	59.14±12.47	-6.46±4.80	-2.68±2.73	-10.0±5.5	-4.6±4.0
	2091-2100	54.73±6.90	60.2±12.23	-6.84±4.88	-1.62±2.44	-10.7±5.6	-2.8±3.6
Eastern Macedonia and Thrace	1961-1990	60.25±9.79	60.32±11.43				
	2071-2080	55.61±7.52	58.07±11.70	-4.64±5.12	-2.25±2.80	-7.2±6.3	-3.8±4.3
	2081-2090	53.59±6.99	57.12±12.28	-6.66±5.21	-3.21±2.92	-10.5±6.2	-5.6±4.3
	2091-2100	52.83±7.03	58.45±11.97	-7.42±5.21	-1.87±2.71	-11.8±6.0	-3.2±4.2
Northern Aegean	1961-1990	71.35±4.95	73.52±4.68				
	2071-2080	69.91±4.65	72.39±4.99	-1.44±0.96	-1.13±0.75	-2.0±1.3	-1.6±1.1
	2081-2090	69.34±4.87	72.38±4.82	-2.00±1.09	-1.14±0.51	-2.8±1.5	-1.6±0.7
	2091-2100	68.94±4.97	72.73±4.68	-2.41±0.86	-0.79±0.69	-3.4±1.2	-1.1±1.0
Cyclades	1961-1990	73.78±3.70	75.21±3.40				
	2071-2080	73.22±3.52	74.54±3.57	-0.56±0.48	-0.67±0.38	-0.7±0.6	-0.9±0.5
	2081-2090	73.02±3.57	74.60±3.26	-0.76±0.56	-0.60±0.30	-1.0±0.7	-0.8±0.4
	2091-2100	72.83±3.70	74.87±3.34	-0.95±0.57	-0.34±0.22	-1.3±0.7	-0.5±0.3
Eastern Aegean	1961-1990	68.92±5.16	69.97±5.22				
	2071-2080	66.74±4.68	68.86±5.43	-2.18±2.48	-1.11±0.64	-3.1±3.2	-1.6±1.0
	2081-2090	66.03±4.88	68.72±5.73	-2.89±2.57	-1.25±0.58	-4.1±3.3	-1.8±1.0
	2091-2100	65.70±4.94	69.39±5.43	-3.22±2.33	-0.58±0.73	-4.6±3.0	-0.8±1.1
Dodecanese	1961-1990	72.44±3.94	74.04±3.14				
	2071-2080	71.87±3.95	73.70±2.91	-0.57±0.74	-0.34±0.80	-0.8±1.1	-0.4±1.1
	2081-2090	71.61±3.92	73.62±3.02	-0.83±0.92	-0.42±0.70	-1.1±1.3	-0.6±1.0
	2091-2100	71.48±4.23	73.97±3.03	-0.95±0.86	-0.06±0.50	-1.3±1.2	-0.1±0.7
Crete	1961-1990	69.38±6.41	68.66±7.71				
	2071-2080	67.66±6.82	67.71±7.68	-1.72±4.10	-0.94±1.18	-2.4±5.4	-1.4±1.6
	2081-2090	67.15±6.97	67.42±7.75	-2.23±4.28	-1.24±0.94	-3.1±5.6	-1.8±1.3
	2091-2100	67.08±6.88	67.97±7.83	-2.30±4.15	-0.69±0.83	-3.3±5.5	-1.0±1.2
Central and Eastern Greece	1961-1990	62.16±6.57	62.52±7.93				
	2071-2080	58.57±4.86	61.03±8.36	-3.59±4.65	-1.49±1.57	-5.4±6.0	-2.5±2.4
	2081-2090	57.04±4.69	60.37±8.36	-5.11±4.33	-2.15±1.43	-7.9±5.3	-3.5±2.2
	2091-2100	57.11±4.78	61.29±8.16	-5.04±4.52	-1.23±1.20	-7.8±5.7	-2.0±1.9
Attica	1961-1990	59.17±8.85	58.29±10.00				
	2071-2080	55.10±8.19	56.41±9.66	-4.07±5.59	-1.89±1.65	-6.5±7.7	-3.2±2.5
	2081-2090	53.73±8.12	55.36±9.54	-5.44±5.36	-2.94±1.73	-8.9±7.2	-5.0±2.7
	2091-2100	53.90±8.42	56.62±9.59	-5.27±5.53	-1.68±1.25	-8.7±7.5	-2.8±2.0
Eastern Peloponnese	1961-1990	61.53±7.24	61.65±8.00				
	2071-2080	57.87±6.24	60.12±8.06	-3.66±4.96	-1.53±0.99	-5.6±6.6	-2.5±1.7
	2081-2090	56.35±6.13	59.26±8.36	-5.18±4.59	-2.40±1.29	-8.1±5.9	-4.0±2.2
	2091-2100	56.41±6.21	60.35±8.19	-5.12±4.86	-1.30±1.23	-8.0±6.4	-2.1±2.0
Western Greece	1961-1990	63.13±10.03	62.86±12.61				
	2071-2080	58.67±8.24	60.58±13.20	-4.46±5.29	-2.28±2.83	-6.6±6.5	-3.8±4.2
	2081-2090	56.37±7.89	60.00±13.50	-6.76±4.84	-2.86±2.90	-10.3±5.5	-4.8±4.1
	2091-2100	55.71±7.84	60.61±13.11	-7.42±4.91	-2.25±2.54	-11.4±5.7	-3.7±3.7
Ionian	1961-1990	72.07±4.83	73.67±4.18				
	2071-2080	71.77±4.20	73.40±2.84	-0.29±1.86	-0.27±1.55	-0.3±2.8	-0.3±2.4
	2081-2090	71.17±4.67	73.53±2.91	-0.90±1.90	-0.14±1.47	-1.2±2.8	-0.1±2.2
	2091-2100	70.67±5.08	73.39±2.47	-1.39±1.97	-0.27±1.96	-1.9±2.9	-0.2±3.0
Western Peloponnese	1961-1990	64.82±6.05	65.35±7.49				
	2071-2080	62.03±4.72	63.81±7.88	-2.79±3.10	-1.54±1.35	-4.1±4.0	-2.4±2.1
	2081-2090	60.51±4.81	63.22±8.09	-4.31±2.88	-2.13±1.63	-6.5±3.7	-3.4±2.6
	2091-2100	60.31±4.68	63.90±7.75	-4.51±3.02	-1.44±1.40	-6.8±3.9	-2.2±2.2
Greece	1961-1990	68.47±4.27	69.49±4.63				
	2071-2080	66.45±2.99	68.42±5.02	-2.02±2.28	-1.07±0.79	-2.8±2.9	-1.6±1.2
	2081-2090	65.50±3.04	68.14±5.03	-2.97±2.20	-1.35±0.72	-4.2±2.7	-2.0±1.0
	2091-2100	65.23±2.99	68.68±4.80	-3.24±2.09	-0.81±0.76	-4.6±2.6	-1.2±1.1

Results are given as the mean value and standard deviation of 13 simulations for Scenario A2 and of 8 simulations for Scenario B2, and are based on the PRUDENCE project.

* The small differences in estimates of climate parameters in the reference period 1961-1990 for the different emission scenarios are due to the fact that climate parameters are estimated on the basis of different sets of climate simulations for the different scenarios.

Table 1.7.2.a

Total incident short-wave radiation (S, W/m²), for time periods 1961-1990*, 2071-2080, 2081-2090 and 2091-2100, as well as changes in these values between the periods 2071-2080, 2081-2090, 2091-2100 and the reference period 1961-1990

Climate zones	Periods	S		ΔS		(%)	
		A2	B2	A2	B2	A2	B2
Western and Central Macedonia	1961-1990	183.4±19.4	188.4±21.4				
	2071-2080	186.7±17.9	192.1±17.7	3.2±4.9	3.7±5.6	1.9±3.2	2.3±3.7
	2081-2090	189.4±17.3	193.2±17.3	6.0±5.6	4.8±5.5	3.5±3.9	2.9±3.8
	2091-2100	189.7±18.0	191.6±17.2	6.3±6.6	3.2±6.3	3.6±4.4	2.0±4.1
Eastern Macedonia and Thrace	1961-1990	181.3±18.8	185.4±20.7				
	2071-2080	185.0±17.2	189.4±16.6	3.7±4.7	4±5.7	2.2±3.2	2.4±3.8
	2081-2090	187.6±16.7	190.6±16.7	6.3±5.6	5.2±5.3	3.7±3.9	3.1±3.7
	2091-2100	187.8±17.0	188.8±16.6	6.5±6.6	3.4±5.9	3.8±4.5	2.2±3.9
Northern Aegean	1961-1990	192.3±20.9	199.3±22.3				
	2071-2080	194.6±20.2	202.3±18.5	2.3±4.2	3.0±5.5	1.3±2.5	1.8±3.4
	2081-2090	196.1±19.8	203.1±18.4	3.8±4.9	3.8±5.3	2.1±3.1	2.2±3.3
	2091-2100	195.8±20.4	201.3±18.1	3.5±5.4	2.1±6.0	1.9±3.3	1.3±3.6
Cyclades	1961-1990	204.1±22.4	212.7±22.6				
	2071-2080	206.5±21.6	214.9±18.7	2.4±3.9	2.2±5.4	1.2±2.2	1.3±3.1
	2081-2090	208.0±21.2	216.3±19.2	3.8±5.0	3.7±4.9	2.0±2.9	1.9±2.9
	2091-2100	207.0±21.6	214.2±18.8	2.8±4.7	1.5±5.5	1.5±2.7	0.9±3.1
Eastern Aegean	1961-1990	200.6±21.6	207.7±21.8				
	2071-2080	203.3±20.8	210.5±17.9	2.7±4.1	2.8±5.4	1.4±2.4	1.6±3.1
	2081-2090	205.0±20.4	211.5±18.5	4.4±4.8	3.8±4.6	2.3±2.9	2±2.8
	2091-2100	204.6±20.8	209.6±18.0	4.0±5.4	1.9±5.4	2.1±3.2	1.1±3
Dodecanese	1961-1990	209.9±22.5	218.8±22.2				
	2071-2080	212.2±21.6	220.6±18.8	2.3±4	1.8±4.4	1.2±2.2	1.0±2.3
	2081-2090	213.6±21.4	221.5±19.4	3.7±4.9	2.7±4.1	1.9±2.7	1.4±2.2
	2091-2100	213.1±21.4	219.8±19.5	3.1±5.1	1.0±3.8	1.6±2.8	0.6±2.0
Crete	1961-1990	207.7±23.0	215.2±25.4				
	2071-2080	210.7±21.7	217.5±21.5	3.0±4.1	2.3±4.7	1.5±2.4	1.3±2.7
	2081-2090	212.2±21.4	219.0±21.5	4.5±4.9	3.8±5.0	2.3±2.9	2.0±3.0
	2091-2100	210.9±21.7	216.9±21.9	3.2±4.7	1.7±4.4	1.6±2.8	1.0±2.5
Central and Eastern Greece	1961-1990	192.5±20.6	199.1±21.2				
	2071-2080	195.7±19.9	202.2±17.6	3.3±4.2	3.1±5.3	1.8±2.6	1.8±3.3
	2081-2090	197.6±19.5	203.6±17.4	5.2±5.1	4.5±4.9	2.8±3.2	2.5±3.1
	2091-2100	197.1±20.4	201.6±17.3	4.7±5.4	2.5±5.5	2.5±3.3	1.5±3.4
Attica	1961-1990	198.3±21.8	205.6±21.2				
	2071-2080	201.7±21.3	208.5±17.7	3.4±3.8	2.9±5.1	1.8±2.3	1.6±3
	2081-2090	203.2±21.2	210.1±17.8	4.8±4.8	4.5±4.4	2.5±2.9	2.4±2.7
	2091-2100	202.3±21.9	208.0±17.2	4.0±4.9	2.3±5.3	2.1±2.9	1.4±3.1
Eastern Peloponnese	1961-1990	198.0±20.5	204.4±20.8				
	2071-2080	202.0±19.8	207.9±17.4	4.0±4.0	3.5±5.2	2.1±2.4	1.9±3.1
	2081-2090	204.1±19.8	209.3±17.9	6.0±4.9	5.0±4.0	3.1±3.0	2.6±2.5
	2091-2100	203.3±20.2	207.1±17.7	5.3±5.3	2.7±4.7	2.7±3.1	1.5±2.7
Western Greece	1961-1990	182.9±20.6	186.7±22.6				
	2071-2080	187.4±19.1	191.3±18.5	4.4±4.7	4.6±6.3	2.6±3.2	2.8±4.1
	2081-2090	190.7±18.5	193.0±18.5	7.8±5.6	6.3±5.4	4.5±4.0	3.7±3.9
	2091-2100	191.7±18.5	191.2±19.1	8.8±7.2	4.5±5.4	5.1±5.0	2.7±3.5
Ionian	1961-1990	188.8±19.6	195.0±22.0				
	2071-2080	191.7±19.2	198.9±18.6	2.9±4.4	3.9±5.7	1.6±2.7	2.3±3.6
	2081-2090	194.5±19.0	200.0±18.8	5.6±4.8	5.0±5.0	3.1±3.1	2.8±3.3
	2091-2100	194.7±18.8	198.1±18.8	5.9±6.3	3.1±5.4	3.3±4.0	1.8±3.3
Western Peloponnese	1961-1990	195.4±19.7	200.5±21.8				
	2071-2080	199.2±18.5	204.4±17.9	3.8±4.6	3.9±5.8	2.1±2.9	2.2±3.5
	2081-2090	201.9±18.5	205.8±18.5	6.6±5.4	5.3±4.6	3.5±3.4	2.8±2.9
	2091-2100	201.7±18.5	203.8±18.8	6.3±6.5	3.3±5.0	3.4±4.0	1.9±3.0
Greece	1961-1990	196.1±20.8	203.0±21.9				
	2071-2080	199.0±19.9	206.0±18.3	2.9±4.2	3.0±5.3	1.6±2.5	1.7±3.2
	2081-2090	201.0±19.6	207.2±18.5	4.9±4.9	4.2±4.8	2.6±3.1	2.3±3.0
	2091-2100	200.5±20.0	205.2±18.4	4.5±5.4	2.3±5.2	2.4±3.3	1.4±3.1

All observations made in the respective position of Table 1.7.1.a, b and c also apply here.

Table 1.7.2.b

Wind velocity (V, m/s) for time periods 1961-1990*, 2071-2080, 2081-2090 and 2091-2100, as well as changes in these values between the periods 2071-2080, 2081-2090, 2091-2100 and the reference period 1961-1990

Climate zones	Periods	V		ΔV		(%)	
		A2	B2	A2	B2	A2	B2
Western and Central Macedonia	1961-1990	2.53±0.88	2.71±1.00				
	2071-2080	2.42±0.79	2.66±0.91	-0.10±0.11	-0.04±0.13	-3.4±3.0	-0.9±4.2
	2081-2090	2.44±0.83	2.64±0.90	-0.08±0.09	-0.07±0.14	-3.1±2.8	-1.8±4.6
	2091-2100	2.45±0.83	2.65±0.94	-0.08±0.09	-0.05±0.11	-2.9±2.8	-1.6±4.2
Eastern Macedonia and Thrace	1961-1990	2.80±0.72	2.89±0.87				
	2071-2080	2.77±0.70	2.97±0.83	-0.03±0.05	0.08±0.15	-1.0±1.6	3.4±6.8
	2081-2090	2.82±0.75	2.95±0.83	0.02±0.06	0.07±0.16	0.6±2.1	3.0±7.2
	2091-2100	2.85±0.78	2.95±0.87	0.05±0.10	0.07±0.15	1.7±3.0	2.8±6.9
Northern Aegean	1961-1990	5.59±0.65	5.60±0.72				
	2071-2080	5.55±0.62	5.60±0.64	-0.04±0.12	0.01±0.22	-0.6±2.0	0.3±4.0
	2081-2090	5.62±0.65	5.56±0.67	0.03±0.10	-0.03±0.16	0.6±1.7	-0.5±3.1
	2091-2100	5.68±0.68	5.65±0.69	0.09±0.17	0.05±0.16	1.6±3.0	1.0±3.0
Cyclades	1961-1990	6.64±0.92	6.67±0.81				
	2071-2080	6.73±0.94	6.74±0.87	0.10±0.12	0.07±0.24	1.5±1.8	1.0±3.7
	2081-2090	6.83±1.00	6.75±0.82	0.20±0.12	0.08±0.20	2.8±1.7	1.2±3.1
	2091-2100	6.87±1.00	6.82±0.82	0.23±0.17	0.16±0.11	3.4±2.3	2.4±1.7
Eastern Aegean	1961-1990	5.56±0.80	5.64±0.93				
	2071-2080	5.62±0.71	5.74±0.82	0.07±0.11	0.10±0.14	1.4±1.9	2.1±2.4
	2081-2090	5.71±0.76	5.76±0.82	0.15±0.10	0.12±0.16	2.9±1.9	2.4±3.0
	2091-2100	5.75±0.75	5.82±0.81	0.19±0.12	0.19±0.18	3.7±2.3	3.6±3.5
Dodecanese	1961-1990	5.96±0.85	6.04±0.88				
	2071-2080	5.92±0.84	5.98±0.90	-0.04±0.07	-0.06±0.17	-0.7±1.1	-1.0±2.8
	2081-2090	5.91±0.86	5.99±0.87	-0.06±0.05	-0.05±0.14	-1.0±0.9	-0.9±2.3
	2091-2100	5.92±0.84	6.03±0.85	-0.05±0.12	-0.01±0.13	-0.8±1.9	-0.1±2.2
Crete	1961-1990	4.99±0.84	4.68±1.35				
	2071-2080	4.96±0.72	4.67±1.20	-0.02±0.16	-0.02±0.21	-0.2±2.5	0.3±3.6
	2081-2090	5.00±0.73	4.68±1.20	0.01±0.15	0.00±0.21	0.6±2.5	0.8±3.6
	2091-2100	5.03±0.75	4.71±1.17	0.04±0.17	0.02±0.22	1.1±3.0	1.5±4.4
Central and Eastern Greece	1961-1990	3.22±1.03	3.29±1.17				
	2071-2080	3.17±0.97	3.34±1.10	-0.05±0.08	0.05±0.14	-1.2±1.8	2.4±5.4
	2081-2090	3.22±1.01	3.31±1.07	0.00±0.06	0.01±0.16	0.1±1.7	1.5±6.2
	2091-2100	3.23±1.02	3.34±1.11	0.01±0.08	0.04±0.16	0.3±2.2	2.2±6.6
Attica	1961-1990	3.30±1.18	3.27±1.38				
	2071-2080	3.31±1.19	3.42±1.34	0.01±0.04	0.14±0.20	0.5±1.0	6.1±10.5
	2081-2090	3.38±1.23	3.39±1.31	0.08±0.07	0.12±0.22	2.4±1.5	5.6±11.5
	2091-2100	3.41±1.26	3.43±1.34	0.11±0.10	0.15±0.23	2.9±2.2	6.4±12.5
Eastern Peloponnese	1961-1990	3.42±1.31	3.44±1.55				
	2071-2080	3.35±1.21	3.42±1.39	-0.07±0.17	-0.02±0.21	-1.6±2.9	1.2±6.0
	2081-2090	3.39±1.25	3.40±1.37	-0.03±0.15	-0.04±0.25	-0.6±2.9	0.7±6.8
	2091-2100	3.41±1.27	3.43±1.42	-0.01±0.15	-0.01±0.20	-0.2±3.4	1.0±6.5
Western Greece	1961-1990	2.38±1.05	2.53±1.21				
	2071-2080	2.31±1.02	2.55±1.17	-0.07±0.09	0.02±0.14	-2.7±2.9	1.7±7.3
	2081-2090	2.32±1.04	2.52±1.16	-0.05±0.08	-0.01±0.14	-2.3±2.9	0.8±7.6
	2091-2100	2.32±1.05	2.54±1.18	-0.06±0.10	0.01±0.15	-2.7±3.5	1.2±8.2
Ionian	1961-1990	4.51±0.75	4.63±0.88				
	2071-2080	4.32±0.68	4.45±0.76	-0.20±0.28	-0.18±0.34	-4.2±5.5	-3.5±6.3
	2081-2090	4.29±0.67	4.42±0.80	-0.22±0.24	-0.21±0.31	-4.7±4.5	-4.3±5.6
	2091-2100	4.27±0.69	4.47±0.80	-0.24±0.24	-0.16±0.31	-5.2±4.9	-3.3±6.0
Western Peloponnese	1961-1990	3.62±0.76	3.88±0.74				
	2071-2080	3.52±0.70	3.87±0.67	-0.11±0.12	-0.01±0.20	-2.8±2.8	0.1±5.5
	2081-2090	3.51±0.73	3.84±0.65	-0.12±0.09	-0.03±0.22	-3.1±2.3	-0.4±5.9
	2091-2100	3.51±0.74	3.86±0.69	-0.11±0.11	-0.01±0.21	-3.1±2.8	-0.1±5.7
Greece	1961-1990	4.72±0.66	4.79±0.74				
	2071-2080	4.68±0.60	4.78±0.67	-0.04±0.09	-0.01±0.13	-0.8±1.6	0.1±2.7
	2081-2090	4.72±0.64	4.77±0.66	-0.01±0.07	-0.02±0.11	-0.1±1.2	-0.2±2.3
	2091-2100	4.74±0.65	4.81±0.68	0.01±0.11	0.02±0.11	0.3±2.2	0.7±2.5

All observations made in the respective position of Table 1.7.1.a, b and c also apply here.

Table 1.7.2.c

Cloud cover fraction (C, %) for time periods 1961-1990*, 2071-2080, 2081-2090 and 2091-2100, as well as changes in these values between the periods 2071-2080, 2081-2090, 2091-2100 and the reference period 1961-1990

Climate zones	Periods	C		ΔC		(%)	
		A2	B2	A2	B2	A2	B2
Western and Central Macedonia	1961-1990	41.0±7.7	41.6±5.2				
	2071-2080	37.2±7.4	38.4±6.0	-3.8±1.8	-3.2±1.6	-9.4±4.6	-8.1±4.5
	2081-2090	35.3±6.8	37.8±5.5	-5.7±2.0	-3.8±1.3	-13.9±4.3	-9.3±3.9
	2091-2100	34.5±6.7	38.5±6.3	-6.5±2.4	-3.1±2.0	-15.8±5.2	-7.9±5.5
Eastern Macedonia and Thrace	1961-1990	41.3±7.7	42.0±5.7				
	2071-2080	37.1±7.4	38.6±6.4	-4.2±1.9	-3.3±1.8	-10.1±4.6	-8.2±4.9
	2081-2090	35.3±6.7	37.8±5.8	-6.0±2.2	-4.2±1.3	-14.4±4.5	-10.1±3.6
	2091-2100	34.6±6.5	38.6±6.5	-6.7±2.6	-3.4±2.2	-16.1±5.5	-8.2±5.6
Northern Aegean	1961-1990	36.0±5.5	35.9±3.1				
	2071-2080	32.1±5.6	32.9±4.1	-3.9±1.7	-3.0±1.4	-11.0±4.9	-8.8±4.7
	2081-2090	30.8±5.1	32.3±3.8	-5.2±1.7	-3.6±1.2	-14.7±4.3	-10.3±4.0
	2091-2100	30.4±5.2	33.0±4.3	-5.6±2.0	-2.9±2.2	-15.6±5.4	-8.3±5.9
Cyclades	1961-1990	32.6±4.3	33.2±3.9				
	2071-2080	28.5±4.4	30.3±4.4	-4.1±1.5	-2.9±1.4	-12.9±4.9	-9.0±4.7
	2081-2090	27.4±4.5	29.5±4.0	-5.2±1.6	-3.6±1.1	-16.3±5.5	-11.1±3.2
	2091-2100	27.7±4.5	30.6±3.8	-4.9±1.6	-2.5±1.8	-15.3±5.3	-7.6±5.1
Eastern Aegean	1961-1990	33.3±4.3	34.0±2.1				
	2071-2080	29.0±3.9	30.8±3.1	-4.2±1.6	-3.2±1.5	-12.7±4.6	-9.5±4.8
	2081-2090	27.7±3.7	30.3±2.4	-5.6±1.6	-3.8±1.2	-16.9±4.2	-11.2±3.5
	2091-2100	27.5±3.6	31.2±2.9	-5.8±2.0	-2.9±2.1	-17.2±5.0	-8.4±6.1
Dodecanese	1961-1990	29.0±4.8	29.6±4.9				
	2071-2080	25.1±5.1	27.1±4.7	-3.8±1.4	-2.5±1.2	-13.6±5.2	-8.5±4.2
	2081-2090	23.9±5.1	26.4±5.1	-5.1±1.5	-3.3±1.0	-17.9±5.7	-11.3±4.2
	2091-2100	23.9±4.9	27.3±4.8	-5.1±1.5	-2.4±1.5	-18.1±5.7	-8.0±5.3
Crete	1961-1990	31.2±6.1	32.4±6.9				
	2071-2080	27.4±6.1	29.6±6.2	-3.9±1.4	-2.8±1.4	-12.8±4.8	-8.5±4.0
	2081-2090	26.0±6.2	28.9±6.2	-5.2±1.6	-3.5±1.1	-17.1±5.8	-10.7±2.4
	2091-2100	26.6±5.9	30.0±6.2	-4.7±1.3	-2.4±1.2	-15.3±4.6	-7.3±3.3
Central and Eastern Greece	1961-1990	37.2±5.7	37.5±3.6				
	2071-2080	33.1±5.2	34.4±4.4	-4.1±1.6	-3.1±1.4	-11.1±3.9	-8.5±4.2
	2081-2090	31.7±4.8	33.8±3.9	-5.5±1.9	-3.7±0.9	-14.8±4.0	-10.0±2.8
	2091-2100	31.5±4.9	34.7±4.4	-5.7±2.3	-2.9±1.6	-15.3±5.4	-7.8±4.7
Attica	1961-1990	34.2±5.5	34.3±3.8				
	2071-2080	29.8±4.8	31.3±4.4	-4.3±1.5	-3.0±1.4	-12.6±3.8	-9.0±4.3
	2081-2090	28.8±4.8	30.6±3.9	-5.3±1.9	-3.7±0.7	-15.6±4.5	-11.0±2.4
	2091-2100	28.9±5.1	31.6±4.4	-5.2±2.3	-2.7±1.6	-15.3±6.0	-8.0±5.0
Eastern Peloponnese	1961-1990	35.7±5.4	36.5±3.6				
	2071-2080	31.1±4.6	33.1±4.5	-4.6±1.6	-3.5±1.4	-12.8±3.8	-9.7±4.2
	2081-2090	29.7±4.5	32.4±3.6	-6.0±1.9	-4.1±0.7	-16.9±4.2	-11.4±2.3
	2091-2100	29.7±4.5	33.4±4.0	-6.1±2.3	-3.1±1.6	-16.8±5.3	-8.6±4.5
Western Greece	1961-1990	43.6±6.7	45.0±4.8				
	2071-2080	39.1±5.9	41.1±5.4	-4.4±2.1	-3.8±2.0	-10±4.1	-8.7±4.8
	2081-2090	36.9±5.5	40.3±4.5	-6.6±2.1	-4.6±1.4	-15.1±3.5	-10.3±3.0
	2091-2100	35.7±5.2	41.2±5.0	-7.9±2.8	-3.8±2.0	-17.8±4.9	-8.5±4.5
Ionian	1961-1990	38.6±6.0	39.8±4.1				
	2071-2080	34.9±6.4	36.2±4.5	-3.7±2.0	-3.6±1.4	-9.7±5.3	-9.1±4.0
	2081-2090	33.0±6.0	35.8±4.5	-5.6±1.7	-3.9±0.8	-14.7±4.6	-10.1±2.8
	2091-2100	32.1±6.3	36.6±4.8	-6.5±2.1	-3.2±1.6	-17.1±5.8	-8.3±4.5
Western Peloponnese	1961-1990	37.6±5.3	39.7±2.2				
	2071-2080	33.2±4.8	36.0±3.3	-4.4±2.0	-3.8±1.8	-11.6±4.7	-9.6±4.7
	2081-2090	31.3±4.7	35.4±2.5	-6.4±2.1	-4.4±1.2	-16.9±4.7	-11.0±3.0
	2091-2100	30.8±4.5	36.3±3.0	-6.8±2.5	-3.5±1.8	-17.8±5.6	-8.8±4.5
Greece	1961-1990	35.8±4.4	36.4±2.1				
	2071-2080	31.7±4.3	33.3±3.1	-4.0±1.6	-3.1±1.4	-11.3±4.3	-8.8±4.2
	2081-2090	30.2±4.2	32.7±2.6	-5.5±1.7	-3.8±1.0	-15.5±4.3	-10.4±2.9
	2091-2100	30.0±4.1	33.6±3.1	-5.7±1.8	-2.9±1.7	-16.1±4.8	-8.0±4.8

All observations made in the respective position of Table 1.7.1.a, b and c also apply here.

Table 1.8.a

Mean values and standard deviation of air temperature at 2 m above ground (T, °C) and rainfall (R, mm/year) from the 12 RCM simulations of the ENSEMBLES project for the thirty-year periods 1961-1990*, 2021-2050 and 2071-2100 (SRES A1B)

Climate zones	Periods	T	ΔT	(%)	R	ΔR	(%)
Western and Central Macedonia	1961-1990	12.33±1.52			658.9±143.7		
	2021-2050	13.94±1.56	1.61±0.44	13.3±4.2	605.8±126.3	-53.0±33.9	-7.8±4.1
	2071-2100	15.90±1.71	3.57±0.84	29.4±7.6	539±114.5	-119.8±47.8	-18±4.9
Eastern Macedonia and Thrace	1961-1990	12.91±1.35			709.8±184.7		
	2021-2050	14.51±1.36	1.60±0.44	12.6±4.0	651.2±169.4	-58.6±26.3	-8.2±2.9
	2071-2100	16.39±1.53	3.49±0.85	27.3±7.4	580.4±155.6	-129.4±49.2	-18.3±4.7
Northern Aegean	1961-1990	15.82±1.22			509.7±205.6		
	2021-2050	17.33±1.15	1.51±0.53	9.7±3.8	501.4±198.8	-8.3±30.3	-1.1±5.6
	2071-2100	19.04±1.25	3.23±1.00	20.7±7.1	450.8±189.1	-59.0±39.9	-11.9±7.0
Cyclades	1961-1990	17.58±0.81			449.5±169.2		
	2021-2050	18.91±0.94	1.33±0.30	7.6±1.6	426.9±158.4	-22.6±33.1	-4.4±6.7
	2071-2100	20.51±1.00	2.92±0.59	16.7±3.4	371.4±166.3	-78.2±26.8	-19±8.0
Eastern Aegean	1961-1990	16.83±0.91			585.3±230.6		
	2021-2050	18.27±1.04	1.44±0.38	8.5±2.2	558.1±219.6	-27.3±49.9	-4.2±7.7
	2071-2100	19.97±1.17	3.14±0.75	18.7±4.5	491.3±215.3	-94.1±32.9	-17.1±6.0
Dodecanese	1961-1990	18.26±0.70			479.4±216.8		
	2021-2050	19.58±0.81	1.32±0.32	7.2±1.7	445.0±197.8	-34.3±39.9	-6.4±7.9
	2071-2100	21.22±0.90	2.96±0.65	16.2±3.6	385.1±196.9	-94.3±29.1	-21.2±7.3
Crete	1961-1990	16.35±0.91			567.8±224.3		
	2021-2050	17.73±1.01	1.38±0.35	8.5±2.2	504.7±183.3	-63.1±50.7	-9.8±6.3
	2071-2100	19.47±1.21	3.12±0.67	19.1±4.1	407±164.4	-160.8±79.6	-28.1±8.0
Central and Eastern Greece	1961-1990	14.48±1.37			507.4±111.8		
	2021-2050	16.02±1.41	1.54±0.42	10.8±3.2	480.5±97.9	-26.9±29.6	-5.0±4.9
	2071-2100	17.88±1.58	3.41±0.80	23.7±5.9	421.8±102.4	-85.6±33.7	-17.2±6.5
Attica	1961-1990	15.32±1.19			379.2±108.3		
	2021-2050	16.86±1.24	1.54±0.42	10.1±3.0	353.6±97.9	-25.5±26.7	-6.6±6.3
	2071-2100	18.69±1.44	3.37±0.80	22.1±5.4	302.5±94.8	-76.7±28.4	-20.8±6.8
Eastern Peloponnese	1961-1990	15.72±1.13			479.6±81.1		
	2021-2050	17.19±1.21	1.46±0.36	9.3±2.4	442.1±79.4	-37.6±20.7	-7.9±4.6
	2071-2100	19.00±1.38	3.27±0.70	20.9±4.6	371.8±82.0	-107.9±27.0	-23.0±7.0
Western Greece	1961-1990	12.28±1.25			1185.4±302.9		
	2021-2050	13.8±1.40	1.52±0.43	12.4±3.5	1084.5±304.0	-100.9±41.1	-9.0±4.3
	2071-2100	15.76±1.63	3.48±0.78	28.4±6.3	932.4±264.7	-253.0±87.4	-21.8±5.8
Ionian	1961-1990	17.31±0.90			786.6±247.8		
	2021-2050	18.59±1.01	1.28±0.37	7.4±2.1	738.6±250.4	-48.0±35.9	-6.6±5.3
	2071-2100	20.28±1.08	2.97±0.63	17.2±3.8	652.0±246.2	-134.6±44.3	-18.2±6.8
Western Peloponnese	1961-1990	14.41±1.16			881.1±229.7		
	2021-2050	15.89±1.30	1.48±0.40	10.3±2.7	786.5±218.6	-94.7±48.1	-10.9±5.7
	2071-2100	17.79±1.51	3.39±0.74	23.6±5.1	655.2±202.6	-225.9±59.7	-26.2±6.0
Greece	1961-1990	15.97±0.94			585.2±165.0		
	2021-2050	17.39±1.03	1.42±0.38	8.9±2.4	546.9±154.2	-38.3±27.4	-6.4±4.2
	2071-2100	19.14±1.16	3.17±0.72	19.9±4.7	476.5±155.3	-108.7±26	-19.3±5.5

* The small differences in estimates of climate parameters in the reference period 1961-1990 for the different emission scenarios are due to the fact that climate parameters are estimated on the basis of different sets of climate simulations for the different scenarios.

Table 1.8.b

Mean values and standard deviation of relative humidity at 2 m above ground (RH, %) and total incident short-wave radiation (S, W/m²), from the 12 RCM simulations of the ENSEMBLES project for the thirty-year periods 1961-1990*, 2021-2050 and 2071-2100 (SRES A1B)

Climate zones	Periods	RH	ΔRH	(%)	S	ΔS	(%)
Western and Central Macedonia	1961-1990	67.01±7.21			180.7±17.3		
	2021-2050	65.27±7.06	-1.74±0.63	-2.6±1.0	182.5±16.8	1.8±1.5	1.0±0.8
	2071-2100	63.53±6.59	-3.48±1.51	-5.1±2.3	184.3±15.3	3.6±2.8	2.1±1.6
Eastern Macedonia and Thrace	1961-1990	68.57±6.25			178.6±16.9		
	2021-2050	66.93±6.24	-1.64±0.46	-2.4±0.7	180.3±16.4	1.8±1.4	1.0±0.8
	2071-2100	65.25±5.80	-3.32±1.21	-4.8±1.8	182.2±15.1	3.6±2.8	2.1±1.6
Northern Aegean	1961-1990	74.20±3.85			186.5±18.6		
	2021-2050	73.26±3.86	-0.94±0.61	-1.3±0.8	187.3±18.4	0.9±1.3	0.5±0.7
	2071-2100	72.52±3.88	-1.68±1.32	-2.3±1.8	188.2±18.5	1.8±2.2	1.0±1.1
Cyclades	1961-1990	73.93±3.08			196.0±20.8		
	2021-2050	73.64±2.96	-0.29±0.41	-0.4±0.6	197.0±20.9	1.0±1.0	0.5±0.5
	2071-2100	73.48±2.66	-0.45±0.6	-0.6±0.8	198.1±21.5	2.1±1.9	1.1±0.9
Eastern Aegean	1961-1990	71.75±3.82			194.3±19.2		
	2021-2050	71.01±3.91	-0.75±0.27	-1.0±0.4	195.3±19.3	1.1±1.1	0.6±0.6
	2071-2100	70.14±3.68	-1.62±0.81	-2.2±1.1	196.7±19.3	2.4±2.0	1.2±0.9
Dodecanese	1961-1990	72.75±2.79			201.0±22.0		
	2021-2050	72.50±2.75	-0.25±0.32	-0.3±0.4	202.1±22.0	1.1±0.8	0.5±0.4
	2071-2100	72.32±2.41	-0.42±0.76	-0.6±1.0	203.4±22.8	2.4±1.7	1.2±0.8
Crete	1961-1990	71.56±3.69			200.6±19.0		
	2021-2050	70.79±3.68	-0.77±0.38	-1.1±0.5	202.2±19.0	1.6±1.3	0.8±0.6
	2071-2100	69.95±3.85	-1.61±1.05	-2.3±1.5	203.9±19.1	3.3±2.5	1.7±1.2
Central and Eastern Greece	1961-1990	66.68±5.93			188.3±17.7		
	2021-2050	65.43±5.85	-1.25±0.58	-1.9±0.9	189.7±17.3	1.4±1.5	0.8±0.8
	2071-2100	64.06±5.54	-2.63±1.46	-3.9±2.3	191.2±16.0	2.9±2.6	1.6±1.4
Attica	1961-1990	66.51±4.32			192.4±17.3		
	2021-2050	65.28±4.26	-1.23±0.64	-1.9±1.0	193.7±17.0	1.3±1.6	0.7±0.8
	2071-2100	63.98±4.04	-2.53±1.59	-3.8±2.5	195.2±16.6	2.8±2.9	1.5±1.5
Eastern Peloponnese	1961-1990	67.50±5.48			195.3±18.5		
	2021-2050	66.50±5.59	-1.01±0.49	-1.5±0.8	196.7±18.3	1.5±1.3	0.8±0.7
	2071-2100	65.31±5.45	-2.20±1.23	-3.3±1.9	198.4±17.5	3.1±2.4	1.6±1.2
Western Greece	1961-1990	71.38±6.17			179.1±18.7		
	2021-2050	69.92±6.23	-1.46±0.46	-2.1±0.7	181.6±18.3	2.5±1.6	1.4±0.9
	2071-2100	67.96±6.18	-3.41±0.98	-4.8±1.4	184.1±16.8	5.0±2.5	2.9±1.4
Ionian	1961-1990	73.16±3.56			186.9±19.7		
	2021-2050	72.84±3.72	-0.32±0.44	-0.5±0.6	188.3±19.6	1.4±0.9	0.7±0.5
	2071-2100	72.47±3.72	-0.69±0.72	-1.0±1.0	189.6±19.5	2.7±2.0	1.5±1.0
Western Peloponnese	1961-1990	70.55±5.2			189.9±19.3		
	2021-2050	69.25±5.27	-1.29±0.35	-1.9±0.5	192.2±19.0	2.2±1.3	1.2±0.7
	2071-2100	67.45±5.26	-3.09±0.94	-4.4±1.4	194.5±18.0	4.5±2.2	2.5±1.2
Greece	1961-1990	71.40±3.71			191.1±18.8		
	2021-2050	70.61±3.70	-0.79±0.25	-1.1±0.4	192.4±18.8	1.3±1.0	0.7±0.5
	2071-2100	69.78±3.42	-1.62±0.73	-2.3±1.0	193.8±18.7	2.7±2.1	1.5±1.0

* The small differences in estimates of climate parameters in the reference period 1961-1990 for the different emission scenarios are due to the fact that climate parameters are estimated on the basis of different sets of climate simulations for the different scenarios.

Table 1.8.c

Mean values and standard deviation of wind velocity (V, m/s) and cloud cover (CC, %) from the 12 RCM simulations of the ENSEMBLES project for the thirty-year periods 1961-1990*, 2021-2050 and 2071-2100 (SRES A1B)

Climate zones	Periods	V	ΔV	(%)	CC	ΔCC	(%)
Western and Central Macedonia	1961-1990	2.90±0.83			41.4±8.3		
	2021-2050	2.88±0.81	-0.01±0.04	-0.4±1.2	39.2±8.0	-2.2±0.6	-5.3±1.3
	2071-2100	2.82±0.77	-0.07±0.09	-2.1±2.7	36.7±7.8	-4.7±1.2	-11.4±3.0
Eastern Macedonia and Thrace	1961-1990	3.54±0.86			41.7±7.5		
	2021-2050	3.56±0.86	0.02±0.03	0.5±0.9	39.4±7.3	-2.2±0.5	-5.4±1.3
	2071-2100	3.57±0.82	0.02±0.08	0.9±2.0	36.9±7.1	-4.8±1.1	-11.6±3.0
Northern Aegean	1961-1990	6.21±0.96			39.2±5.9		
	2021-2050	6.26±0.95	0.05±0.08	0.8±1.4	37.0±5.7	-2.1±0.6	-5.5±1.7
	2071-2100	6.38±0.96	0.18±0.18	2.9±2.9	34.7±5.7	-4.5±1.1	-11.7±3.1
Cyclades	1961-1990	6.51±1.24			36.5±6.3		
	2021-2050	6.51±1.24	0.01±0.06	0.1±0.9	34.2±6.4	-2.3±0.6	-6.4±2.0
	2071-2100	6.64±1.28	0.13±0.12	2.0±1.8	31.8±6.4	-4.7±1.0	-13.2±3.8
Eastern Aegean	1961-1990	5.74±1.13			35.6±5.5		
	2021-2050	5.75±1.11	0.01±0.05	0.3±1.1	33.3±5.4	-2.3±0.5	-6.5±1.5
	2071-2100	5.87±1.13	0.13±0.12	2.4±2.0	30.8±5.3	-4.8±1.1	-13.7±3.7
Dodecanese	1961-1990	6.08±0.69			34.6±7.4		
	2021-2050	6.03±0.65	-0.05±0.11	-0.8±1.8	32.2±7.4	-2.4±0.5	-7.2±2.0
	2071-2100	6.01±0.62	-0.07±0.18	-1.1±2.9	29.7±7.5	-4.9±1.1	-14.7±5.0
Crete	1961-1990	4.61±1.25			36.6±5.9		
	2021-2050	4.59±1.24	-0.02±0.04	-0.3±0.9	34.1±5.5	-2.5±0.7	-6.8±1.6
	2071-2100	4.64±1.23	0.04±0.08	0.9±1.7	31.4±5.2	-5.2±1.4	-14.2±3.2
Central and Eastern Greece	1961-1990	3.47±1.08			37.9±7.5		
	2021-2050	3.47±1.07	0.00±0.03	0.1±0.8	35.8±7.1	-2.1±0.6	-5.6±1.5
	2071-2100	3.46±1.04	-0.01±0.06	0.2±1.8	33.5±6.8	-4.4±1.2	-11.6±3.1
Attica	1961-1990	3.73±1.15			36.9±7.0		
	2021-2050	3.75±1.14	0.02±0.03	0.5±0.8	34.7±6.6	-2.2±0.7	-6.0±1.8
	2071-2100	3.80±1.14	0.07±0.07	2.2±1.9	32.5±6.3	-4.4±1.3	-12.0±3.4
Eastern Peloponnese	1961-1990	4.16±1.27			35.3±6.7		
	2021-2050	4.15±1.27	0.00±0.04	-0.1±0.9	33.1±6.3	-2.2±0.7	-6.2±1.9
	2071-2100	4.18±1.27	0.02±0.11	0.6±2.2	30.9±6.1	-4.4±1.3	-12.6±3.7
Western Greece	1961-1990	3.09±1.11			44.9±7.9		
	2021-2050	3.06±1.10	-0.04±0.04	-1.1±1.3	42.4±7.6	-2.5±0.8	-5.7±1.6
	2071-2100	3.01±1.07	-0.09±0.07	-2.5±1.7	39.4±7.6	-5.5±1.1	-12.4±2.9
Ionian	1961-1990	4.95±0.86			40.6±6.0		
	2021-2050	4.88±0.84	-0.07±0.06	-1.3±1.1	38.3±6.0	-2.3±0.7	-5.8±1.8
	2071-2100	4.78±0.80	-0.17±0.09	-3.4±1.4	35.5±5.9	-5.1±1.0	-12.9±2.9
Western Peloponnese	1961-1990	3.60±1.09			40.8±7.0		
	2021-2050	3.57±1.08	-0.03±0.04	-0.8±1.1	38.3±6.7	-2.5±0.8	-6.2±1.9
	2071-2100	3.53±1.06	-0.07±0.07	-2.0±1.6	35.4±6.6	-5.5±1.1	-13.6±3.1
Greece	1961-1990	5.02±0.87			38.0±5.8		
	2021-2050	5.00±0.86	-0.01±0.04	-0.3±0.9	35.8±5.7	-2.3±0.5	-6±1.4
	2071-2100	5.01±0.84	0.00±0.07	0.1±1.4	33.3±5.6	-4.8±1.0	-12.7±3.1

* The small differences in estimates of climate parameters in the reference period 1961-1990 for the different emissions scenarios are due to the fact that climate parameters are estimated on the basis of different sets of climate simulations for the different scenarios.

ation in the six climate parameters for the 13 climate zones can be found on the website pages of the Bank of Greece dedicated to the Climate Change Impacts Study Committee (CCISC).²⁶

Presented in Tables 1.7.1.a, b, c and 1.7.2.a, b, c are the annual mean values of the six climate parameters for the reference period 1961-1990 and for the decades 2071-2080, 2081-2090 and 2091-2100, as well as the variation in annual mean values in the case of Scenarios A2 and B2 between the periods 2071-2080, 2081-2090, 2091-2100 and the reference period 1961-1990 for each of the country's 13 climate zones. The respective estimates for the periods 1961-1990, 2021-2050 and 2071-2100 in the case of Scenario A1B are presented in Table 1.8.a, b, c. The results of the assessment are discussed separately for each of the six climate parameters immediately below.

Mean air temperature

The climate simulations under all four emission scenarios (Tables 1.7.1.a, b, c, 1.7.2.a, b, c and 1.8.a, b, c) point to an overall mean warming in Greece over the coming decades, relative to the reference period 1961-1990. This increase in temperature is projected to be most pronounced under Scenario A2 and smallest under Scenario B1. Warming is also projected to be greater in the continental regions than in the islands, and greater in summer and autumn than in winter and spring.

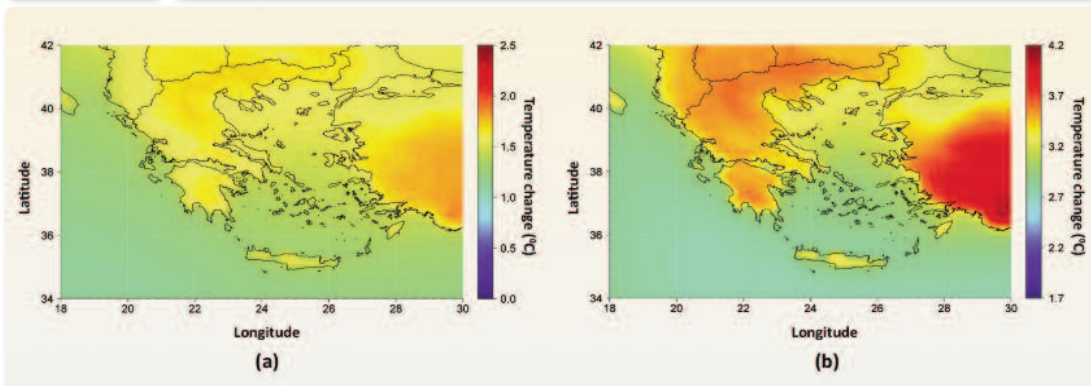
Under the more extreme Scenario A2, in the decade 2091-2100 the mean air temperature countrywide is projected to be 3.9°C higher in winter and spring, 5.4°C higher in summer, 4.7°C higher in autumn and 4.5°C higher year-round. The increase in winter temperature is projected to range between 4°C and 4.5°C in the continental regions, but will be less pronounced in the island regions where it will not exceed 3.5°C, except in the Northern Aegean, where it will reach 4 °C. Spring temperatures are expected to be 4.5°C higher in the continental regions and 3.5°C higher in the island regions. The temperature increase in summer is expected to be greater than in the other seasons, and is projected to range from 6°C to 7°C in the continental regions and from 4.5°C to 5°C on the islands. Lastly, the temperature increase in autumn is projected to be more uniform across the different climate zones and should range between 4.3°C and 5.2°C.

As for the somewhat milder Scenario A1B, the projected variation in annual mean air temperature, relative to the reference period 1961-1990, can be seen in Figure 1.25 (for the period 2021-2050 on the left panel, and for the period 2071-2100 on the right panel). As can be seen on the left panel (a), all of Greece's regions should have 1.5°C higher annual mean temperatures in 2021-2050. As mentioned earlier, the temperature increase will be greater in summer and smaller in winter. It should also be noted that the differences in estimated air temperature vari-

²⁶ <http://www.bankofgreece.gr/Pages/en/klima/>

Figure 1.25

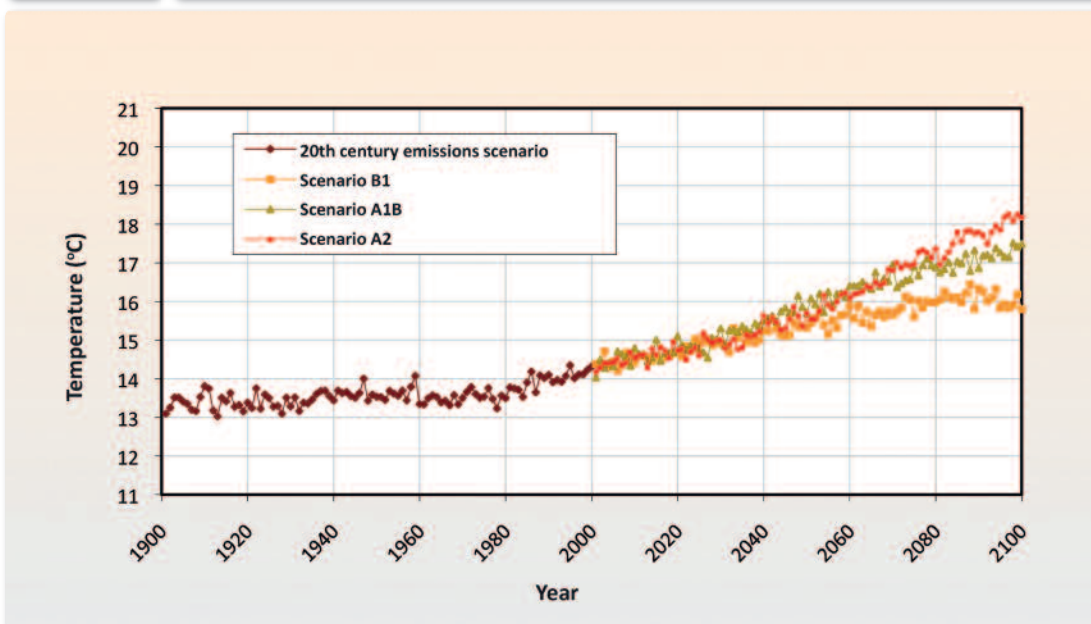
Variation in mean air temperature in (a) 2021-2050 and (b) 2071-2100, relative to 1961-1990



Mean value of 12 RCMs from the ENSEMBLES project. Scenario A1B.

Figure 1.26

Variation across time in the average annual temperature in Greece in the course of the 2000-2100 period under Scenarios B1, A1B and A2



Average of 10 simulations with AOGCMs.

ation presented by the various emission scenarios are small for the near future (Figure 1.26, Kapsomenakis, 2009). During the decade 2091-2100, the mean temperature countrywide is projected to be higher than in the reference period by 3.2°C in winter, 4.2°C in summer and ~3.5°C in spring and autumn, as well as on annual basis. The increase in winter temperature will range across the different climate zones between 3°C and 3.5°C, with higher values projected for Northern Greece and lower values projected for the islands. The increase in summer tempera-

ture is expected to approach 4.5-5°C in the continental regions, but should not exceed 4°C on the islands.

Under Scenario B2, the annual mean warming at the end of the 21st century is projected to be ~1.3°C lower than under Scenario A2. The difference in projected warming between the two scenarios will be smallest in winter and spring (1°C) and more pronounced in autumn (1.5°C) and summer (1.7°C).

Lastly, the warming projected under Scenario B1 will be less pronounced than under all of the other scenarios considered. In particular, the mean air temperature countrywide for the decade 2091-2100 will be higher, with respect to the reference period, by 2°C in winter, 2.2°C in spring, 3°C in summer and 2.4°C in autumn as well as on an annual basis. An analysis of the results found the differences in temperature variations across the different climate zones to be smaller under Scenario B1 than under the other scenarios considered.

It should be noted that under all four scenarios the warming trend increases throughout the 21st century. During the period 2071-2100 in particular, this trend is stronger under Scenarios A2 (0.5°C/decade) and A1B (0.4°C/decade), milder under Scenario B2 (0.25°C/decade) and milder yet under Scenario B1, the only scenario under which the warming trend slackens off toward the end of the century (0.1°C/decade). The difference in projected warming between the four scenarios is therefore greatest at the close of the 21st century, as can be seen in Figure 1.26.

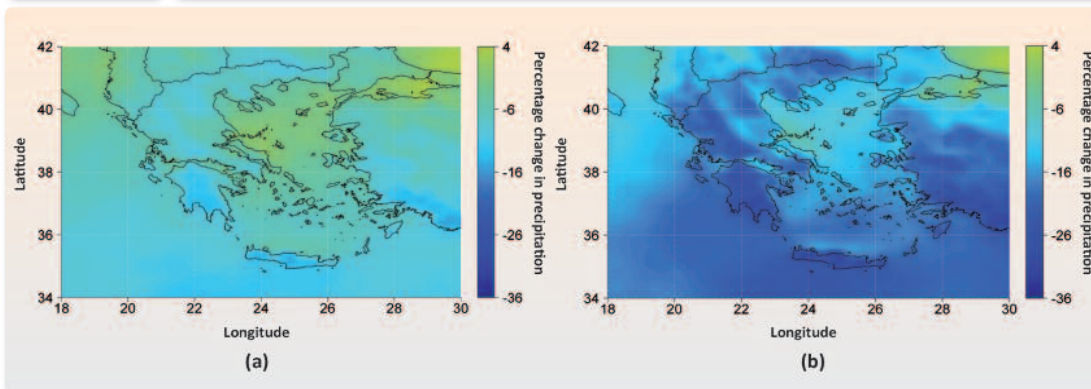
Precipitation

According to the results of the climate model simulations, annual precipitation levels countrywide are projected to decline under all three emission scenarios considered. The decrease is particularly important under Scenarios A2 and A1B and milder under Scenario B2.

In the case of Scenario A2, precipitation levels countrywide during the period 2071-2100 are expected to decrease, relative to the reference period, by 16% in winter, 19% in spring, 47% in summer, 10% in autumn and 17% on an annual basis. The percentage decrease in annual mean precipitation is projected to be greatest in the western continental areas and in the Eastern Peloponnese (over 20%), followed by the rest of Greece (15-20%), with the exception of the Northern Aegean where the decrease in annual precipitation should not exceed 10%. In winter, when Greece receives most of its precipitation, the percentage decrease is projected to be greatest in the eastern continental regions, the Western Peloponnese and the Southern Aegean (over 18%), smallest in the Northern Aegean (under 8%), while ranging between 9% and 12% in the rest of Greece. The greatest percentage decrease in precipitation is projected for summer, when it will exceed 40% in the larger part of Greece. In absolute terms, however, the decrease in summer precipitation will – with the exception of Northern Greece – be small, as even today summer precipitation ranges from limited to minimal. In spring, precipitation should decrease by more than 20% in the larger part of Greece, and in other regions by ~15%. Lastly, autumn precipita-

Figure 1.27

Percentage changes in average annual total precipitation in (a) 2021-2050 and (b) 2071-2100, relative to 1961-1990



Mean value of the 12 RCMs from the ENSEMBLES project. Scenario A1B.

tion is expected to decrease significantly by over 18% in Western Greece, the Western Peloponnese and Eastern Macedonia-Thrace.

Turning to Scenario A1B, the percentage changes in annual mean precipitation projected for the periods 2021-2050 and 2071-2100, relative to the reference period, are represented in Figure 1.27. In 2021-2050, precipitation levels countrywide will decrease relative to the reference period by about 5% (Table 1.8.a). In percentage terms, annual mean precipitation is projected to decrease most in Crete and the Peloponnese (close to 15%), followed by the rest of Greece (between 5% and 10%), but to increase slightly in the Northern Aegean (Figure 1.27, panel (a)). The decrease in precipitation countrywide is projected to be greatest toward the end of the century. More specifically, in 2071-2100, mean precipitation is projected to decrease by 16% in winter, 26.5% in spring, 37% in summer, 12.5% in autumn and 19% on an annual basis. The percentage decrease in annual mean precipitation will be greatest in Crete and the Peloponnese (close to 25%), while ranging around 20% in the rest of Greece and remaining below 15% in the Northern Aegean (See Figure 1.27, panel (b)). The percentage decrease in winter precipitation is expected to be largest in Greece's southern island areas and the Peloponnese (over 20%), followed by Western Greece, the Ionian and the Eastern Aegean islands (about 15%), and the rest of Greece (about 10%). The percentage decrease in summer precipitation should be around or even above 40% in most of Greece, while even in the Northern Aegean, i.e. the region with the smallest projected percentage decrease, it will exceed 20%. Spring precipitation should decrease in most of Greece by more than 20%. Lastly, in autumn, the percentage decrease is projected to be greatest in Crete and the Western Peloponnese (20%), whereas in Central and Eastern Greece and the Northern Aegean it will not exceed 7%.

Under Scenario B2, the decrease in precipitation projected for the period 2071-2100, relative to the reference period, will be smaller. A significant decrease in winter and spring precipitation (of

~10%) is projected only for Southern Greece. Autumn precipitation will decrease significantly only in Western Greece (by ~8%), and in contrast will increase by as much as 10% in the island regions. Lastly, summer precipitation is projected to decrease significantly countrywide. In absolute terms, however, the decrease in summer precipitation will be sizeable only in Northern Greece.

Relative humidity at 2 m above ground

Annual mean relative humidity is projected to decrease in Greece under all three Scenarios A2, A1B and B2, with the changes projected under Scenario B2 expected to be much more moderate than under Scenario A2, and the changes projected under Scenario A1B figuring somewhere in the middle. As also indicated by the simulations, the variation in relative humidity – under all three scenarios – will be much milder in the island regions than in the continental climate zones, and much milder in the near future than at the close of the 21st century.

In greater detail, under extreme Scenario A2, annual mean relative humidity is projected to decrease countrywide by 4.5% in 2091-2100, relative to the reference period 1961-1990. The percentage decrease in annual mean relative humidity is projected to be about 10% in the western and northern continental regions, between 6% and 8% in the remaining continental regions, but less than 4% in the islands. Winter relative humidity is estimated to decrease by 6% to 8% in the continental regions – with the exception of the Western Peloponnese (3.5%) – whereas an even smaller decrease is projected for the island regions. The largest percentage decrease in relative humidity is expected in summer, with relative humidity more than 20% lower in the western and northern continental regions, close to 15% lower in the remaining the continental regions, but only between 3% and 7% lower on the islands. In spring, similarly, the decrease in relative humidity should be more pronounced in Western and Northern Greece (close to 10%) and in the remaining continental regions (around 8%) than on the islands (below 5%). Lastly, in autumn, the changes in relative humidity are projected to be similar to those in winter.

Turning to Scenario A1B, the largest percentage decrease in relative humidity is, once again, projected for summer. More specifically, summer mean relative humidity in 2091-2100 is expected to be 12% lower in Greece's western and northern continental regions, 6% to 8% lower in the remaining continental regions, and 3% to 5% lower in the islands. The change in winter relative humidity, however, is not expected to be substantial on a countrywide basis. In spring, mean relative humidity is projected to be 6% lower in the continental regions, 4% lower in the islands of the Northern Aegean, the Eastern Aegean and Crete, and less than 2% lower in the remaining islands. Lastly, autumn relative humidity is expected to decrease slightly in the western and northern continental regions, but to remain essentially unchanged elsewhere.

In the case of Scenario B2, the changes in seasonal and annual relative humidity are projected to be small, with the exception of the summer, when the decrease in relative humidity is projected to reach as much as 10% in continental Greece.

The decrease in relative humidity is attributable in part to the rise in temperatures, which results in higher saturation specific humidity. Thus, when the water vapour content of the atmosphere can no longer increase, as in the case of Greece's continental regions particularly in summer, mean relative humidity drops.

Cloud cover

As shown by the results of the climate simulations for the three scenarios considered, cloud cover is projected to decrease countrywide in the coming decades, relative to the reference period 1961-1990. The decrease in cloud cover is projected to be more pronounced under Scenario A2 and least pronounced under Scenario B2.

Based on the projections, the percentage decrease in annual mean cloud cover countrywide in 2091-2100 relative to the reference period will reach 16% and 8% under Scenarios A2 and B2, respectively. It should be noted that the spatial distribution of the projected changes was found to be similar under both scenarios. Depending on the climate zone, the percentage decrease in winter cloud cover ranges between 10% and 14% under Scenario A2, and between 4% and 8% under Scenario B2. Similar results were obtained for spring. The largest percentage decreases in cloud cover are projected for summer, reaching 36% and 20%, respectively, under Scenarios A2 and B2 countrywide. In absolute terms, however, the change in summer cloud cover will be small, with the exception of the western and northern regions, given that low level of summer cloud cover even today. Lastly, autumn cloud cover is expected to fall to 14% and 7%, respectively, under Scenarios A2 and B2.

Future cloud cover is projected to decrease under Scenario A1B as well, with the percentage decreases in mean cloud cover in the different climate zones generally assuming intermediate values, between those obtained under Scenario A2 and under Scenario B2.

Incident short-wave radiation

According to the results of the studied simulations, incident short-wave radiation is — according to Scenarios A2, A1B and B2— expected to increase slightly in Greece. It should be noted that this increase is, to some extent, correlated with the anticipated decrease in cloud cover.

In greater detail, under Scenario A2, annual incident radiation is projected to increase countrywide by 4.5 W/m² in 2091-2100, relative to the reference period. The increase is expected to exceed 6 W/m² in Northern Greece, but at the other end, to be less than 3 W/m² in the southern island regions. In addition, the increase will in general be greater in Western than in Eastern Greece. In winter, the increase in incident radiation is expected to be greater in the southern regions, in some cases reaching 5 W/m², and smaller in the northern regions where it should not exceed 3 W/m². Summer incident radiation is projected to increase countrywide by 3.5 W/m², with the most significant increase projected for Western and Northern Greece (8-10 W/m²), in

contrast with the southern island regions, where incident radiation should remain broadly unchanged. The highest increase in incident radiation countrywide is projected to take place in spring, reaching 9 W/m^2 , with the highest levels of increase anticipated for Western Greece (15 W/m^2), followed by other western and northern regions (above 10 W/m^2) and the rest of the country (between 6.5 W/m^2 and 9 W/m^2). Lastly, in autumn, the increase in incident short-wave radiation is projected to be relatively smaller (2 W/m^2 countrywide).

Turning to Scenario A1B, annual mean incident solar radiation is projected to increase countrywide by 2.4 W/m^2 in the period 2091-2100. The increase will range between 4.5 W/m^2 in Western Greece and 2 W/m^2 in the Cyclades, the Eastern Aegean and the Dodecanese. In winter, the increase in incident solar radiation in the larger part of Greece should range between 3 W/m^2 and 5 W/m^2 , with the exception of Northern Greece, where it is not expected to exceed 2.5 W/m^2 . In summer, incident solar radiation is not projected to change significantly countrywide. The highest increase in incident solar radiation countrywide is projected to occur in spring, when it would reach 10 W/m^2 . The increase will be greatest in the western continental regions, where it is expected to exceed 13 W/m^2 , but will also be substantial in the rest of Greece, where it will range between 8 W/m^2 and 11 W/m^2 . Lastly, incident short-wave radiation in autumn is expected to decline. The decrease will be uniform countrywide and is expected to reach 3 W/m^2 .

Lastly, under Scenario B2, the increase in incident solar radiation that is projected countrywide is smaller than under Scenario A2. More specifically, as indicated by the simulations, annual incident solar radiation countrywide will be 2.3 W/m^2 higher at the end of the 21st century, relative to the reference period. Season-wise, the greatest increase in incident solar radiation is projected to occur in spring and the smallest in autumn. In terms of spatial distribution, the highest increase in incident solar radiation is expected to occur in Western and Northern Greece, whereas the smallest increase is projected for the southern island regions.

Wind speed

No change is projected in the annual mean wind speed countrywide, according to all three Scenarios (A2, A1B and B2). However, certain specific regions are expected to experience significant changes in wind speed toward the end of the 21st century, on a seasonal and annual basis.

More specifically, under extreme Scenario A2, the annual mean wind speed is projected to increase in Eastern Greece (except in the Dodecanese, where it will remain unchanged), and to decline in the western regions. In winter, the mean wind speed will decrease countrywide, by as much as 7% in the western regions but by no more than 2% in the Cyclades and the Eastern Aegean islands. In summer, on the other hand, the mean wind speed countrywide will increase by about 5%. This increase is attributed to the strengthening of the Etesians in the Aegean, as

projected by the models. In greater detail, the mean summer wind speed will increase by more than 10% in the Cyclades and the Eastern Aegean islands, and by close to 5% in the other eastern regions (except for the Dodecanese). In Western Greece and the Dodecanese, the wind speed will not change substantially. In the intermediate seasons, the mean wind speed country-wide is projected to remain essentially unchanged. However, in the Cyclades and the Eastern Aegean islands an increase in wind speed is projected both for spring and autumn, on account of the higher intensity and frequency of the Etesians early and late in the season. In other eastern regions, the wind speed should increase slightly in autumn, but is not expected to change substantially in spring. By contrast, wind intensity in Western Greece is expected to decline, particularly in spring.

Turning to the projections under the milder scenario (B2), the changes in seasonal and annual mean wind speed in different regions of Greece will have the same sign as under Scenario A2, but lower absolute values, with the exception of the summer wind speed in the Aegean, where the variation in intensity of the Etesians is projected to be roughly equal under both Scenarios.

Lastly, similar results were also obtained using the intermediate Scenario (A1B). On a seasonal basis, the mean wind speed countrywide will increase in summer by nearly 4%, on account of a strengthening of the Etesians in the Aegean. It should be noted that, whereas the PRUDENCE models (Scenarios A2 and B2) place the highest strengthening of the Etesians in the Central Aegean, the ENSEMBLES models (Scenario A1B) project the highest strengthening (above 10%) to take place in the Northern Aegean. The winter mean wind speed will, in contrast, decline countrywide, and will be more pronounced in the Ionian and in Western Greece (5%) than in eastern continental Greece and the Aegean islands (3%). During the intermediate seasons, the changes in wind speed will be similar to those estimated under Scenarios A2 and B2. It is worth noting the upward trend in the intensity of the Etesians over the period 2071-2100 under all three scenarios.

1.16 Assessment of extreme weather events and their regional impact in Greece

The severity of the climate change impact is more likely to be associated with changes in the frequency of extreme weather events than with a drawn-out ‘average’ climate evolution, given that, in the case of extreme events, a simple change in mean value above a critical threshold can bring about a disproportionate, non-linear impact.

The complexity of the natural and social systems’ interactions with the climate system makes it difficult to assess and describe the impacts of climate change in a comprehensive and

straight-forward manner. Instead, one has to use indicators gauging changes in observable and measurable characteristics of natural systems and human societies that are heavily dependent on climate change and can point to changes in the broader system. For instance, a longer or shorter growing season can serve as an indicator of a climate change impact on agriculture.

For the purpose of the present study, we used the datasets from the regional climate model RACMO2, developed by the Royal Meteorological Institute of the Netherlands (KNMI), with a horizontal resolution of 0.25° (~25 km). These datasets were compiled in the context of the EU-financed project ENSEMBLES,²⁷ in which the National Observatory of Athens took part. The objective of the ENSEMBLES project was the study of climate change in Europe and the quantification of uncertainty in climate projections. The specific model was selected because, during an assessment exercise of all the models forming the basis for the simulations under the ENSEMBLES project, RACMO2 was found to be more accurate in simulating temperature and rainfall extremes. The datasets cover a 30-year reference period, 1961-1990, for the current climate, and two future periods, 2021-2050 and 2071-2100, for the study of climate change using Scenario A1B of the IPCC. For each of Greece's 13 climate zones, we computed the change in the relevant climate indices between each future period (2021-2050 and 2071-2100) and the reference period (1961-1990). Scenario A1B is a mid-line scenario in terms of carbon dioxide emissions and economic growth (Alcamo et al., 2007). The first future period, 2021-2050, was chosen with the specific needs of policy-makers in mind, in order to assist them with nearer-term planning, whereas the second period, 2071-2100, serves to underscore the extent of the changes toward the end of the 21st century. Using the data from this model, it was possible to study the variation in climate parameters and indices between the reference period and each one of the two future periods, and to determine climate change for each of Greece's 13 climate zones.

Maximum summer and minimum winter temperatures

As can be seen from the projected changes in mean minimum winter temperature represented in Figure 1.28, minimum winter temperatures in all of Greece's regions will be ~1.5°C higher in 2021-2050 and ~3.5°C higher in 2071-2100, than in the reference period 1961-1990. These results concur with large-scale findings, which have recorded a significant upward trend in minimum temperatures over the past few decades. The warming trend will be more pronounced in the more mountainous areas, especially in the mountain ranges of Pindos and of Northern Greece, where it is projected to reach 2°C in 2021-2050 and 4°C in 2071-2100.

The increase in this parameter is likely to have an impact on forests, presently adapted to colder weather conditions. If the conditions become prohibitive, certain categories of forests (e.g. fir) would have to shift to higher altitudes.

²⁷ www.ensembles-eu.org

Figure 1.28

Variation in the mean minimum winter temperature in (a) 2021-2050 and (b) 2071-2100, relative to 1961-1990 (in °C)

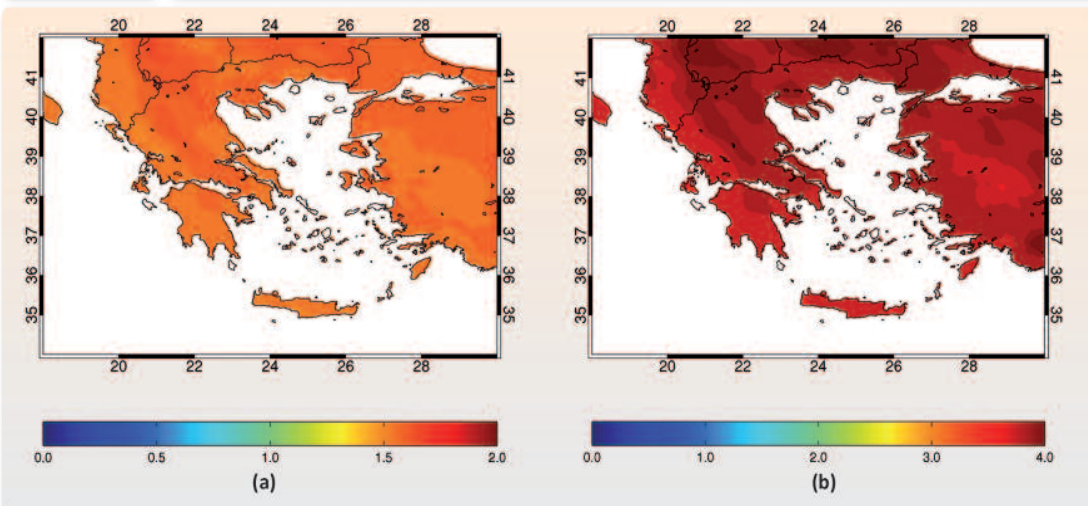
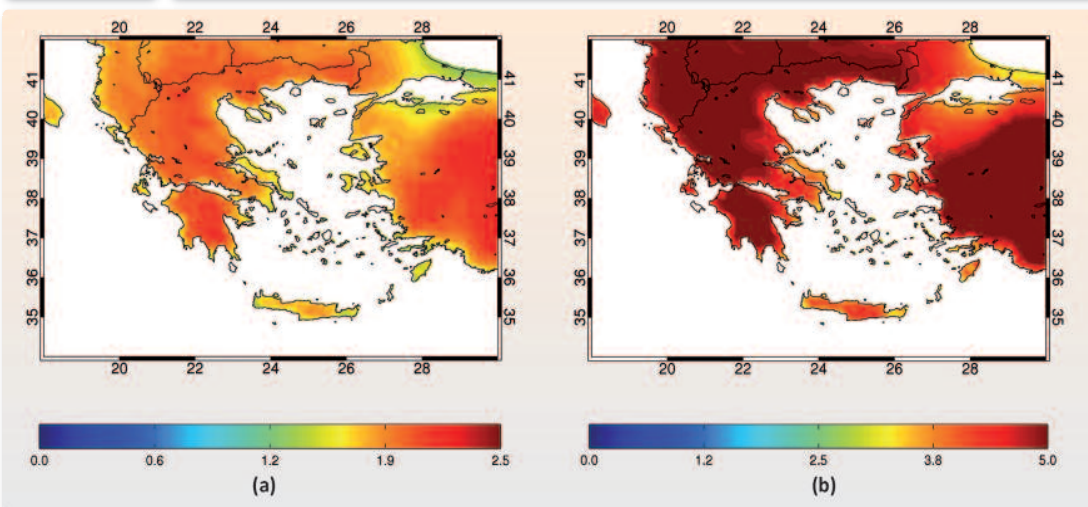


Figure 1.29

Variation in the mean maximum summer temperature in (a) 2021-2050 and (b) 2071-2100, relative to 1961-1990 (in °C)



The projected changes in mean maximum summer temperatures are represented in Figure 1.29. The increase in mean maximum summer temperatures in the period 2021-2050 will be greater than that of the winter minimums and will exceed 1.5°C and in some cases reach as much as 2.5°C. In the period 2071-2100, the increase in mean maximum summer temperatures may be as much as 5°C. Most affected will be the continental inland regions,

situated far from the cooling effects of the sea, whereas regions with strong sea breezes (Crete, Aegean islands) will experience a significantly smaller variation in maximum summer temperatures.

Warm days and warm nights

The projected variation in the number of days with maximum temperatures above 35°C, as represented in Figure 1.30, is expected to have a significant impact on human discomfort, especially in urban areas, as the number of hot days countrywide is clearly projected to increase. The most noticeable changes are projected for the low-lying inland regions of Central Greece, Thessaly, the Southern Peloponnese as well as Central Macedonia, where up to 20 additional very warm days are expected per year in 2021-2050 and up to 40 in 2071-2100, relative to the reference period 1961-1990. The change is expected to be somewhat milder in Crete and Attica, where the number of additional very warm days per year should not exceed 15 in 2021-2050 and 30 in 2071-2100, and milder yet in the Aegean and the Ionian islands, which will count 10 additional very warm days per year in 2021-2050 and 15 additional ones in 2071-2100, due to the proximity of the sea and the tempering effect of sea breezes.

Another temperature-related and significant parameter is the change in the annual number of warm nights. Nights are defined as warm (or tropical) when the minimum temperature does not fall below 20°C. This parameter is closely associated with human health, as a tropical night following an extremely hot day can increase human discomfort. As can be seen from Figure 1.31, the annual number of tropical nights is projected to increase almost everywhere in Greece, but substantially more so in the coastal and island regions than in the continental mainland

Figure 1.30

Variation in the number of days with maximum temperature > 35°C in (a) 2021-2050 and (b) 2071-2100, relative to 1961-1990

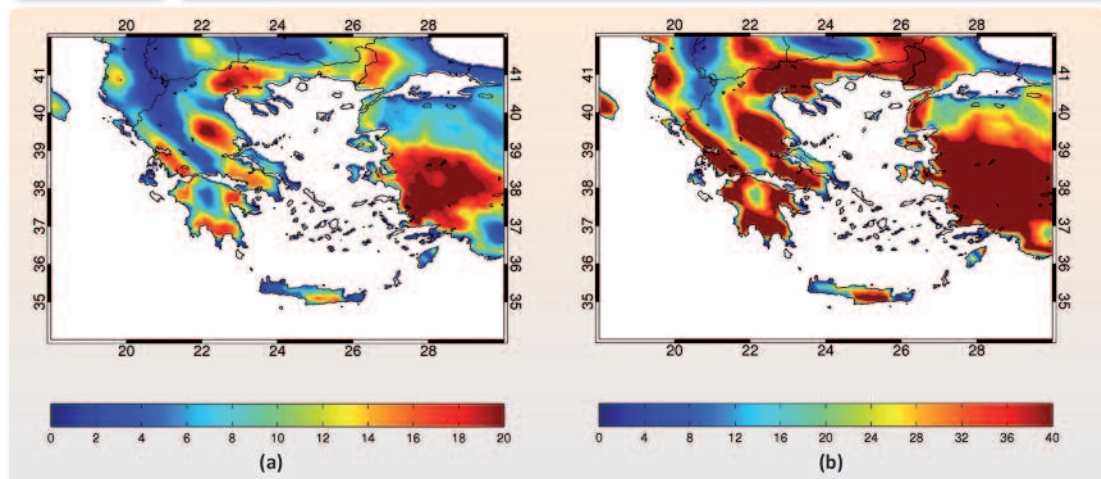
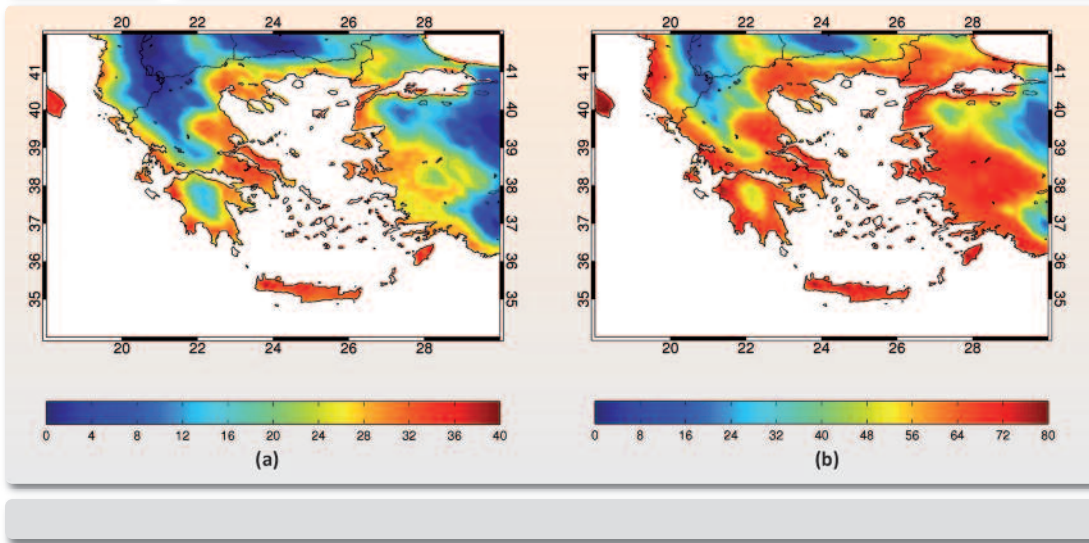


Figure 1.31**Variation in the number of days with minimum temperature > 20°C in (a) 2021-2050 and (b) 2071-2100, relative to 1961-1990**

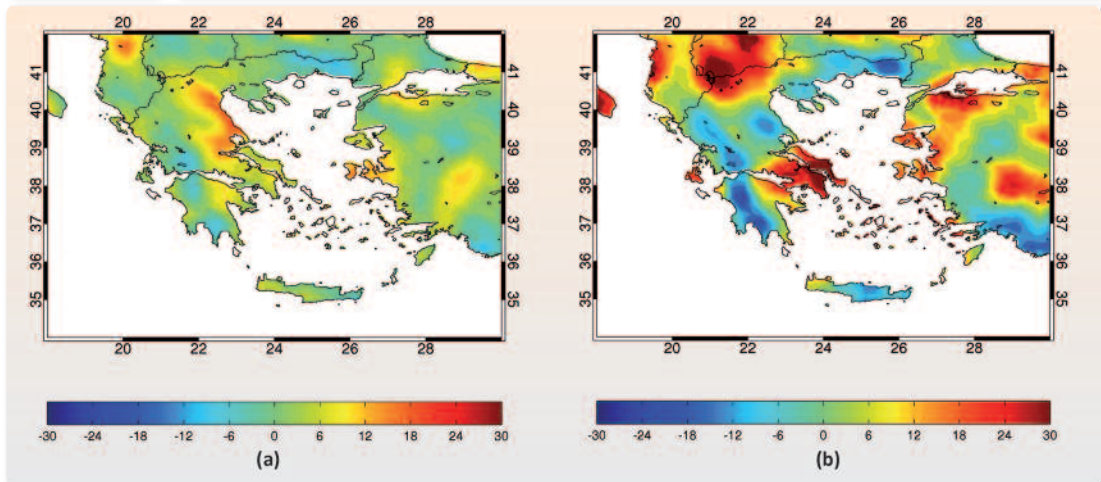
regions. Crete, the coastal regions of Eastern Greece and the Aegean islands are expected to have 40 additional warm nights per year in 2021-2050 and 80 additional warm nights per year in 2071-2100. In Western Greece and Eastern Macedonia-Thrace, however, the increase in the annual number of warm nights will be less than 30 in 2021-2050 and 70 in 2071-2100, with even smaller increases projected for Western Macedonia (15 or less additional warm nights per year in 2021-2050 and 30 or less in 2071-2100).

Days with precipitation and dry days

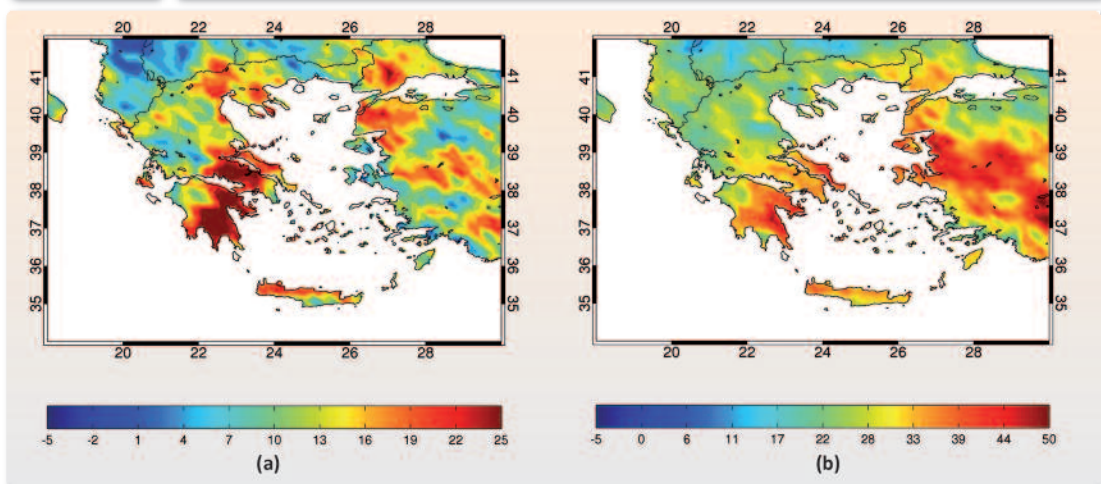
Apart from maximum temperature extremes and their association with human discomfort, another source of concern is flash flooding, especially if its frequency were to increase on account of climate change. As can be seen from Figure 1.32, the percentage variation in annual maximum consecutive 3-day precipitation is projected to increase. Together with the projected decrease in total annual rainfall, this means that extreme precipitation events will increase in intensity, thereby raising the flood risk. As can be seen from the left panel of Figure 1.32, maximum consecutive 3-day precipitation period during 2021-2050 will remain essentially unchanged, relative to the reference period 1961-1990, in regions like Western Greece, Eastern Macedonia-Thrace and Crete, but will increase significantly in others. In the eastern continental regions, in particular, maximum consecutive 3-day precipitation is projected to increase by 20%. These contrasts become even more pronounced toward the end of the 21st century, with the amount of extreme rainfall projected to decrease by 10-20% in regions of Western Greece and Thrace, but to increase by 30% in the Eastern Central Greece and the NW Macedonia. Small variations are projected for the rest of the country.

Figure 1.32

Percentage change in annual maximum consecutive 3-day precipitation in (a) 2021-2050 and (b) 2071-2100, relative to 1961-1990

**Figure 1.33**

Variation in maximum length of dry spell (in consecutive dry days) in (a) 2021-2050 and (b) 2071-2100, relative to 1961-1990

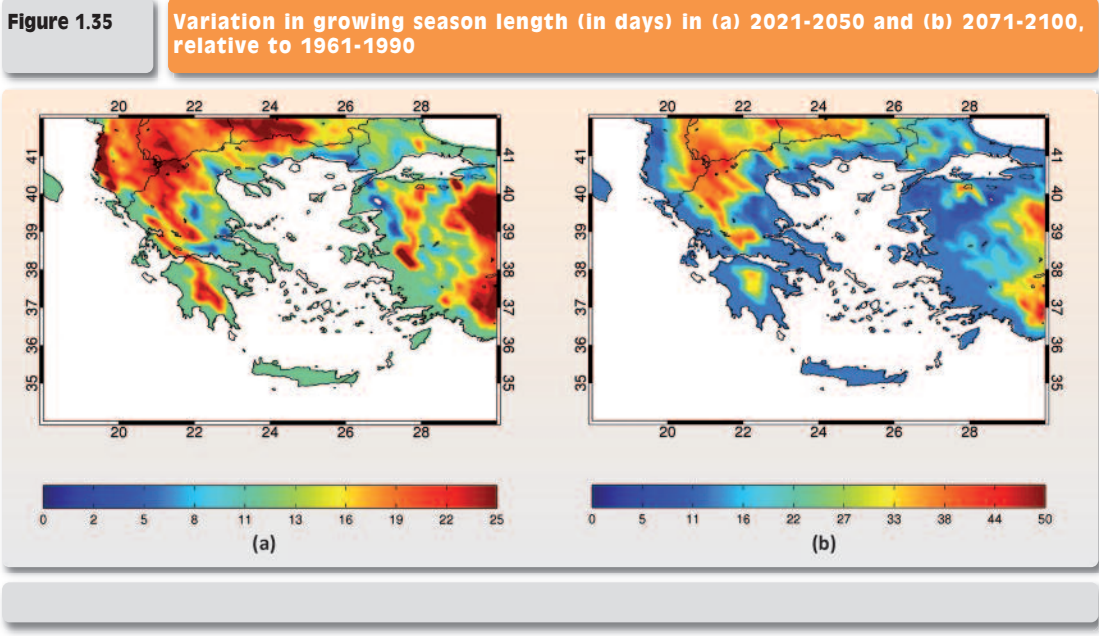
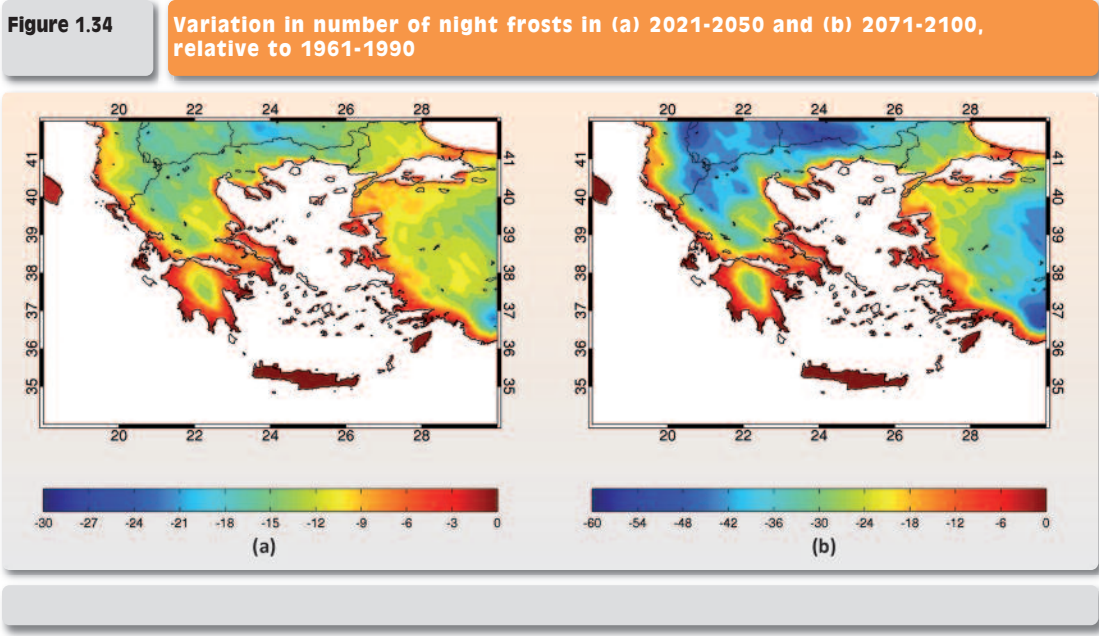


Projections were also made regarding the variation in the maximum duration of dry spells, i.e. consecutive dry days, defined as days with no or less than 1 mm precipitation. As can be seen from Figure 1.33, the length of dry spells will clearly increase. The smallest variations in dry spell length are projected for Greece's western regions in 2021-2050 (less than 10 more consecutive dry days) and for Western and Northern Greece in 2071-2100 (less than 20 more consecutive dry days). The largest increases in dry spell length are projected for the eastern continental regions (Eastern Central Greece, the Eastern Peloponnese and Euboeia) and Northern

Crete, which will have more than 20 additional consecutive dry days in 2021-2050 and as many as 40 more consecutive dry days in 2071-2100.

Frost days and growing season

The projected changes in the number of frost days per year are represented in Figure 1.34. This is an important parameter for agricultural regions, especially those where frost-sensitive crops, like citrus fruit, are grown. The number of frost days per year is projected to decrease in



Macedonia and Thrace by 15 in 2021-2050 and by 40 in 2071-2100, and in the continental regions of Thessaly and the Peloponnese by 10 to 15 in 2021-2050 and by 25 in 2071-2100. Smaller decreases are projected for the rest of Greece, mainly because of the small number of frost days that these regions have even today.

In addition to the number of frost days, we also examined the length of the growing season, defined as the period favourable to plant and crop growth between the last spring frost and the first autumn frost. The projected changes in the length of the growing season are represented in Figure 1.35. The observable lengthening can be attributed to the earlier occurrence of the last spring frost and to the later occurrence of the first autumn frost. The largest increases in growth season length (in the order of 25 days for 2021-2050 and 45 days for 2071-2100) are projected for the country's continental mountain regions. Length increases of 10-15 days for 2021-2050 and 15-25 days for 2071-2100 are projected for the rest of the country.

Energy demand for heating and cooling

In order to estimate future energy demand, we used the degree-days method, which consists in calculating the daily difference (in °C) between a mean temperature and a base temperature. The base temperature can be given a value such that heating or cooling consumption would be at a minimum. Since the choice of such a base temperature would result in the degree-day index taking on positive values in the warm season and negative values in the cold season, we chose to use two separate indices: (a) Heating Degree Days (HDD) and (b) Cooling Degree Days (CDD), using the following mathematical formulas:

$$\text{HDD} = \max (T^* - T, 0)$$

$$\text{CDD} = \max (T - T^{**}, 0)$$

where T^* and T^{**} are the respective base temperatures for HDD and CDD that can be either the same or different, and T is the daily mean temperature, as obtained from the daily temperatures of the regional climate models for the reference period and the future periods. The HDD (CDD) index is usually summed up for a specific period (annual or seasonal), and therefore provides a measure of the severity of winter (summer) conditions in terms of outdoor dry-bulb temperature. This, in turn, is a measure of the likely aggregate energy demand for reasonable heating (cooling) during that period in a particular location. In the present study, we adopted a base temperature of 15°C for our HDD calculations and 25°C for our CDD calculations, in line with the recent study by Giannakopoulos et al. (2009a; 2009b).

One major impact of global warming is that the electricity demand for cooling will increase in summer. This could lead to more frequent network overloads and power disruptions, calling into question the ability to meet demand. The projected changes in the number of days per year with significant cooling needs (defined as days with a temperature 5°C or more above the CDD base temperature) are represented in Figure 1.36. As can be seen, the low-lying continental

Figure 1.36

Variation in number of days with strong cooling demand in (a) 2021-2050 and (b) 2071-2100, relative to 1961-1990

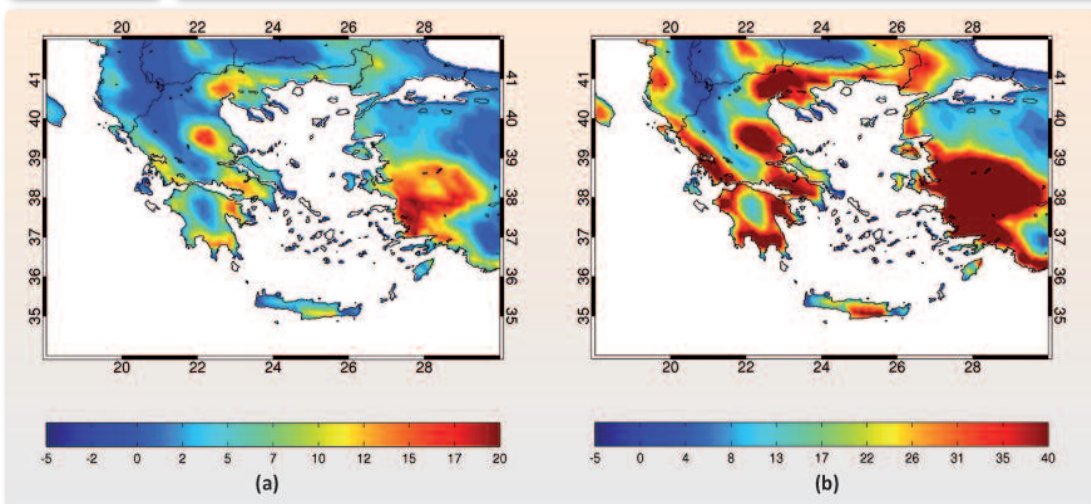
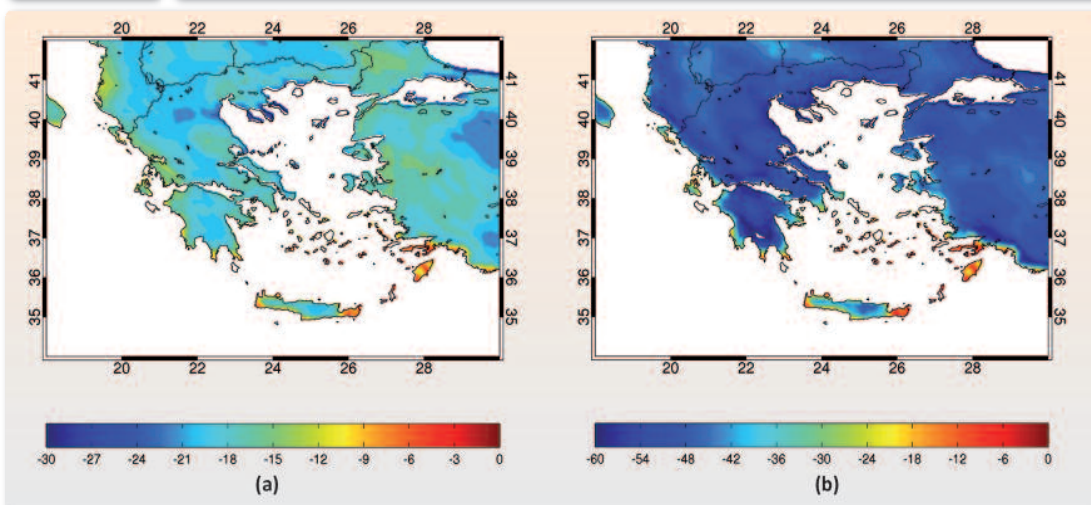


Figure 1.37

Variation in number of days with strong heating needs in (a) 2021-2050 and (b) 2071-2100, relative to 1961-1990



regions are projected to have an additional 10-20 days per year with a significant demand for cooling in the period 2021-2050 and 30-40 additional days per year in the period 2071-2100, relative to the reference period 1961-1990. In the island and mountain regions, the respective increases will be smaller.

One positive aspect of climate change is that energy needs for heating in winter are expected to decline. As shown by the projected changes in the number of days requiring heavy heating,

represented in Figure 1.37, the electricity demand for heating in winter will clearly decline in almost all parts of Greece, by roughly 20 days per year in 2021-2050 and by 45 days per year in 2071-2100.

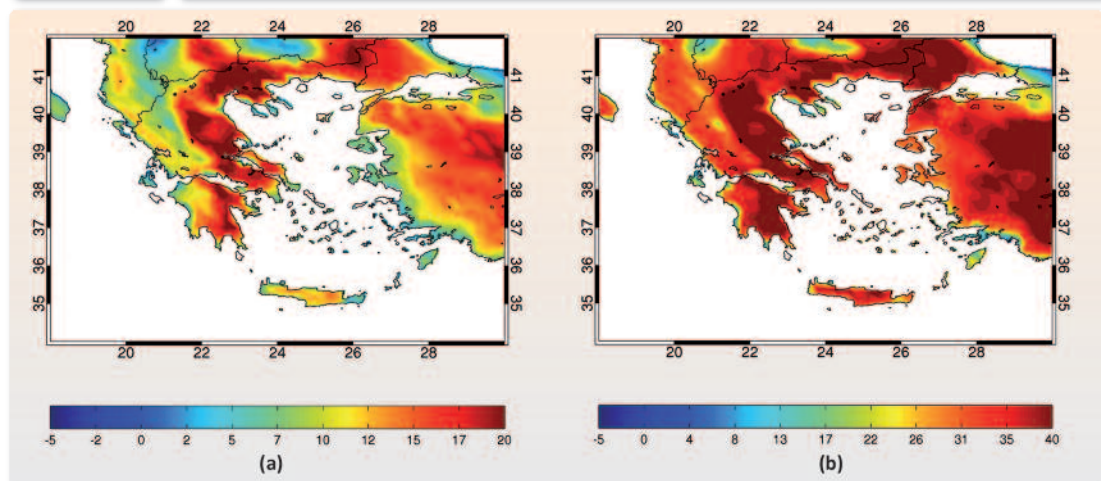
Forest fires

Forest fires, like all other ecosystem processes, are highly sensitive to climate change, as fire behaviour responds immediately to fuel moisture, which in turn is affected by precipitation, relative humidity, air temperature and wind speed. The projected rise in temperature as a result of climate change should therefore increase fuel dryness and reduce relative humidity, more markedly in those regions where rainfall will decrease. The increased frequency of extreme climate events is expected to have a significant impact on the fire vulnerability of forests.

The Forest Fire Weather Index (FWI) is a daily meteorological-based index, designed in Canada and used worldwide to estimate the wildland fire potential for a standard fuel type. It is computed from six standard components, each measuring a different aspect of fire danger. The first three components refer to forest fuel moisture codes that simulate daily changes in the moisture contents of three classes of forest fuel with different drying rates. The other three components are fire behaviour indices representing the rate of fire spread, the total amount of fuel available for combustion and the frontal fire intensity. The FWI is a numerical rating of a fire's intensity and is used to estimate the difficulty of fire control. The system depends solely on weather readings taken each day at noon: temperature, relative humidity, wind speed and rainfall. In the present study, RCM daily outputs of maximum temperature (Tmax), relative humidity (RH), wind speed at 10 m above ground and total rainfall were used as input variables to the

Figure 1.38

Variation in number of days with extremely high risk of fire in (a) 2021-2050 and (b) 2071-2100, relative to 1961-1990



FWI system. The FWI system was developed for Canadian forests, but has found a wide application in other countries and environments, such as Mexico, SE Asia, Florida, Argentina. For the Mediterranean basin, several studies have shown that the FWI system and its components were well suited to the estimation of fire risk in the region (Moriondo et al., 2006). FWI values over 15 were found to be indicative of an elevated fire risk, while FWI values over 30 indicate extreme fire risk (Good et al., 2008).

The projected changes in the number of extreme fire danger days are presented in Figure 1.38. Apart from forest regions, this parameter is equally important to agricultural and tourist areas. In all of Eastern Greece, from Thrace down to the Peloponnese, extreme fire danger days are likely to increase by 20 in 2021-2050 and 40 in 2071-2100. Smaller increases are projected for Western Greece, mostly on account of the higher humidity conditions.

Days with increased thermal discomfort

Heat effects on human comfort (or discomfort) are assessed by computing the humidex (Masterton and Richardson, 1979). This index, used generally during warmer periods to describe how hot or humid the weather feels to the average individual, is derived by combining temperature and humidity values into one number to reflect the perceived temperature. Humidex (equivalent to dry temperature in °C) is computed with the following formula:

$$T(h) = T_{max} + 5/9 * (e - 10)$$

where e is the vapour pressure (given by $6.112 * 10^{(7.5 * T_{max} / (237.7 + T_{max})) * h / 100}$), T_{max} is the maximum air temperature (°C) at 2 m above ground and h is the relative humidity (%).

Figure 1.39

Variation in number of days with high thermal discomfort (humidex > 38°C) in (a) 2021-2050 and (b) 2071-2100, relative to 1961-1990

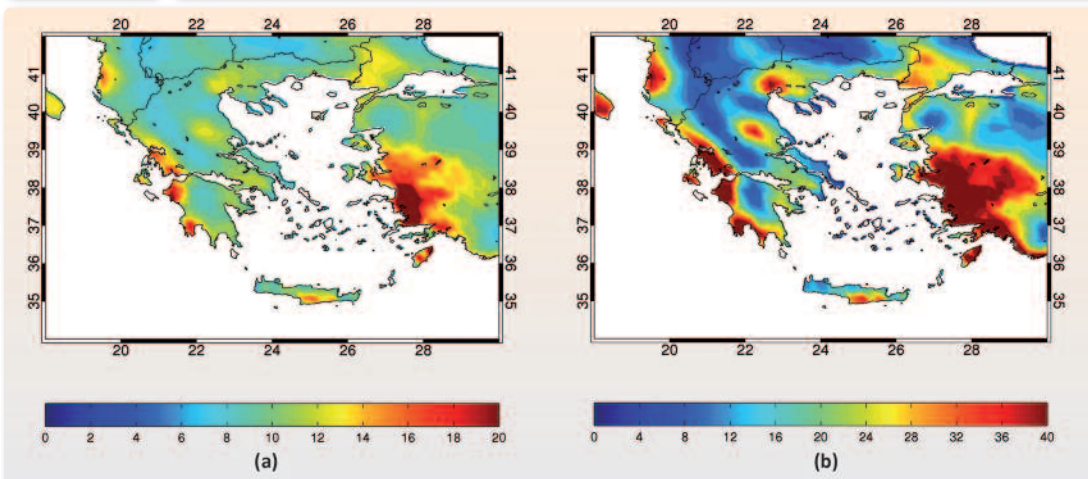


Table 1.9

Variation in examined climate indicators for each of Greece's 13 climate zones

	WG	CEG	ATT	WCM	EMT	WP	EP	C	D	CY	EA	NA	I
Minimum winter temperature (°C)	2	1.5	1.5	1.5	1.5	1.5	1.5	1.5	1.5	1.5	1.5	1.5	1.5
	4	3.5	3.5	3.5	3.5	3.5	3.5	3.5	3.5	3.5	3.5	3.5	3.5
Maximum summer temperature (°C)	2	2	1.7	2	2	2	2.5	1.5	1.5	1.5	1.5	1.5	1.5
	4	4.5	4	4	4	4	4.5	3.5	3.5	3.5	3.5	3.5	3.5
Tmax>35 °C (days)	20	20	15	20	15	20	20	15	10	10	10	10	10
	40	40	35	40	40	40	40	35	15	15	15	15	15
Tmin>20 °C (days)	20	35	40	15	20	25	25	40	40	30	30	25	25
	50	65	70	20	50	60	60	70	70	60	60	50	50
Maximum 3-day rainfall (%)	0	20	10	10	0	0	15	0	0	0	15	0	0
	-10	0	25	20	0	-15	10	0	0	0	15	10	20
Length of dry spell (days)	10	15	20	10	10	15	20	20	10	10	10	10	15
	20	25	35	20	25	30	45	40	30	30	40	30	30
Number of frosts (days)	0	-10	-5	-15	-15	-5	-10	0	0	0	0	0	0
	0	-25	-5	-40	-30	0	-15	0	0	0	0	0	0
Growing season length (days)	20	10	10	15	10	10	10	10	10	10	10	10	10
	35	20	15	35	20	15	15	15	15	15	15	15	15
Days with strong cooling demand	10	15	10	0	10	10	10	10	5	5	5	5	5
	35	40	35	10	30	35	35	30	25	20	25	20	20
Days with strong heating demand	-10	-15	-15	-15	-15	-10	-15	-10	-5	-5	-10	-15	-10
	-35	-40	-35	-35	-40	-30	-40	-25	-20	-20	-25	-30	-25
Extreme fire risk (days)	10	20	15	20	20	15	20	15	10	10	10	10	10
	30	40	35	40	40	30	40	35	25	25	30	30	25
High thermal discomfort (days)	20	15	15	5	10	20	10	15	20	10	10	10	20
	40	30	25	10	20	40	25	30	40	20	25	20	40

Climate zones: Western Greece (WG), Central and Eastern Greece (CEG), Attica (ATT), Western and Central Macedonia (WCM), Eastern Macedonia-Thrace (EMT), Western Peloponnese (WP), Eastern Peloponnese (EP), Crete (C), Dodecanese (D), Cyclades (CY), Eastern Aegean (EA), Northern Aegean (NA) and Ionian (I).

Changes with a negative sign indicate a decrease, while those without any sign indicate an increase. The first value in each cell corresponds to the 2021-2050 period and the second one to the 2071-2100 period.

Six humidex categories have been established to inform the general public of discomfort conditions:²⁸

- <29°C: no discomfort
- 30-34°C: some discomfort
- 35-39°C: discomfort; avoid intense exertion
- 40-45°C: great discomfort; avoid exertion

²⁸ http://www.eurometeo.com/english/read/doc_heat

- 46-53°C: significant danger; avoid any activity
- >54°C: imminent danger; heatstroke

The projected changes in the number of consecutive days during summer with a humidex value above 38°C are represented in Figure 1.39. Interestingly, the coastal and island regions were found to be most affected, contrary to our findings for heat wave occurrences which showed the continental regions to be most vulnerable. In particular, in the coastal regions of the Ionian and the Dodecanese islands, the period with humidex>38°C is projected to be 20 days longer in 2021-2050 and 40 days longer in 2071-2100, with obvious repercussions on human discomfort and, ultimately, health. In the low-lying continental regions and in Crete, the period with humidex>38°C is projected to be some 15 days longer in 2021-2050 and 25 days longer in 2071-2100, whereas the mountainous regions will not experience significant changes and will retain their cool summer climate.

Table 1.9 summarises the findings of our analysis, presented per respective climate indicator, for each of Greece's 13 climate zones.

Statistical distributions for five large cities in Greece

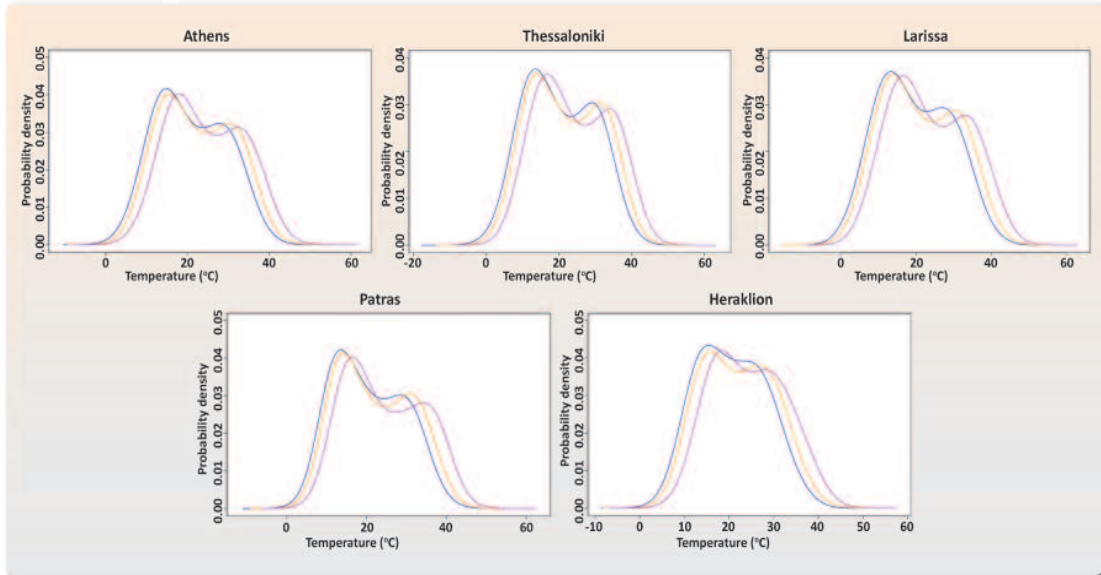
This section further analyses the projections of the KNMI/RACMO2 model,²⁹ focusing on the statistical distribution of maximum temperatures as well as on extreme summer events for Greece's five largest urban centres. The kernel density estimations of maximum temperature (a non-parametric way to estimate the probability density function) for each of these large cities are represented in Figure 1.40. For all five cities, the temperature distribution curve for the reference period 1961-1990 (blue line) has two maxima corresponding, respectively, to the onset of the cold season (left maximum) and the warm season (right maximum). The distribution curves for the two future periods (2021-2050 in orange and 2071-2100 in violet) shift progressively to the right, reflecting a mean climate warming. As can be seen from the tails of the distribution curves, the temperature during extremely hot weather events (right tail of the curves) is projected to be 1-2°C higher.

Turning to the occurrence of abnormally hot summers, Figure 1.41 illustrates the frequency of deviations of the summer mean maximum temperature (June-August mean values) from the climatological summer mean (1961-1990), for each of the 30 years of the period 1961-1990 (blue histogram) and 2071-2100 (coral histogram). In most cases, the histograms for the two periods overlap only slightly (violet histogram), suggesting that the 'cooler' summers at the end of the century are likely to be as warm as the hottest summers of the recent past. Of particular interest is the case of Athens: the summer of 1987, which – with its major heat wave that cost

²⁹ The model used is known as 'RACMO2', i.e. the second version of the regional atmospheric climate model of the Royal Netherlands Meteorological Institute (KNMI).

Figure 1.40

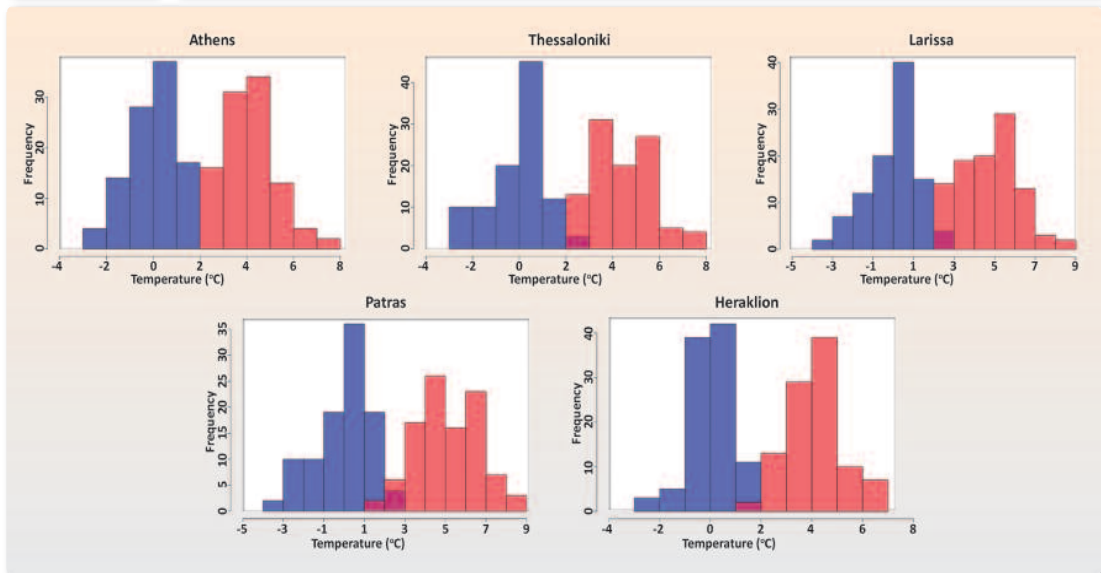
Kernel density estimates of maximum temperature for five major Greek cities



Kernel densities: non-parametric estimates of the probability density function.
Blue line: 1961-1990, orange line: 2021-2050, violet line: 2071-2100.

Figure 1.41

Frequency of deviation of mean summer maximum temperature (June to August) from the 1961-1990 average for five major Greek cities



Periods 1961-1990 in blue; 2071-2100 in pink; overlap in purple.

hundreds of lives in July— was the hottest summer of the reference period 1961-1990 (1.7°C warmer than the climatological mean 1961-1990), would be considered quite cool (and even outside the probable distribution range) at the end of the century.

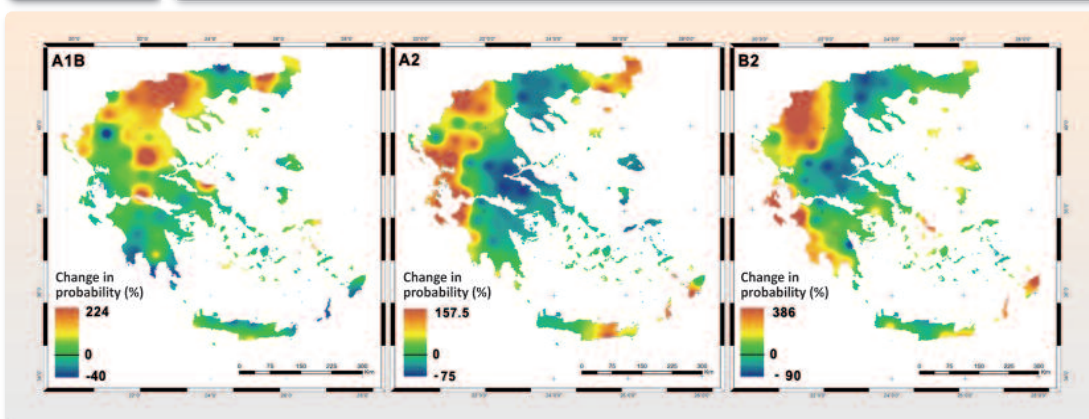
1.17 Changes in the intensity and distribution of landslides and floods in Greece

In the present section, we examine the variability of climate parameters and their likely regime, and the impact that such variability is likely to have on flood and landslide hazards. The datasets used for the purpose of the analysis were taken from an ECHAM5 model run for Scenario A1B and from a HadCM3 model run for Scenarios A2 and B2.

With regard to landslides, we examined the effect of rainfall intensity variability, a factor crucial to landslide occurrence (Caine, 1980; Koukis and Ziourkas, 1989). This meant that we first had to study the probability of rainfall exceeding certain thresholds beyond which landslides become highly probable (Caine, 1980), as well as possible changes in this probability. This probability change served as a means of assessing changes in landslide probability and,

Figure 1.42

Percentage change in probability of exceedance of rainfall intensity threshold for landslides



Between the reference period (1960-1990) and the 2070-2100 period for Scenarios A2 and B2, and the 2090-2099 period for Scenario A1B.

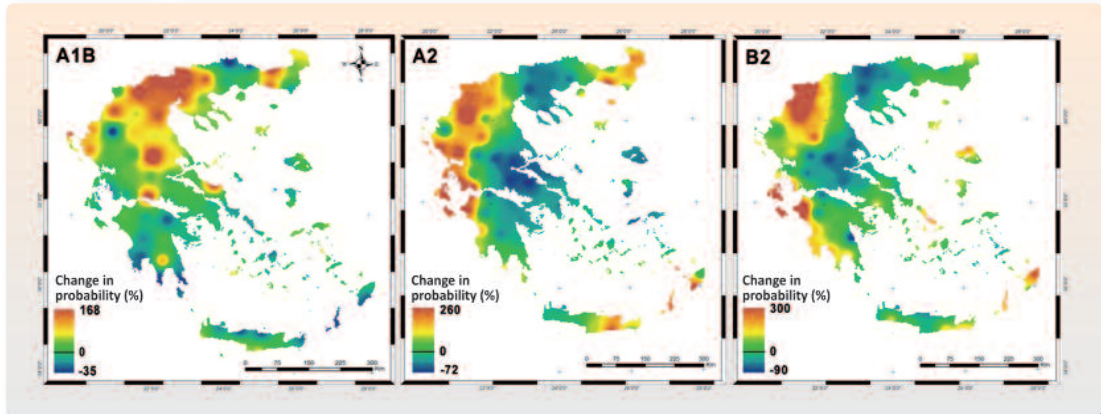
Table 1.10

Variation in probability of exceedance of rainfall threshold for landslides, based on the HadCM3 model for Scenarios A2 and B2 and the ECHAM5 model for Scenario A1B

Period	Probability of exceedance	Percentage change in probability		
		2070-2100		2090-2099
Scenario		A2	B2	A1B
Global threshold	0.011	+38.4	+10.6	+ 29.3
Local threshold	0.007	+44.6	+11.9	+ 33.7

Figure 1.43

Percentage change in probability of exceedance of rainfall intensity threshold above which flood risk becomes high



Between the reference period (1960-1990) and the 2070-2100 period for Scenarios A2 and B2, and the 2090-2099 period for Scenario A1B.

Table 1.11

Average percentage change in probability of exceedance of rainfall intensity threshold above which flood risk becomes high

Scenario	Period	Average percentage change in probability of exceedance
A1B	2090-2099	+ 30.15
A2	2070-2100	+ 24.7
B2	2070-2100	+ 6.45

The reference period is 1961-1990.

thus, in landslide hazard. For the purpose of our calculations, we used the global threshold proposed by Caine (1980) and the regional threshold proposed by Calcaterra et al. (2000) for the Mediterranean.

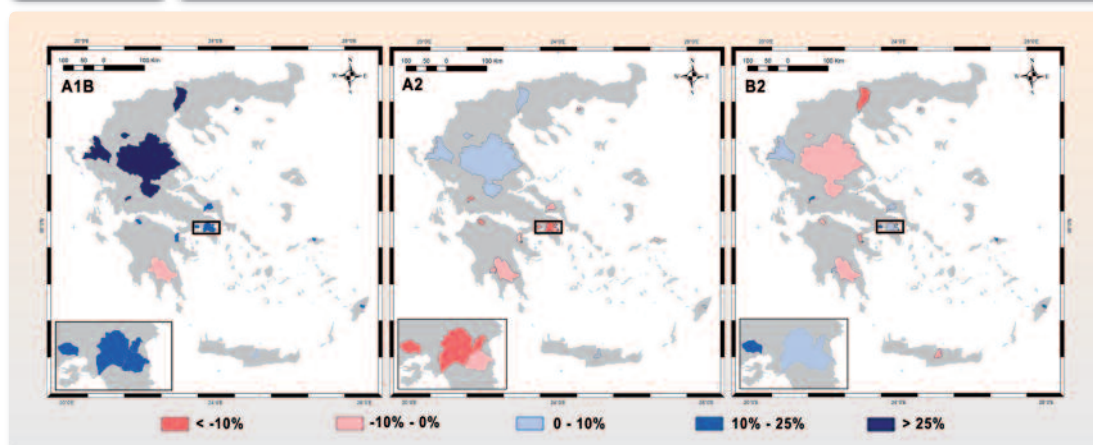
The final results were obtained by calculating the percentage change in probability of rainfall exceeding the thresholds between the reference period (1960-1990) and the periods 2071-2100 (for Scenarios A2 and B2) and 2090-2099 (for Scenario A1B). The results present similar spatial distributions with regard to both thresholds, and point to significant increases, but also decreases, in landslide probability depending on the region (Figure 1.42). More specifically, the landslide probability increases 1.5 times (Scenario A2) and 3 times (Scenario B2) in Western Macedonia, Western Greece and the Western Peloponnese, while smaller increases of 1.4 times (Scenario A2) and 2 times (Scenario B2) are projected for Eastern Crete, the Dodecanese and Evros (Eastern Thrace). In contrast, the landslide probability is projected to be 50% lower (Sce-

nario A2) and 90% lower (Scenario B2) in Central Greece, Central Macedonia and the Peloponnese. Under Scenario A1B, the landslide probability is projected to increase by up to 2 times in the largest part of Greece, with the greatest increases observed in Central Macedonia and Thessaly (100-224%), whereas decreases are projected for the Southern Peloponnese and some parts of the Dodecanese. In terms of average changes, significant differences (in the order of 10-45%) are observed in the results of the three scenarios (Table 1.10), with Scenario B2 presenting the smallest changes and Scenario A2 the largest.

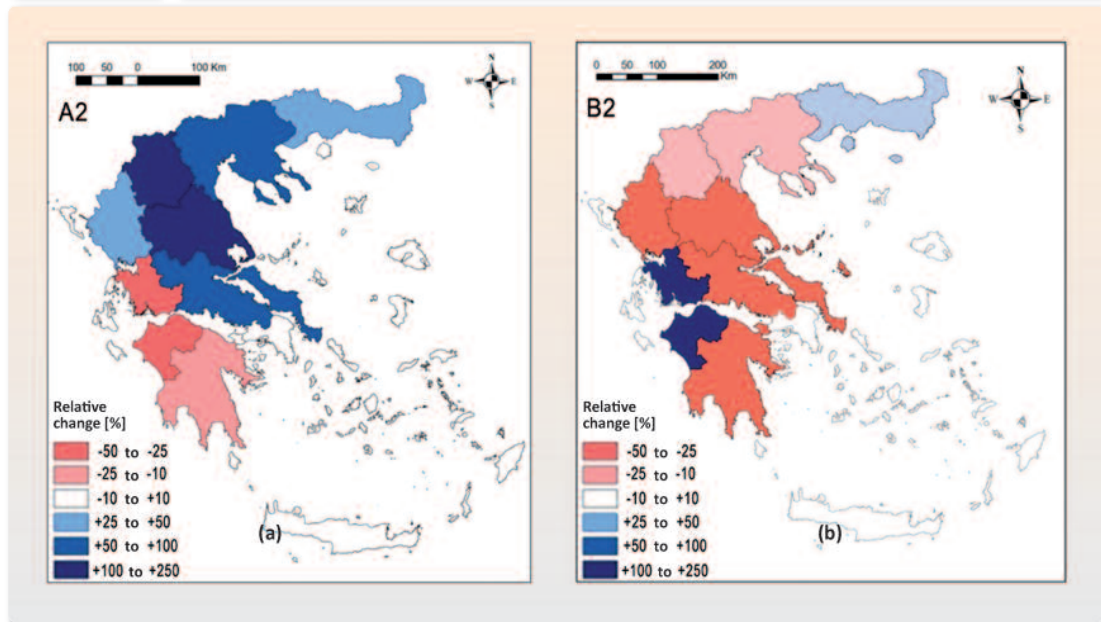
Turning to floods, we examined the future variability of heavy rainfall, as well as the effect of such variability on the flood occurrence regime. This indicator was chosen because of its established association with flood phenomena (Loukas et al., 2002; Lehner et al., 2006; Georgakakos, 2006; Norbiato et al., 2008). In order to achieve this, we analysed the projected changes in the probability of rainfall intensity exceeding the thresholds beyond which flooding becomes highly probable (Cannon et al., 2008; Diakakis, 2011). The results point to significant variation in flooding probability across the different regions depending on the climate scenario (Figure 1.43) and to increases in average values under all the scenarios for the periods 2071-2100 and 2090-2099 (Table 1.11). Specifically, the probability of flooding was projected to be 2.6 times higher (Scenario A2) and 3 times higher (Scenario B2) in the Western Peloponnese, Epirus and Western Macedonia, but 50% lower (Scenario A2) and 90% lower (Scenario B2) in Central Greece and Central Macedonia. Under Scenario A1B, the probability increases by as much as 168% almost everywhere in the country, with the highest increases recorded for Central Macedonia and Thessaly, but decreases by as much as 35% in the Southern Peloponnese, Northern Crete and the Dodecanese.

Figure 1.44

Percentage change in peak discharge rate with a 5-year return period in the 19 catchment areas studied



Calculated using Sutcliffe's (1978) method. Changes under Scenarios A2 and B2 were calculated using the results of HadCM3 model simulations for the time periods 1961-1990 and 2071-2100. Changes under Scenario A1B were calculated using the results of ECHAM5 model for the time periods 1990-1999 and 2090-2099.

Figure 1.45**Relative percentage change in the estimated annual cost of direct damage from floods**

Under Scenarios A2 and B2 (HadCM3) between the periods 1960-1990 and 2070-2100 (Ciscar et al., 2009, modified).

In order to assess the future variation of flood hazards, we examined the projected changes in discharge of 19 selected hydrological basins of different sizes and geomorphology, selected in such a manner as to ensure that the geographical range was representative of the country as a whole. The projected changes were assigned a sign and magnitude. Using the method proposed by Sutcliffe (1978), we calculated the change in peak flows with a 5-year return period for these basins (Figure 1.44). The change in flood damage was calculated on the basis of models developed to assess the country-specific consequences of flooding (Ciscar et al., 2009), as well as the estimated change in flow of major waterways (Figure 1.45).

In summary, based on the results of our climate modelling and subsequent analysis, the future variation of flood and landslide risk regimes presents, on average, an increasing trend. However, in certain regions, the probability of such disaster event occurrence will decline. The values of change obtained are similar to the ones reached by other researchers, for instance Frei et al. (2006). The range of values obtained both in the present study and in other studies with results of a similar scope (Huntingford et al., 2003; Barnett et al., 2006; Frei et al., 2006) highlights the degree of uncertainty surrounding the projection of extreme values. The results should be interpreted with caution, as flood and landslide risks both depend on additional factors such as change in vegetation, land-use and anthropogenic impact (Alcamo et al., 2007), which are not assessable in full, but are expected to play a significant role in the occurrence of such disasters.

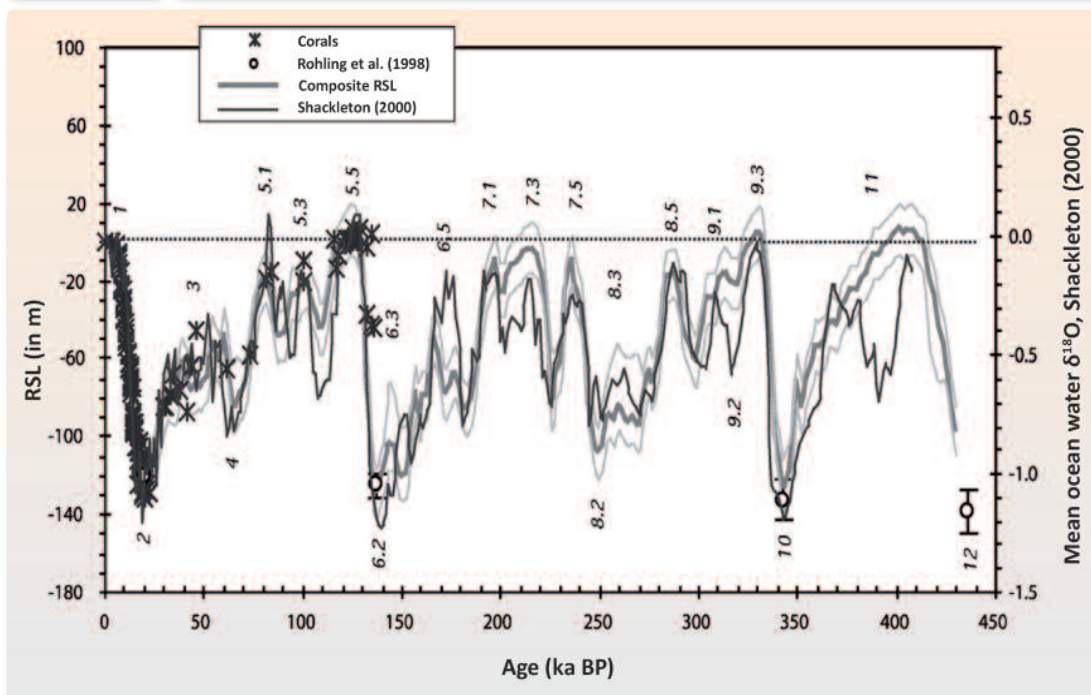
1.18 Change in mean sea level and its impact on Greece's shorelines

1.18.1 Global sea level changes in the geological past

Based on the records of global sea level change over the last 500,000 years (ka), for which available paleoclimatic data are more accurate, it has been estimated that the sea level during interglacial Marine Isotope Stage (MIS) 11 (400 ka BP, e.g. Bowen, 2009; Rohling et al., 2010), MIS 9c (320 ka BP), MIS 7e and MIS 7a (respectively, 237 ka BP and 197 ka BP, e.g. Siddall et al., 2003; Rabineau et al., 2006) may well have been close to current levels (Figure 1.46). During the more recent interglacial MIS 5 (120-125 ka BP), the sea level is estimated to have been 4-9 m higher than present (e.g. Stirling et al., 1998; McCulloch and Esat, 2000; Kopp et al., 2009), with a peak rate of increase of 10-16 mm/year (Rohling et al., 2008). This rate is similar to the rise of 10-20 mm/year estimated for the exceptionally long MIS 11 interglacial period (400 ka BP), as well as for the four 'warm' episodes within MIS 3 (60-25 ka BP; Siddall et al., 2008). The latest increase in sea level (20-6 ka BP) was in the order of 10 mm/year (Rohling et al., 2010).

The global mean sea level is estimated to have risen 120-130 m since the last glacial maximum (about 21 ka) (e.g. Shackleton, 2000; Waelbroeck et al., 2002; Siddall et al., 2003; Peltier

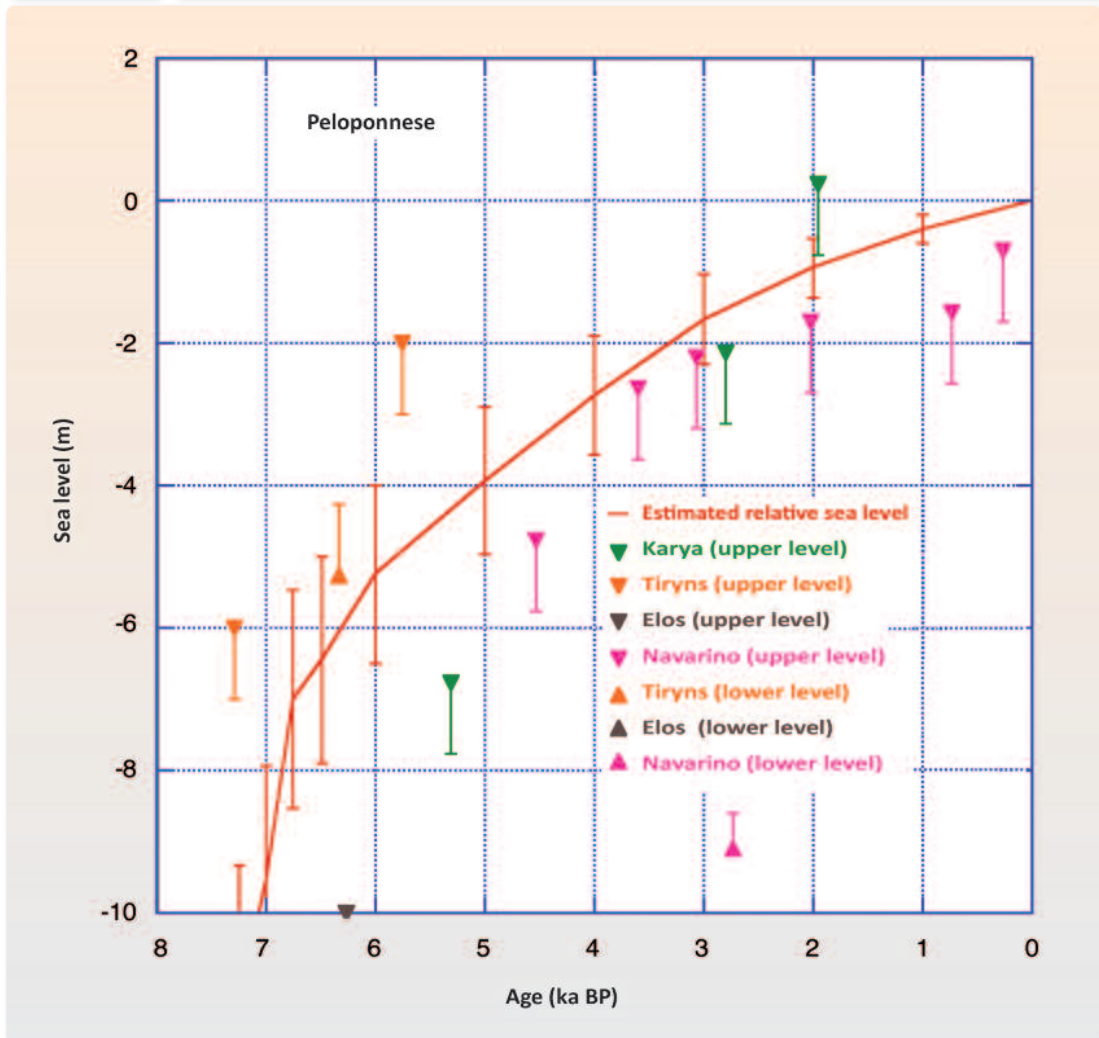
Figure 1.46 Composite relative sea level (RSL) over the past 450 ka



Crosses: coral reef RSL data. Empty circles: RSL low stands estimated by Rohling et al. (1998). Right axis: variations in mean ocean water $\delta^{18}\text{O}$ derived by Shackleton (2000) from atmospheric $\delta^{18}\text{O}$ (black line). The numbers above sea-level curves represent marine isotope stages (MIS). Chart from Waelbroeck et al. (2002).

Figure 1.47

Estimated variation curve in paleo-sea level of the Peloponnese



Comparison with observed sea levels in selected areas. The above chart shows upper and lower levels of estimated sea level. Field data from Kraft and Rapp (1975) and Kraft et al. (1977, 1980), and summarised by Lambeck (1995b).

and Fairbanks, 2006). During the current interglacial, the rate of sea level increase is estimated to have been close to 11 mm/year from 14 to 7 ka BP (Bard et al., 1996), and to have dropped to 1 mm/year over the last 6 ka (Lambeck, 1995; Lambeck and Purcell, 2005; Figure 1.46). Recent studies have shown that the sea level is still on the rise today (IPCC, 2007; Poulos et al., 2009a; Woodworth et al., 2009).

Focusing more specifically on the area of Greece, the sea level during 21-18 ka BP (end of the last glacial period) was 105-120 m lower than it is today (e.g. Pirazzoli and Pluet, 1991; Lambeck and Bard, 2000), but according to Lambeck (1995; 1996) and Lambeck and Purcell (2005), it rose rapidly between 11.5 ka and 6 ka, due to glacio-eustatic fluctuations, to 2 m below current sea level (Northern Aegean) and to 6 m below current sea level (Southern

Table 1.12

Past sea level (SL) and rate of sea level rise for various time intervals, along with the geographical origin of indicated data

Time period	Past sea-level (SL)	Rate of SL rise	Geographical origin of data	References
From 21 to 18 ka BP	Between -120 m and -105 m			
From 8 to 6 ka BP		8.5 mm/year	Euboia	Kambouroglou et al. (1988)
From 10 to 5 ka BP		4 mm/year	Thessaloniki	Vouvalidis et al. (2005)
8.3 ka BP	-28 m		Thessaloniki	Chronis (1986)
From 8 to 7 ka BP		12.3 mm/year	Akarnania	Vött (2007)
From 7.6 to 6.2 ka BP	-11 m		Plain of Argolis	Jacobsen and Farrand (1987), van Andel (1987)
From 7 to 6.5 ka BP		6.0 mm/year	Peloponnese	Lambeck and Purcell (2005)
Last 6 ka BP	-2 m		Northern Aegean	Lambeck (1995), Lambeck and Purcell (2005)
Last 6 ka BP	-6 m		Southern Aegean	Lambeck (1995), Lambeck and Purcell (2005)
From 6 ka BP to 0 BC		2.5 mm/year	Cyprus	Gifford 1980
Last 6 ka BP		1 m/1000 years	Peloponnese	Lambeck and Purcell (2005)
From 6 to 2.5 ka BP		0.2–1.4 mm/year	Akarnania	Vött (2007)
Last 4 ka BP		1.0 mm/year	Thessaloniki	Vouvalidis et al. (2005)
From 5.5 to 1.3 ka BP		1.68 mm/year	Marathon	Pavlopoulos et al. (2006)

Aegean). Indicatively, the rate of sea level rise during 8-6 ka BP was about ~8.5 mm/year in Southern Euboia (Kambouroglou et al., 1988), 12.3 mm/year in SW Akarnania (Vött, 2007) and 6 mm/year in the Peloponnese (Lambeck and Purcell, 2005; Figure 1.47). During the last 5,000-6,000 years, the sea level continued to rise at a rate of <1 mm/year, without ever exceeding the current levels and without excluding small variations in the rate of increase (Lambeck and Purcell, 2005; Pavlopoulos et al., 2007; Vött, 2007; Poulos et al., 2008a). Table 1.12 summarises typical rates of sea level rise over time for various Greek coastal regions.

1.18.2 Current and future mean sea levels

As shown by instrumental measurements (tide gauges, satellite altimetry), mean sea level has been rising at a rate of 1.8 mm/year since the late-19th century, while based on satellite measurements for the last 15 years, this rate has accelerated to 3 mm/year (Bindoff et al., 2007). As reported in IPCC (2007), by 2100 the air temperature is projected to rise by 1.1-2.9°C under the most conservative scenario (B1) and by as much as 2.4-6.4°C under the worst-case scenario

(A1FI). Meanwhile, sea level rise for the period 2090-2099, relative to the period 1980-1999, is projected to range between 0.18 m and 0.38 m under Scenario B1, and between 0.26-0.59 m under Scenario A1FI. However, subsequent studies anticipate an even greater sea level rise by 2100. According to the semi-empirical model advanced by Rahmstorf (2007) relating the rates of change in global surface temperature to sea level, a rise in temperature of 1°C corresponds to a sea level rise of 10-30 cm. Applying this ratio to the rise in temperature of 1.4-5.8°C projected by the SRES scenarios (IPCC, 2007), we obtain sea level rise figures of 0.5-1.4 m. The most adverse projections are reported in Pfeffer et al. (2008), with sea level rise likely to reach 0.8 m to 2 m. According to this study, the IPCC (2007) has not successfully modelled the dynamic development (decline) of the Greenland and Antarctic glaciers, a view recently also supported by other researchers (e.g. Rohling et al., 2009; Grinsted et al., 2010).

1.18.3 A comparison of sea level projections with paleoclimatic data

The current rates of sea level rise are markedly lower than those of past interglacials (e.g. 120 ka BP), some interstadial phases of the last glacial period (40-41 ka BP) and the beginning of the current interglacial (14-8 ka BP).

Looking at the course of sea level changes during the Holocene, it would seem that the sea level is currently nearing its upper limits, given on one hand the highstand recorded since the beginning of the 'warm' period (similar to other previous warm periods) and the slowdown in the rate of sea level rise in the past 5,000-6,000 years. Still, the course of sea level changes remains uncertain, as signalled by the significant acceleration in the rate of increase (3 mm/year) in the last 15 years. This development, likely associated with greenhouse gas-induced global warming, in turn a cause of 'glacier waning', leads us to the conclusion that today's higher rate of sea level rise is likely to pick up further, to values not unheard of in the geological past. One would also have to factor in the impact of orbital forcing on the course of the current climate cycle, as orbital forcing would be directly linked to the onset of the next glacial period.

1.18.4 Coastline classification into geomorphologic-geodynamic categories and map representation

Given that the sea level rise by 2100 is, depending on the scenario, projected to be between 0.2 m and 2 m, we chose to examine which parts of Greece's coastline would find themselves 'endangered' if the sea level were to rise by 1 m.

However, the vulnerability of a coastal region cannot be safely estimated on the basis of the rate and scale of sea level rise alone. Other local factors, such as tectonics, sediment transport (from inland) and coastal geomorphology/lithology, also need to be taken into account.

Tectonics obviously play a highly important role in tectonically active areas, as a rise in sea level can be offset (amplified) by tectonic uplift (subsidence). Typical examples in Greece are

Figure 1.48

Classification map of Greece's coastal zones



Greece's coastal areas can be classified into: a) coastal areas of medium vulnerability to sea level rise (in green), usually of low altitude and consisting of soft sediments of the Neogene and Quaternary age; b) coastal areas of high vulnerability to sea level rise (in red), low-lying and formed of deltaic deposits; and c) rocky coastal areas of low vulnerability to sea level rise (black sections) of high altitude.

the coastal zone of the Northern Peloponnese, with an uplift rate of 0.3 to 1.5 mm/year, Crete with 0.7 to 4 mm/year and Rhodes with 1.2 to 1.9 mm/year. Thus, a supposed average value of sea level rise of 4.3 mm/year would be reduced to 3.5 mm/year due to the counteraction of a mean tectonic uplift of 0.8 mm/year.

A change (i.e. increase) in sediment discharge and deposition in large river delta-front estuaries can cause the delta front to advance and locally offset the sea level rise. Conversely, a decrease in river sediment discharge could reinforce the incursion of the sea following a sea level rise.

Lastly, another important determinant of coastal vulnerability to sea level rise is the coast's morphology and, specifically, the slope and lithological composition, factors directly associated with erosion rates. An erosion rate can range from very high (several metres per year) in the case of coastlines with a low-lying geomorphology and an 'erodible' lithology, to low (mms per year) in the case of hard coastal limestone formations (e.g. cliffs).

Taking all of the above factors into consideration and using a map scale of 1:50,000, Greece's coastal areas can be subdivided into the following three main zones (Figure 1.48):

1) Deltaic coastal areas. Represented in red in Figure 1.48, these low-lying coastal areas are formed of loose, unconsolidated sediment deposits and are highly vulnerable to sea level rise.

2) Coastal areas consisting of non-consolidated sediments of Neogene and Quaternary age. Represented in green, these coastal areas, usually of low altitude, are prone to recessional erosion and present a medium vulnerability to sea level rise.

3) Rocky coastal areas. These coastal areas (without any specific colouring/markings in Fig. 1.48) consist mostly of hard rock of low vulnerability to erosion and sea level rise, form the bulk of Greece's coastline.

The estimation of the length of these three types of coastal areas, as illustrated in Figure 1.48, shows that out of the total ~16,300 kms of coastline, 960 km (6%) correspond to deltaic areas of high vulnerability (red colour); 2,400 km (15%) correspond to non-consolidated sediments of medium vulnerability (green colour), and the remaining 12,810 km (79%) correspond to rocky coastal regions of low vulnerability. Thus, the total coastline length presenting medium to high vulnerability to sea level rise amounts to 3,360 km or 21% of Greece's total shoreline.

1.18.5 Estimates of shoreline retreat due to the rise in mean sea level

Table 1.13 presents indicative approximate values of flooded coastal areas and shoreline retreat (without any correction for tectonic and geodynamic effects) in response to possible sea level rises, respectively, of 0.5 m and 1 m in high-risk deltaic areas, such as the Axios river delta, the Aliakmon river delta and the Alfeios river delta (Poulos et al., 2008b). The shoreline retreat was estimated to range between 30 m and 2,750 m in response to a possible sea level rise of 0.5 m, and between 400 and 6,500 m in response to a rise of 1 m.

Assessing the severity of a possible sea level rise impact on coastal regions involves a degree of uncertainty, concerning:

(a) The intensity of the sea level rise, with projections ranging between 0.2 m and 2 m. The sea level rise will be determined by the interaction between several factors, both natural (e.g. astronomical forcing) and anthropogenic (e.g. greenhouse gases). The severity of each factor will determine the overall evolution of the current climate cycle, which should soon be crossing the finish line of the current 'warm' interglacial period.

Table 1.13

Estimated coastline retreat (in m) and coastal inundation from a potential sea-level rise of 0.5 m and 1 m, for various deltaic areas of Thermaikos Gulf and Kyparissiakos Gulf (Poulos et al., 2008b)

Coastal area	Sea-level rise (m)	Coastline retreat, Bruun's model (m)	Coastline retreat due to		Total coastline retreat (m)	Inundated area (km ²)
			sea-level rise (m)	coast erosion (m)		
Alfeios Delta (northern part)	0.5	51.1	175	15	190	224
	1.0	102.2	810	-110	700	683
Alfeios Delta (southern part)	0.5	54.5	15-30	0-15	30	35
	1.0	109.0	10-100	400	400-450	344
Axios Delta	0.5	52.7	250-2,000	0	250-2,000	10,825
	1.0	213.6	2,000-2,500	0	2,000-2,500	28,482
Aliakmon Delta	0.5	63.6	50-1,750	0	50-1,750	4,875
	1.0	195.4	250-2,500	0	250-2,500	8,950
Deltaic plain of Loudias-Aliakmonas	0.5		500-2,750	0	500-2,750	8,900
	1.0		5,000-6,500	0	5,000-6,500	25,575

(b) The relationship between tectonic uplift and the eustatic sea level rise. In several areas of Greece, the high tectonic uplift may locally offset and sometimes even exceed the eustatic sea level rise.

(c) The sedimentation of clastic materials in coastal areas, which is determined by geological and climatic conditions, as well as by anthropogenic intervention (e.g. dams, river sand mining). In the case of river delta areas for instance, these factors could alter their vulnerability to sea level rise.

Bibliography

A. In Greek

- Αιγινήτης, Δ. (1908), *Το Κλίμα της Ελλάδος*, τ. 2, *Το Κλίμα της Αττικής*, Αθήναι.
- Αιγινήτης, Δ. (1926), “Αι ανομβρικοί και τα αναγκαία έργα υδρεύσεως και αρδεύσεως εν Ελλάδι”, *Πρακτικά Ακαδημίας Αθηνών*, τ. Γ΄, 244-58.
- Αριστοτέλης, “Πολιτικά”, 1330.
- WWF Ελλάς (2009), “Το αύριο της Ελλάδας: επιπτώσεις της κλιματικής αλλαγής στην Ελλάδα κατά το άμεσο μέλλον”, Αθήνα, Σεπτέμβριος.
- Δουβής, Κ. (2009), “Μελέτη των ακραίων κλιματικών φαινομένων στην Ελλάδα με μεθόδους υποκλιμάκωσης”, Διδακτορική Διατριβή, Αθήνα.
- Ζερεφός, Χ. (2007), “Η κλιματική αλλαγή στην Επιστήμη και στην Τέχνη”, *Πρακτικά Ακαδημίας Αθηνών*, τ. 82, τεύχος Α΄.
- Ζερεφός, Χ. (2009), “Εισαγωγικά Μαθήματα στη Φυσική της Ατμόσφαιρας”, Χ. Ζερεφός, Εκδόσεις Πατάκη.
- Κανδύλης, Φ., Χ. Ρεπαπής και Στ. Κοτίνη-Ζαμπάκα (1989), “Οι κλιματικές μεταβολές κατά τα τελευταία 100 έτη, όπως εκδηλώνονται στην Ανατολική Μεσόγειο”, 2ο Πανελλήνιο Συνέδριο Γεωγραφίας, Αθήνα, 147-54, Δεκέμβριος.
- Καψωμενάκης, Ι. (2009), “Εκτίμηση των προβλεπομένων από τα πρότυπα προσομοίωσης κλιματικών αλλαγών στην Ελλάδα με μεθόδους υποκλιμάκωσης”, Διδακτορική Διατριβή, Αθήνα.
- Κοτίνη-Ζαμπάκα, Στ. (1983), “Συμβολή στην κατά μήνα μελέτη του κλίματος της Ελλάδος”, Διδακτορική Διατριβή, Θεσσαλονίκη.
- Κούκης, Γ. και Κ. Ζιούρκας (1989), “Κατολισθητικές κινήσεις στον ελληνικό χώρο. Στατιστική Θεώρηση”, *Ορ. Πλούτος*, 58, 39-58.
- Μαριολόπουλος, Η.Γ. (1938), “Το Κλίμα της Ελλάδος”, Αθήναι.
- Μαριολόπουλος, Η.Γ. (1982), “Επιτομή του Κλίματος της Ελλάδος”, *ΚΕΦΑΚ Ακαδημίας Αθηνών*, *Δημοσίευμα*, 7.
- Πλάτων, “Νόμοι”, Βιβλ. 6.
- Ρεπαπής, Χ.Κ., Κ.Μ. Φιλάνδρας και Δ.Α. Μεταξάς (2002), “Μεταβλητότητα του κλίματος στην Ανατολική Μεσόγειο, στην Ελλάδα και ειδικότερα στην Αθήνα”, *ΚΕΦΑΚ Ακαδημίας Αθηνών*, *Δημοσίευμα*, 16.
- Φουντά, Δ. (2009), “Τάσεις ακραίων καιρικών φαινομένων στην Αθήνα τα τελευταία 150 χρόνια-Μελλοντικές εκτιμήσεις”, Διημερίδα ΕΚΔΔ-ΕΑΑ με θέμα ‘Φυσικές Καταστροφές και Ανανεώσιμες Πηγές Ενέργειας: Οικονομική και Περιβαλλοντική Σημασία για την Ελλάδα’, Αθήνα, 5-6 Φεβρουαρίου.

B. In other languages

Adhémar, J. (1842), “Révolutions de la Mer: Déluges”, Carilian-Goeury et V. Dalmont, Paris, 184.

Akkemik, Ü. and A. Aras (2005), “Reconstruction (1689-1994 AD) of April-August precipitation in the southern part of central Turkey”, *International Journal of Climatology*, 25, 537.

Aksu, A.E., D. Yaşar, P.J. Mudie and H. Gillespie (1995), “Late Glacial–Holocene palaeoclimatic and paleoceanographic evolution of the Aegean Sea: micropaleontological and stable isotopic evidence”, *Marine Micropaleontology*, 25, 1-28.

Alcamo, J., J.M. Moreno, B. Nováky, M. Bindi, R. Corobov, R.J.N. Devoy, C. Giannakopoulos, E. Martin, J.E. Olesen and A. Shvidenko (2007), “Europe. Climate Change 2007: Impacts, Adaptation and Vulnerability”, Contribution of Working Group II to the Fourth Assessment Report of the Intergovernmental Panel on Climate Change, in Parry, M.L., O.F. Canziani, J.P. Palutikof, P.J. van der Linden and C.E. Hanson (eds), Cambridge University Press, Cambridge, UK, 541-80.

Alley, R.B., P.A. Mayewski, T. Sowers, M. Stuiver, K.C. Taylor and P.U. Clark (1997), “Holocene climatic instability: A prominent, widespread event 8200 yr ago”, *Geology*, 1997, 25, 6, 483-6.

Alley, R.B. (2000), “Ice-core evidence of abrupt climate changes”, *Proceedings of the National Academy of Sciences of the United States of America*, 97, 4, 1331-4.

Almogi-Labin, A., M. Bar-Matthews, D. Shriki, E. Kolosovsky, M. Paterne, B. Schilman, A. Ayalon, Z. Aizenshtat and A. Matthews (2009), “Climatic variability during the last 90 ka of the southern and northern Levantine Basin as evident from marine records and speleothems”, *Quaternary Science Reviews*, 28, 2882-96.

Alpert, P., M. Baldi, R. Ilani, S. Krichak, C. Price, X. Rodo, H. Saaroni, B. Ziv, P. Kishcha, J. Barkan, A. Mariotti and E. Xoplaki (2006), Chapter 2: “Relations between climate variability in the Mediterranean region and the tropics: ENSO, the Indian and the African monsoons, hurricanes and Saharan dust”, *Elsevier*, doi:10.1016/S1571-9197(06)80005-4.

Alverson, K.D., R.S. Bradley and T.F. Pedersen (eds) (2003), “Paleoclimate, Global Change and the Future”, The IGBP Series, *Springer-Verlag*, New York.

Antonioli, F., S. Silenzi and S. Frisia (2001), “Tyrrhenian holocene palaeoclimate trends from spelean serpulids”, *Quaternary Science Reviews*, 20, 1661.

Arz, H.W., F. Lamy and J. Pätzold (2006), “A pronounced dry event recorded around 4.2 kyr in brine sediments from the Northern Red Sea”, *Quaternary Research*, 66, 432-41.

Asioli, A., F. Trincardi, J.J. Lowe, D. Ariztegui, L. Langone and F. Oldfield (2001), “Sub-millennial scale climatic oscillations in the central Adriatic during the Lateglacial: palaeoceanographic implications”, *Quaternary Science Reviews*, 20, 11, 1201-21.

Atkinson, T.C., K.R. Briffa and G.R. Coope (1987), “Seasonal temperatures in Britain during the last 22,000 years, reconstructed using beetle remains”, *Nature*, 325, 587-92.

Austin, W.E.N. and D. Kroon (1996), "Late glacial sedimentology, foraminifera and stable isotope stratigraphy of the Hebridean continental shelf, northwest Scotland", in Andrews, J.T., W.E.N. Austin and H. Bergsten and A.E. Jennings (eds), "Late Quaternary of the North Atlantic Margins", *Geological Society Special Publication*, 111, 187-214.

Axaopoulos, P. and S. Sofianos (2009), "Long Term Variability of Sea Surface Temperature in Mediterranean Sea", 7th International Conference of the Balkan Physical Union, edited by A. Angelopoulos and T. Fildisis, American Institute of Physics.

Barber, D.C., A. Dyke, C. Hillaire-Marcel, A.E. Jennings, J.T. Andrews, M.W. Kerwin, G. Bilodeau, R. McNeely, J. Southon, M.D. Morehead and J.-M. Gagnon (1999), "Forcing of the cold event of 8,200 years ago by catastrophic drainage of Laurentide lakes", *Nature*, 400, 344-8.

Bar-Matthews, M., A. Ayalon and A. Kaufman (1997), "Late Quaternary palaeoclimate in the eastern Mediterranean region from stable isotope analysis of speleothems at Soreq Cave, Israel", *Quaternary Research*, 47, 155-68.

Bar-Matthews, M., A. Ayalon, M. Gilmour, A. Matthews and C.J. Hawkesworth (2003), "Sea-land oxygen isotopic relationships from planktonic foraminifera and speleothems in the Eastern Mediterranean region and their implication for paleorainfall during interglacial intervals", *Geochimica et Cosmochimica Acta*, 67, 3181-99.

Bar-Matthews, M. and A. Ayalon (2005), "Evidence from speleothem for abrupt climatic changes during the Holocene and their impact on human settlements in the Eastern Mediterranean region: Dating methods and stable isotope systematics", in Fouache, E. and K. Pavlopoulos (eds) "Sea level changes in Eastern Mediterranean during Holocene – indicators and human impacts", *Zeitschrift für Geomorphologie N.F.*, Supplement Volume 137, 45-59, Berlin-Stuttgart.

Bard, E., B. Hamelin, M. Arnold, L. Montaggioni, G. Cabioch, G. Faure and F. Rougerie (1996), "Sea level record from Tahiti corals and the timing of deglacial meltwater discharge", *Nature*, 382, 241-4.

Bard, E. and M. Frank (2006), "Climate change and solar variability: What's new under the sun? Frontiers", *Earth and Planetary Science Letters*, 248, 1-14.

Barker, S. and H. Elderfield (2002), "Foraminiferal calcification response to Glacial-Interglacial changes in atmospheric CO₂", *Science*, 297, 833-83.

Barnett, D.N. et al. (2006), "Quantifying uncertainty in changes in extreme event frequency in response to doubled CO₂ using a large ensemble of GCM simulations", *Clim. Dyn.*, 26, 489-511.

Barrett, P. J. (1996), "Antarctic paleoenvironment through Cenozoic times – a review", *Terra Antarctica*, 3, 103-19.

Beer, J. (2000), "Polar ice as an archive for solar cycles and the terrestrial climate. The Solar Cycle and Terrestrial Climate", Proc. 1st Solar and Space Weather Euroconference, SP-463, ESA, Santa Cruz de Tenerife, Spain, 671-6.

Belkin, I.M. (2009), “Rapid warming of Large Marine Ecosystems”, *Progress in Oceanography*, 81, 1-4, 207-13.

Berger, A.L. and M.F. Loutre (1991), “Insolation values for the climate of the last 10 million years”, *Quaternary Science Reviews*, 10, 297-317.

Berger, A., M.F. Loutre and J.L. Mélice (1998), “Instability of the astronomical periods from 1.5 Myr BP to 0.5 Myr AP”, *Paleoclimates*, 2, 239-80.

Berger, J-F. and J. Guilaine (2009), “The 8,200 cal BP abrupt environmental change and the Neolithic transition: A Mediterranean perspective”, *Quaternary International*, 200, 1-2, 31-49.

Berman, T., N. Paldor and S. Brenner (2003), “Annual SST cycle in the Eastern Mediterranean, Red Sea and Gulf of Elat”, *Geophysical Research Letters*, 30, 5, 1261, doi:10.1029/2002GL015860.

Bindoff, N.L., J. Willebrand, V. Artale, A. Cazenave, J. Gregory, S. Gulev, K. Hanawa, C. Le Quéré, S. Levitus, Y. Nojiri, C.K. Shum, L.D. Talley and A. Unnikrishnan (2007), “Observations: Oceanic Climate Change and Sea Level”, in: Solomon, S., D. Qin, M. Manning, Z. Chen, M. Marquis, K.B. Averyt, M. Tignor and H.L. Miller (eds), “Climate Change 2007: The Physical Science Basis”, Contribution of Working Group I to the Fourth Assessment Report of the Intergovernmental Panel on Climate Change, Cambridge University Press, Cambridge, United Kingdom and New York, USA.

Bond, G., B. Kromer, J. Beer, R. Muscheler, M. Evans, W. Showers, S. Hoffmann, R. Lottibond, I. Hajdas and G. Bonani (2001), “Persistent solar influence on North Atlantic climate during the Holocene”, *Science*, 294, 2130-6.

Bowen, D.Q. (2009), “Sea level 400,000 years ago (MIS 11): analogue for present and future sea-level”, *Climate of the Past Discussion*, 5, 1853-82.

Bradley, R.S. (1999), “Paleoclimatology. Reconstructing Climates of the Quaternary”, *International Geophysics*, Academic Press.

Brasseur, P., J.M. Beckers, J.M. Brankart and R. Schoenauen (1996), “Seasonal temperature and salinity fields in the Mediterranean Sea: climatological analyses of an historical dataset”, *Deep-Sea Research*, 43, 2, 159-92.

Broecker, W. S. and T.L. Stocker (2006), “The Holocene CO₂ rise: Anthropogenic or natural?”, *Eos Trans. AGU*, 87, 3, 27.

Brönnimann, S., E. Xoplaki, C. Casty, A. Pauling and J. Luterbacher (2007), “ENSO influence on Europe during the last centuries”, *Climate Dynamics*, 28, 181-97.

Büntgen, U., D. Frank, H. Grudd and J. Esper (2008), “Long-term summer temperature variations in the Pyrenees”, *Climate Dynamics*, 31, 6, 15-631.

Büntgen, U., D. Frank, V. Trouet and J. Esper (2010), “Diverse climate sensitivity of Mediterranean tree-ring width and density”, *Trees-Structures and Function*, 24, 2, 261-73.

Cacho, I., J. O. Grimalt, M. Canals, L. Sbaffi, N. J. Shackleton, J. Schönfeld and R. Zahn (2001), "Variability of the western Mediterranean Sea surface temperature during the last 25,000 years and its connection with the Northern Hemisphere climatic changes", *Paleoceanography*, 16(1), 40-52, doi:10.1029/2000PA000502.

Caine, N. (1980), "Rainfall intensity-duration control of shallow landslides and debris flows", *Geograf. Ann.* 62A, 23-7.

Calcaterra, D., M. Parise, B. Palma and L. Pelella (2000), "The influence of meteoric events in triggering shallow landslides in pyroclastic deposits of Campania Italy", in Bromhead, E., N. Dixon and M.L. Ibsen (eds), Proc. 8th Int Symp on Landslides, vol. 1 Cardiff, AA Balkema, 209-14.

Caldeira, K. and M.E. Wickett (2003), "Anthropogenic carbon and ocean pH", *Nature*, 425, 365.

Cannon, S.H. and J.E. Gartner (2005), "Wildfire-related debris flow from a hazards perspective", in Jakob, M. and O. Hungr (eds), "Debris flow Hazards and Related Phenomena", Springer, Berlin-Heidelberg, 363-85.

Cannon S.H., J.E. Gartner, R.C. Wilson, J.C. Bowers and J.L. Layber (2008), Storm rainfall conditions for floods and debris flows from recently burned areas in southwestern Colorado and southern California, *Geomorphology*, 96, 250 -269.

Casford, J.S.L., E.J. Rohling, R.H. Abu-Zied, C. Fontanier, F.J. Jorissen, M.J. Leng, G. Schmiedl and J. Thomson (2003), "A dynamic concept for eastern Mediterranean circulation and oxygenation during sapropel formation", *Palaeogeography, Palaeoclimatology, Palaeoecology*, 190, 103-19.

Castañeda, I.S., E. Schefuß, J. Pätzol, J.S.S. Damsté, S. Weldeab and S. Schouten (2010), "Millennial-scale sea surface temperature changes in the Eastern Mediterranean (Nile River Delta Region) over the last 27,000 years", *Paleoceanography*, in press.

Ciscar J-C, ed. (2009). *Climate change impacts in Europe. Final report of the PESETA research project*. Brussels, European Commission (JRC Scientific and Technical Reports).

Croll, J. (1875), "Climate and time in their geological relations. A theory of secular changes of the earth's climate", Dadly, Ibister & Co, London.

Dahl-Jensen, D., K. Mosegaard, N. Gundestrup, G. D. Clow, S. J. Johnsen, A. W. Hansen and N. Balling (1998), "Past temperature directly from the Greenland Ice Sheet", *Science*, 282, 268-71, doi:10.1126/science.282.5387.268.

De Lange, G.J., J. Thomson, A. Reitz, C.P. Slomp, M.S. Principato, E. Erba and C. Corselli (2008), "Synchronous basin-wide formation and redox-controlled preservation of a Mediterranean sapropel", *Nature Geosciences*, 1, 606-10.

De Rijk, S., A. Hayes and E.J. Rohling (1999), "Eastern Mediterranean sapropel S1 interruption: an expression of the onset of climatic deterioration around 7ka BP", *Marine Geology*, 153, (1-4), 337-43, doi:10.1016/S0025-3227(98)00075-9.

Del Rio Vera, J. et al. (2006), “Mediterranean Sea level analysis from 1992 to 2005”, presented at ESA workshop, Venice, Italy (www.earth.esa.int/workshops/venice06/participants/838paper_838_delriovera.pdf).

deMenocal, P., J. Ortiz, T. Guilderson, J. Adkins, M. Sarnthein, L. Baker and M. Yarusinsky (2000a), “Abrupt onset and termination of the African Humid Period: rapid climate responses to gradual insolation forcing”, *Quaternary Science Reviews*, 19, 1-5, 1, 347-61.

deMenocal, P., J. Ortiz, T. Guilderson and M. Sarnthein (2000b), “Coherent High- and Low-Latitude Climate, Variability During the Holocene Warm Period”, *Science*, 288, 2198-202.

Denton, G.H. and W. Karlén (1973), “Holocene climatic variations: their pattern and possible cause”, *Quaternary Research*, 3, 155-205.

Diakakis, M. (in press), “Rainfall thresholds for flood triggering. The case of Marathonas in Greece”, *Natural Hazards*.

Diffenbough, N.S., J.S. Pal, F. Giorgi and X. Gao (2007), “Heat stress intensification in the Mediterranean climate change hotspot”, *Geophysical Research Letters*, 34, L11706, doi: 10.1029/2007GL030000.

Drysdale, R., G. Zanchetta, J. Hellstrom, R. Maas, A. Fallick, M. Pickett, I. Cartwright and L. Piccini (2006), “Late Holocene drought responsible for the collapse of Old World civilizations is recorded in an Italian cave flowstone”, *Geology*, 34, 101-4.

Duplessy, J.-C., E. Cortijo and N. Kallel (2005), “External Geophysics, Climate and Environment Marine records of Holocene climatic variations”, *Comptes Rendus Geoscience*, 337, 87-95.

ECSN (1995), “European Climate Support Network”, *KNMI*, De Bilt.

Efstratiou, N., A. Karetsou, E. Banou and D. Margomenou (2004), “The Neolithic settlement of Knossos: new light on an old picture”, in Cadogan, G. (ed.), *Knossos: Palace, City, State*, vol. 12, British School at Athens Studies, London.

Emeis, K.-C., H.-M. Schulz, U. Struck, T. Sakamoto, H. Doose, H. Erlenkeuser, M. Howell, D. Kroon and M. Paterne (1998), “Stable isotope and alkenone temperature records of sapropels from sites 964 and 967: Constraining the physical environment of sapropel formation in the eastern Mediterranean sea”, in Robertson, A.H.F., K.-C. Emeis, C. Richter and A. Camerlenghi (eds), 1998 *Proceedings of the Ocean Drilling Program, Scientific Results*, Vol. 160.

Emeis, K.-C., U. Struck, H.-M. Schulz, R. Rosenberg, S. Bernasconi, H. Erlenkeuser, T. Sakamoto and F. Martinez-Ruiz (2000), “Temperature and salinity variations of Mediterranean Sea surface waters over the last 16,000 years from records of planktonic stable oxygen isotopes and alkenone unsaturation ratios”, *Palaeogeography, Palaeoclimatology, Palaeoecology*, 158, 259-80.

Emeis, K.-C., H. Schulz, U. Struck, M. Rossignol-Strick, H. Erlenkeuser, M.W. Howell, D. Kroon, A. Mackensen, S. Ishizuka, T. Oba, T. Sakamoto and I. Koizumi (2003), “Eastern

Mediterranean surface water temperatures and $\delta^{18}\text{O}$ composition during deposition of sapropels in the late Quaternary”, *Paleoceanography*, 18, 1, 1005.

Enzel, Y., R. Bookman, D. Sharon, H. Gvirtzman, U. Dayan, B. Ziv and M. Stein (2003), “Late Holocene climates of the Near East deduced from Dead Sea level variations and modern regional winter rainfall”, *Quaternary Research*, 60, 263-73.

EPICA community members (2004), “Eight glacial cycles from an Antarctic ice core”, *Nature*, 429, 623-8, doi:10.1038/nature02599, 2004.

Esper, J., D. Frank, U. Büntgen, A. Verstege, J. Luterbacher and E. Xoplaki (2007), “Long-term drought severity variations in Morocco”, *Geophysical Research Letters*, 34, L17702, doi:10.1029/2007GL030844.

Feidas, H., T. Makrogiannis and E. Bora-Senta (2004), “Trend analysis of air temperature time series in Greece and their relationship with circulation using surface and satellite data: 1955-2001”, *Theoretical and Applied Climatology*, 79, 185-208, doi: 01007/s00704-004-0064-5.

Feidas, H., Ch. Nouloupoulou T. Makrogiannis and E. Bora-Senta (2007), “Trend analysis of precipitation time series in Greece and their relationship with circulation using surface and satellite data: 1955-2001”, *Theoretical and Applied Climatology*, 87, 155-77, doi:101007/s00704-006-0200-5.

Felis, T., G. Lohmann, H. Kuhnert, S. J. Lorenz, D. Scholz, J. Pätzold, S.A. Al-Rousan and S.M. Al-Moghrabi (2004), “Increased seasonality in Middle East temperatures during the last interglacial period”, *Nature*, 429, 164.

Felis, T. and N. Rimbu (2010), “Mediterranean climate variability documented in oxygen isotope records from northern Red Sea corals – A review”, *Global and Planetary Change*, 71, 3-4, 232-41.

Fischer, E. M., S. Seneviratne, I. Lüthi and D.C. Schär (2007), “Contribution of land-atmosphere coupling to recent European summer heat waves”, *Geophysical Research Letters*, 34, L06707.

Fleitmann, D. et al. (2003), “Holocene forcing of the Indian monsoon recorded in a stalagmite from southern Oman”, *Science*, 300, 1737-40.

Founda, D., K.H. Papadopoulos, M. Petrakis, C. Giannakopoulos and P. Good (2004), “Analysis of mean, maximum and minimum temperature in Athens from 1897 to 2001 with emphasis on the last decade: trends, warm events, and cold events” *Global and Planetary Change*, 44, 27-38.

Founda, D. and C. Giannakopoulos (2009), “The exceptionally hot summer of 2007 in Athens, Greece – A typical summer in the future climate?”, *Global and Planetary Change*, 67, 227-36.

Founda, D., C. Giannakopoulos, F. Pierros, M. Petrakis and C. Zerefos (2009), “Precipitation regime in Athens (Greece) in the past, recent and future climate”, *Geophysical Research Abstracts*, 11, EGU2009-7616.

Founda, D. (2011), “Evolution of the air temperature in Athens and evidence of climatic change: A review”, *Advances in Building Energy Research* (in press).

Frei, C. et al. (2006), “Future change of precipitation extremes in Europe: Intercomparison of scenarios from regional climate models”, *J. Geophys. Res.*, 111, D06105, doi:10.1029/2005JD005965.

Frisia, S., A. Borsato, A. Mangini, C. Spötl, G. Madonia and H. Sauro (2006), “Holocene climate variability in Sicily from a discontinuous stalagmite record and the Mesolithic to Neolithic transition”, *Quaternary Research*, 66, 388-400.

Gao, C., A. Robock and C. Ammann (2008), “Volcanic forcing of climate over the past 1500 years: An improved ice core-based index for climate models”, *Journal of Geophysical Research-Atmospheres*, 113(D23): D23111.

Gao, X., J.S. Pal and F. Giorgi (2006), “Projected changes in mean and extreme precipitation over the Mediterranean region from a high resolution double nested RCM simulation”, *Geophysical Research Letters*, 33, L03706, doi: 10.1029/2005GL024954.

Gasse, F. (2000), “Hydrological changes in the African tropics since the last glacial maximum”, *Quaternary Science Reviews*, 19, 189-211.

Gasse, F. (2001), “Hydrological changes in Africa”, *Science*, 292, 2259-60.

Georgakakos, K.P. (2006), “Analytical results for operational flash flood guidance”, *J Hydrol*, 317, 81-103.

Geraga, M., G. Mylona, St. Tsaila-Monopoli, G. Papatheodorou and G. Ferentinos (2008), “Northeastern Ionian Sea: Palaeoceanographic variability over the last 22 ka”, *Journal of Marine Systems*, 74, 1-2, 623-38.

Geraga, M., St. Tsaila-Monopoli, Ch. Ioakim, G. Papatheodorou and G. Ferentinos (2000), “An evaluation of paleoenvironmental changes during the last 18,000 yr BP in the Myrtoon Basin, S.W. Aegean Sea”, *Palaeogeography, Palaeoclimatology, Palaeoecology*, 156, 1-17.

Geraga, M., St. Tsaila-Monopoli, Ch. Ioakim, G. Papatheodorou and G. Ferentinos (2005), “Short-term climate changes in the southern Aegean Sea over the last 48,000 years”, *Palaeogeography, Palaeoclimatology, Palaeoecology*, 220, 311-32.

Giannakopoulos, C., P. Le Sager, M. Bindi, M. Moriondo, E. Kostopoulou and C.M. Goodess (2009a), “Climatic changes and associated impacts in the Mediterranean resulting from a 2°C global warming”, *Global and Planetary Change*, 68, 209-24.

Giannakopoulos, C., P. Hadjinicolaou, C. Zerefos and G. Demosthenous (2009b), “Changing energy requirements in the Mediterranean under changing climatic conditions”, *Energies*, 2(4), 805-15.

Gibelin, A.L. and M. Deque (2003), “Anthropogenic climate change over Mediterranean region simulated by a global variable resolution model”, *Climate Dynamics*, 20, 327-39.

Giorgi, F. and X. Bi (2005), “Regional changes in surface climate interannual variability for the 21st century from ensembles of global model simulations”, *Geophysical Research Letters*, 32, L13701, doi: 10.1029/2005GL023002.

Giorgi, F. (2006), “Climate change hot-spots”, *Geophysical Research Letters*, 33, L08707, doi: 10.1029/2006GL025734.

Giorgi, F. and P. Lionello (2008), “Climate change projections for the Mediterranean region”, *Global and Planetary Change*, 63, 90-104.

Glueck, M.F. and C.W. Stockton (2001), “Reconstruction of the North Atlantic Oscillation, 1429-1983”, *International Journal of Climatology*, 21, 12, 1453-65.

Gogou, A., I. Bouloubassi, V. Lykousis, M. Arnaboldi, P. Gaitani and P.A. Meyers (2007), “Organic geochemical evidence of abrupt late Glacial-Holocene climate changes in the North Aegean Sea”, *Palaeogeography, Palaeoclimatology, Palaeoecology*, 256, 1-20.

Good, P., M. Moriondo, C. Giannakopoulos and M. Bindi (2008), “The meteorological conditions associated with extreme fire risk in Italy and Greece: Relevance to climate model studies”, *International Journal of Wildland Fire*, 17, 155-65.

Goubanova, K. and L. Li (2007), “Extremes in temperature and precipitation around the Mediterranean basin in an ensemble of future climate scenario simulations”, *Global and Planetary Change*, 57, 27-42, doi: 10.1016/j.gloplacha.2006.11.012.

Grinsted, A., J.C. Moore and S. Jevrejeva (2010), “Reconstructing sea level from paleo and projected temperatures 200 to 2100 AD”, *Climate Dynamics*, 34, 461-72.

Guiot, J. (1987), “Late quaternary climatic change in France estimated from multivariate pollen time series”, *Quaternary Research*, 28, 1, 100-18.

Gurjar, B.R., T.M. Butler, M.G. Lawrence and J. Lelieveld (2007), “Evaluation of emissions and air quality in megacities”, *Atmos. Env.*, doi:10.1016/j.atmosenv.2007.10.048.

Hassid, S., M. Santamouris, N. Papanikolaou, A. Linardi, N. Klitsikas, C. Georgakis and D.N. Assimakopoulos (2000), “The Effect of the Athens Heat Island on Air Conditioning Load”, *J. Energy and Buildings*, 32, 2, 131-41.

Hatzioannou L., D. Retalis, S. Pasiardis, D. Nikolakis, D. Asimakopoulos and N. Lourantos (1998), “Study of the Precipitation Time Series in SE Greece and Cyprus”, Proceedings of the 4th Greek Scientific Conference in Meteorology-Climatology-Atmospheric Physics, Athens, 22-25 September.

Hegerl, G.C., F.W. Zwiers, P. Braconnot, N.P. Gillett, Y. Luo, J.A. Marengo Orsini, N. Nicholls, J.E. Penner and P.A. Stott (2007), “Understanding and Attributing Climate Change”, in Solomon, S., D. Qin, M. Manning, Z. Chen, M. Marquis, K.B. Averyt, M. Tignor and H.L. Miller (eds), “Climate Change 2007: The Physical Science Basis”, Contribution of Working Group I to the Fourth Assessment Report of the Intergovernmental Panel on Climate Change, Cambridge University Press, Cambridge, United Kingdom and New York, NY, USA.

Hegerl, G., J. Luterbacher, F. González-Rouco, S. Tett, T. Crowley and E. Xoplaki (2011), “Influence of human and natural forcing on European seasonal temperatures”, *Nature Geoscience*, 4, 99-103.

Heiss, G.A. (1994), “Coral reefs in the Red Sea: growth, production and stable isotopes”, *GEOMAR Report*, 32, 1-141.

Hertig, E. and J. Jacobeit (2007), “Assessments of Mediterranean precipitation changes for the 21st century using statistical downscaling techniques”, *International Journal of Climatology*, 28, 1025-45.

Hodell, D.A., M. Brenner, J.H. Curtis and T. Guilderson (2001), “Solar forcing of drought frequency in the Maya Lowlands” *Science*, 292, 1367-70.

Huang, S.P., H.N. Pollack and P.Y. Shen (2000), “Temperature trends over the past five centuries reconstructed from borehole temperatures”, *Nature*, 403 (6771), 756-8.

Hulme, M., J. Mitchell, W. Ingram, J. Lowe, T. Johns, M. New and D. Viner (1999), “Climate change scenarios for global impacts studies”, *Global Environmental Change*, 9, S3-S19.

Huntingford, C. et al. (2003), “Regional climate-model predictions of extreme rainfall for a changing climate” *Q. J. R. Meteorol. Soc.*, 129, 1607-21.

IPCC (1996), “Climate Change 1995: The Science of Climate Change”, in Houghton, J.T., L.G. Meira Filho, B.A. Callander, N. Harris, A. Kattenberg and K. Maskell (eds), Contribution of Working Group I to the Second Assessment report of the Intergovernmental Panel on Climate Change, Cambridge University Press, Cambridge, United Kingdom, and New York, NY, USA, and Melbourne, Australia, 572.

IPCC (2001), “Climate Change 2001: The Scientific Basis”, in Houghton, J.T., Y. Ding, D.J. Griggs, M. Noguer, P.J. van der Linden, X. Dai, K. Maskell and C.A. Johnson (eds), Contribution of Working Group I to the Third Assessment Report of the Intergovernmental Panel on Climate Change, Cambridge University Press, Cambridge, United Kingdom, and New York, NY, USA, 881.

IPCC (2007), “Climate change 2007: The physical science basis”, in Solomon, S., D. Qin, M. Manning, Z. Chen, M. Marquis, K.B. Averyt, M. Tignor, H.L. Miller (eds), Contribution of Working Group I to the Fourth Assessment Report of the Intergovernmental Panel on Climate Change, Cambridge University Press, Cambridge, New York, 996.

IPCC (2013), in press.

Jansen, E., J. Overpeck, K.R. Briffa, J.-C. Duplessy, F. Joos, V. Masson-Delmotte, D. Olago, B. Otto-Bliesner, W.R. Peltier, S. Rahmstorf, R. Ramesh, D. Raynaud, D. Rind, O. Solomina, R. Villalba and D. Zhang, (2007), “Palaeoclimate”, in Solomon, S., D. Qin, M. Manning, Z. Chen, M. Marquis, K.B. Averyt, M. Tignor and H.L. Miller (eds), “Climate Change 2007: The Physical Science Basis”, Contribution of Working Group I to the Fourth Assessment Report of the Intergovernmental Panel on Climate Change, Cambridge University Press, Cambridge, United Kingdom, and New York, NY, USA.

Jolly, D., S.P. Harrison, B. Damnati and R. Bonnefille (1998), “Simulated climate and biomes of Africa during the Late Quaternary: comparison with pollen and lake status data”, *Quaternary Science Reviews*, 17, 629-57.

Jones, P.D. and A. Moberg (2003), “Hemispheric and large-scale surface air temperature variations: An extensive revision and an update to 2001”, *Journal of Climate*, 16, 206-23.

Jouzel, J., V. Masson-Demotte, O. Cattani, G. Dreyfus, S. Falourd, G. Hoffmann, B. Minster, J. Nouet, J.M. Barnola, J. Chappellaz, H. Fischer, J.C. Gallet, S. Johnsen, M. Leuenberger, L. Loulergue, D. Luethis, H. Oerter, F. Parrenin, G. Raisbeck, D. Raynaud, A. Schilt, J. Schwander, E. Selmo, R. Souchez, R. Spahni, B. Stauffer, J. P. Steffensen, B. Stenni, T.F. Stocker, J.L. Tison, M. Werner and E.W. Wolff (2007), “Orbital and millennial Antarctic climate variability over the past 800,000 years” *Science*, 317, 793-6.

Kambouroglou E., H. Maroukian and A. Sampsos (1988), “Coastal evolution and archaeology north and south of Khalkis (Euboea) in the last 5000 years”, in Raban, A. (ed.), *Archaeology of Coastal Changes*, BAR Int. Ser., Oxford, 404, 71-9.

Karabörk, M. and E. Kahya (2009), “The links between the categorised Southern Oscillation indicators and climate and hydrologic variables in Turkey”, *Hydrological Processes*, 23, 13, 1927-36.

Karlén, W. and J. Kylenstierna (1996), “On solar forcing of Holocene climate: evidence from Scandinavia”, *The Holocene*, 6, 359-65.

Keeling, R.F., A. Kortzinger and N. Gruber (2010), “Ocean Deoxygenation in a Warming World”, *Annual Review of Marine Science*, 2, 199-229.

Keigwin, L.D. (1996), “The Little Ice Age and Medieval Warm Period in the Sargasso Sea”, *Science*, 29, 274, 5292, 1503-8.

Kobashi T., J.P. Severinghaus, J.-M. Barnola, K. Kawamura, T. Carter, T. Nakaegawa (2010), “Persistent multi-decadal Greenland temperature fluctuation through the last millennium”, *Climatic Change*, Vol. 100, 3-4, 733-56.

Kopp, R.E., F.J. Simons, J.X. Mitrovica, A.C. Maloof and M. Oppenheimer (2009), “Probabilistic assessment of sea level during the last interglacial stage”, *Nature*, 462, 863-7.

Kostopoulou, E. and P.D. Jones (2005), “Assessment of climate extremes in the Eastern Mediterranean”, *Meteorology and Atmospheric Physics*, 89, 69-85.

Kraft, J.C., S.E. Aschenbrenner and G.J. Rapp (1977), “Palaeogeographic reconstructions of coastal Aegean archaeological sites”, *Science* 195, 941-7.

Kraft, J.C., J.G.R. Rapp and S.E. Aschenbrenner (1980), “Late Holocene palaeogeomorphic reconstructions in the area of the Bay of Navarino: Sandy Pylos”, *Journal of Archaeological Science*, 7, 187-210.

Kuglitsch, F.G., A. Toreti, E. Xoplaki, P.M. Della-Marta, C.S. Zerefos, M. Türkeş and J. Luterbacher (2010), “Heat Wave Changes in the Eastern Mediterranean since 1960”, *Geophysical Research Letters*, 37, L04802.

Kuniholm, P. I. and C.L. Striker (1987), “Dendrochronological investigations in the Aegean and neighboring regions, 1983-1986”, *Journal of Field Archaeology*, 14, 385.

Lambeck, K. (1995), “Late Pleistocene and sea-level change in Greece and south-western Turkey: a separation of eustatic, isostatic and tectonic contributions”, *Geophysical Journal International*, 122, 1022-44.

Lambeck, K. (1996), “Sea-level changes and shoreline evolution in Aegean Greece since Upper Paleolithic time”, *Antiquity*, 70, 588-611.

Lambeck, K. and E. Bard (2000), “Sea-level change along the French Mediterranean coast for the past 30,000 years”, *Earth and Planetary Science Letters*, 175, 203-22.

Lambeck, K. and A. Purcell (2005), “Sea-level change in the Mediterranean Sea since the LGM: model predictions for tectonically stable areas”, *Quaternary Science Reviews*, 24, 1969-88.

Lehner, B., P. Döll, J. Alcamo, H. Henrichs and F. Kaspar (2006), “Estimating the impact of global change on flood and drought risks in Europe: a continental, integrated analysis”, *Climatic Change*, 75, 273-99.

Lionello, P., P. Malanotte-Rizzoli, R. Boscolo, P. Alpert, V. Artale, L. Li, J. Luterbacher, W. May, R. Trigo, M. Tsimplis, U. Ulbrich and E. Xoplaki (2006), The Mediterranean climate: an overview of the main characteristics and issues. In Lionello et al. (eds), *Mediterranean Climate Variability*, Elsevier, Amsterdam, The Netherlands, pp. 1-26.

Lionello, P. and M.B. Galati (2008), “Links of the significant wave height distribution in the Mediterranean sea with the Northern Hemisphere teleconnection patterns”, *Advances in Geoscience*, 17, 13-8.

Lisiecki, L.E. and M.E. Raymo (2005), “A Pliocene-Pleistocene stack of 57 globally distributed benthic $\delta^{18}\text{O}$ records”, *Paleoceanography*, 20, PA1003.

Livada, I., M. Santamouris, K. Niachou, N. Papanikolaou and G. Mihalakakou (2002), “Determination of places in the great Athens area where the heat island effect is observed”, *Theor. Appl. Climatol.*, 71, 219-30.

Loukas, A., L. Vasiliades and N.R. Dalezios (2002), “Potential climate change impacts on flood-producing mechanisms in southern British Columbia, Canada, using the CGCMA1 simulation results”, *J. Hydrol.*, 259, 163-88.

Loulergue, L., A. Schilt, R. Spahni, V. Masson-Delmotte, T. Blunier, B. Lemieux, J.M. Barnola, D. Raynaud, T.F. Stocker and J. Chappellaz (2008), “Orbital and millennial-scale features of atmospheric CH_4 over the past 800,000 years”, *Nature*, 435, 383-6.

Loutré, M.F. and A. Berger (2000), “Future climatic changes: are we entering an exceptionally long interglacial?”, *Climate Change*, 46, 61-90.

Loutré, M.F. and A. Berger (2003), “Marine Isotope Stage 11 as an analogue for the present interglacial”, *Global and Planetary Change*, 36, 209-17.

Luterbacher, J., R. Rickli, E. Xoplaki, C. Tinguely, C. Beck, C. Pfister and H. Wanner (2001), The late Maunder Minimum (1675-1715) – A key period for studying decadal scale climatic change in Europe, *Climate Change*, 49: 441-462.

Luterbacher, J. and E. Xoplaki (2003), “500-Year Winter Temperature and Precipitation Variability over the Mediterranean Area and its Connection to the Large-Scale Atmospheric Circulation”, in Bolle, H.-J. (ed.), “Mediterranean Climate. Variability and Trends”, *Springer Verlag*, Berlin, Heidelberg, 133-53.

Luterbacher, J. et al. (2006), “Mediterranean climate variability over the last centuries: a review”, in Lionello, P., P. Malanotte-Rizzoli and R. Boscolo (eds), “The Mediterranean climate: an overview of the main characteristics and issues”, *Elsevier*, Amsterdam, 27-148.

Luterbacher, J, S.J. Koenig, J. Franke, G. van der Schrier, E. Zorita, A. Moberg, J. Jacobeit, P.M. Della-Marta, M. Küttel, E. Xoplaki, D. Wheeler, T. Rutishauer, M. Stössel, H. Wanner, R. Brázdil, P. Dobrovolný, D. Camuffo, C. Bertolin, A. van Engelen, F.J. Gonzalez-Rouco, R. Wilson, C. Pfister, D. Limanówka, Ø. Nordli, L. Leijonhufvud, J. Söderberg, R. Allan, M. Barriendos, R. Glaser, D. Riemann, Z. Hao and C.S. Zerefos (2010), “Circulation dynamics and its influence on European and Mediterranean January-April climate over the past half millennium: results and insights from instrumental data, documentary evidence and coupled climate models”, *Climatic Change*, 101, 201-34.

Luterbacher, J., R. García-Herrera, A. R. Allan, M. C. Alvarez-Castro, G. Benito, J. Booth, U. Büntgen, D. Colombaroli, B. Davis, J. Esper, T. Felis, D. Fleitmann, D. Frank, D. Gallego, E. Garcia-Bustamante, J. F. González-Rouco, H. Goosse, T. Kiefer, M. G. Macklin, S. Manning, P. Montagna, L. Newman, M. J. Power, V. Rath, P. Ribera, N. Roberts, S. Silenzi, W. Tinner, B. Valero-Garces, G. van der Schrier, C. Tzedakis, B. Vannière, H. Wanner, J. P. Werner, G. Willeit, E. Xoplaki, C. S. Zerefos and E. Zorita (2011) “A review of 2000 years of paleoclimatic evidence in the Mediterranean”, in Lionello, P. et al. (eds), “The Mediterranean Climate: from past to future”, *Elsevier*, Amsterdam, The Netherlands, in press.

Maheras, P., K. Tolika, C. Anagnostopoulou, M. Vafiadis, I. Patrikas and H. Floca (2004), “On the relationship between circulation types and changes in rainfall variability in Greece”, *International Journal of Climatology*, 24, 1695-1712.

Malanotte-Rizzoli, P., B.B. Manca, M. Ribera d’Alcala, A. Theocharis, A. Bergamasco, D. Bregant, G. Budillon, G. Civitarese, D. Georgopoulos, A. Michelato, E. Sansone, P. Scarazato and E. Souvermezoglou (1997) “A synthesis of the Ionian Sea hydrography, circulation and water mass pathways during POEM-Phase I”, *Progress in Oceanography* 39, 153-204.

Mantis, H.T., C.C. Repapis, C.M. Philandras, A.G. Paliatsos and G.T. Amanatidis (1997), “The spatial and temporal structure of precipitation in the Eastern Mediterranean: Background for climate change”, Proc. of the Eastern Europe and Global Change Symposium, 3-10 October 1994, Kassandra, Halkidiki, Greece, 125-31.

Marchal, O., I. Cacho, T.S. Stocker, J.O. Grimalt, E. Calvo, B. Martrat, N. Shackleton, M. Vautravers, E. Cortijo, S. van Kreveld, C. Andersson, N. Koc, M. Chapman, L. Scaffi, J.-C. Duplessy, M. Sarnthein, J.-L. Turon, J. Duprat and E. Jansen (2002), “Apparent long-term cooling of the sea surface in the northeast Atlantic and Mediterranean during the Holocene”, *Quaternary Science Reviews*, 21, 455-83.

Marino, G. (2008), “Palaeoceanography of the interglacial eastern Mediterranean Sea”, Thesis, Utrecht.

Maslin, M.A., X.S. Li, M.-F. Loutre and A. Berger (1998), “The contribution of orbital forcing to the progressive intensification of Northern Hemisphere glaciation”, *Quaternary Science Reviews*, 17, 411-26.

Masson-Delmotte, V., A. Landais, N. Combourieu-Nebout, U. v. Grafenstein, J. Jouzel, N. Cailion, J. Chappellaz, D. Dahl-Jensen, S.J. Johnsen and B. Stenni (2005), “Rapid climate variability during warm and cold periods in polar regions and Europe” *C. R. Geosciences*, 337, 935-46.

Masson-Delmotte, V., G. Dreyfus, P. Braconnot, S. Johnsen, J. Jouzel, M. Kageyama, A. Landais, M.-F. Loutre, J. Nouet, F. Parrenin, D. Raynaud, B. Stenni and E. Tuenter (2006), “Past temperature reconstructions from deep ice cores: relevance for future climate change”, *Climate of the Past*, 2, 145-65.

Masterton, J.M. and F.A. Richardson (1979), “Humidex. A method of quantifying human discomfort due to excessive heat and humidity”, Downsview, Ontario, Canada, AES, Environment Canada, CLI 1-79.

Matzarakis, A. and P.T. Nastos (2011), “Human-Biometeorological assessment of heat waves in Athens”, *Theoretical and Applied Climatology*, doi 10.1007/s00704-010-0379-3.

Mayewski, P.A., L.D. Meeker, M.S. Twickler, S. Whitlow, Q. Yang, W.B. Lyons and M. Prentice (1997), “Major features and forcing of high-latitude northern hemisphere atmospheric circulation using a 110,000-year long glaciochemical series”, *Journal of Geophysical Research*, 102, 26345-66.

Mayewski, P.A., E. Rohling, J.C. Stager, W. Karlen, K.A. Maasch, L.D. Meeker, E.A. Meyerson, F. Gasse, S. van Kreveld, K. Holmgren, J. Lee-Thorp, G. Rosqvist, F. Rack, M. Staubwasser, R.R. Schneider and E.J. Steig (2004), “Holocene climate variability”, *Quaternary Research*, 62, 243-55.

McCormack, F.G., A.G. Hogg, P.G. Blackwell, C.E. Buck, P.J. Higham and P.J. Reimer (2004), “SHCAL04 Southern Hemisphere calibration. 0-11.0 cal kyr BP”, *Radiocarbon*, 48, 1087-92.

McCulloch, M.T. and T. Esat (2000), “The coral record of last interglacial sea levels and sea surface temperatures”, *Chemical Geology*, 169, 107-29.

McCulloch, M., M. Taviani, P. Montagna, M. López Correa, A. Remia and G. Mortimer (2010), “Proliferation and demise of deep-sea corals in the Mediterranean during the Younger Dryas”, *Earth and Planetary Science Letters*, 298, 143-52.

McGarry, S., M. Bar-Matthews, A. Matthews, A. Vaks, B. Schilman and A. Ayalon (2004), “Constraints on hydrological and paleotemperature variations in the Eastern Mediterranean region in the last 140 ka given by the δD values of speleothem fluid inclusions”, *Quaternary Science Reviews*, 7-8, 919-93.

Meehl, G. A., T. F. Stocker, W. Collins, P. Friedlingstein, A. Gaye, J. M. Gregory, A. Kitoh, R. Knutti, J. Murphy, A. Noda, S.C.B. Raper, I. Watterson, A. Weaver and Z.-C. Zhao (2007), “Global Climate Projections”, Chapter 10 of IPCC Fourth Assessment Report, IPCC, Cambridge, Cambridge University Press.

Metaxas, D.A. (1973), “Air-Sea interaction in the Greek seas and resulted Etesians wind characteristics”, Univ. Ioannina, Greece, Tech. Report, 5.

Metaxas, D.A. and C.C. Repapis (1977), “Evaporation in the Mediterranean”, *Riv. Meteor. Aeron.*, 37, 311-22.

Metaxas, D.A., A. Bartzokas and A. Vitsas (1991), “Temperature fluctuations in the Mediterranean Area during the last 100 years”, *Int. J. Climatol.*, 11, 897-908.

Mihalakakou, G., H. Flokas, M. Santamouris and C. Helmis (2002), “Application of Neural Networks to the simulation of the heat island over Athens, Greece, using synoptic types as a predictor” *J Appl. Meteorol.*, 41, 519-27.

Mihalakakou, G., M. Santamouris, N. Papanikolaou and C. Cartalis (2004), “Simulation of the urban heat island phenomenon in Mediterranean climates”, *Pure and applied Geophysics*, 161, 429-51.

Milankovitch, M. (1941), “Canon of Insolation and the Ice Age Problem”, *Royal Serbian Sciences*, Special Publication 132, Section of Mathematical and Natural Sciences, 33, 633, Belgrade.

Miller, K.G., J.D. Wright and J.V. Browning (2005), “Visions of ice sheets in a greenhouse world”, *Marine Geology*, 217, 215-31.

Monks, P. (2005), “Gas-phase radical chemistry in the troposphere”, *Chem. Soc. Rev.*, 34, 376-95.

Montagna, P., M. McCulloch, M. Taviani, C. Mazzoli and B. Vendrell (2006), “Phosphorus in cold-water corals as a proxy for seawater nutrient chemistry”, *Science*, 312, 1788-91.

Montagna, P., S. Silenzi, S. Devoti, C. Mazzoli, M. McCulloch, G. Scicchitano and M. Taviani (2008), “High-resolution natural archives provide new tools for climate reconstruction and monitoring in the Mediterranean Sea”, *Rendiconti Lincei*, 19(b), 121-40.

Montagna, P., M. McCulloch, M. Taviani, J. Trotter, S. Silenzi and C. Mazzoli (2009), “An improved sampling method for coral P/Ca as a nutrient proxy”, *Geochimica et Cosmochimica Acta*, 25, 1888-1947.

Moriondo, M., P. Good, R. Durao, M. Bindi, C. Giannakopoulos and J. Corte-Real (2006), “Potential impact of climate change on fire risk in the Mediterranean area”, *Climate Research*, 13, 85-95.

Müller, S.A., F. Joos, N.R. Edwards and T.F. Stocker (2006), “Water mass distribution and ventilation time scales in a cost-efficient, three-dimensional ocean model”, *Journal of Climate* 19, 5479-99.

Nakićenović, N., J. Alcamo, G. Davis, B. de Vries, J. Fenhann, S. Gaffin, K. Gregory, A. Grübler, T.Y. Jung, T. Kram, E.L. La Rovere, L. Michaelis, S. Mori, T. Morita, W. Pepper, H. Pitcher, L. Price, K. Raihi, A. Roehrl, H.-H. Rogner, A. Sankovski, M. Schlesinger, P. Shukla, S. Smith, R. Swart, S. van Rooijen, N. Victor and Z. Dadi (2000), “IPCC Special Report on Emissions Scenarios”, Cambridge University Press, Cambridge, UK.

Nastos, P.T. and C.S. Zerefos (2007), “On extreme daily precipitation totals at Athens, Greece”, *Advances in Geosciences*, 10, 59-66.

Norbiato, D., M. Borga, S.D. Esposti, E. Gaume and S. Anquetin (2008), “Flash flood warning based on rainfall thresholds and soil moisture conditions: an assessment for gauged and ungauged basins”, *J Hydrology*, 362, 274-90.

O’Brien, S.R., P.A. Mayewski, L.D. Meeker, D.A. Meese, M.S. Twickler and S.I. Whitlow (1995), “Complexity of Holocene climate as reconstructed from a Greenland ice core”, *Science*, 270, 1962-4.

Otto-Bliesner, B.L. et al. (2006), “Simulating Arctic climate warmth and icefield retreat in the last interglaciation”, *Science*, 311, 1751-3.

Pal, J.S., F. Giorgi, X. Bi (2004), “Consistency of recent European summer precipitation trends and extremes with future regional climate projections”, *Geophysical Research Letters*, 31, L13202, doi: 10.1029/2004GL019836.

Park, H.S. (1986), “Features of the heat island in Seoul and its surrounding cities”, *Atmos. Environ.* 20, 1859-66.

Pavlopoulos, K., M. Triantaphyllou, E. Karymbalis, P. Karkanis, K. Kouli and T. Tsourou (2007), “Landscape evolution recorded in the embayment of Palamari (Skyros Island, Greece) from the beginning of the Bronze Age until recent times”, *Géomorphologie: relief, processus, environment*, 1, 37-48.

Paz, S., H. Kutiel and E. H. Steinberger (1998), “Variations in rainfall along the eastern Mediterranean coast”, *Proceedings of the 4th Pan-Hellenic Symposium on Meteorology, Climatology and Atmospheric Physics*, Athens, Greece, Vol. 2, 299-304, September 22-25.

Peltier, W.R. and R.G. Fairbanks (2006), “Global glacial ice volume and last glacial maximum duration from an extended Barbados sea level record”, *Quaternary Science Reviews*, 25, 3322-37.

Perissoratis, C. and D.J.W. Piper (1992), “Age, regional variation and shallowest occurrence of S1 sapropel in the northern Aegean Sea”, *Geomarine Letters*, 12, 49-53.

Pfeffer, W.Y., J.T. Harper and S. O’Neel (2008), “Kinematic constraints on Glacier Contributions to 21st-Century Sea-Level Rise”, *Science*, 321, 5894, 1340-3.

Philandras, C.M., D.A. Metaxas and P.T. Nastos (1999), “Climate variability and urbanization in Athens”, *Theor. Appl. Climatol.* 63, 65-72.

Pirazzoli, P.A. and J. Pluet (1991), “World atlas of Holocene sea-level changes”, *Elsevier Oceanography Series*, 58.

Pollack, H.N. and J.E. Smerdon (2004), “Borehole climate reconstructions: Spatial structure and hemispheric averages”, *J. Geophys. Res.*, 109 (D11), D11106, doi:10.1029/2003JD004163.

Ponel, P. and G.R.Coope (1990), “Lateglacial and Early Flandrian Coleoptera from La Taphanel, Massif Central, France: Climatic and Ecological Implications”, *Journal of Quaternary Science*, 5, 3, 235-49.

Poulos, S.E., P.G. Drakopoulos and M.B. Collins (1997), “Seasonal variability in sea surface oceanographic conditions in the Aegean Sea (eastern Mediterranean): an overview”, *Journal of Marine Systems*, 13, 225-44.

Poulos, S.E., G. Ghionis and H. Maroukian (2009a), “The consequences of a future eustatic sea-level rise on the deltaic coasts of Inner Thermaikos Gulf (Aegean Sea) and Kyparissiakos Gulf (Ionian Sea), Greece”, *Geomorphology*, 107 (1-2), 1-17.

Poulos, S.E., G. Ghionis and H. Maroukian (2009b), “The consequences of a future eustatic sea-level rise on the deltaic coasts of Inner Thermaikos Gulf (Aegean Sea) and Kyparissiakos Gulf (Ionian Sea), Greece”, *Geomorphology*, 107 (1-2), 18-24.

Rabineau, M., S. Berné, J.-L. Olivet, D. Aslanian, F. Guillocheau and P. Joseph (2006), “Paleo sea levels reconsidered from direct observation of paleoshoreline position during Glacial Maxima (for the last 500,000 yr)”, *Earth and Planetary Science Letters*, 252, 119-37.

Rahmstorf, S. (2007), “Sea-Level Rise: A semi-Empirical Approach to Projecting Future”, *Science*, 315, 368-70.

Rayner, N.A. et al. (2006), “Improved analyses of changes and uncertainties in sea surface temperature measured in situ since the mid-nineteenth century”, the HadSST2 dataset, *J. Climate*, 19, 446-69.

Reimer, P.J., M.G.L. Baillie, E. Bard, A. Bayliss, J.W. Beck, C.J.H. Bertrand, P.G. Blackwell, C.E. Buck, G.S. Burr, K.B. Cutler, P.E. Damon, R.L. Edwards, R.G. Fairbanks, M. Friedrich, T.P. Guilderson, A.G. Hogg, K.A. Hughen, B. Kromer, G. McCormac, S. Manning, C.B. Ramsey, R.W. Reimer, S. Remmele, J.R. Southon, M. Stuiver, S. Talamo, F.W. Taylor, J. van der Plicht and C.E. Weyhenmeyer (2004), “INTCAL04 terrestrial radiocarbon age calibration, 0–26 cal kyr BP”, *Radiocarbon*, 48, 1029-58.

Repapis, C.C., C.S. Zerefos and V. Tritakis (1977), “On the Etesians over the Aegean”, *Πρακτικά Ακαδημίας Αθηνών*, τ. 52, 571-605.

Repapis, C.C. and C.M. Philandras (1988), “A note on the air temperature trends of the last 100 years as evidenced in the Eastern Mediterranean time series”, *Theor. Appl. Climatol.*, 39, 93-107.

Repapis, C.C., C.J.E. Schuurmans, C.S. Zerefos and J. Ziomas (1989), “A note on the frequency of occurrence of severe winters as evidenced in monastery and historical records from Greece, during the period 1200-1900 A.D” *Theor. Appl. Climatol.* 39, 213-7.

Repapis, C.C., C.M. Philandras, P.D. Kalabokas, P. Zanis and C.S. Zerefos (2007), “Is the last years abrupt warming in the National Observatory of Athens records a climate change manifestation?”, *Global Nest*, v. 9, No 2, 107-16.

Roberts, G., P. Artaxo, J. Zhou, E. Swietlicki and M.O. Andreae (2002), “Sensitivity of CCN spectra on chemical and physical properties of aerosol: A case study from the Amazon Basin”, *J. Geophys. Res.*, 107, 10.1029/2001JD000583.

Rohling, E.J. and F.J. Hilgen (1991), “The eastern Mediterranean climate at times of sapropel formation: a review”, *Geologie & Mijnbouw*, 70, 253-64.

Rohling, E.J. (1994), “Review and new aspects concerning the formation of Eastern Mediterranean sapropels”, *Marine Geology*, 122, 1-28.

Rohling, E., J. Casford, R. Abu-Zied, S. Cooke, D. Mercone, J. Thomson, I. Croudace, F. Jorissen, H. Brinkhuis, J. Kallmeyer et al. (2002), *Rapid Holocene climate changes in the Eastern Mediterranean*, I, 35-46, doi: 10.1007/0-306-47547-2_3.

Rohling, E.J., P.A. Mayewski, R.H. Abu-Zied, J.S.L. Casford and A. Hayes (2002b), “Holocene atmosphere – ocean interactions: records from Greenland and The Aegean Sea”, *Climate Dynamics*, 18, 587-93.

Rohling, E.J. and H. Pälike (2005), “Centennial-scale climate cooling with a sudden cold event around 8,200 years ago”, *Nature*, 434, 975-9.

Rohling, E.J., K. Grant, Ch. Hemleben, M. Siddall, A. Hoogakker, M. Bolshaw and M. Kucera (2008), “High rates of sea-level rise during the last interglacial period”, *Nature Geoscience*, 1, 38-42.

Rohling, E.J., K. Grant, M. Bolshaw, A.P. Roberts, M. Siddall, Ch. Hemleben and M. Kucera (2009), “Antarctic temperature and global sea level closely coupled over the past five glacial cycles”, *Nature Geoscience*, 2, 500-4.

Rohling, E.J., K. Braun, K. Grant, M. Kucera, A.P. Roberts, M. Siddall and G. Trommer (2010), “Comparison between Holocene and Marine Isotope Stage-11 sea-level histories”, *Earth and Planetary Science Letters*, 291, 97-105.

Rosenzweig, C., G. Casassa, D.J. Karoly, A. Imeson, C. Liu, A. Menzel, S. Rawlins, T.L. Root, B. Seguin and P. Tryjanowski (2007), “Assessment of observed changes and responses in natural and managed systems. Climate Change 2007: Impacts, Adaptation and Vulnerability”, Contribution of Working Group II to the Fourth Assessment Report of the Intergovernmental Panel on Climate Change, in Parry, M.L., O.F. Canziani, J.P. Palutikof, P.J. van der Linden and C.E. Hanson (eds), Cambridge University Press, Cambridge, UK, 79-131.

Rossignol-Strick, M. (1985), “Mediterranean Quaternary sapropels, an immediate response of the African monsoon to variations of insolation”, *Palaeogeography, Paleoclimatology, Palaeoecology*, 49, 237-63.

Rossignol-Strick, M. (1995), “Sea-land correlation of pollen records in the eastern Mediterranean for the glacial-interglacial transition: biostratigraphy versus radiometric time-scale”, *Quaternary Science Reviews*, 14, 893-915, Pergamon, Elsevier, Oxford.

Ruddiman, W. F. (2007), “The early anthropogenic hypothesis: Challenges and responses”, *Reviews of Geophysics*, 45, RG4001, doi:10.1029/2006RG000207.

Saaroni, H., B. Ziv, J. Edelson and P. Alpert (2003), “Long term variations in summer temperature over the Eastern Mediterranean” *Geophysics, Research Letters*, 30, No 18, 1946, doi:10.1029/2003GL017742.

Santamouris, M., N. Papanikolaou, I. Livada, I. Koronakis, C. Georgakis, A. Argiriou and D. N. Assimakopoulos (2001), “On the Impact of Urban Climate to the Energy Consumption of Buildings”, *Solar Energy*, 70, 3, 201-16.

Sbaffi, L., F.C. Wezel, N. Kallel, M. Paterne, I. Cacho, P. Ziveri and N. Shackleton (2001), “Response of the pelagic environment to palaeoclimatic changes in the central Mediterranean Sea during Late Quaternary”, *Marine Geology*, 178, 39-62.

Scafetta, N. and B.J. West (2006), “Phenomenological solar contribution to the 1900-2000 global surface warming”, *Geophysical Research Letters*, 33 L05708, doi: 10.1029/2005GL025539.

Schilman, B., M. Bar-Matthews, A. Almogi-Labin and B. Luz (2001), “Global climate instability reflected by Eastern Mediterranean marine records during the late Holocene”, *Palaeogeography, Palaeoclimatology, Palaeoecology*, 176, 157.

Seki, O., G.L. Foster, D.N. Schmidt, A. Mackensen, K. Kawamura and R.D. Pancost (2010), “Alkenone and boron-based Pliocene pCO₂ records”, *Earth and Planetary Science Letters*, 292, 1-2, 201-11.

Serre-Bachet, F., J. Guiot and L. Tessier (1992), “Dendroclimatic evidence from southwestern Europe and northwestern Africa”, in Bradley, R.S. and P.D. Jones (eds), *Climate Since A.D. 1550*, Routledge, London, 349-65.

Severinghaus, J.P., T. Sowers, E.J. Brook, R.B. Alley and M.L. Bender (1998), “Timing of abrupt climate change at the end of the Younger Dryas interval from thermally fractionated gases in polar ice”, *Nature*, 391, 141-6.

Shackleton, N.J. (2000), “The 100,000-year ice-age cycle identified and found to lag temperature, carbon dioxide, and orbital eccentricity”, *Science*, 289, 1897-1902.

Siddall, M., E. J. Rohling, A. Almogi-Labin, Ch. Hemleben, D. Meischner, I. Schmelzer and D.A. Smeed (2003), “Sea-level fluctuations during the last glacial cycle”, *Nature*, 423, 853-8.

Siddall, M., E.J. Rohling, W.G. Thompson and C. Waelbroeck (2008), “Marine isotope stage 3 sea level fluctuations: Data synthesis and new outlook”, *Reviews of Geophysics*, 46, RG4003.

Silenzi, S., F. Antonioli and R. Chemello (2004), “A new marker for sea surface temperature trend during the last centuries in temperate areas: Vermetid reef”, *Global and Planetary Change*, 40, 105.

Sisma-Ventura, G., B. Guzman, R. Yam, M. Fine, A. Shemesh (2009), “The reef builder gastropod *Dendropoma petreum* – A proxy of short and long term climatic events in the Eastern Mediterranean”, *Geochimica et Cosmochimica Acta*, 73,15, 4376-83.

Skliris, N., A. Mantziadou, S. Sofianos and A. Gkanasos (2010), “Satellite-derived variability of the Aegean Sea ecohydrodynamics”, *Continental Shelf Research*, 30, 403-18.

Solomon, S., D. Qin, M. Manning et al. (2007), “Climate change 2007: The physical science basis”, Contribution of Working Group I to the 4th Assessment Report of the IPCC, Cambridge University Press.

Somot, S., F. Sevault and M. Déqué (2006), “Transient climate change scenario simulation of the Mediterranean Sea for the twenty-first century using a high-resolution ocean circulation model”, *Climate Dynamics*, 27, 7-8, 851-79.

Soria, A., C.M. Goodess, O.B. Christensen, A. Iglesias, L. Garrote, M. Moneo, M. Moreno, A. Pye, S. Quiroga and S. van Regemorter (2009), in Ciscar, J.-C. (ed.), “Climate change impacts in Europe: Final report of the PESETA research project, Joint Research Centre Scientific and Technical Report (EUR 24093 EN)”, European Commission, Luxembourg: Office for Official Publications of the European Communities, November.

Stathopoulou, M. and C. Cartalis (2006), “Mapping quality of life in Metropolitan Athens using satellite and census data”, 1st EARSeL Workshop of the SIG Urban Remote Sensing, Humboldt-Universität zu Berlin, 2-3 March.

Stathopoulou, M., A. Synnefa, C. Cartalis, M. Santamouris, T. Karlessi and H. Akbari (2009), “A surface heat island study of Athens using high resolution satellite imagery and measurements of the optical and thermal properties of commonly used building and paving materials”, *International Journal of Sustainable Energy*, 28, 1, 59-76.

Staubwasser, M. and H. Weiss (2006), “Holocene climate and cultural evolution in late pre-historic–early historic West Asia” *Quaternary Research*, 66, 372-87.

Steinhilber, F., J. Beer and C. Frohlich (2009), “Total solar irradiance during the Holocene”, *Geophysical Research Letters*, 36, L19704.

Stirling, C.H., T.M. Esat, K. Lambeck and M.T. McCulloch (1998), “Timing and duration of the Last Interglacial: Evidence for a restricted interval of widespread coral reef growth”, *Earth and Planetary Science Letters*, 160, 745-62.

Stuiver, M. and T.F. Braziunas (1989), “Atmospheric ¹⁴C and century-scale solar oscillations”, *Nature*, 338, 405-7.

Stuiver, M. and T.F. Braziunas (1993), “Sun, ocean, climate and atmospheric $^{14}\text{CO}_2$: an evaluation of causal and spectral relationships”, *The Holocene*, 3, 289-305.

Sutcliffe, J.V. (1978), “Methods of flood estimation: a guide to the Flood Studies Report”, Wallingford, *Institute of Hydrology*, 50.

The Geological Society (2010), “Climate change: evidence from the geological record”, A statement from the Geological Society of London, November.

Theocharis, A. and D. Georgopoulos (1993), “Dense water formation over the Samothraki and Limnos Plateaux in the north Aegean Sea (eastern Mediterranean Sea)”, *Continental Shelf Research*, 13, 919-39.

Till, C. and J. Guiot (1990), “Reconstruction of precipitation in Morocco since 1100 A.D. based on *Cedrus atlantique* tree-ring width”, *Quaternary Research*, 33, 337-51.

Tolika, K., C. Anagnostopoulou, P. Maheras and M. Vafiadis (2008), “Simulation of future changes in extreme rainfall and temperature conditions over the Greek area: a comparison of two statistical downscaling approaches”, *Global and Planetary Change*, 63, 132-51.

Tolika, K., P. Maheras and I. Tegoulis (2009), “Extreme temperatures in Greece during 2007: Could this be a ‘return to the future’?”, *Geophysical Research Letters*, 36, L10813, doi: 10.1029/2009GL038538.

Touchan, R., G.M. Garfin, D.M. Meko, G. Funkhouser, N. Erkan, M.K. Hughes and B.S. Wallin (2003), “Preliminary reconstructions of spring precipitation in southwestern Turkey from tree-ring width”, *International Journal of Climatology*, 23, 157-71.

Touchan, R., E. Xoplaki, G. Funkhouser, J. Luterbacher, M.K. Hughes, N. Erkan, Ü. Akkemik and J. Stephan (2005), “Reconstructions of spring/summer precipitation for the Eastern Mediterranean from tree-ring widths and its connection to large-scale atmospheric circulation”, *Climate Dynamics*, 25, 75-98.

Touchan, R., Ü. Akkemik, M.K. Hughes and N. Erkan (2007), “May-June precipitation reconstruction of southwestern Anatolia, Turkey, during the last 900 years from tree rings”, *Quaternary Research*, 68, 196-202.

Touchan, R., K.J. Anchukaitis, D.M. Meko, S. Attalah, C. Baisan and A. Aloui (2008), “Long term context for recent drought in northwestern Africa”, *Geophysical Research Letters*, 35, L13705, doi:10.1029/2008GL034264.

Trenberth, K.E., P.D. Jones, P. Ambenje, R. Bojariu, D. Easterling, A. Klein Tank, D. Parker, F. Rahimzadeh, J.A. Renwick, M. Rusticucci, B. Soden and P. Zhai (2007), “Observations: Surface and Atmospheric Climate Change”, in Solomon, S., D. Qin, M. Manning, Z. Chen, M. Marquis, K.B. Averyt, M. Tignor and H.L. Miller (eds), “Climate Change 2007: The Physical Science Basis”, Contribution of Working Group I to the Fourth Assessment Report of the Intergovernmental Panel on Climate Change, Cambridge University Press, Cambridge, United Kingdom and New York, NY, USA.

Triantaphyllou, M.V., P. Ziveri, A. Gogou, G. Marino, V. Lykousis, I. Bouloubassi, K.-C. Emeis, K. Kouli, M. Dimiza, A. Rosell-Melé, M. Papanikolaou, G. Katsouras and N. Nunez (2009), “Late Glacial-Holocene climate variability at the south-eastern margin of the Aegean Sea”, *Marine Geology*, 266, 182-97.

Triantaphyllou, M.V., A. Antonarakou, K. Kouli, M. Dimiza, G. Kontakiotis, M. Papanikolaou, P. Ziveri, P.G. Mortyn, V. Lianou, V. Lykousis and M.D. Dermitzakis (2009b), “Comparing Late Glacial-Holocene plankton ecozones and pollen assemblage zones: basis for a multi-proxy ecostratigraphy in the South-Eastern Aegean Sea (E. Mediterranean)”, *Geomarine Letters*, 29, 4, 249-67.

Triantaphyllou, M.V., P. Ziveri, A. Gogou, G. Marino, V. Lykousis, I. Bouloubassi, K.-C. Emeis, K. Kouli, M. Dimiza, A. Rosell-Melé, M. Papanikolaou, G., Katsouras and N. Nunez (2009), “Late Glacial-Holocene climate variability at the south-eastern margin of the Aegean Sea”, *Marine Geology*, 266, 1-4, 182-97.

Tsimplis M., V. Zervakis, S. Josey, E. Peneva, M.V. Struglia, E. Stanev, P. Lionello, P. Malanotte-Rizzoli, V. Artale, A. Theocharis, E. Tragou and T. Oguz (2006), “Changes in the oceanography of the Mediterranean Sea and their link to climate variability” in Lionello, P. et al. (ed.), “Mediterranean climate variability”, *Elsevier*, 228-82.

Tzedakis, P.C. (2007), “Seven ambiguities in the Mediterranean palaeoenvironmental narrative”, *Quaternary Science Reviews*, 26, 2042-66.

Tzedakis, P. C. (2010), “The MIS 11 – MIS 1 analogy, southern European vegetation, atmospheric methane and the ‘early anthropogenic hypothesis’”, *Climate of the Past*, 6, 131-44.

Vergnaud-Grazzini, C., M. Devaux and J. Znaidi (1986), “Stable isotope anomalies in the Mediterranean Pleistocene records”, *Marine Micropaleontology*, 10, 35-69.

Vinther, B.M., P.D. Jones, K.R. Briffa, H.B. Clausen, K.K. Andersen, D. Dahl-Jensen and S.J. Johnsen (2010), “Climatic signals in multiple highly resolved stable isotope records from Greenland”, *Quaternary Science Reviews*, 29, 522-38.

Vonmoos, M., J. Beer and R. Muscheler (2006), “Large variations in Holocene solar activity – constraints from ¹⁰Be in the GRIP ice core”, *Journal of Geophysical Research*, 111, A10105. doi:10.1029/2005JA011500.

Vött, A. (2007), “Relative sea level changes and regional tectonic evolution of seven coastal areas in NW Greece since the mid-Holocene”, *Quaternary Science Reviews*, 26, 7-8, 894-919.

Vrekoussis, M., M. Kanakidou, N. Mihalopoulos, P. J. Crutzen, J. Lelieveld, D. Perner, H. Berresheim and E. Baboukas (2004), “Role of the NO₃ radicals in oxidation processes in the eastern Mediterranean troposphere during the MINOS campaign”, *Atmos. Chem. Phys.*, 4, 169-82.

Vrekoussis, M., F. Wittrock, A. Richter and J.P Burrows (2009), “Temporal and spatial variability of glyoxal as observed from space”, *Atmos. Chem. Phys.*, 9, 4485-504.

Vrekoussis, M., F. Wittrock, A. Richter and J.P Burrows (2010), "GOME-2 observations of oxygenated VOCs: What can we learn from the ratio glyoxal to formaldehyde on a global scale?", *Atmos. Chem. Phys.*, 10, 10145-10160, doi:10.5194/acp-10-10145-2010.

Waelbroeck, C., L. Labeyrie, E. Michel, J.C. Duplessy, J.F. McManus, K. Lambeck, E. Balbon and M. Labracherie (2002), "Sea-level and deep-water temperature changes derived from benthic foraminifera isotopic records", *Quaternary Science Reviews*, 21, 295-305.

Wang, Y.M., J.L. Lean and N.R. Sheeley (2005), "Modeling the sun's magnetic field and irradiance since 1713", *The Astrophysical Journal*, 625, 522-38.

Wanner, H., J. Beer, J. Bütikofer, T.J. Crowley, U. Cubasch, J. Flückiger, H. Goosse, M. Grosjean, F. Joos, J.O. Kaplan, M. Küttel, S.A. Müller, I.C. Prentice, O. Solomina, T.F. Stocker, P. Tarasov, M. Wagner and M. Widmann (2008), "Mid- to Late Holocene climate change: an overview", *Quaternary Science Reviews*, 27, 1791–1828, doi:10.1016/j.quascirev.2008.06.013.

Williams, J. (2004), "Organic trace gases in the atmosphere, an overview", *Environ. Chem.* 2004, 1, 125-36, doi:10.1071/EN04057.

Woodworth, P.L., N. J. White, S. Jevrejeva, S.J. Holgate, J.A. Church and W.R. Gehrels (2009), "Evidence for the accelerations of sea level on multi-decade and century timescales", *International Journal of Climatology*, 29, 777-89.

Worley, S.J., S.D. Woodruff, R.W. Reynolds, S.J. Lubker and N. Lott (2005), "ICOADS Release 2.1 data and products", *International Journal of Climatology* (CLIMAR-II Special Issue), 25, 823-42.

Xoplaki, E., P. Maheras and J. Luterbacher (2001), "Variability of climate in meridional Balkans during the periods 1675-1715 and 1780-1830 and its impact on human life", *Climatic Change*, 48, 581.

Xoplaki, E., 2002: *Climate variability over the Mediterranean*. PhD Thesis, University of Bern, Switzerland.

Xoplaki, E., F.J. Gonzalez-Rouco, D. Gyalistras, J. Luterbacher, R. Rickli and H. Wanner (2003), "b. Interannual summer air temperature variability over Greece and its connection to the large-scale atmospheric circulation and Mediterranean SSTs 1950-1999", *Climate Dynamics*, 20, 537-54.

Xoplaki, E., J.F. Gonzalez-Rouco, J. Luterbacher and H. Wanner (2004), "Wet season Mediterranean precipitation variability: influence of large-scale dynamics", *Climate Dynamics*, 23, 63-78.

Xoplaki, E., J. Luterbacher, H. Paeth, D. Dietrich, N. Steiner, M. Grosjean and H. Wanner (2005), "European spring & autumn temperature variability and change of extremes over the last half millennium", *Geophysical Research Letters*, 32, L15713.

Zachariasse, W.J., F.J. Jorissen, C. Perissoratis, E.J. Rohling and V. Tsapralis (1997), “Late Quaternary foraminiferal changes and the nature of sapropel S1 in Skopelos basin”, Proceedings of 5th Hellenic Symposium on Oceanography and Fisheries, I, Greece, 391-4.

Zachos, J.C., M. Pagani, L. Sloan, E. Thomas and K. Billups (2001), “Trends, rhythms, and aberrations in global climate 65 Ma to present”, *Science*, 292, 686-93.

Zanis, P., I. Kapsomenakis, C. Philandras, K. Douvis, D. Nikolakis, E. Kanellopoulou, C. Zerefos and C. Repapis (2009), “Analysis of an ensemble of present day and future regional climate simulations for Greece”, *International Journal of Climatology*, 29, 1614-33, doi: 10.1002/joc.1809.

Zerefos, C., K. Philandras, C. Douvis, I. Kapsomenakis, G. Tselioudis and K. Eleftheratos (2010), “Long term changes of precipitation in Greece”, 12th Plinius Conference on Mediterranean Storms, MedCLIVAR session, Corfu, September 3.

Zoulia, I., M. Santamouris and A. Dimoudi (2008), “Monitoring the effect of urban green areas on the heat island in Athens”, *Environ Monit Assess*, doi: 10.1007/s10661-008-0483-3.

WMO (2006), “Statement on the status of the global climate in 2005”, World Meteorological Organization, 998, Geneva.

